

University College London
UCL

**Synthesis of Truncated Analogues of ProTx-II
as a Novel Form of Pain Relief**

Zoë Wright

Submitted in partial fulfilment of the requirements for the degree of

Doctor of Philosophy

Declaration

I, Zoë Wright, confirm that the work presented in this thesis is my own. Where information has been derived from other sources, I confirm that this has been indicated in the thesis.

Signed:

Date:

Abstract

Chronic pain affects almost 10 million people in the UK but despite this, few effective treatments exist. Research has shown that targeting the Na_v1.7 ion channel provides a novel approach to treatment. ProTx-II, a 30 amino acid peptide isolated from Tarantula venom, is highly selective for the channel (IC₅₀ value - 0.3nm *in vitro*) but *in vivo* results were less promising.

ProTx-II contains three interlocking disulfide bonds connected in a distinctive pattern. To investigate the structure-activity relationship between the peptide and the ion channel, truncated analogues based on the individual cysteine rings were synthesised.

This thesis investigates the effect of replacing the disulfide bond with a thioether linkage through the incorporation of a novel diastereoisomer of the non-natural amino acid lanthionine to produce hydrolytically stable compounds. Lanthionine can be thought of as two alanine residues connected by a thioether linkage at the β-carbon. Improvements in the synthesis allowed for the first large scale production of lanthionine enabling multiple attempts at peptide synthesis to be carried out. Work was also begun on the synthesis of cystathionine, a second thioether linker containing an extra CH₂ group between the amino acid centres.

Novel methodologies were investigated for the incorporation of a new diastereomer of lanthionine containing two L-amino acid centres using a new microwave-based methodology. This methodology has so far produced the largest known synthetic rings containing a lanthionine bridge, along with the first interlocking disulfide and thioether bridged compounds.

The analogues produced were modelled using *in silico* mutagenesis techniques and the effect of these analogues on the hNa_v1.7 receptor was investigated using an automated patch clamp assay. Finally, analysis of the connectivity of ProTx-II was carried out using a combination of digestion and MS/MS experiments.

Table of Contents

Declaration

Abstract

Table of Contents

List of Figures and Tables

Acknowledgements

Abbreviations

1	Chapter 1: Introduction	19
1.1	Identification of a Novel Biological Target	20
1.2	Voltage-Gated Sodium Ion Channels and Action Potentials	20
1.3	Small Molecule Ion Channel Inhibitors	25
1.4	Toxins as Ion Channel Inhibitors	26
1.4.1	Conotoxins	27
1.4.2	Other Multiply-Bridged Peptides	30
1.4.3	Toxins Isolated from Tarantula Venoms	31
1.5	ProTx-II as an Inhibitor of Na _v 1.7	32
1.6	Disulfide Bond Replacements	35
1.6.1	Replacement of a Disulfide Bond with a Diselenide Bond	35
1.6.2	Replacement of Sulfur Atoms with Carbon Atoms	36
1.6.3	Replacement of a Disulfide Bond with Lactam Ring Formation	37
1.6.4	Replacement of a Disulfide Bond with Cystathionine	38
1.6.5	Replacement of a Disulfide Bond with Lanthionine	40
1.7	Lanthionine and the Lantibiotics	41
1.7.1	Chemical Syntheses of Lanthionine	42
1.8	Synthesis of Lantibiotics	46
1.8.1	Formation of a Lanthionine Bridge On-Resin	46
1.8.2	Incorporation of a Pre-Formed Protected Lanthionine into a Solid Phase Peptide Synthesis Strategy	48

1.9	Conclusions and Aims	55
	References	55
2	Synthesis of Orthogonally Protected Lanthionine for Use in Solid Phase Peptide Synthesis	59
2.1	Introduction	59
2.2	Small Scale Synthesis	60
2.2.1	Overview of the Small Scale Synthesis	60
2.2.2	Optimisation of the Synthesis	61
2.2.2a	Preparation of the Protected Amino Acids	61
2.2.2b	Optimisation of the Coupling Procedure	63
	i) Investigation into the Vederas Route	65
	ii) Hybrid Route Investigations	65
	iii) Optimisation of the Bregant and Tabor Route	66
2.2.2c	Optimisation of the Trityl Deprotection and Alloc Protection Steps	70
2.2.2d	Optimisation of the <i>tert</i> -Butyl Deprotection Step	72
2.2.2e	Conclusions from the Small Scale Synthesis Work	72
2.3	Large Scale Synthesis	74
2.3.1	Reaction Monitoring and Safety Concerns	74
2.3.2	Results and Summary of the Large Scale Synthesis Work	78
2.4	Conclusions	80
	References	80
3.	Chapter 3: Synthesis of ProTx-II (22) and Truncated Analogues	82
3.1	Synthesis of ProTx-II (22)	83
3.1.1	Cyclisation and Structure Determination of ProTx-II (22)	83
3.2	Synthesis of Disulfide Bridge Truncated Analogues	88
3.2.1	Synthesis of Single Ring Disulfide Analogues	88
3.2.2	Synthesis of Double Ring Disulfide Analogues	90
3.2.3	Conclusions	92

3.3	Synthesis of Thioether Bridge Truncated Analogues	92
3.3.1	Introduction	92
3.3.2	Synthesis of Single Ring Lanthionine Analogues	94
3.3.3	Synthesis of Double Ring Lanthionine Analogues	99
3.4	Synthesis of Triple Ring Lanthionine Analogues	101
3.5	Conclusions	109
	References	110
4	Chapter 4: Towards the Synthesis of Orthogonally Protected Cystathionine for Use in Solid Phase Peptide Synthesis	112
4.1	Introduction	112
4.2	Synthesis of Regioisomer 1 (245)	116
4.3	Conclusions from the Synthesis of Regioisomer 1 (245)	120
4.4	Synthesis of Regioisomer 2 (246)	121
4.5	Conclusions from the Synthesis of Regioisomer 2 (246)	126
4.6	Conclusions	127
	References	127
5.	Chapter 5: Biological and <i>in silico</i> Evaluation of the Analogues of ProTx-II	128
5.1	<i>In Silico</i> Analysis of Structures	128
5.1.1	Modelling of the Single Ring Analogues of ProTx-II	130
5.1.2	Modelling of the Double Ring Analogues of ProTx-II	133
5.1.3	Modelling of the Triple Ring Analogues of ProTx-II	138
5.1.4	Conclusions from the Modelling Calculations	141
5.2	An Introduction to Patch Clamping	142
5.2.1	Manual Patch Clamping	142
5.2.2	Automated Patch Clamping	145
5.3	Preliminary Patch Clamping Results	145
5.4	Further Results from B'Sys	147
5.5	Analysis of the Structure of ProTx-II	148

5.6	Probing Disulfide Bond Connectivity	151
5.7	Conclusions	155
	References	156
6.	Chapter 6: Conclusions and Future Work	158
7.	Chapter 7: Experimental	161
7.1	General Experimental	161
7.2	Experimental for the Synthesis of Lanthionine (Chapter 2)	162
7.2.1	Key to NMR Assignments:	162
7.2.2	Experimental for Small Scale Synthesis	163
7.2.3	Experimental for Large Scale Synthesis	180
7.3	Experimental for Peptide Synthesis (Chapter 3)	186
7.3.1	General Experimental for Peptide Synthesis	186
7.3.2	Synthesis of ProTX-II and Disulfide Analogues	190
7.3.3	Optimisation of the Synthesis of Lanthionine-Containing Analogues	201
7.3.4	Synthesis of Lanthionine-Containing Analogues	203
7.3.5	Attempted Syntheses of Double Ring Analogues of ProTx-II	217
7.4	Experimental for the Synthesis of Cystathionine (Chapter 4)	229
7.4.1	Key to NMR Assignments:	229
7.4.2	Experimental for Cystathionine Synthesis Work	230
7.5	Experimental for the Analysis of the Connectivity of ProTX-II (Chapter 5)	247
7.5.1	Preparation of ProTx-II (22)	247
7.5.2	Maleimide Experiments	251
7.5.3	Digestion Experiments	252
7.5.4	Computer Modelling	253
	References	253
	Appendix: LC-MS Data from Mitsunobu Experiments	254

List of Figures and Tables

1	Chapter 1: Introduction	19
	Table 1.1: The WHO Pain Ladder	19
	Figure 1.1: Schematic Diagram of a Nerve Cell	21
	Figure 1.2: Schematic Diagram of an Action Potential	21
	Figure 1.3: Schematic Diagram Showing the Stages of an Action Potential	22
	Figure 1.4: Schematic Diagram of a Sodium Channel	23
	Table 1.2: The Mammalian Sodium Channel Isoforms	24
	Figure 1.5: Comparison of Vertebrate and Bacterial Sodium Ion Channels	24
	Figure 1.6: Structure of the Bacterial Sodium Ion Channel Isolated from <i>A. butzleri</i>	25
	Figure 1.7: Structures of First Generation Sodium Ion Channel Blockers	25
	Figure 1.8: Generic Structures of Second Generation Sodium Ion Channel Blockers	26
	Figure 1.9: Structures of Lidocaine (7) and QX-314 (8)	26
	Figure 1.10: Structure of Tetrodotoxin (9)	27
	Table 1.3: Summary of Sensitivity to Tetrodotoxin (9)	27
	Table 1.4: Classification of Conotoxins by Site of Inhibition	28
	Figure 1.11: Structure of α -GI (10) and α -ImI (11)	28
	Figure 1.12: Structure of μ -GIIIA (12) and μ -GIIIB (13)	29
	Figure 1.13: Comparison of the Structures of an ICK peptide (14) and a DDH peptide (15)	29
	Figure 1.14: Structure of Prialt (16)	29
	Figure 1.15: Structure of Bracelet and Möbius Cyclotides	30
	Figure 1.16: Structure of Kalata-B1 (17)	30
	Figure 1.17: Structure of Ssm6a (18)	31
	Figure 1.18: Structures of GsMTx-4 (19) and HwTx-IV (20)	31
	Figure 1.19: Structures of ProTx-I (21) and ProTx-II (22)	31
	Figure 1.20: Homology Model of ProTx-II (22)	32
	Figure 1.21: Solution NMR Structure of ProTx-II (22)	33

Figure 1.22: Structures of the Peptides Used in the Investigations	33
Table 1.5: Summary of Results from Park <i>et al.</i>	34
Figure 1.23: Structure of ProTx-II-NHCH ₃ (23)	34
Figure 1.24: Structure of WT-Iml (11)	35
Figure 1.25: Selenocysteine analogues of Iml	36
Figure 1.26: Unsaturated (27) and Saturated (28) Dicarba-analogues of Iml	36
Figure 1.27: Incorporation of Ring Closing Metathesis and Hydrogenation into an SPPS Strategy	37
Figure 1.28: Example Orthogonal Synthesis of ST Analogue Using On-resin Lactamization	38
Figure 1.29: Structure Comparisons 39 – Disulfide Bond, 40 – Cystathionine Bond, Regioisomer 1, 41 – Cystathionine Bond, Regioisomer 2	39
Figure 1.30: Tachyplesin-1 (42) and Generic Structural Analogues (43)	39
Figure 1.31: γ - (44) and δ -Analogues (45) of Compstatin	40
Figure 1.32: Cystathionine-Containing analogues of Iml	40
Figure 1.33: Structure Comparisons 39 – Disulfide Bond, 49 – Lanthionine Bond, 40 – Cystathionine Bond, Regioisomer 1, 41 – Cystathionine Bond, Regioisomer 2	40
Figure 1.34: Structure of Somatostatin (50), Sandostatin (51) and Examples of the Goodman Lanthionine-Containing Analogues (52 and 53)	41
Figure 1.35: Structure of Nisin (54)	42
Figure 1.36: Synthesis of Lanthionine <i>via</i> Michael Addition	42
Figure 1.37: Synthesis of Lanthionine <i>via</i> Chloroalanine (58) Reaction with Cysteine (59)	43
Figure 1.38: Synthesis of Lanthionine (63) <i>via</i> Iodoalanine (61) Reaction with Cysteine (62)	43
Figure 1.39: Synthesis of Lanthionine <i>via</i> Bromoalanine (64) Reaction with Cysteine (56)	43
Figure 1.40: Formation of Aziridine (69)	43
Figure 1.41: Synthesis of Lanthionine (72) and Nor-Lanthionine (73)	44
Figure 1.42: Synthesis of Lanthionine <i>via</i> Mitsunobu Reaction	44
Figure 1.43: Synthesis of Lanthionine <i>via</i> Desulfurisation	45
Figure 1.44: Synthesis of Orthogonally Protected Lanthionine (81)	45
Figure 1.45: Synthesis of Nisin Ring A	46

Figure 1.46: Total Synthesis of Nisin (54)	47
Figure 1.47: Synthesis of Subtilin Ring B (96)	48
Figure 1.48: Synthesis of Nisin Ring C (101)	49
Figure 1.49: Structure of Lanthionine (102) for Use in SPPS Strategy	49
Figure 1.50: Synthesis of an Analogue of Nisin Ring C (109)	50
Figure 1.51: Synthesis of Lactocin S (117)	51
Figure 1.52: Structure of Lanthionine (118) and Methyl Lanthionine (119)	52
Figure 1.53: Structure of Lacticin 3147 A1 (120) and Lacticin 3147 A2 (121)	52
Figure 1.54: Synthesis of Lacticin 3147 A1 (120)	53
Figure 1.55: Structures of Orthogonally Protected Lanthionines (102) and (130) and an Analogue of Nisin Rings D and E (131)	54
2. Chapter 2: Synthesis of Orthogonally Protected Lanthionine for Use in Solid Phase Peptide Synthesis	59
Figure 2.1: Structure of ProTX-II (22)	59
Figure 2.2: Structure of Lanthionine in S,R (49) and R,R 132 Forms	60
Figure 2.3: Synthesis of Orthogonally Protected Lanthionine 142	61
Figure 2.4: Large Scale Synthesis of the Doubly Protected Cysteine (63)	62
Figure 2.5: Synthesis of Doubly Protected Iodoalanine 139	63
Figure 2.6: Formation of α -iodo- β -alanine Derivative 145 <i>via</i> the Aziridine 143 and Subsequent Reaction to Give Norlanthionine (146)	64
Figure 2.7: Phase transfer coupling conditions	64
Figure 2.8: Formation of Diastereoisomers <i>via</i> Competing Elimination Reaction	65
Figure 2.9: Vederas Route to Orthogonally Protected Lanthionine 141	65
Figure 2.10: Hybrid Route to Formation of Lanthionine	66
Figure 2.11: Formation of Doubly Protected Bromoalanine 155	67
Figure 2.12: Summary of Results from Coupling Investigations	67
Table 2.1: Summary of Results from Coupling Investigations	67
Figure 2.13: Proposed Large Scale Coupling Procedure	68
Figure 2.14: New Mitsunobu Conditions to give Iodoalanine 139	69

Figure 2.15: Summary of the <i>in situ</i> Investigations into Coupling Reactions	69
Table 2.2: Summary of the <i>in situ</i> Investigations into Coupling Reactions	69
Figure 2.16: Large Scale Coupling Procedure	70
Figure 2.17: Reaction Conditions for Trityl Deprotection and Alloc Protection Steps	71
Table 2.3: Reaction Conditions for Trityl Deprotection and Alloc Protection Steps	71
Figure 2.18: Results from Trial Deprotection Reactions	71
Table 2.4: Results from Trial Deprotection Reactions	72
Figure 2.19: Summary of the Trityl to Alloc Protecting Group Reaction	72
Figure 2.20: New Synthesis for the Production of Orthogonally Protected Lanthionine	142 74
Figure 2.21: Generally Accepted Mechanism for a Mitsunobu Reaction	75
Figure 2.22: Possible Structures of Intermediates and Side Products Observed by LC-MS during the Mitsunobu Iodination Reaction	76
Figure 2.23: A Second Mechanistic Pathway for the Mitsunobu Reaction	77
Figure 2.24: A Possible Mechanistic Pathway for the Iodination Reaction	78
Figure 2.25: Summary of the Large Scale Synthesis	79
3. Chapter 3: Synthesis of ProTX-II (22) and Truncated Analogues	82
Figure 3.1: Structure of ProTX-II (22) and Suggested Analogues for Synthesis	82
Table 3.1: Short Investigation into Cleavage Times	83
Table 3.2: Investigation into Cyclisation Conditions	84
Figure 3.2: Double Digestion of ProTX-II	84
Figure 3.3: Post Source Decay Experimental Results	85
Figure 3.4: Possible Connectivity in Synthesised ProTX-II (22)	86
Figure 3.5: Structures of PaTx-I (190) and ProTX-II (22)	86
Figure 3.6 HPLC Trace Showing Injection of Synthesised ProTX-II	87
Figure 3.7: HPLC Trace Showing Injection of Purchased ProTX-II	87
Figure 3.8: HPLC Trace Showing Combined Injection of Synthesised and Purchased ProTX-II	88
Figure 3.9: Single Ring Disulfide Analogues	89
Table 3.3: Summary of Investigations into the Effect of Resin on Yield	89

Figure 3.10: Double Ring Disulfide Analogues	90
Table 3.4: Summary of Investigations into the Use of Orthogonal Protecting Groups	91
Figure 3.11: Methodology for the Incorporation and Cyclisation of Orthogonally Protected Lanthionine (142) Into a Peptide Sequence	93
Figure 3.12: Single Ring Thioether Analogues	95
Figure 3.13: Structure of the Desired Peptide 205 and the Peptide Without Lanthionine Incorporation 209	95
Table 3.5: Summary of Preliminary Investigations into the Use of the Microwave for Incorporation of Lanthionine (142) into the Peptide Sequence	97
Table 3.6: Summary of Further Investigations into the Use of the Microwave for Incorporation of Lanthionine (142) into the Peptide Sequence	97
Figure 3.14: Structures of the Single Ring Thioether Analogues	98
Figure 3.15: Double Ring Thioether Analogues	100
Figure 3.16: Triple Ring Thioether Analogues	102
Figure 3.17: Step-wise Insertion of Amino Acids into the Peptide Sequence	104
Figure 3.18: Mechanism of Interaction with Hmb-protected Amino Acid	106
Figure 3.19: Structure of Peptides Incorporating Hmb-protected Amino Acid	106
Figure 3.20: Synthetic Strategy for Formation of the Triple Ring Analogues Incorporating Hmb Protection and Addition of Lanthionine Using the Microwave Protocol	107
Figure 3.21: Structure of the S(Tmp) protected Cysteine (242)	108
Figure 3.22: Formation of Peptide 215	109
4 Chapter 4: Synthesis of Orthogonally Protected Cystathionine for Use in Solid Phase Peptide Synthesis	112
Figure 4.1: Structural Comparison of Disulfide and Thioether Linkages	112
Figure 4.2: Orthogonally Protected Thioether Moieties for Use in Peptide Synthesis	113
Figure 4.3: Van der Donk Synthesis of Cystathionines (245) and (246)	114
Figure 4.4: Possible Synthetic Strategies for the Synthesis of Cystathionines (245) & (246)	115
Figure 4.5: Proposed Synthetic Strategy for Synthesis of Cystathionine (245)	116
Figure 4.6: Attempts to Couple Iodoalanine 139 and Protected Homocysteine 257 to form Cystathionine	117

Table 4.1: Attempts to Couple Iodoalanine 139 and Protected Homocysteine 257 to form Cystathionine	117
Figure 4.7: Alternative Synthetic Strategy for Synthesis of Cystathionine (245)	118
Figure 4.8: Alternative Synthetic Strategy for Synthesis of Protected Cysteine (253)	118
Figure 4.9: Attempts to Synthesise allyl/Alloc Homoserine (254)	119
Table 4.2: Summary of Attempts to Iodinate Homoserine (254)	119
Figure 4.10: Alternative Synthetic Strategy for Synthesis of Protected Homoserine 258	119
Figure 4.11: Synthesis of Cystathionine (256)	120
Table 4.3: Synthesis of Cystathionine (256)	120
Figure 4.12: Proposed Synthetic Strategy for Synthesis of Cystathionine (246)	121
Figure 4.13: Attempts to Synthesise allyl/Alloc Homoserine (248)	122
Table 4.4: Attempts to Synthesise allyl/Alloc Homoserine (248)	122
Figure 4.14: Attempts to Open Alloc Lactone 270	123
Table 4.5: Attempts to Open Alloc Lactone 270	123
Figure 4.15: Attempted Synthesis of Cystathionine (246)	124
Figure 4.16: Attempts to Synthesise allyl/Alloc Protected Homocysteine 274	124
Figure 4.17: Synthesis of Homocysteine 275	125
Figure 4.18: Alternative Strategy for the Synthesis of Cystathionine (246)	125
Figure 4.19: Formation of Dehydroalanine (278) and the Subsequent Coupling Reaction	126
5. Chapter 5: Biological and <i>in silico</i> Evaluation of the Analogues of ProTx-II	128
Figure 5.1: Comparison of PaTx-I (left) and ProTx-II (right) Structure Generated by MOE™ Software	129
Figure 5.2: Comparison of Solution NMR Structure of ProTx-II With Structure Predicted by MOE™ Software	130
Figure 5.3: Structure of C-terminal Single Ring (192) and Location of the Residues Within ProTx-II (22)	130
Figure 5.4: Structure of Middle Single Ring (193) and Location of the Residues Within ProTx-II (22)	131
Figure 5.5: Structure of N-terminal Single Ring (194) and Location of the Residues Within ProTx-II (22)	131

Figure 5.6: Comparison of the Structures of the C-Terminal Single Ring	132
Figure 5.7: Comparison of the Structures of the Middle Single Ring	133
Figure 5.8: Comparison of the Structures of the N-Terminal Single Ring	133
Figure 5.9: Structure of C-Terminal Double Ring (195) and Location of the Residues Within ProTx-II (22)	134
Figure 5.10: Structure of N-Terminal Double Ring (196) and Location of the Residues Within ProTx-II (22)	134
Figure 5.11: Structure of C-Terminal Double Ring Analogues	135
Figure 5.12: Comparison of Solution Phase NMR of ProTx-II (22) Against Predicted Structure for C-Terminal Double Ring Analogue with the Middle Ring Containing the Thioether Bridge (211)	136
Figure 5.13: Structure of the N-Terminal Double Ring Analogues	137
Figure 5.14: Structure of Triple Ring Analogue with C-Terminal Lanthionine Bridge (214)	138
Figure 5.15: Structure of Triple Ring Analogue with Middle Lanthionine Bridge (215)	139
Figure 5.16: Structure of Triple Ring Analogue with N-Terminal Lanthionine Bridge (216)	139
Figure 5.17: Comparison of the Triple Ring Structures with the Solution Phase ProTx-II (22) NMR Structure	140
Figure 5.18: Unmyelinated vs Myelinated Neurons	142
Figure 5.19: Propagation of the Nerve Impulse in an Unmyelinated Neuron	143
Figure 5.20: Propagation of the Nerve Impulse in a Myelinated Neuron	143
Figure 5.21: Schematic Diagram of a Patch Clamp Experiment	144
Table 5.1: Composition of the Pipette Solution	144
Table 5.2: Structures of Peptides Submitted for the First Round of Testing	146
Table 5.3: Summary of Testing Results from B'Sys	147
Figure 5.22: Reaction of a Free Sulfhydryl Group with 2,3-Dibromomaleimide (284)	149
Table 5.4: Results from the Maleimide End-Capping Experiments	149
Table 5.5: Summary of Analytical HPLC Results	150
Figure 5.23: Comparison of the Solution Phase NMR Structures of the DDH motif in HwTx-II (289) against the ICK motif of ProTx-II (22)	151
Figure 5.24: Products from the Digestion of ProTx-II using Trypsin and Glu-C	152

Figure 5.25: Possible Products from the MS/MS Experiments	154
6. Conclusions and Future Work	158
7. Experimental	161
Figure 7.1: Summary of Results from Coupling Investigations	172
Table 7.1: Summary of Results from Coupling Investigations	173
Table 7.2: Summary of Preliminary Investigations into the Use of the Microwave for Incorporation of Lanthionine (142) into the Peptide Sequence	202
Table 7.3: Summary of Further Investigations into the Use of the Microwave for Incorporation of Lanthionine (142) into the Peptide Sequence	203
Figure 7.2: Attempts to Synthesise allyl/Alloc Homoserine (248)	239
Table 7.4: Attempts to Synthesise allyl/Alloc Homoserine (248)	239
Table 7.5: Attempts to Open Alloc Lactone 270	241
Figure 7.3: HPLC Trace Showing Injection of Tocris ProTx-II	249
Figure 7.4: HPLC Trace Showing Combined Injection of Tocris ProTx-II and Original Cyclisation Method for Synthesis of ProTx-II in-house	249
Figure 7.5: HPLC Trace Showing Smartox ProTx-II	250
Figure 7.6: HPLC Trace Showing Combined Injection of Smartox ProTx-II and Original Cyclisation Method for Synthesis of ProTx-II in-house	250
Figure 7.7: HPLC Trace Showing Combined Injection of Smartox ProTx-II and Park Cyclisation Method for Synthesis of ProTx-II in-house	251
Table 7.6: Results from the Maleimide End-Capping Experiments	252

Acknowledgements

First and foremost, I would like to thank Prof. Alethea Tabor for agreeing to take me on as a PhD student and for supervising me during the last four years; I am really grateful I had the opportunity to work for you. Thank you also to my second supervisor Dr. Erik Årstad and my industrial supervisors Dr. Luis Castro, Dr. Adrian Hall and Dr. Andy Takle at Eisai for their help throughout the project. Thank you to Eisai for generously funding my PhD project and for allowing me to do all the scale-up work at their research centre in Hatfield. I'd also like to thank Ian Kilford for teaching me how to do large scale synthesis.

Thank you also to Dr. Abil Aliev in NMR and the entire mass spectrometry department for their help throughout my time at UCL. Thanks also to Dr. Cali Hyde, Adam Cryar and Dr. Kostas Thalassinos for their help with extra mass spec analysis and Essen Bioscience and B'Sys for carrying out the testing against the ion channel.

I would like to thank all members of the Hailes and Tabor group past and present – it's been alright, eh? I'd especially like to thank Dr. Nick Mitchell, whose constant guidance and support helped me on a near daily basis and to whom I will be forever grateful. I'd also like to thank Dr. Fred Campbell, Dr. James Sayer and Dr. Dave Steadman for all of their help in the early years. Thank you as well to Dr. Robin Bofinger who has kept me company during so many late nights in the lab and to Alex, Eleanor and Leila – we're all nearly done now! Finally, thank you to Fiona, my, perhaps unwilling, partner in so many scrapes: thank you for everything, it's been a blast. And The Prodigy wrote a song about us. I think that's probably all I need to say. There isn't enough space to mention everyone but thank you to all of you – it's been a pleasure and a privilege to work alongside you all.

A huge thank you goes to my proof-reading elves who, despite having no clue what this thesis is about, have checked every page diligently and without complaint. Thank you so much for taking the time to do this: I owe you all big time. I'm not quite sure how many cakes I'll need to bake to say thank you but if I start now, I might be done in a few decades...

A huge thanks to the Ladies of Tufnell Park for everything and a shout out to the Mews for making sure I wasn't homeless and plying me with wine on a worryingly frequent basis. Last but not least, thank you to my family for unending support throughout this process and encouragement when I needed it most.

If this were an Oscars speech, I'd have to start crying uncontrollably now and professing my undying love for each and every one of you. Luckily, I'm crippingly British so I will just say it's been quite good.

This thesis is dedicated to Carol with love. I did it in the end xxxxx

Abbreviations

The following abbreviations are used throughout this thesis.

$[\alpha]_D$	specific rotation
aq.	aqueous
Ar	aryl
Bn	Benzyl
br	Broad
<i>n</i> Bu	Butyl
<i>t</i> Bu	<i>tertiary</i> butyl
c	concentration
C	Celsius
cat.	catalytic amount
CI	Chemical Ionisation
cm	centimetre
cm ⁻¹	wavenumber
D	doublet
dd	doublet of doublets
Da	Dalton
DDH	Disulfide Directed β -Hairpin
de	diastereoisomeric excess
DEAD	diethyl azodicarboxylate
DIPEA	N,N-diisopropylethylamine
DMF	dimethylformamide
DMSO	dimethylsulfoxide
dq	doublet of quartets
dt	doublet of triplets
DTT	1,4-dithiothreitol
δ_H	Proton (¹ H) NMR chemical shift
δ_C	Carbon (¹³ C) NMR chemical shift
eq.	equivalents
EI	Electron Ionisation
ESI	Electrospray Ionisation
Et	ethyl
FAB	Fast Atom Bombardment
Fmoc	9-fluorenylmethyloxycarbonyl
G	gram
GSH	reduced glutathione
GSSG	glutathione disulfide
h	hour
HBTU	O-benzotriazole- <i>N,N,N',N'</i> -tetramethyl-uronium-hexafluoro-phosphate
HOAt	1-hydroxy-7-azabenzotriazole
HPLC	High Performance Liquid Chromatography
HRMS	High Resolution Mass Spectrometry
Hz	Hertz
ICK	Inhibitory Cysteine Knot
IR	Infra-red
<i>J</i>	coupling constant
lit.	literature

L	Litre
LC-MS	Liquid Chromatography-Mass Spectrometry
LRMS	Low Resolution Mass Spectrometry
M	Meter
M	multiplet
M	Molar
M ⁺	molecular ion
M+H ⁺	protonated molecular ion
M–H ⁺	deprotonated molecular ion
m-CPBA	meta-chloroperoxybenzoic acid
Me	methyl
min	Minute
mL	millilitre
mM	millimolar
mol	Mole
mmol	millimole
MOE	Molecular Operating Environment
mp	melting point
MS	Mass Spectrometry
<i>MW</i>	molecular weight
<i>MWCO</i>	molecular weight cut-off
<i>m/z</i>	mass to charge ratio
NB	<i>para</i> -nitrobenzyl
NCS	<i>N</i> -chlorosuccinimide
nm	nanometre
NMM	<i>N</i> -methyl morpholine
NMR	Nuclear Magnetic Resonance
Nz	<i>para</i> -nitrobenzyloxycarbonyl
<i>O</i>	Ortho
OMe	Methoxy
<i>p</i>	para
PDB	Protein Data Bank
PEG	poly(ethylene glycol)
ppm	parts per million
PyAOP	(7-azabenzotriazol-1-yloxy)tripyrrolidinophosphonium hexafluorophosphate
q	Quartet
quant.	Quantitative
rt	room temperature
s	Singlet
SAR	Structure-Activity Relationship
sat.	Saturated
t	Triplet
TCEP	<i>tris</i> (2-carboxyethyl)phosphine
<i>tert</i>	Tertiary
TFA	trifluoroacetic acid
THF	tetrahydrofuran
TLC	Thin Layer Chromatography
μM	micromolar
UV	ultraviolet
ν _{max}	infrared absorption
V	Volume

1. Chapter 1: Introduction

This thesis details work towards the treatment of chronic nociceptive pain. Chronic pain is described as any pain which persists or recurs for a period of more than three months,¹ while nociceptive pain is that felt in the peripheral nerves and is caused by noxious (chemical, mechanical or thermal) stimuli. Nociception is defined as the encoding and processing of harmful stimuli in the nervous system² and is the mechanism by which the body identifies potentially dangerous situations. The stimuli are processed by free nerve endings referred to as pain receptors or nociceptors.

Chronic nociceptive pain has a variety of causes, from a herniated disc to cancer, and can be associated with debilitating levels of pain, making it difficult to maintain normality in daily life.¹ Each year, approximately 5 million people develop chronic pain in the UK but only about two thirds recover.³ It is estimated that back pain alone costs the exchequer in excess of £5 billion per annum.⁴ Currently, pain is managed according to the World Health Organisation (WHO) guidelines,^{5,6} which state that pain is treated in a “step-wise” manner, starting with mild ‘over-the-counter’ drugs and increasing with need up to the prescription of powerful opioids such as morphine and fentanyl. The so-called ‘pain ladder’ is divided into three main phases (Table 1.1).

Entry	Pain Level	Prescription	Example
Bottom Rung	Mild	Non-opioid + adjuvant	paracetamol + ibuprofen
Middle Rung	Moderate	Weak opioid + non-opioid + adjuvant	codeine + paracetamol + diclofenac
Highest Rung	Severe	Strong opioid + non-opioid + adjuvant	morphine + paracetamol + gabapentin

Table 1.1: The WHO Pain Ladder^{5,6}

The stronger painkillers such as morphine and fentanyl act at the μ and κ -opioid receptors, which belong to a group of G protein-coupled receptors with opioids as ligands. Targeting these receptors is associated with a number of different side effects including respiratory depression, drowsiness and euphoria.^{7,8} Fentanyl is 50 – 80 times more potent than morphine and whilst it shows little hypnotic activity, it is associated with bradycardia.⁸ In the case of many agonists of the μ and κ -opioid receptors, there are considerable problems with dependence as well as with all of the side effects mentioned above. As such, it is not desirable to prescribe these drugs for long term use, meaning there is a real clinical need for new treatment alternatives by targeting alternative biological pathways.

1.1 Identification of a Novel Biological Target

In the late 2000s, two key pieces of research helped to identify a novel target for the treatment of chronic pain. The first work centred around three consanguineous families in Pakistan, who were all found to share an inability to experience pain but were otherwise healthy.⁹ All members of the family were found to have suffered from fractures and frequent cuts and bruises but were otherwise healthy and considered of normal intelligence by both their families and physicians. The inability to experience pain was found to be caused by an autosomal-recessive trait associated with the gene *SCN9A*. This gene was found to code for the α -subunit of the voltage-gated sodium ion channel, $\text{Na}_v1.7$, which is strongly expressed in nociceptive neurons.¹⁰ Cox *et al.* showed that *SCN9A* is an essential requirement for nociception in humans, as the absence of the gene prevents the experience of pain.⁹

The second piece of research which pointed towards targeting the $\text{Na}_v1.7$ ion channel was from patients suffering from Erythromelalgia or “man on fire” syndrome.¹¹ This condition is characterised by a burning sensation and patients are often very sensitive to changes in temperature and pressure, especially those caused by mild exercise. There are currently no cures for this disease and treatment consists of applying cold presses and prescription of drugs for nerve problems such as the anti-epileptic gabapentin or tricyclic antidepressants such as amitriptyline.¹² Yang *et al.* showed that the increased sensitivity to pain was again caused by mutations to *SCN9A*, which this time caused abnormal excitability of sensory and sympathetic neurones.¹¹

Taken together, these two pieces of research suggest that the $\text{Na}_v1.7$ ion channel could be a new biological target for the treatment of chronic pain.

1.2 Voltage-Gated Sodium Ion Channels and Action Potentials

Nociceptive pain occurs as a result of the stimulation of peripheral nerves leading to the production of impulses which relay information to the brain. Nerve impulses, or action potentials, are short-lasting electrical excitation events, which are characterised by the sudden change in the membrane potential of the cell. Once stimulation reaches a threshold excitation level, the nerve impulse is carried along the axon (Figure 1.1).

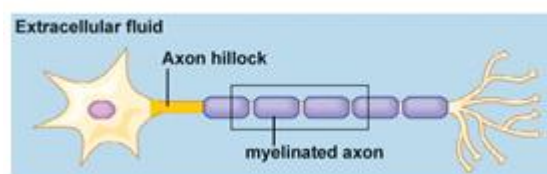


Figure 1.1: Schematic Diagram of a Nerve Cell¹³

Sodium and potassium gated ion channels are instrumental in the conduction of the nerve impulse along the neuron (Figures 1.2 and 1.3).

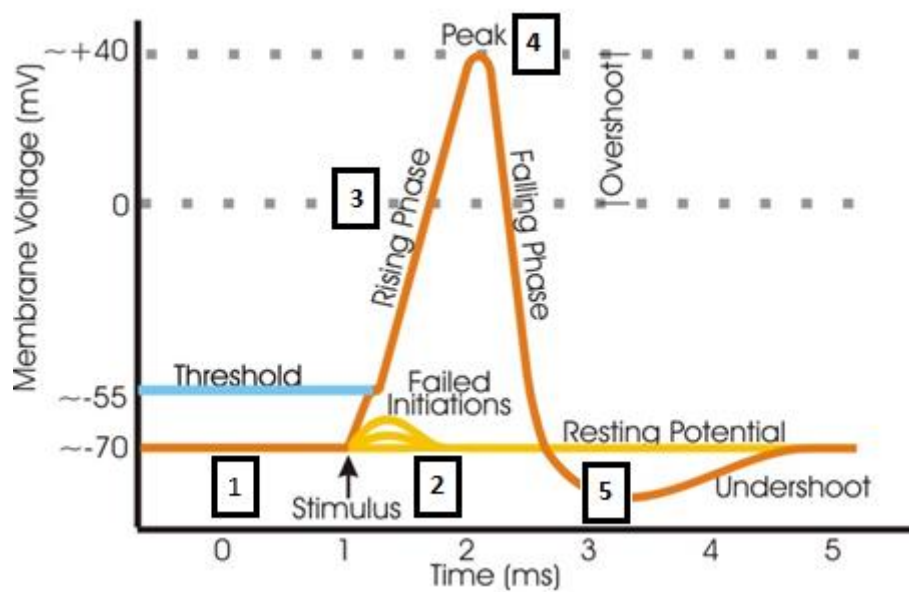


Figure 1.2: Schematic Diagram of an Action Potential¹⁴

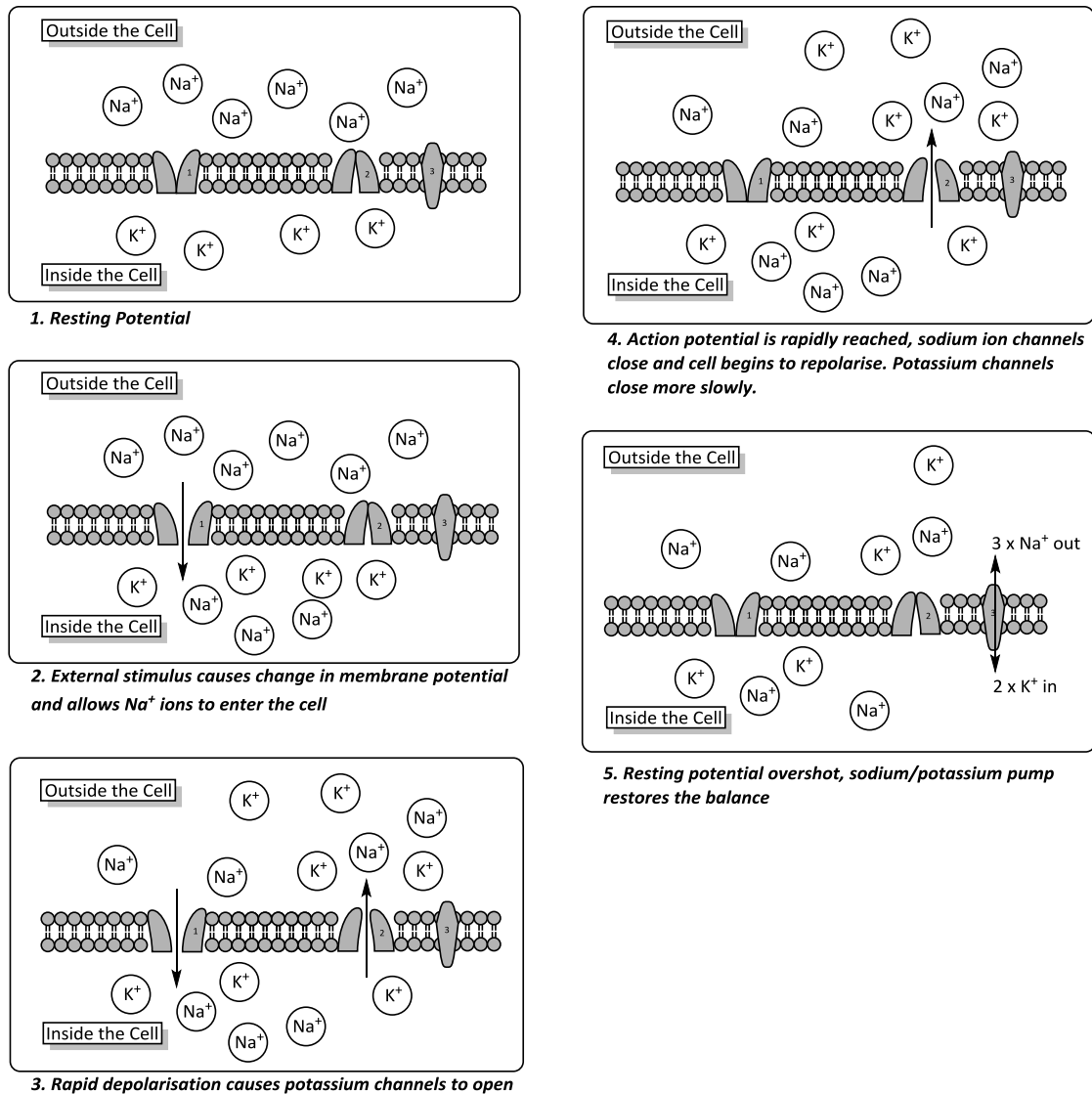


Figure 1.3: Schematic Diagram Showing the Stages of an Action Potential

The change in membrane potential causes a conformational alteration to occur in the sodium channels, which allows Na^+ ions to travel down the concentration gradient into the cell, leading to depolarisation of the neuron. This in turn leads to the opening of the potassium channels and further depolarisation of the cell. The peak of the action potential is rapidly reached and the sodium ion channels close, allowing the neuron to begin repolarising. The slower sequential closure of the potassium channels allows some K^+ ions to continue leaking out of the cell during this repolarisation period and the original resting potential is consequently overshoot. The sodium/potassium ion pump then begins to restore the balance by removing three sodium ions from the neuron and replacing them with two potassium ions, leading to the overall net negative charge within the neuron.

Sodium channels are responsible for most of the initial depolarisation events within a cell and are consequently of great interest as potential targets for analgesic drugs. The channels

consist of a main highly functionalised α -subunit, containing the active site, and three β -subunits (Figure 1.4). The latter modify the kinetics and voltage dependence of channel gating. The α -subunit consists of four pseudo-homologous domains (I – IV), each containing six transmembrane helices (S1 – S6). The S1 – S4 helices line the narrow outer entry to the pore, while S5 and S6 mark the inner, wider exit of the pore into the cell itself. In each of the domains, the S4 segment is highly conserved and is responsible for initiating channel activation in response to depolarisation of the membrane, using the positively charged amino acid residues located at every third position.¹⁵

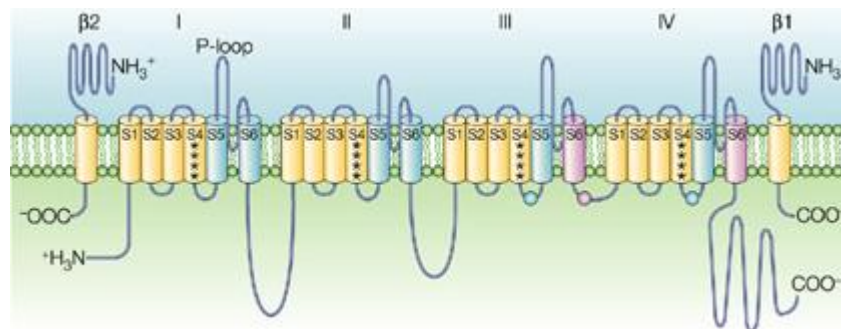


Figure 1.4: Schematic Diagram of a Sodium Channel¹⁶

The main α -subunit consists of four homologous repeats (I-IV). The cylinders represent probable transmembrane segments. The blue helical segments (S5 and S6) form the pore region. S4 (marked by asterisks) is the voltage sensor region. Pink S6 segments show the region of modulatory drug binding.

To date, nine mammalian isoforms of the sodium ion channel have been identified and functionally expressed (Table 1.2) and they have been shown to be identical in more than 50% of the amino acid sequence.

Channel Name	Channel Distribution	Physiological Function
Na_v1.1	Central Neurons Cardiac Myocytes	Action Potential Initiation Repetitive Firing Excitation/Contraction Coupling
Na_v1.2	Central Neurons	Action Potential Initiation Repetitive Firing
Na_v1.3	Central Neurons Cardiac Myocytes	Action Potential Initiation and Conduction Repetitive Firing
Na_v1.4	Skeletal Muscles	Action Potential Initiation and Conduction
Na_v1.5	Cardiac Myocytes	Action Potential Initiation and Conduction
Na_v1.6	Brain	Action Potential Initiation and Transmission in Central Neurons and Myelinated Axons
Na_v1.7	Dorsal Root Ganglion (DRG) Neurons Sympathetic Neurons Schwann Cells	Action Potential Initiation and Transmission in Peripheral Neurons Involved in Nociception
Na_v1.8	DRG Neurons Axons	Slowly Inactivates Na ⁺ Current in DRG Neurons
Na_v1.9	DRG Neurons Axons	Modulates Excitability of Cell Membrane Depolarisation

Table 1.2: The Mammalian Sodium Channel Isoforms⁵

Currently, there are no crystal structures available for any of the mammalian sodium ion channel isoforms. In 2001, Ren *et al.*¹⁷ published their work on the first sodium ion channel to be isolated and functionally expressed from a bacterium, which was shown to be the probable ancestor of vertebrate sodium and calcium channels.¹⁸ However it took another decade before Catterall *et al.*¹⁹ published their work on the crystal structure of the bacterial sodium ion channel isolated from *Arcobacter butzleri* (Figure 1.5).

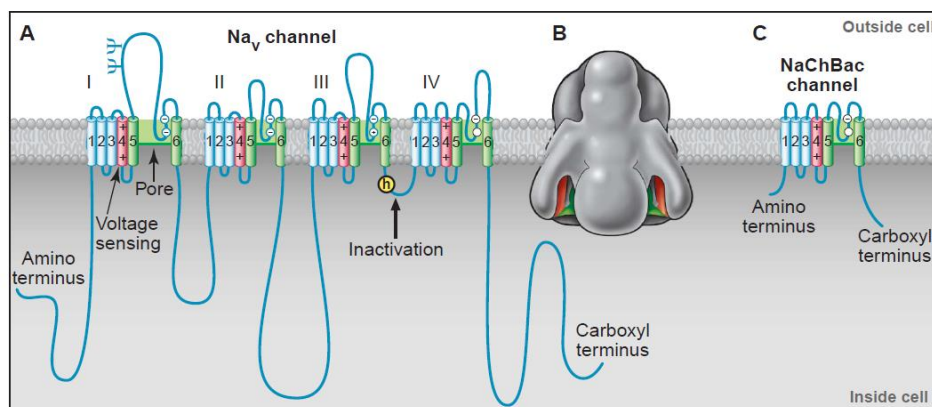


Figure 1.5: Comparison of Vertebrate and Bacterial Sodium Ion Channels¹⁸
 (A) schematic arrangement of the α -subunit of the mammalian Na_v1.2 ion channel (I-IV represent the homologous subdomains) (B) 3D structure of the sodium ion channel (C) bacterial voltage-gated sodium ion channel

A

B1

B2

1.3 Small Molecule Ion Channel Inhibitors

Chemical structures of compounds 1, 2, and 3 are shown. Compound 1 is a complex molecule featuring a benzimidazole core, a fluorene-like system, and a trifluoromethyl group. Compound 2 is a substituted benzamide derivative. Compound 3 is a substituted pyridine derivative with a hydroxyl group and a piperidine ring.

The first generation of sodium ion channel blockers tend to act on the highly conserved part of the α -subunit of the channel, which means that they show a lack of selectivity towards the nine subtypes and hence a relatively small therapeutic window.²⁰

25

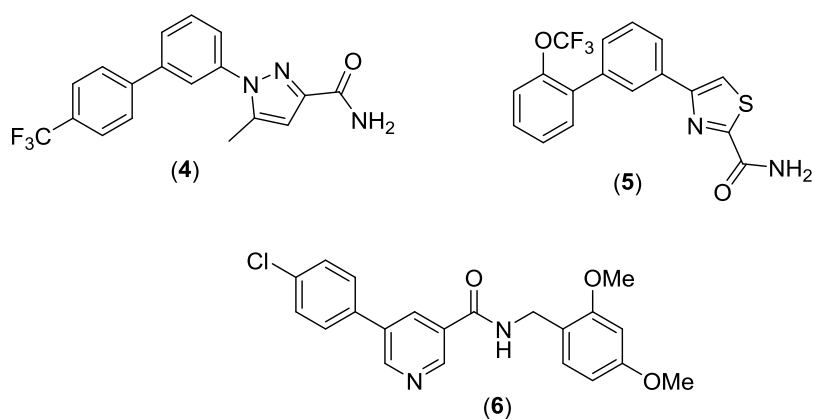


Figure 1.8: Generic Structures of Second Generation Sodium Ion Channel Blockers, biarylpyrazole (4), biarylthiazole (5) and A-803467 (6)

The first generation molecules show far better “drug-like” properties and their use in a clinical setting supports this observation. However, as their target is the highly conserved inner pore, it is unlikely that continuing research in this area will lead to any subtype-specific molecules. Whilst the second generation drugs confer some selectivity, it is at the expense of “drug-like” properties including molecular weight, lipophilicity, aqueous solubility and selectivity towards other targets such as hERG.²⁰ Currently, trials are ongoing with these compounds but none are available for use in a clinical setting.

Although work has focussed on these second generation molecules, some interesting research by Roberson *et al.* has shown that in some cases it is possible to make the generic channel blockers work in a more selective manner.²² They found that by injecting a combination of lidocaine (7) with its *N*-ethyl bromide derivative QX-314 (8), it was possible to produce long lasting pain relief for up to nine hours after injection in rats (Figure 1.9). It was reasoned that this occurred because the normally too hydrophilic QX-314 (8) could enter the nociceptor *via* permeation through the TrpV1 channel using lidocaine (7) as the TrpV1 activator. This more targeted approach for the delivery of drugs to the nociceptor would be particularly important in post-operative analgesia as it would decrease the requirement for the prescription of opiates and could allow for earlier hospital discharge and better pain control.²²

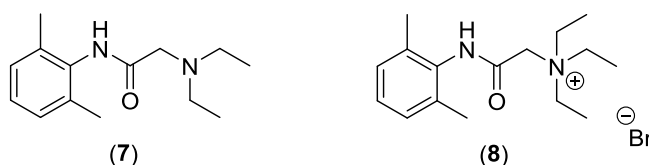


Figure 1.9: Structures of Lidocaine (7) and QX-314 (8)

By far the most famous of the sodium ion channel blockers is tetrodotoxin (TTX, 9) which is isolated from the venom of the puffer fish. In a seminal paper released in 1967,²³ Narahashi and Moore showed that TTX (9) reacted selectively with the sodium ion channels over

potassium and calcium channels. It was later found that this occurred through the guanidinium group, which physically blocks the extracellular opening to the pore, preventing sodium ions from entering the channel (Figure 1.10).²⁴ This is unusual when compared to other generic channel blockers such as lidocaine, which tend to block from inside the channel.²⁴

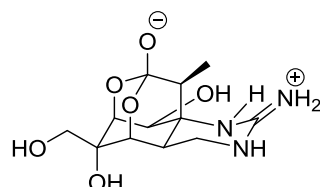


Figure 1.10: Structure of Tetrodotoxin (9)

It has subsequently been found that not all mammalian sodium ion channels are responsive to tetrodotoxin and in fact, sodium ion channels are often defined as TTX resistant (TTX-R) or TTX sensitive (TTX-S) (Table 1.3).

Channel Name	Channel Distribution	Tetrodotoxin (9) Sensitivity
Na_v1.1	Central Neurons Cardiac Myocytes	TTX-S
Na_v1.2	Central Neurons	TTX-S
Na_v1.3	Central Neurons Cardiac Myocytes	TTX-S
Na_v1.4	Skeletal Muscles	TTX-S
Na_v1.5	Cardiac Myocytes	TTX-R
Na_v1.6	Brain	TTX-S
Na_v1.7	Dorsal Root Ganglion Neurons Sympathetic Neurons Schwann Cells	TTX-S
Na_v1.8	DRG Neurons Axons	TTX-R
Na_v1.9	DRG Neurons Axons	TTX-R

Table 1.3: Summary of Sensitivity to Tetrodotoxin (9)²⁴

1.4 Toxins as Ion Channel Inhibitors

Although TTX (9) shows some selectivity towards individual subtypes, it again does not show enough selectivity to be of use in a clinical setting. However, there are many other toxins with improved properties; the diverse functions of ion channels have made them the target of many other toxins from a variety of sources including, but not limited to, snakes, insects, scorpions, spiders, sea anemones and the male duckbilled platypus.²⁵ Despite the vast array of animals and plants producing toxins, the active constituents act *via* one of two mechanisms: either through pore blocking (physically occluding the pore and preventing the passage of ions through the channel) or by acting as a gating modifier through binding to a region of the channel involved with the gating procedure.²⁵

1.4.1 Conotoxins

One of the most studied groups of toxins is the conotoxins. Isolated from the venom of marine snails of the genus *Conus*, these peptides form part of a complex mixture of biologically active components. The conotoxins represent the majority of the *Conus* venom peptide collection and are characterised by their multiple disulfide bonds. They have been shown to target a wide range of ion channels and receptors with unmatched potency and selectivity,²⁶ which has allowed them to become a significant area of research with hopes of finding new therapies and diagnostic tools.²⁷ Traditionally the conotoxins are classified according to their site of inhibition (Table 1.4) before being further divided into families based on disulfide framework and the species from which the peptide was isolated. However, as the number of classified conotoxins increases, it has become increasingly difficult to make such broad distinctions between classes as structural features appear to be conserved across subfamilies.²⁶

Name	Site of Inhibition
α	nicotinic acetylcholine receptors in nerves and muscles
δ	sodium ion channels
κ	potassium ion channels
μ	sodium ion channels
ω	calcium ion channels

Table 1.4: Classification of Conotoxins by Site of Inhibition

The α -conotoxins act on the nicotinic acetylcholine receptors (nAChRs) and represent the largest group of venom peptides isolated from cone snail venoms.²⁶ They have attracted widespread attention as their selectivity for muscle and neuronal nAChRs has allowed for characterisation of a number of different receptors and investigation of the structure-activity relationship (SAR). For example, α -GI acts as a potent antagonist of the muscle-type nAChR in both binding assays and animal-isolated tissues (**10**, Figure 1.11) and α -Iml (**11**) is of interest because it interacts with neuronal nAChRs and has potential for the treatment of pain (Figure 1.11).

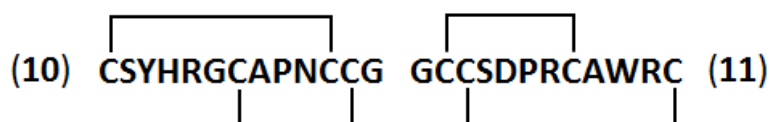


Figure 1.11: Structure of α -GI (**10**) and α -Iml (**11**)

The μ -conotoxins have been shown to compete with TTX (**9**) for the extracellular binding site and show preference for the TTX-S channels over the resistant ones.²⁸ They consist of 16-25 amino acids including six cysteine residues and have been shown to be highly selective for the Na_v1.4 ion channel.^{28,29} Like TTX, the μ -conotoxins are known to be pore-blockers, which

interact with the negatively charged residues associated with the selectivity filter of voltage-gated sodium channels.²⁶ For example, μ -GIIIA and μ -GIIIB (**12** and **13**, Figure 1.12), isolated from the venom of *Conus geographus*, are shown to have selectivity for the muscle sodium ion channels but have no appreciable effect on either nerve or brain channels.³⁰

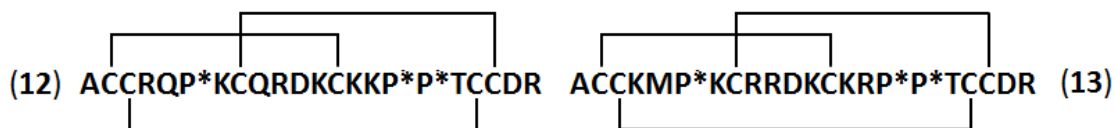


Figure 1.12: Structure of μ -GIIIA (**12**) and μ -GIIIB (**13**)
P* = 4-hydroxyproline

Despite the different targets for the δ -, κ - and ω -conotoxins, all three of these subtypes share the same secondary structural feature of conserved disulfide bond connectivity in the pattern 1-4, 2-5, 3-6. This gives a tightly bound structure in which two disulfide bonds form a loop through which the third disulfide bond passes, making them part of the inhibitory cystine knot (ICK) peptide family (**14**, Figure 1.13). An alternative connectivity to the ICK structure is exhibited by HwTx-II, which connects the disulfide bonds in the pattern 1-3, 2-5, 4-6 and is known as the disulfide-directed β -hairpin (DDH, **15**, Figure 1.13). The DDH motif was first identified by the King group and they postulated that it is a structural ancestor to the more complex ICK binding pattern (Figure 1.13).³¹

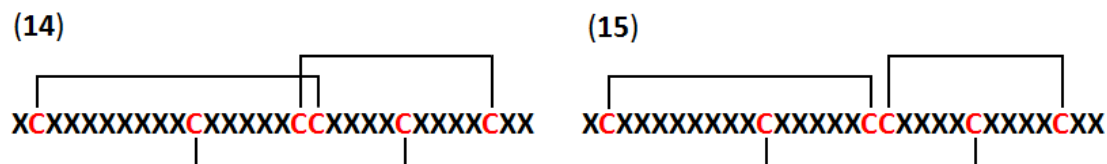


Figure 1.13: Comparison of the Structures of an ICK peptide (**14**) and a DDH peptide (**15**)

Currently, one ω -conotoxin is on the market for use as an analgesic in the treatment of severe and chronic pain: Ziconotide (**16**). Marketed as Prialt by Eisai Ltd, Ziconotide works by blocking the $\text{Ca}_v2.2$ channel, which prevents the release of pro-nociceptive neurochemicals and hence prevents pain (Figure 1.14). However, due to a lack of efficacy if delivered either orally or intravenously, this compound can only be administered intrathecally, which has a number of risks associated with it.



Figure 1.14: Structure of Prialt (**16**)

In addition to animals, it has been found that these small disulfide-rich peptides can also be produced by plants. In the last 20 years, a new class of compounds has emerged known as the cyclotides. These are comprised of approximately 30 amino acids and, as well as the six

highly conserved cysteine residues observed in the conotoxins, the peptides display head-to-tail cyclisation to give a fully cyclised backbone to the cysteine knot structure. The peptides are divided into two categories; in about half of the peptides, a cys-pro bond is present, which gives the impression of a twist within the circular backbone. These peptides are known as Möbius cyclotides. Conversely, those without the twist are known as Bracelet cyclotides (Figure 1.15).

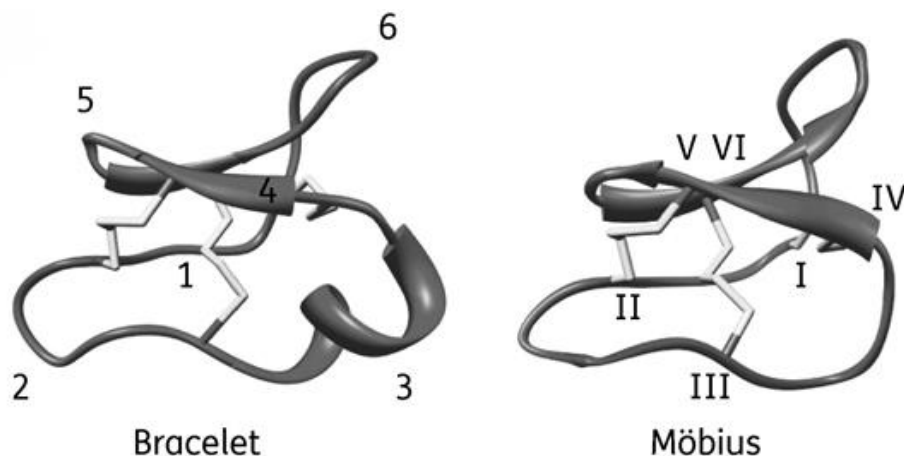


Figure 1.15: Structure of Bracelet and Möbius Cyclotides³²

The first of the cyclotides to be structurally identified was kalata-B1 (**17**),³³ which was isolated from the tropical African plant *Oldenlandia affinis* and used in local medicine to accelerate labour and childbirth (Figure 1.16). Other cyclotides include the circulins, which are used as anti-HIV agents and the neurotensin antagonist cyclopsychotride.³⁴



Figure 1.16: Structure of Kalata-B1 (**17**)³³

Head-to-tail cyclisation has been shown to increase the stability of a peptide as it prevents degradation by cellular exopeptidases and thus increases physiological stability *in vivo*.³⁵ This has led to many attempts to cyclise peptides using a variety of methods including solution phase peptide bond formation using HOAt and PyAOP,³⁶ use of successive N to S acyl shifts³⁷ and genetic code reprogramming methods.³⁵

1.4.2 Other Multiply-Bridged Peptides

In 2013, the SSm6a peptide (**18**, Figure 1.17) was isolated from the venom of a centipede. It was found to be 150-fold more selective for the Na_v1.7 ion channel over all other subtypes apart from Na_v1.2, with which it showed a 32-fold selectivity, with an IC₅₀ value of 25 nM.³⁸ The peptide contains six cysteine residues, which are linked in an unusual combination of 1-5,

2-4, 3-6 and is predominantly α -helical in structure. The promising IC_{50} value and selectivities indicate that this peptide could be an interesting lead compound for the development of future analgesics but, with 46 residues, it will be too large to cross the blood-nerve barrier in its current form.

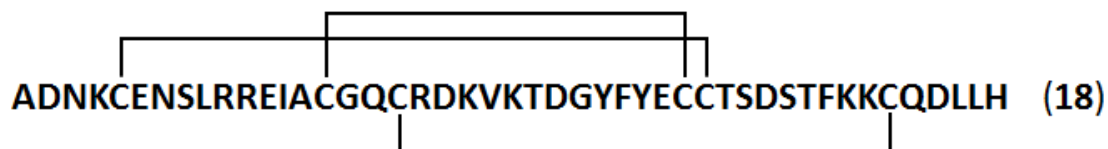


Figure 1.17: Structure of *Ssm6a* (18)

1.4.3 Toxins Isolated from Tarantula Venoms

As has been previously mentioned, the unique ICK structure of the cyclotides and conotoxins has led to the discovery of the first real examples of ion channel selectivity. This has been exemplified by the spider toxins; in the past decade, a number of different toxins isolated from the venom of tarantulas have been shown to have selectivities for specific ion channels. These include, but are not limited to, GsMTx-4 (19, Figure 1.18), which is isolated from the Chilean Rose Spider^{39,40} and is an inhibitor of the mechanosensitive TRP channels and HwTx-IV (20, Figure 1.18), which has an IC_{50} value of approximately 500 nM against the $Na_v1.7$ ion channel.⁴¹

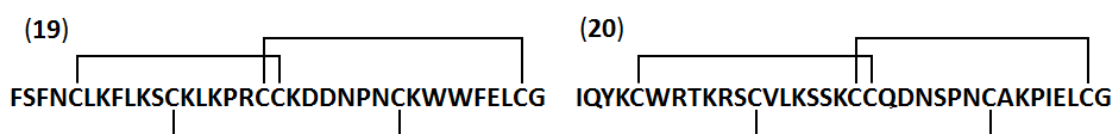


Figure 1.18: Structures of *GsMTx-4* (19) and *HwTx-IV* (20)

In 2007, Schmalhofer *et al.*⁴² published their work on a toxin isolated from the Peruvian Green Velvet Tarantula, *Thrixopelma pruriens*. The peptide, known as ProTx-II (22, Figure 1.19), was shown to have the highest selectivity for the $Na_v1.7$ ion channel to date ($IC_{50} = 0.3$ nM) and was 100-fold more selective for this channel than the other subtypes *in vitro*. The peptide was first isolated from tarantula venom by Middleton *et al.*,⁴³ along with another peptide named ProTx-I (21, Figure 1.19). Upon publication, these peptides were the first known examples of tarantula toxins which acted by inhibiting sodium channel activation.⁴³

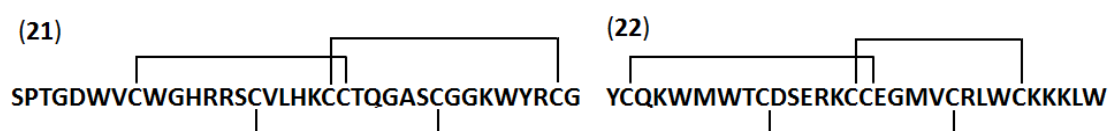


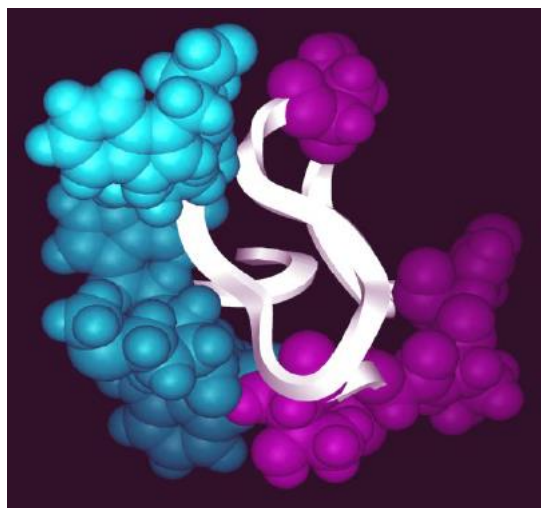
Figure 1.19: Structures of *ProTx-I* (21) and *ProTx-II* (22)

ProTx-I has been shown to be active against a number of sodium ion channels including $Na_v1.8$ ($IC_{50} = 27$ nM) and $Na_v1.2$, $Na_v1.5$, $Na_v1.7$ (IC_{50} values all 50 – 100 nM). Most

interestingly, it can also be used to selectively bind to the Ca_v3.1 channel (IC₅₀ = 0.2 μM) over the Ca_v3.2 channel, allowing for distinction between the two subtypes.⁴⁴

1.5 ProTx-II as an Inhibitor of Na_v1.7

Middleton *et al.*⁴³ characterised both ProTx-I and ProTx-II as members of the ICK family through a series of enzymatic digestion experiments with analysis of the products *via* mass spectrometry (these are discussed further in Chapter 3). However, it was not until 2014 that the structure of ProTx-II was finally confirmed using solution-phase NMR.⁴⁵ Prior to this, the only structural information available came from some homology modelling carried out by the Blumenthal group,⁴⁶ who studied the interactions of ProTx-II on the Na_v1.5 channel. Using the Protein Data Bank coordinates for another ICK peptide HpTx-2, which is isolated from the venom of the *Heteropoda venatoria* spider and is shown to act against the K_v4.2 channel,⁴⁷ the group performed *in silico* mutagenesis techniques to create the bioactive surface of ProTx-II (Figure 1.20).



Peptide Sequences

HpTx-2: DCGKLFSGCDTNADCCEGYVCRLWCKLDW

ProTx-II:

YCQKWMWTCDSERKCCEGMVCRLWCKKKLW

Figure 1.20: Homology Model of ProTx-II (**22**)⁴⁶

Key: Essential Residues in Cyan, Non-Essential Residues in Magenta

Their results show that the bioactive surface contains both hydrophobic and cationic residues and that the peptide can bind phospholipids. The peptide has been shown to modify the action of both sodium and calcium voltage ion channels but not potassium channels by inhibiting peak current and shifting the voltage dependence of activation to more depolarised potentials.^{43,48} This led to the belief that ProTx-II (**22**) bound to the “site 4” binding site on the sodium channel, namely to part of domain II between segments 3 and 4. To investigate this possibility, the group created 16 mutants of the Na_v1.5 channel but found that no change

in binding was observed with these mutants and that pre-saturation with TTX (**9**) also had little effect. From this result, it was possible to conclude that ProTx-II (**22**) does not act as a pore blocker in the Na_v1.5 channel and that it has an as yet unidentified binding site, which is not characteristic of other known channel activators. As the peptide has the ability to bind to liposomes,⁴⁸ it is possible that the toxin may partially insert into the membrane as part of its mode of action. So far, it has been established that ProTx-II (**22**) does not bind in the same manner as other ICK peptides to sodium ion channels. The unique, undefined binding site accounts for its selectivity towards the Na_v1.7 ion channel and provides an interesting avenue for further research.

Continuation of this work by Park *et al.*⁴⁵ has helped to identify which residues are important for binding to the Na_v1.7 ion channel, as well as highlighting certain structural motifs. The NMR structure showed that a short β -sheet region was present and that the C-terminus was conformationally labile (Figure 1.21).

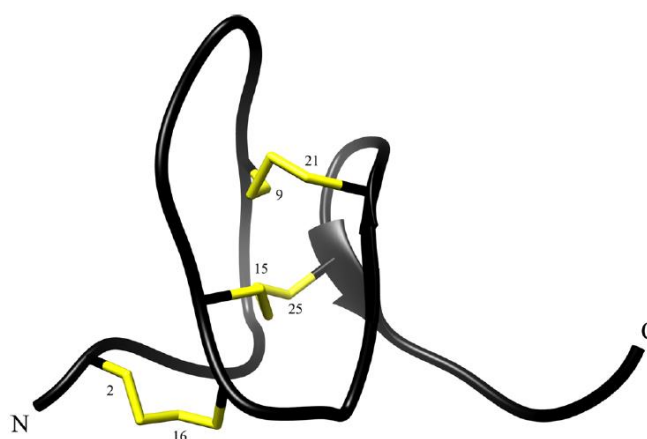


Figure 1.21: Solution NMR Structure of ProTx-II (**22**)⁴⁹

As well as elucidating the NMR structure, the group produced a series of analogues of ProTx-II to investigate effects on potency and selectivity. They first compared the binding of ProTx-II to PaTx-I (a structurally similar peptide with a different C-terminus, Figure 1.22) and found that whilst the IC₅₀ value for PaTx-I against Na_v1.7 was quite high (IC₅₀ = 420 nM against 1 nM for ProTx-II), when the PaTx-I tail is replaced with the KKKLW motif found at the C-terminus of ProTx-II, the IC₅₀ value is comparable (Table 1.5, Entries 1 – 3).

Peptide Sequences

ProTx-II: YCQKWMWTCDSERKCCEGMVCRLWCKKKLW

PaTx-I: YCQKWMWTCDSARKCCEGLVCRLWCKKII

VsTx-2: YCQKWMWTCDEERKCCEGLVCRLWCKKKIEEG

JzTx-12: YCQKWMWTCDSERKCCEGYVCELWCKYNL

Figure 1.22: Structures of the Peptides Used in the Investigations

Entry	Sequence	IC ₅₀ against Na _v 1.7 (nM)
1	ProTx-II	1
2	PaTx-I	420
3	PaTx-I (ProTx-II tail)	1
4	VsTx-2	9300
5	VsTx-2 (ProTx-II tail)	290
6	JzTx-12	1500
7	JzTx-12 (ProTx-II tail)	Not active

Table 1.5: Summary of Results from Park et al.⁴⁵

To see if only the tail section was important in binding, the group also investigated the effect of adding the KKKLW motif to two other peptides, both of which show only modest levels of activity with Na_v1.7. Whereas the activity of VsTx-2 was found to increase (Table 1.5, Entries 4 and 5), the activity of JzTx-12 decreased with this modification (Table 1.5, Entries 6 and 7), showing that the final motif is not the only important part for binding. The group found that Ser-11, Glu-12, Tyr-19 and Arg-22 are also important for conferring potency in the molecule. Finally, their focus on C-terminal modifications also showed that the preferred conformation for potency is the α -helix and that by changing the carboxylic acid group, it was possible to increase potency still further in the order:



The last of the compounds in fact forms the most potent Na_v1.7 ion channel selective compound to date (**23**, Figure 1.23) with an IC₅₀ value of just 42 pM.

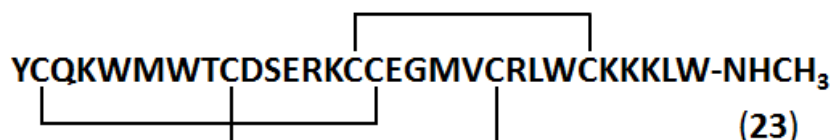


Figure 1.23: Structure of ProTx-II-NHCH₃ (**23**), the most potent Na_v1.7 selective compound to date

The high potency and selectivity of ProTx-II (**22**) make it an ideal lead candidate for the treatment of chronic pain. However, peptides lack oral bioavailability as a consequence of their susceptibility to degradation in the intestines and blood, and inefficient transport across the intestinal wall.^{28,50} In addition, disulfide bonds present an extra level of difficulty due to their susceptibility to reduction in extracellular environments including the blood.⁵¹ For example, they are particularly sensitive to glutathione, which is present in the blood, and disulfide bond isomerases, which can lead to oxidative refolding of the peptide giving unwanted conformations.⁵⁰ Craik and co-workers have shown that all three disulfide bonds are required in cyclotides, as well as the head-to-tail cyclisation of the backbone, in order to maintain activity, and that loss of the innermost disulfide bond causes inactivity.^{33,34}

1.6 Disulfide Bond Replacements

With these problems in mind, considerable effort has been directed towards the investigation into disulfide bond replacements which are not susceptible to reduction or oxidative refolding.

1.6.1 Replacement of a Disulfide Bond with a Diselenide Bond

One of the first attempts to solve this problem was by Alewood and co-workers⁵¹ who investigated replacing disulfide bonds with isosteric but non-reducible diselenide bonds, through the introduction of Boc-L-Sec(MeBzl)-OH into a solid phase synthetic strategy. Upon cleavage from the resin with HF, this method has the advantage of using mild aerobic oxidation conditions to form the diselenide bond from the deprotected selenocysteines. Their work focussed on the synthesis of analogues of the conotoxin Iml (**11**), which is a potent antagonist of the neuronal nicotinic acetylcholine receptor (Figure 1.24).



Figure 1.24: Structure of WT-Iml (**11**)

They showed that crosslinking between selenocysteine and cysteine was disfavoured, meaning that when using a mixture of the two amino acids, the correct connectivity was always observed. In addition they showed that when all four cysteines were replaced by the selenocysteine analogue, the correct connectivity was still observed, indicating that the same factors controlling the formation of disulfide bonds are important for the formation of the diselenide (Figure 1.25).⁵¹

Having shown that the connectivity was not affected by the change in amino acid, the group next compared the stability of the peptides in human blood plasma. Whereas significant scrambling was observed in WT-Iml, no scrambling was observed in the isomer in which all four amino acids had been replaced by selenocysteine under the same conditions. Perhaps the more surprising result however, was that when just one pair of cysteines was replaced with selenocysteine, scrambling was still not observed, which the group attributed to a difference in redox potential between cysteine and selenocysteine. Interestingly, the group subsequently found that replacement with selenocysteine slightly improved potency.⁵² This was attributed to a change in hydrophobicity upon selenocysteine replacement, which, combined with small changes in bond length and torsion angle, was thought to increase the hydrophobic interactions within the binding site.

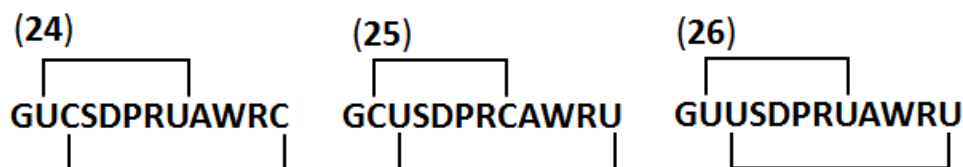


Figure 1.25: Selenocysteine analogues of lml, where U = selenocysteine

1.6.2 Replacement of Sulfur Atoms with Carbon Atoms

As well as replacement by selenocysteine, work has also been carried out by Norton and co-workers⁵³ to form a dicarba-bridged analogue of lml by using ring-closing metathesis on-resin (Figure 1.26). In their strategy, one disulfide bond is replaced by an unsaturated carbon-carbon bond. Unlike the diselenide bond, which is slightly larger than the disulfide bond, the dicarba bridge is slightly shorter (2.02 Å and 1.34 Å respectively). By using an unsaturated double bond, it was possible to form two different isomers of the dicarba-lml with either cis or trans configuration. The work showed that whilst the cis conformation showed similar activity to the native WT-lml, no activity was observed for the trans isomer, nor was it found to adopt a single stable conformation in solution. It is not possible to give a general prediction for whether the cis or trans dicarba-analogue of a peptide would give the greater activity, meaning that experiments would need to be carried out on a system-by-system basis. As an alternative to this problem, the paper suggests that use of the fully saturated version could infer a greater flexibility in the structure and would negate the need to form both the cis and trans isomers of the peptide.

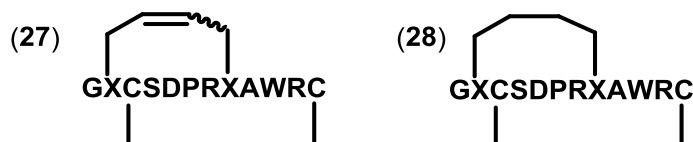


Figure 1.26: Unsaturated (27) and Saturated (28) Dicarba-analogues of lml

Ring-closing metathesis has also been used by Vederas and co-workers, who showed that by replacing the disulfide bond in a type IIa bacteriocidin with an unsaturated carbon-carbon bond, the structural integrity of the peptide was maintained and only a modest drop in antimicrobial activity was observed.⁵⁴ Similarly, when they formed carbocyclic analogues of oxytocin and the antagonist atosibin, they found a slight decrease in activity but an increased half-life in placental tissue.⁵⁵

Elaridi *et al.*⁵⁶ furthered this work by combining on-resin ring closing metathesis using allyl glycine with rhodium catalysed hydrogenation of prenyl glycine. By using allyl and prenyl glycine, the group found they could control the diastereoselectivity of the reactions to give the desired products, with no formation of the mismatched bonds observed (Figure 1.27).

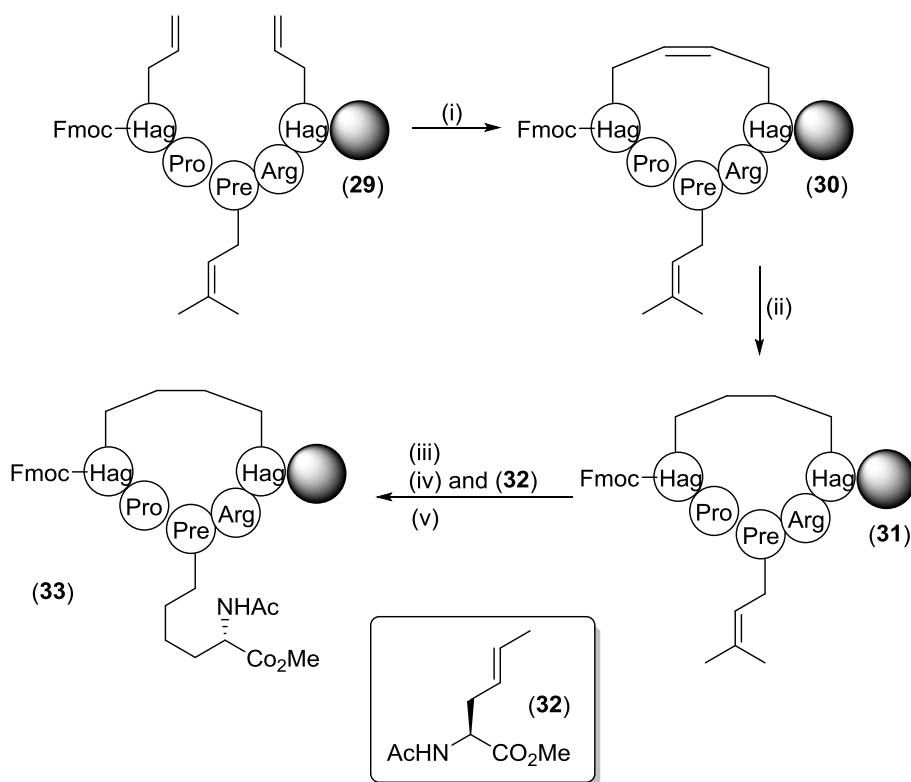


Figure 1.27: Incorporation of Ring Closing Metathesis and Hydrogenation into an SPPS Strategy

Reagents and Conditions: (i) 40 mol% 2nd Gen Grubbs, CH₂Cl₂, LiCl, DMF (ii) Rh(I)(PPh₃)₃Cl, H₂ CH₂Cl₂, MeOH (iii) 40 mol% 2nd Gen Grubbs, C₄H₈, CH₂Cl₂, LiCl, DMF (iv) 40 mol% 2nd Gen Grubbs, CH₂Cl₂, LiCl, DMF (v) Rh(I)(PPh₃)₃Cl, H₂ CH₂Cl₂, MeOH

Firstly, the allyl groups were reacted selectively with the Grubbs catalyst to give the unsaturated ring (**30**). This was then be selectively reduced using a rhodium-catalysed hydrogenation reaction to give (**31**). Preparation of the prenyl group for the second ring-closing metathesis reaction, followed by reaction with (**32**) gave the unsaturated chain product, which was again reduced using rhodium to give the desired product (**33**). The remarkable result in this synthesis was the selectivity: the prenyl group did not react with Wilkinson's catalyst and no mixed metathesis or any other unwanted side products are formed, meaning there was complete control over the ring formation to give the desired product. However, the major limitation to this work was that it is not possible to perform ring-closing metathesis rings on sterically hindered structures,⁵⁵ meaning that this could prove problematic for any system where neighbouring amino acids have bulky side chains or in particularly tightly bound structures, such as the ICK peptides.

1.6.3 Replacement of a Disulfide Bond with Lactam Ring Formation

As an alternative to ring-closing metathesis, Hargittai *et al.*⁵⁷ replaced the disulfide bond with a lactam ring through the formation of an amide bond on-resin. By using orthogonal protecting groups (allyl and alloc) they could selectively deprotect the amino acids and form

the desired product (Figure 1.28). For their model system, they used the α -conotoxin SI, which is an agonist against the nicotinic acetylcholine receptor.

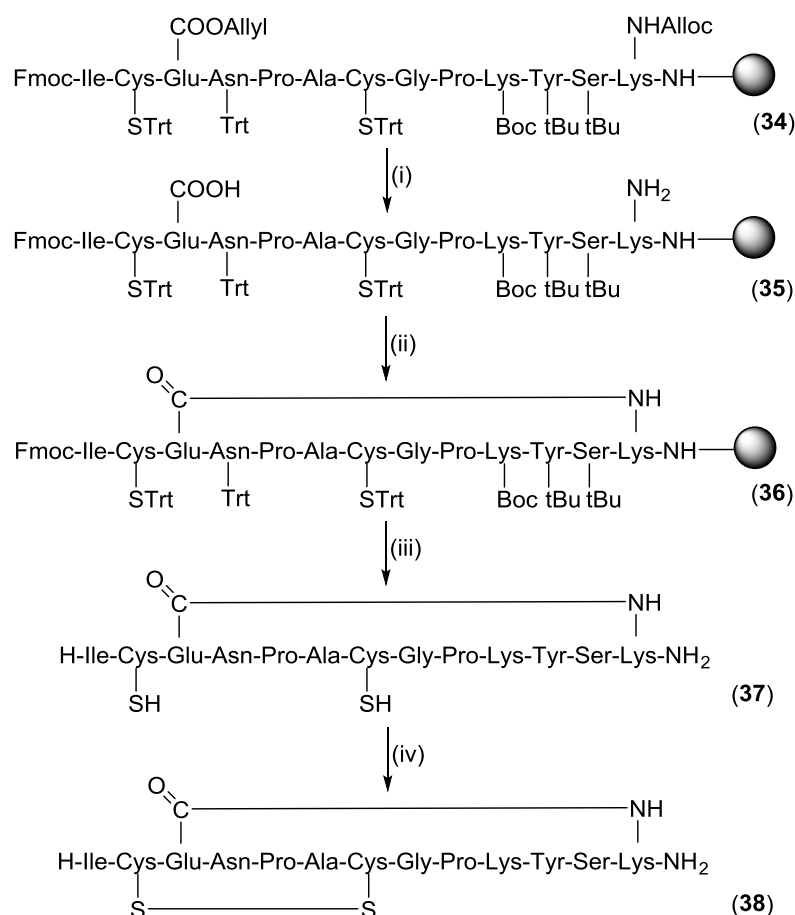


Figure 1.28: Example Orthogonal Synthesis of ST Analogue Using On-resin Lactamization
 Reagents and Conditions: (i) $\text{Pd}(\text{PPh}_3)_4$, NMM, HOAc, DMF (ii) HATU, NMM, DMF
 (iii) piperidine, DMF, then EDT (iv) DMSO, Na_2HPO_4

The group found that formation of the smaller loop (Cys 2 – Cys 7) by on-resin lactamization occurred three times faster than formation of the larger loop (Cys 3 – Cys 13). However, whereas both orientations of the lactam in the large ring showed significant binding in the radioligand binding assay, neither lactam analogue of the smaller ring was found to have any activity. Replacement of a disulfide bond with a lactam ring gives rise to a large change in the electronics of the compound and could perhaps have a detrimental effect on the potency of the compound, as well as still being susceptible to breakdown *in vivo* by peptidases, meaning this disulfide bond replacement may have limited utility.

1.6.4 Replacement of a Disulfide Bond with Cystathionine

Although these replacements have been shown to have reasonable reactivity in some cases against their original disulfide counterparts, they all show vastly differing electronics to a disulfide bond and neither the ring-closing metathesis nor lactamization reactions give a true bioisosteric analogue. However, as early as 1991, research was published showing the

replacement of a disulfide bond by a cystathionine linker,⁵⁸ which can be thought of as a disulfide bond in which one sulfur has been replaced by a carbon atom (Figure 1.29).

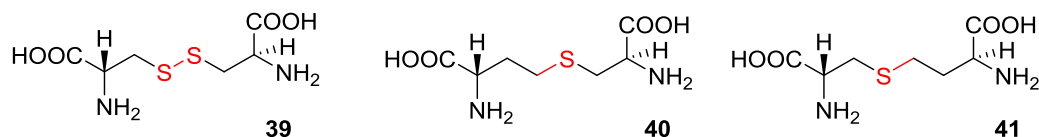


Figure 1.29: Structure Comparisons **39** – Disulfide Bond, **40** – Cystathionine Bond, Regioisomer 1, **41** – Cystathionine Bond, Regioisomer 2

Cui *et al.*⁵⁹ formed a series of analogues of Tachyplesin-1 (**42**, Figure 1.30), a peptide known to have high antimicrobial activity. The peptides formed have one or more S atoms replaced with carbon to form a series of analogues (Figure 1.30).

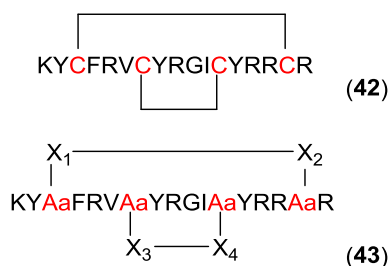


Figure 1.30: Tachyplesin-1 (**42**) and Generic Structural Analogues (**43**) (X = S or C)

The most interesting result came from the replacement of just one sulfur atom with a carbon; that is, the peptide contained one cystathionine and one disulfide link. In this case, the activity was the same or only slightly reduced with respect to the original peptide. The group found that as the number of carbon atoms replacing sulfurs increased, the minimal inhibitory concentration (MiC) also increased until, when all four sulfurs were replaced with carbon atoms, the compound was up to 16-fold less potent than the parent peptide. Computer modelling showed that this was as a result of a dramatic variation in torsional strain, which caused large structural distortions in the peptide structure.

In 2011, van der Donk and co-workers⁶⁰ published their work on cystathionine-containing analogues of compstatin, a 13 amino acid peptide known to inhibit complement activation and containing one disulfide bond. They showed that the position of the sulfur had serious consequences in activity; whilst the δ -Cth analogue (**45**, Figure 1.31) maintained binding and inhibition properties, all activity was lost in the γ -Cth analogue (**44**, Figure 1.31).

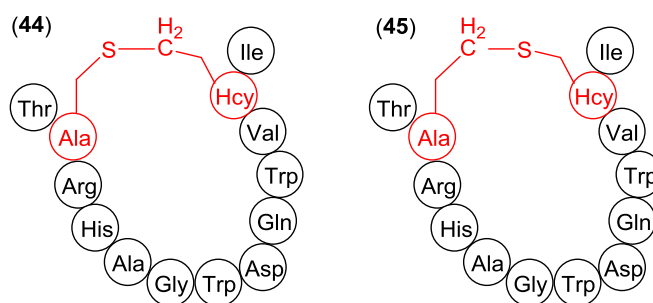


Figure 1.31: γ - (**44**) and δ -Analogues (**45**) of Compstatin (HCy = cystathionine)

The most interesting result however was that the reduction of the disulfide bond had a far more pronounced effect on potency than substitution of cystathionine or the subsequent oxidation of the sulfur, showing that cystathionine is a good replacement in this system. Finally, in addition to their work with replacement of disulfide bonds with the diselenide equivalent in Iml, Alewood and co-workers also experimented with a cystathionine replacement.⁶¹ They produced analogues in which each disulfide bond in turn was replaced by the cystathionine linker before forming the dual cystathionine analogue. These were shown to be structurally homologous by NMR and revealed no or very modest losses in biological activity (Figure 1.32).

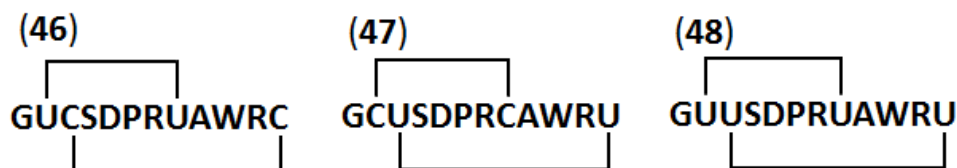


Figure 1.32: Cystathionine-Containing analogues of Iml (U = cystathionine)

1.6.5 Replacement of a Disulfide Bond with Lanthionine

The great advantage of using a thioether linkage in place of the disulfide bond is that these compounds tend to be far more stable in reducing environments including the blood.^{50,51,60} Whilst some work has been done on the replacement of a disulfide bond with the isosteric cystathionine, little work has been published on the replacement with lanthionine (Figure 1.33).

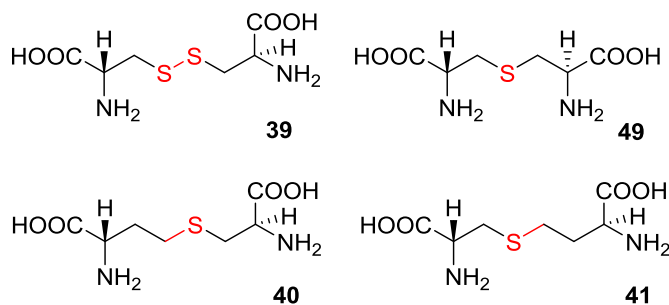


Figure 1.33: Structure Comparisons **39** – Disulfide Bond, **49** – Lanthionine Bond, **40** – Cystathionine Bond, Regioisomer 1, **41** – Cystathionine Bond, Regioisomer 2

Replacement of a disulfide bond with lanthionine has the dual advantage of preventing ring opening by disulfide bond cleavage and subtly changing the size of the ring to allow investigation into the structure-activity relationship between the peptide and the binding site. Previous work by Goodman and co-workers,⁶² has shown that lanthionine analogues of sandostatin (**52** and **53**), itself a clinically used analogue of somatostatin, were found to have increased selectivity to the SSTR5 receptor with respect to the parent peptide sandostatin (Figure 1.34).

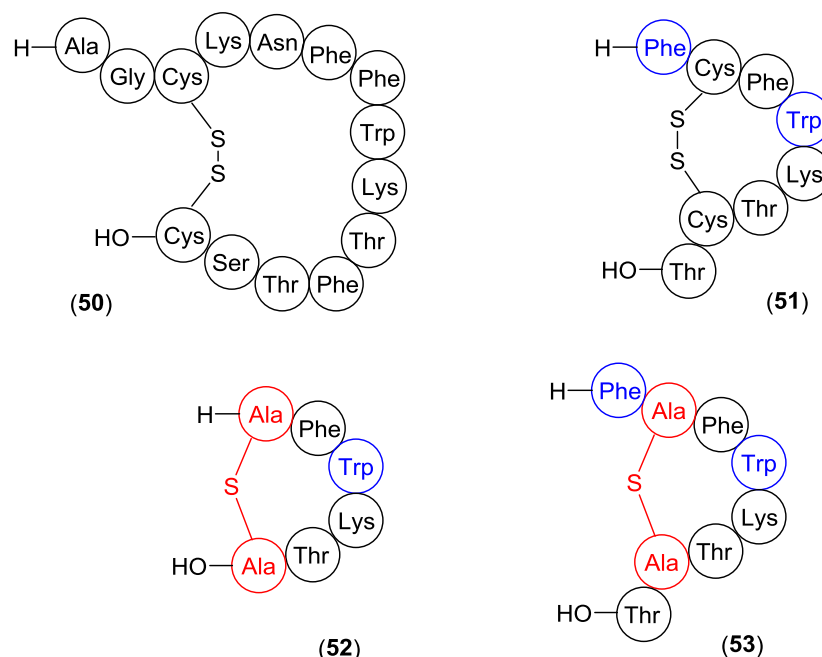


Figure 1.34: Structure of Somatostatin (**50**), Sandostatin (**51**) and Examples of the Goodman Lanthionine-Containing Analogues (**52** and **53**) (blue indicates a D-amino acid)

The analogues showed a weaker inhibition of growth hormone release but showed an increased stability against enzymatic degradation and an increased half-life *in vivo*. In this work, the lanthionine bridge was formed on-resin, which lead to some racemisation at the stereocentre.

1.7 Lanthionine and the Lantibiotics

Lanthionine is found in a group of peptides known as the lanthionine-containing antibiotics, or lantibiotics. The most studied of the lantibiotics is Nisin, a 34 amino acid peptide used as a food preservative (**54**, Figure 1.35). It has been shown to bind with lipid II and thus interferes with cell wall biosynthesis in bacteria.^{63,64} This novel mode of action has led to a lot of research in the area with the aim of developing a potential new class of antibiotics.

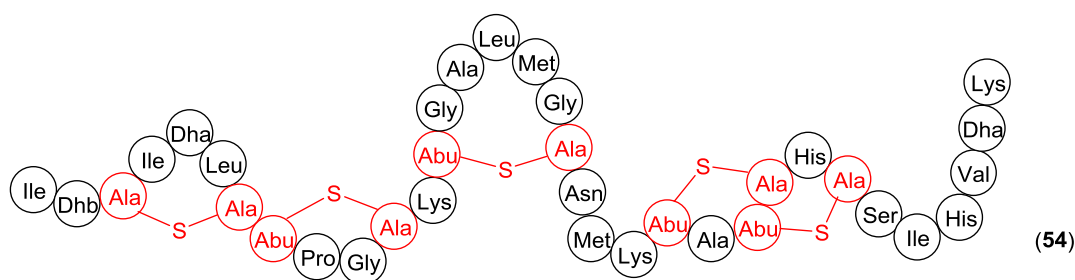


Figure 1.35: Structure of Nisin (**54**)

In nature, the lanthionine bridges are made during a complex post-translational modification procedure involving, amongst other reactions, Michael addition of a cysteine to a dehydroalanine residue.⁶³ In the laboratory, a number of different approaches have been used to synthesise lantibiotics; a lot of work has focussed on the use of protein engineering to generate these thioether bridges in mutant lantibiotics using cell culture.^{65,66} In addition to this, enzymatic work pioneered by Levengood *et al.*^{67,68,69} has shown that it is possible to synthesise lantibiotic analogues containing non-proteinogenic amino acids by harnessing the synthetase enzymes involved in lantibiotic synthesis, which are able to accept a wide range of substrates for processing.

1.7.1 Chemical Syntheses of Lanthionine

Chemists have also tried to synthesise lanthionine by mimicking the post-translational modifications observed in nature. Work by Bradley and co-workers⁷⁰ has shown that the thioether bridge can be formed by adding a protected cysteine (**56**) to a protected dehydroalanine (**55**) in the presence of a catalytic amount of cesium carbonate to give lanthionine (**57**, Figure 1.36).

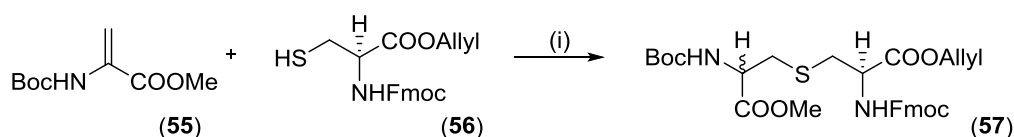


Figure 1.36: Synthesis of Lanthionine via Michael Addition

Reagents and Conditions: (i) Cs_2CO_3 , MeCN

Unfortunately, unlike in nature, complete stereochemical control is not achieved and a mixture of diastereoisomers is observed. As an alternative, the first reported synthesis of lanthionine^{69,71} uses the reaction between a β -chloroalanine (**58**) and cysteine (**59**, Figure 1.37).

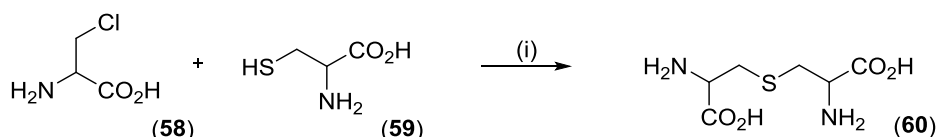


Figure 1.37: Synthesis of Lanthionine via Chloroalanine (**58**) Reaction with Cysteine (**59**)

Reagents and Conditions: (i) KOH (aq), 50 °C

However, the strongly basic conditions could result in elimination to form the dehydroalanine, which would again lead to a mixture of diastereoisomers in the product. This is also observed when using the carbamate protected iodoalanine, which produces the desired product with a diastereomeric excess of 70% (Figure 1.38).⁷²

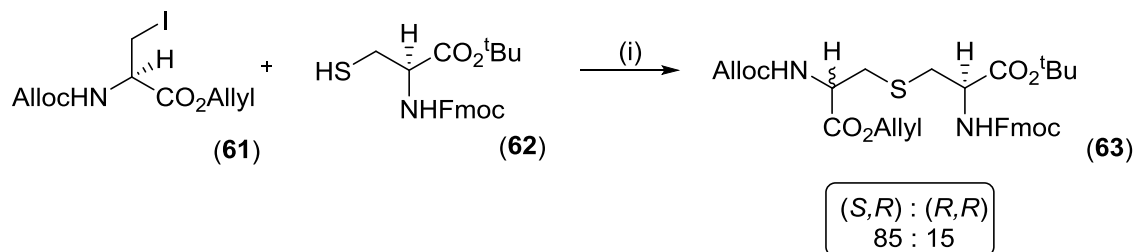


Figure 1.38: Synthesis of Lanthionine (**63**) via Iodoalanine (**61**) Reaction with Cysteine (**62**)
Reagents and Conditions: (i) Cs_2CO_3 , DMF

As carbamate protecting groups are so prone to elimination to give dehydroalanine, other approaches using different protecting groups have been trialled. Zhu and Schmidt⁷³ have shown that by using a milder base with the bromoalanine derivative (**64**), it is possible to form the desired product without formation of the dehydroalanine, which results in complete stereochemical control (Figure 1.39).

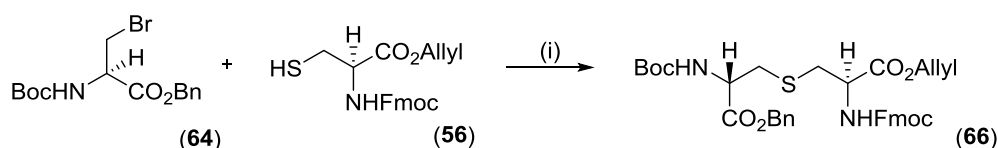


Figure 1.39: Synthesis of Lanthionine via Bromoalanine (**64**) Reaction with Cysteine (**56**)
Reagents and Conditions: (i) NaHCO_3 (pH 8.5), tetrabutylammonium hydrogen sulfate, EtOAc

Similarly, instead of the Boc protecting group, the trityl group can also be used. However, this protecting group comes with a different challenge as, although the formation of dehydroalanine is disfavoured, the formation of the corresponding aziridine is now favoured (Figure 1.40).^{74,75}

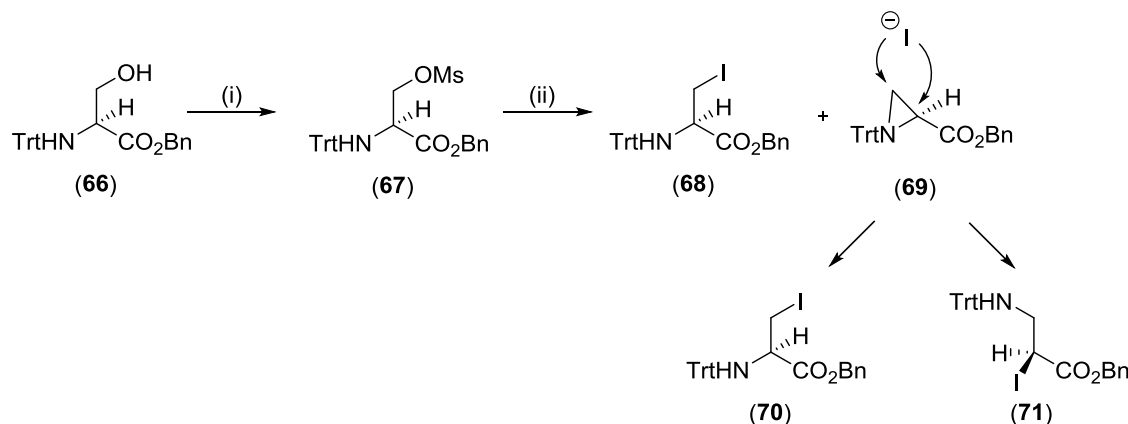


Figure 1.40: Formation of Aziridine (**69**)
Reagents and Conditions: (i) MeSO_2Cl , Et_3N (ii) NaI, acetone

The aziridine (**69**) then has two possible points of attack available at which the iodine can add, leading to the formation of two regioisomers (**72** and **73**). Upon reaction with cysteine, this then leads to the formation of the desired product as the minor isomer, with the major product being the nor-lanthionine analogue (**73**, Figure 1.41).

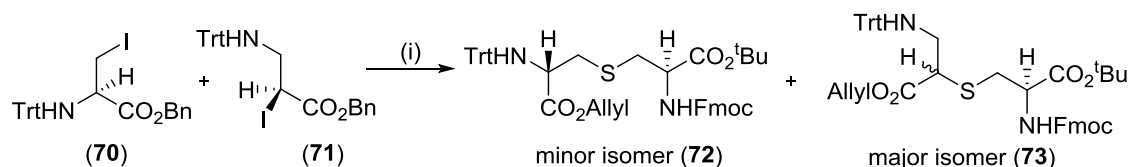


Figure 1.41: Synthesis of Lanthionine (**72**) and Nor-Lanthionine (**73**)

Reagents and Conditions: (i) Fmoc-Cys-O^tBu (**62**), Cs₂CO₃, DMF

To prevent the formation of the unwanted nor-lanthionine, the Tabor group came up with two separate approaches; in the first, they performed the iodination reaction at low temperature. This allowed the formation of the desired iodoalanine in favour of the unwanted regioisomer. Although small amounts of the aziridine were formed in this manner, upon coupling with the protected cysteine (**62**), none of the unwanted product was observed, suggesting no ring opening of the aziridine occurs at low temperature.

As an alternative, they also formed lanthionine *via* a Mitsunobu reaction using more reactive reagents than the traditional triphenylphosphine and DEAD combination. They found that by using ADDP and PMe₃ with catalytic amounts of zinc tartrate, they could form the desired lanthionine product directly from the reaction of trityl allyl serine (**75**) with protected cysteine (**62**).⁷⁵ However, the disadvantage of this reaction route is the long reaction time of 7 days (Figure 1.42).

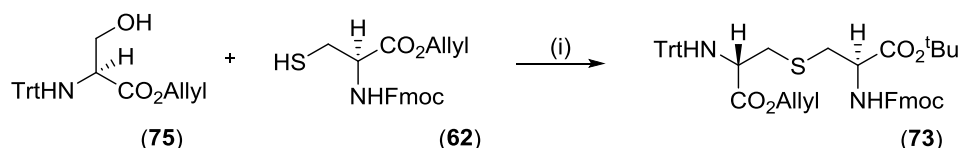


Figure 1.42: Synthesis of Lanthionine via Mitsunobu Reaction

Reagents and Conditions: (i) ADDP, PMe₃, zinc tartrate

An alternative approach to formation of lanthionine is *via* the desulfurisation of a pre-prepared cystine derivative. First reported by Harpp and Gleason,⁷⁶ it was extended by Hennen and co-workers⁷⁷ to give unsymmetrical thioether bridged compounds. In their work, symmetrical cystines were first oxidised to give thiosulfonates, which could then be reacted with a differentially protected cysteine to give an unsymmetrical cystine (**78**). The use of an aminophosphine caused contraction of the cystine to the desired lanthionine (Figure 1.43).

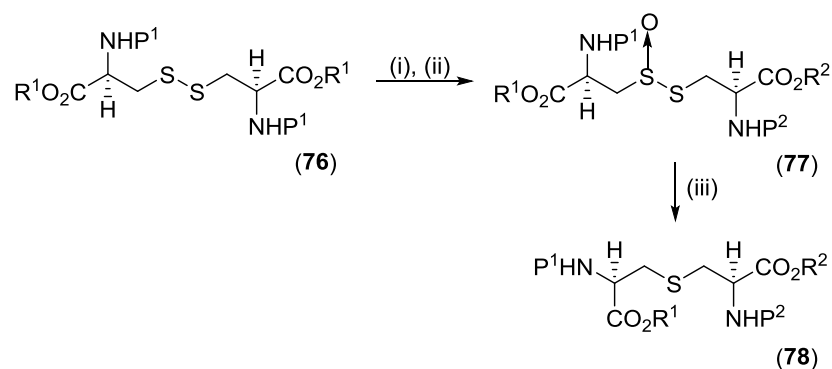


Figure 1.43: Synthesis of Lanthionine via Desulfurisation
Reagents and Conditions: (i) mCPBA, CH₂Cl₂ (ii) Fmoc-Cys-O^tBu, 1.1 eq. tris(dialkylamino)phosphine hexaethylphosphorus triamide, benzene (iii) 2.5 eq. tris(dialkylamino)phosphine hexaethylphosphorus triamide, benzene

However, the final reaction with the phosphine is reversible, which means that only modest yields of the desired product are achieved along with mixtures of symmetrical cystine derivatives.

Finally, Goodman and co-workers^{78,69} showed that the preparation of orthogonally protected lanthionine (**81**) could be formed from serine β-lactone (**79**, Figure 1.44).

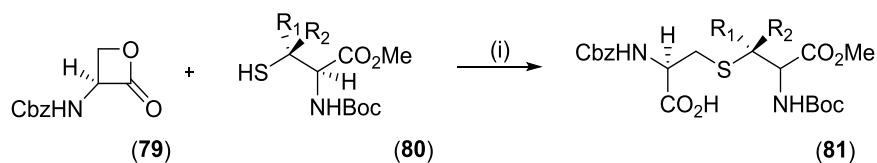


Figure 1.44: Synthesis of Orthogonally Protected Lanthionine (81)
Reagents and Conditions: (i) Cs₂CO₃, DMF

Although all of these syntheses show promise and have allowed for production of lanthionine, each synthesis has shown problems including, but not limited to, racemisation of the product, formation of unwanted side products and poor yields. As such, in order to form large quantities of lanthionine, it was necessary to re-evaluate the current routes available and design a more robust synthesis.

1.8 Synthesis of Lantibiotics

1.8.1 Formation of a Lanthionine Bridge On-Resin

Using this method, Fukase *et al.*⁷⁹ were able to achieve the first synthetic total synthesis of Nisin. In their approach, they made each ring separately using the desulfurisation approach by Harpp and Gleason⁷⁶ and then coupled each of the rings together using 1-ethyl-3-(3-dimethylaminopropyl)-carbodiimide and HOBt (Figures 1.45 and 1.46).

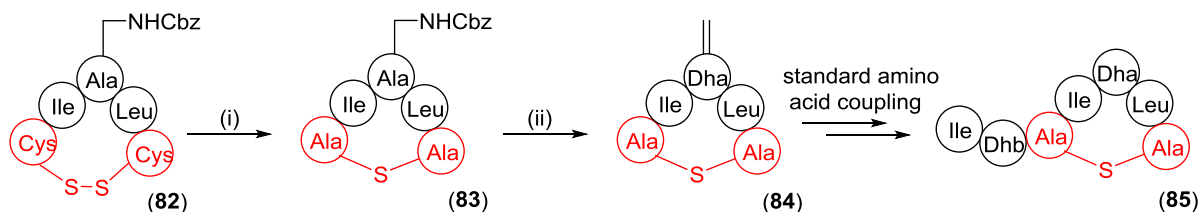


Figure 1.45: Synthesis of Nisin Ring A

Reagents and Conditions: (i) $P(NEt_2)_3$, DMF (ii) 1. H_2 , Pd, 2. $HCHO$, $NaBH_3CN$, 3. CH_3I , $KHCO_3$

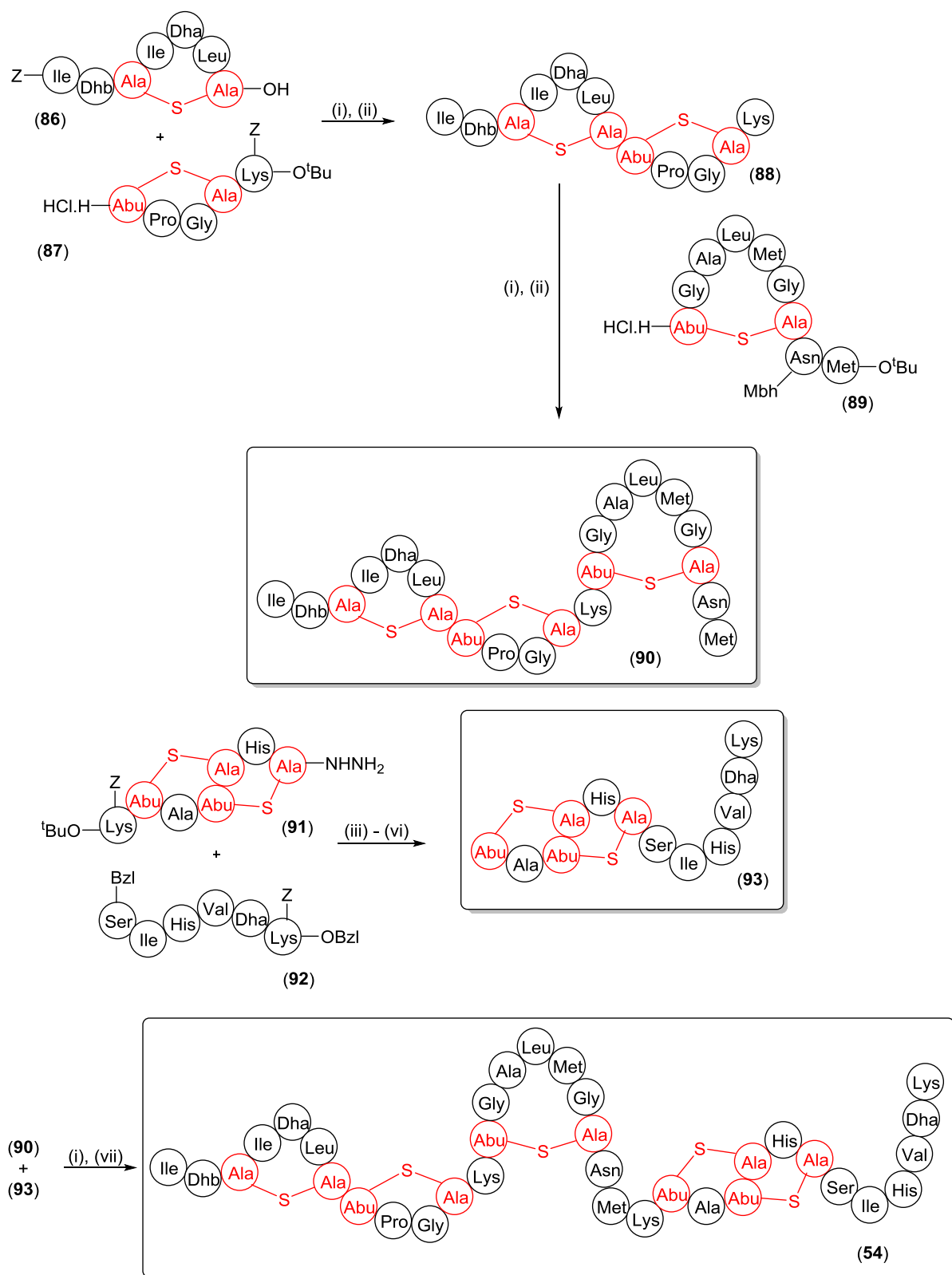


Figure 1.46: Total Synthesis of Nisin (**54**)⁷⁹

Reagents and Conditions: (i) 1-ethyl-3-(3-dimethylaminopropyl)-carbodiimide, HOBT (ii) TFA (iii) "azide method" (iv) Boc_2O (v) TFA (vi) HCl (vii) HF-anisole

The biomimetic nature of the Michael addition was also exploited by van der Donk and co-workers⁸⁰ who extended it to include the use of the unnatural amino acid

phenylselenocysteine (Sec(Ph)). This was added into a solid phase peptide synthesis (SPPS) strategy before subsequent oxidation and elimination with NaIO_4 to give the required dehydroalanine residue. This could then again be reacted *via* a Michael addition with a deprotected cysteine residue to give the desired thioether bridge. This methodology was then used to form Ring B in subtilin (Figure 1.47).

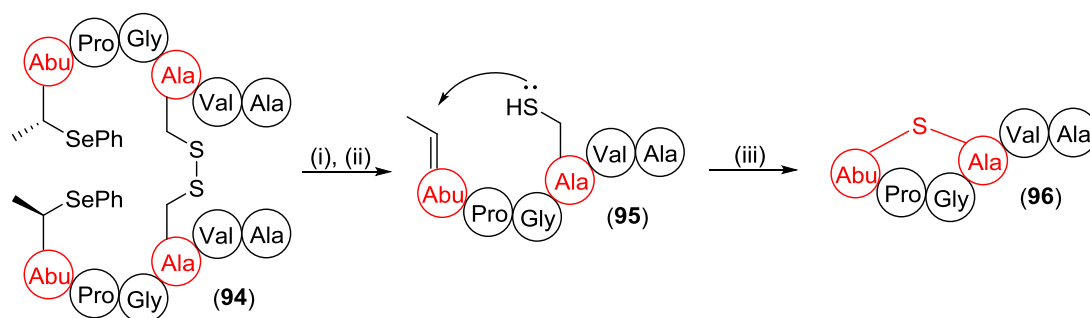


Figure 1.47: Synthesis of Subtilin Ring B (**96**)
Reagents and Conditions: (i) NaIO_4 (ii) TCEP (iii) pH 8

1.8.2 Incorporation of a Pre-Formed Protected Lanthionine into a Solid Phase Peptide Synthesis Strategy

Although these reactions do give the desired stereochemistry, they are very reliant on the correct orientation of both halves of the molecule and indeed, if the dehydroalanine and cysteine residues are reversed in the above Michael addition, then a mixture of diastereoisomers is observed.⁸⁰ One way to circumvent this problem would be to add a pre-formed lanthionine moiety into a peptide synthesis strategy. Provided that the insertion and cyclisation steps could be controlled, this would guarantee that the desired stereochemistry was observed and should prevent the formation of the wrong isomer.

This approach was first attempted by Goodman *et al.*⁷⁸ who showed that their orthogonally protected lanthionine (**97**) could be incorporated into a peptide sequence using standard Boc chemistry. Reaction with acetic acid gives simultaneous cleavage from the oxime resin and peptide cyclisation to give the desired cyclic peptide, Nisin Ring C (**101**, Figure 1.48).

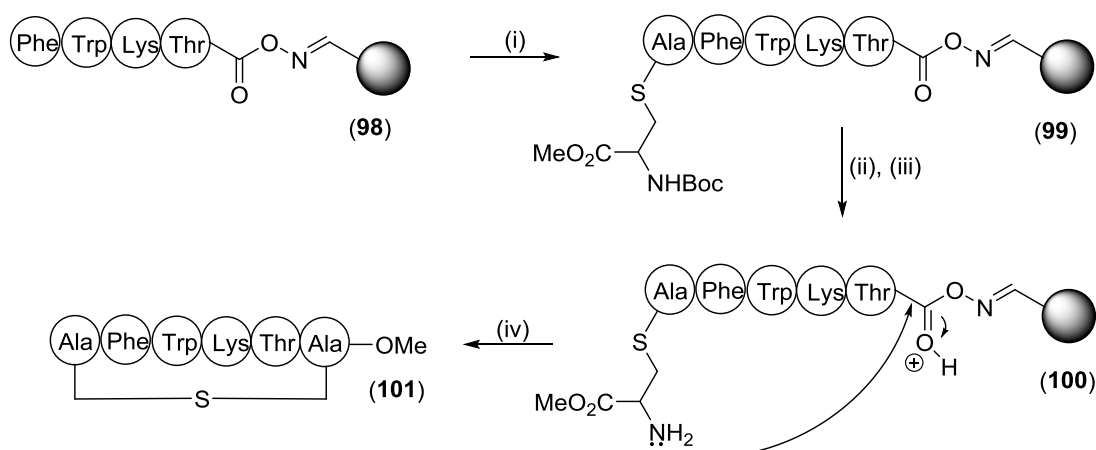


Figure 1.48: Synthesis of Nisin Ring C (**101**)⁷⁸

Reagents and Conditions: (i) BOP, DMF (ii) TFA, CH₂Cl₂ (iii) DIPEA, CH₂Cl₂ (iv) AcOH, DMF, CH₂Cl₂

Whilst this approach gives both regioselective and stereoselective control, the disadvantage of this method is that it can only be used to form single lanthionine rings as cyclisation necessitates concurrent cleavage from the oxime resin. In this instance, this would mean that any subsequent additions to the peptide would need to be carried out in solution rather than on-resin.

As an alternative to this, work by Bregant and Tabor used a different protecting group SPPS strategy.⁷² The linear thioether precursor they used had orthogonal protecting groups to allow for controlled chain growth during a solid phase strategy (Figure 1.49).

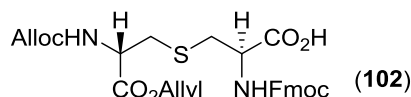


Figure 1.49: Structure of Lanthionine (**102**) for Use in Solid Phase Peptide Synthesis Strategy⁷²

To begin, the chain was built up using the standard Fmoc SPPS protocol (Fmoc deprotection using 40% piperidine, followed by amino acid addition using HBTU and DIPEA) to give **103**. The lanthionine moiety was incorporated using the non-uronium based coupling reagents HOAt (1-Hydroxy-7-azabenzotriazole) and PyAOP (1H-7-Azabenzotriazole-1-yl)-oxytrispyrrolidinophosphonium hexafluorophosphate) in the presence of DIPEA to generate **104**. Once the lanthionine moiety was successfully installed, the classical Fmoc SPPS protocol was used to build up the amino acid chain to the desired length **105**. To cyclise the peptide, the Fmoc group was again removed using 40% piperidine and simultaneous removal of the allyl and Alloc protecting groups was achieved using tetrakis(triphenylphosphine) palladium and 1,3-dimethylbarbitic acid to give the fully deprotected peptide **106**. Cyclisation again employed the HOAt and PyAOP conditions to give **107**. The free amino group was then ready to react with the next Fmoc protected amino acid to give **108**. To complete the synthesis, one last Fmoc deprotection using 40% piperidine was carried out followed by TFA-mediated

cleavage from the resin with simultaneous side chain deprotection to give the desired analogue of Nisin Ring C (**109**, Figure 1.50).

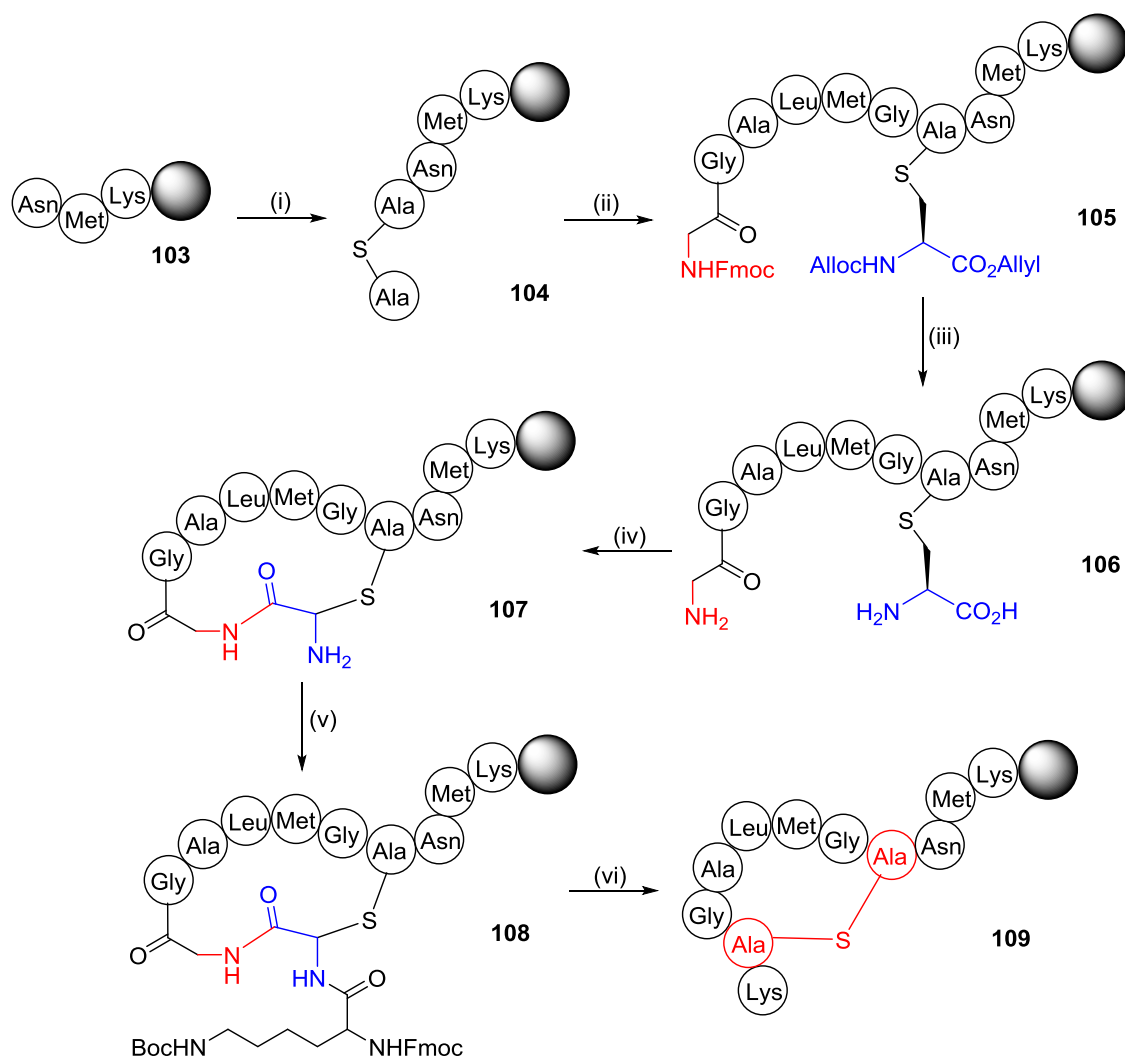


Figure 1.50: Synthesis of an Analogue of Nisin Ring C (**109**)⁷²

Reagents and Conditions: (i) HOAt, PyAOP, DIPEA, lanthionine (**102**), DMF (ii) 40% piperidine in DMF, then amino acid, HBTU, DIPEA, DMF (iii) 40% piperidine in DMF, then Pd(PPh₃)₄, 1,3-dimethylbarbitic acid, DMF, CH₂Cl₂ (iv) HOAt, PyAOP, DIPEA, DMF (v) FmocLysOH, HBTU, DIPEA, DMF (vi) 40% piperidine in DMF (vii) TFA, ethanedithiol, triisopropylsilane, water

Using this methodology, Vederas and co-workers were able to form multiple lanthionine rings on-resin to give the first solid-supported synthesis of a lantibiotic, lactocin S (**117**, Figure 1.51).⁸¹

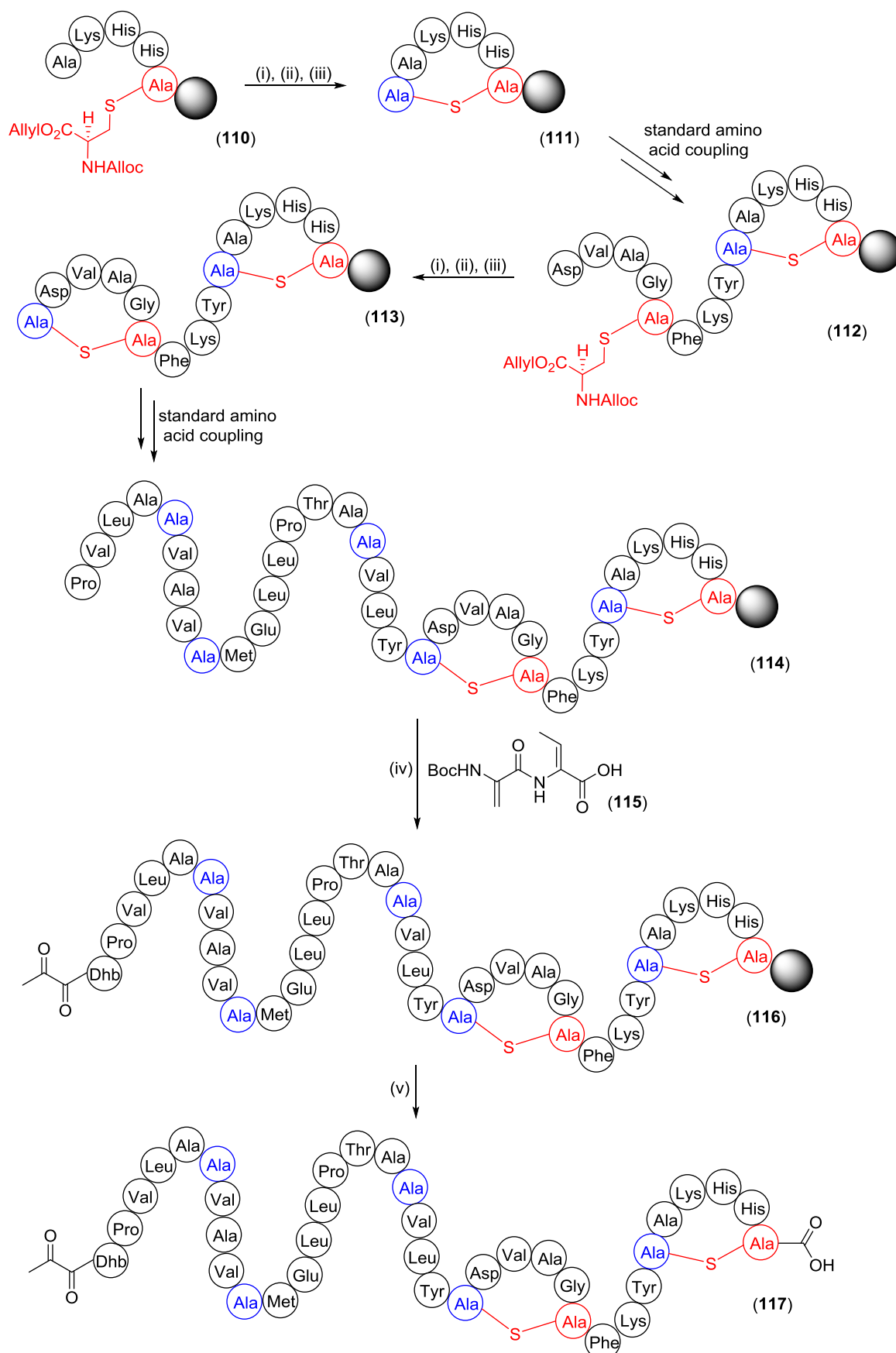


Figure 1.51: Synthesis of Lactocin S (**117**)⁸¹ (blue indicates a D-amino acid)
 Reagents and Conditions: (i) $\text{Pd(PPh}_3)_4$, PhSiH_3 (ii) 20% piperidine, DMF (iii) PyBOP, HOBT, NMM, DMF (iv) PyBOP, HOBT, NMM, DMF (v) TFA, water, anisole

The first lanthionine bridge was formed by initially deprotecting the allyl and Alloc groups using $\text{Pd(PPh}_3)_4$ and phenylsilane, before removing the Fmoc group with piperidine. Cyclisation was achieved using PyBOP and HOBt as the coupling reagents to give intermediate (**111**). Standard coupling conditions were then used to grow the chain to give (**112**) before again deprotecting and cyclising the peptide to give the second lanthionine bridge (**113**). SPPS continued until the installation of the final two amino acids (**115**), which were pre-prepared using solution phase chemistry and then coupled to the product using PyBOP and HOBt. Cleavage from the resin using TFA and anisole gave the desired product, Lactocin S (**117**), with a yield of 10% over 71 steps.

This methodology was further extended by the Vederas group to include methyl lanthionine (**119**, Figure 1.52) in the solid phase synthesis of Lacticin 3147.^{82,83}

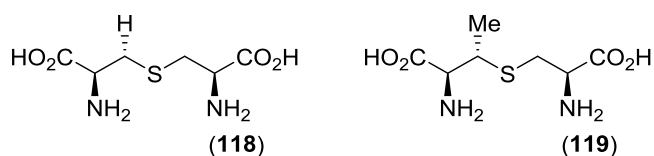


Figure 1.52: Structure of Lanthionine (**118**) and Methyl Lanthionine (**119**)

By using two different sets of orthogonal protecting groups, it was possible to form both the successive and interlocking rings in both components of Lacticin 3147, known as A1 and A2 (**120** and **121**, Figure 1.53).

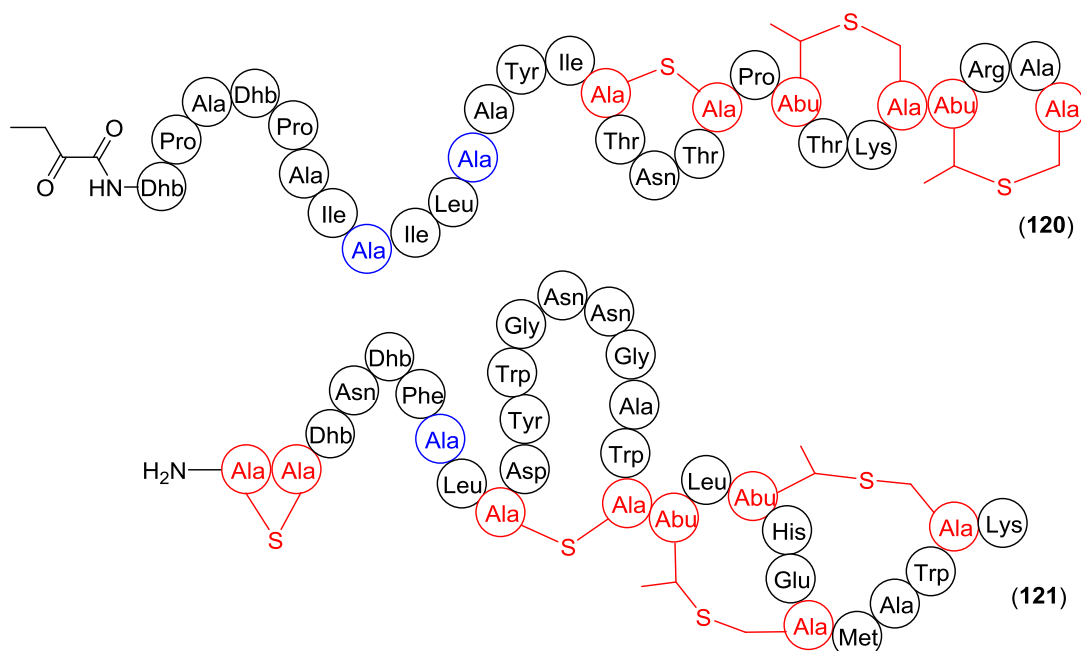


Figure 1.53: Structure of Lacticin 3147 A1 (**120**) and Lacticin 3147 A2 (**121**)^{82,83}

To form the interlocking rings in (**121**), orthogonal protecting groups were employed; for the first incorporation of methyllanthionine, the allyl and Alloc groups were used and for the

second molecule, *para*-nitrobenzyloxycarbonyl (Nz) and *para*-nitrobenzyl (NB) were employed (Figure 1.54).

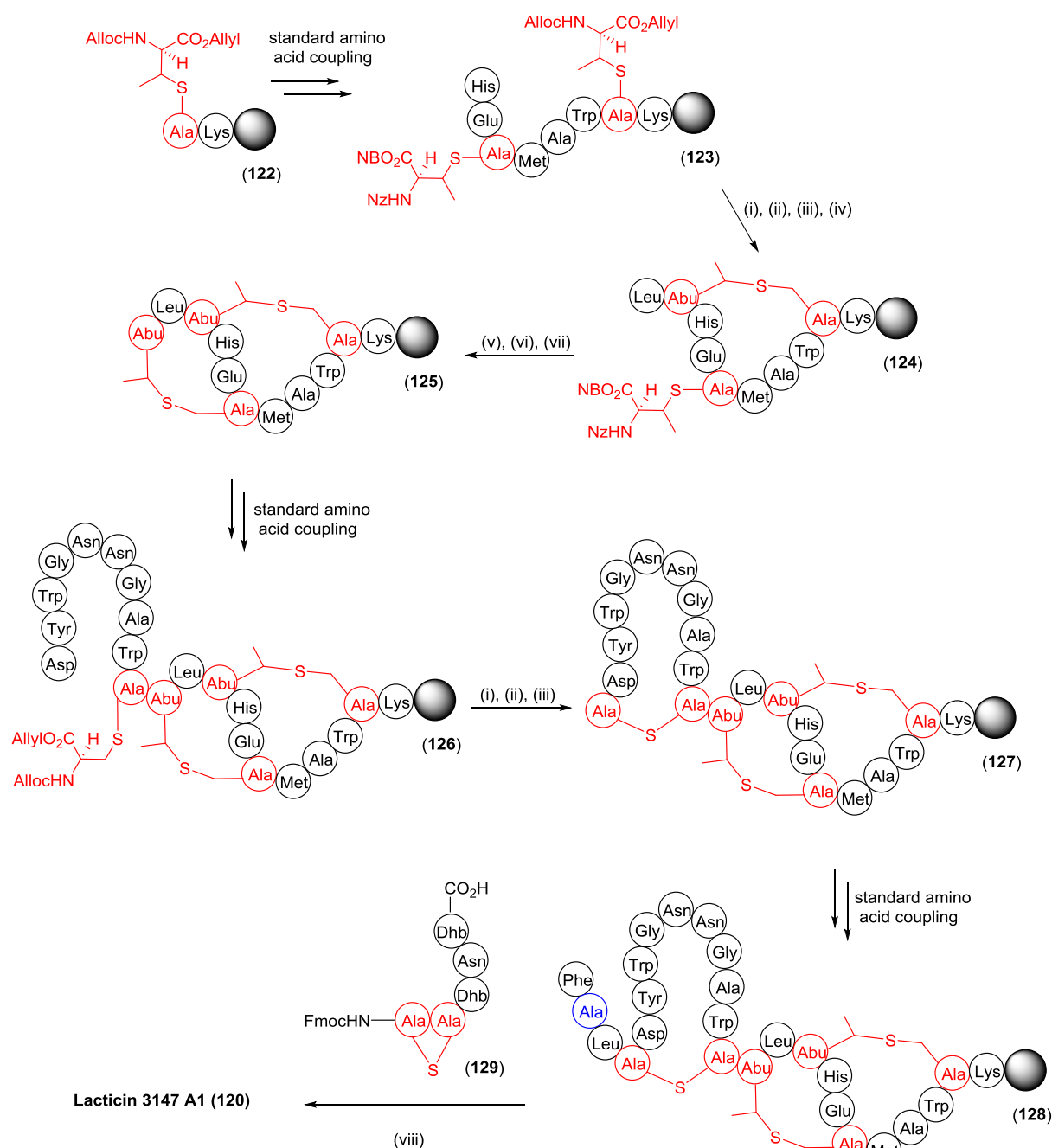


Figure 1.54: Synthesis of Lacticin 3147 A1 (**120**)⁸³ (blue indicates a D-amino acid)

Reagents and Conditions: (i) $\text{Pd}(\text{PPh}_3)_4$, PhSiH_3 (ii) 20% piperidine, DMF (iii) PyBOP, HOBT, NMM, DMF (iv) Fmoc-Leu-OH (v) SnCl_2 , HCl (vi) 20% piperidine, DMF (vii) PyBOP, HOBT, NMM, DMF (viii) 1. 20% piperidine, DMF 2. TFFH, DBH, **129** 3. TFA, water, anisole

The peptide chain was grown using standard Fmoc methodology to install both the standard amino acids and the orthogonally protected methyl lanthionine moieties. Synthesis of the first ring was achieved by deprotection with $\text{Pd}(\text{PPh}_3)_4$ followed by cyclisation using PyBOP and HOBT to give intermediate (**124**). Standard Fmoc conditions were used to install the following leucine before simultaneous deprotection of the Nz and NB groups was carried out

using 6 M SnCl_2 in HCl, which upon cyclisation gave intermediate (**125**). Installation of lanthionine to give the final ring in the sequence again employed the allyl/Alloc group protecting strategy to give (**127**), before addition of the last amino acids gave intermediate (**128**). The last five amino acids (**129**) were synthesised off-resin due to the extensive and densely packed modifications⁸³ and were installed into the peptide chain on-resin using fluoro-*N,N,N',N'*-tetramethylformamidine hexafluorophosphate and DIPEA to give (**120**). Finally, cleavage from the resin gave the desired product, Lacticin 3147 A1. This is the first reported total synthesis of both these peptides using SPPS techniques and shows that a remarkably complex structure can be formed by employing the correct protecting groups.

At the same time, work published by the Tabor group⁸⁴ showed that it was possible to make an analogue of the interlocking rings D & E in Nisin (**131**, Figure 1.55) by employing two different orthogonally protected lanthionines. In their work, they used the previously reported allyl/Alloc protecting group on one moiety (**102**, Figure 1.55) and trimethylsilyl (TMSE) and β -(trimethylsilyl)ethoxycarbonyl (TEOC) on the other lanthionine moiety (**130**, Figure 1.55).

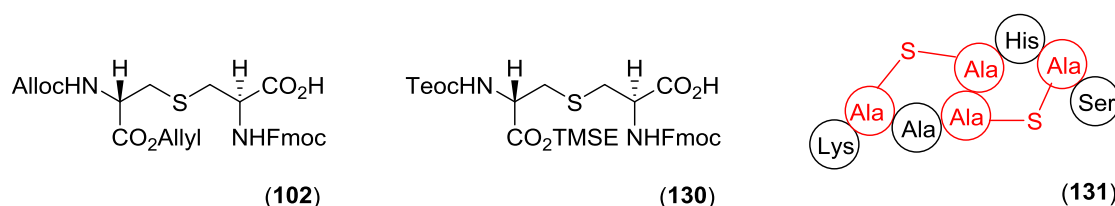


Figure 1.55: Structures of Orthogonally Protected Lanthionines (**102**) and (**130**) and an Analogue of Nisin Rings D and E (**131**)⁸⁴

Again, standard SPPS strategies were employed to form the peptide chain and simultaneous deprotection of the TMSE and TEOC groups was achieved using TBAF, before cyclisation to form the second ring was carried out with PyAOP and HOAt.

Although all of these strategies have shown it is possible to incorporate an orthogonally protected lanthionine moiety into a SPPS strategy, none of the methods above have been applied to a system as complicated as an ICK peptide. In recent years, work by both the Tabor and van der Donk groups has shown that it is possible to make interlocking thioether bridges but as yet, no one has published the formation of complex systems containing interlocking disulfide and lanthionine bridges. Thus, in order to form true analogues of ProTx-II (**22**), a new methodology was required which could be utilised to form the desired peptides.

1.9 Conclusions and Aims

Research has indicated that ProTx-II (**22**) shows good therapeutic potential for the selective inhibition of the Na_v1.7 ion channel over other subtypes but has difficulty crossing the blood-nerve barrier. Currently, little is known about the structure of the Na_v1.7 ion channel or of the binding site specifically. The first aim of this project was to investigate the structure-activity relationship of the ligand on the Na_v1.7 ion channel *via* the synthesis of shorter analogues of ProTx-II (**22**) and by replacing one or more of the disulfide bonds with thioether linkages. All of the above work has focussed on the synthesis of naturally occurring peptides which incorporate a D-amino acid into the structure of the peptide. However, in order to incorporate a lanthionine moiety into ProTx-II, it was necessary to form a new diastereoisomer of lanthionine synthesised from L-amino acids, as the parent peptide consists entirely of L-amino acids. As mentioned in section 1.7, there are many promising syntheses of orthogonally protected lanthionine but they are all either low yielding, do not produce stereochemically pure product or cannot be used in a solid phase peptide synthesis strategy. In order to allow this research to be carried out, a large amount of orthogonally protected lanthionine was required. For this reason, the first part of the project aimed to investigate a robust synthesis for the production of multi-gram quantities of diastereomerically pure lanthionine.

Although some work has been published on the formation of interlocking lanthionine bridges, no work has been published on interlocking lanthionine and disulfide bridges. In this work, a new methodology for the formation of these structures was implemented to form a number of analogues of ProTx-II (**22**), with the aim of increasing the stability of the peptides by replacing the disulfide bond with a thioether linkage.

Finally, these peptides were tested against the hNa_v1.7 ion channel using an automated patch clamp assay to assess the potency of the compounds and their structures were assessed using homology modelling techniques.

¹ Porter, R. S.; Kaplan, J. S. ed., *The Merck Manual of Diagnosis and Therapy*, Chronic Pain, 19th Edition, (2011)

² Loeser, J. D.; Treede, R. D., *Pain*, **137**, 3, 473-477 (2008)

³ Chief Medical Officer for England, 2009

⁴ <https://www.britishpainsociety.org/media-resources/#faqs> (last accessed 09/02/2015)

⁵ <http://www.who.int/cancer/palliative/painladder/en/> (last accessed 09/02/2015)

⁶ World Health Organization, *Cancer pain relief. With a guide to opioid availability*, 2nd Edition, Geneva: WHO, ISBN 92-4-154482-1 (1996)

- ⁷ Benyamin, R.; Trescot, A. M.; Datta, S.; Buenaventura, R.; Adlaka, R.; Sehgal, N.; Glaser, S. E.; Vallejo, R., *Pain Physician*, **11**, 2 (suppl), S105-120 (2008)
- ⁸ Smith, S.; Scarth, E.; Sasada, M., *Drugs in Anaesthesia and Intensive Care*, 4th Edition, OUP (2012)
- ⁹ Cox, J. J.; Reiman, F.; Nicholas, A. K.; Thornton, G.; Roberts, E.; Springell, K.; Karbani, G.; Jafri, H.; Mannan, J.; Raashid, Y.; Al-Gazali, L.; Hamamy, H.; Valente, E. M.; Gorman, S.; Williams, R.; McHale, D. P.; Wood, J. N.; Gribble, F. M.; Woods, C. G., *Nature*, **444**, 14, 894-898 (2006)
- ¹⁰ Sangameswaran, L.; Fish, L. M.; Koch, B. D.; Rabert, D. K.; Delgado, S. G.; Ilnicka, M.; Jakeman, L. B.; Novakovic, S.; Wong, K.; Sze, P.; Tzoumaka, E.; Stewart, G. R.; Herman, R. C.; Chan, H. C.; Eglen, R. M.; Hunter, J. C., *J. Biol. Chem.*, **272**, 12805-14809 (1997)
- ¹¹ Yang, Y.; Wang, Y.; Li, S.; Xu, Z.; Li, H.; Ma, L.; Fan, J.; Bu, D.; Liu, B.; Fan, Z.; Wu, G.; Jin, J.; Ding, B.; Zhu, X.; Shen, Y., *J. Med. Genet.*, **41**, 3, 171-174 (2004)
- ¹² <http://www.nhs.uk/conditions/erythromelalgia/Pages/Introduction.aspx> (last accessed 09/02/2015)
- ¹³ Stanfield, C. L., *Principles of Human Physiology*, 5th Edition (2013). Reprinted by permission of Pearson Education, Inc., New York, New York
- ¹⁴ http://upload.wikimedia.org/wikipedia/commons/c/cc/Action_potential_vert.png (last accessed 09/02/2015)
- ¹⁵ Catterall, W. A.; Goldin, A. L.; Waxman, S. G., *Pharmacol Rev*, **57**, 397-409 (2005)
- ¹⁶ Adapted from Rogawski, M. A.; Loeschner, W., *Nature Reviews Neuroscience*, **5**, 553-564 (2004)
- ¹⁷ Ren, D.; Navarro, B.; Xu, H.; Yue, L.; Shi, Q.; Clapham, D. E., *Science*, **294**, 2372-2375 (2001)
- ¹⁸ Catterall, W. A., *Science*, **294**, 2306-2308 (2001)
- ¹⁹ Payandeh, J.; Scheuer, T.; Zheng, N.; Catterall, W. A., *Nature*, **475**, 353-359 (2011)
- ²⁰ Nardi, A.; Damann, N.; Hertrampf, T.; Kless, A.; *ChemMedChem*, **7**, 10, 1712-1740 (2012)
- ²¹ Jarvis, M. F.; Honore, P.; Shieh, C. C.; Chapman, M.; Joshi, S.; Zhang, X. F.; Kort, M.; Carroll, W.; Marron, B.; Atkinson, R.; Thomas, J.; Liu, D.; Krambis, M.; Liu, Y.; McGaraughty, S.; Chu, K.; Roeloffs, R.; Zhong, C.; Mikusa, J. P.; Hernandez, G.; Gauvin, D.; Wade, C.; Zhu, C.; Pai, M.; Scanio, M.; Shi, L.; Drizin, I.; Gregg, R.; Matulenko, M.; Hakeem, A.; Gross, M.; Johnson, M.; Marsh, K.; Wagoner, P. K.; Sullivan, J. P.; Faltynek, C. R.; Krafter, D. S., *Proc. Natl. Acad. Sci.*, **104**, 20, 8520-8525 (2007)
- ²² Roberson, D. P.; Binshtok, A. M.; Blas, F.; Bean, B. P.; Woolf, C. J., *Br. J. Pharmacol.*, **164**, 48-58 (2011)
- ²³ Moore, J. W.; Narahashi, T., *Fed. Proc.*, **26**, 6, 1655-1663 (1967)
- ²⁴ Narahashi, T., *Proc. Jpn. Acad., Ser. B*, **84**, 147-154 (2008)
- ²⁵ Ferrat, G.; Darbon, H., *Toxin Reviews*, **24**, 361-383 (2005)
- ²⁶ Akondi, K. B.; Muttenthaler, M.; Dutertre, S.; Kaas, Q.; Craik, D. J.; Lewis, R. J.; Alewood, P. F., *Chem. Rev.*, **114**, 11, 5815-5847 (2014)
- ²⁷ McIntosh, J. M.; Jones, R. M., *Toxicon*, **39**, 1447-1451 (2001)
- ²⁸ Norton, R. S., *Molecules*, **15**, 2825-2844 (2010)
- ²⁹ Nielsen, K. J.; Watson, M.; Adams, D. J.; Hammarström, A. K.; Gage, P. W.; Hill, J. M.; Craik, D. J.; Thomas, L.; Adams, D.; Alewood, P. F.; Lewis, R. J., *J. Biol. Chem.*, **277**, 30, 27247-27255 (2002)
- ³⁰ Cruz, L. J.; Gray, W. R.; Olivera, B. M.; Zeikus, R. D.; Kerr, L.; Yoshikami, D.; Moczydlowski, E., *J. Biol. Chem.*, **260**, 16, 9280-9288 (1985)
- ³¹ Wang, X.-H.; Connor, M.; Smith, R.; Maciejewski, M. W.; Howden, M. E. H.; Nicholson, G. M.; Christie, M. J.; King, G. F., *Nature Structural Biology*, **7**, 6, 505-513 (2000)
- ³² Pránting, M.; Lööv, C.; Burman, R.; Göransson, U.; Andersson, D. I., *J. Antimicrob. Chemother.*, **65**, 9, 1964-1971 (2010)
- ³³ Saether, O.; Craik, D. J.; Campbell, I. D.; Sletten, K.; Juul, J.; Norman, D. G., *Biochemistry*, **34**, 4147-4158 (1995)
- ³⁴ Craik, D. J., *Toxicon*, **39**, 1809-1813 (2001)
- ³⁵ Katoh, T.; Goto, Y.; Reza, M. S.; Suga, H., *Chem. Commun.*, **47**, 9946-9958 (2011)
- ³⁶ Jaulent, A. M.; Leatherbarrow, R. J., *Protein Engineering, Design and Selection*, **17**, 9, 681-687 (2004)
- ³⁷ Shariff, L.; Zhu, Y.; Cowper, B.; Di, W.-L.; Macmillan, D., *Tetrahedron*, **70**, 7675-7680 (2014)
- ³⁸ Yang, S.; Xiao, Y.; Kang, D.; Liu, J.; Li, Y.; Undheim, E. A. B.; Klint, J. K.; Rong, M.; Lai, R.; King, G. F., *Proc. Natl. Acad. Sci.*, **110**, 43, 17534-17539 (2013)
- ³⁹ Park, S. P.; Kim, B. M.; Koo, J. Y.; Cho, H.; Lee, C. H.; Kim, M.; Na, H. S.; Oh, U., *Pain*, **137**, 1, 208-217 (2008)
- ⁴⁰ Bowman, C. L.; Gottlieb, P. A.; Suchyna, T. M.; Murphy, Y. K.; Sachs, F., *Toxicon*, **49**, 2, 249-270 (2007)

- ⁴¹ Sermadrias, I.; Revell, J.; Linley, J. E.; Sandercock, A.; Ravn, P., *PLoS ONE*, **8**, 12, e83202 (2013)
- ⁴² Schmalhofer, W. A.; Calhoun, J.; Burrows, R.; Bailey, T.; Kohler, M. G.; Weinglass, A. B.; Kaczorowski, G. J.; Garcia, M. L.; Koltzenburg, M.; Priest, B. T., *Mol. Pharmacol.*, **74**, 1476-1484 (2008)
- ⁴³ Middleton, R. E.; Warren, V. A.; Kraus, R. L.; Hwang, J. C.; Liu, C. J.; Dai, G.; Brochu, R. M.; Kohler, M. G.; Gao, Y.-D.; Garsky, V. M.; Bogusky, M. J.; Mehl, J. T.; Cohen, C. J.; Smith, M. M., *Biochemistry*, **41**, 14734-14747 (2002)
- ⁴⁴ Ohkubo, T.; Yamazaki, J.; Kitamura, K., *J. Pharmacol. Sci.*, **112**, 452-458 (2010)
- ⁴⁵ Park, J. H.; Carlin, K. P.; Wu, G.; Ilyin, V. I.; Musza, L. L.; Blake, P. R.; Kyle, D. J., *J. Med. Chem.*, **57**, 6623-6631 (2014)
- ⁴⁶ Smith, J. J.; Cummins, T. R.; Alphy, S.; Blumenthal, K. M., *J. Biol. Chem.*, **282**, 17, 12687-12697 (2007)
- ⁴⁷ Bernard, C.; Legros, C.; Ferrat, G.; Bischoff, U.; Marquardt, A.; Pongs, O.; Darbon, H., *Protein Sci*, **9**, 11, 2059-2067 (2000)
- ⁴⁸ Smith, J. J.; Alphy, S.; Seibert, A. L.; Blumenthal, K. M., *J. Biol. Chem.*, **280**, 12, 11127-11133 (2005)
- ⁴⁹ Reproduced with permission from Park, J. H.; Carlin, K. P.; Wu, G.; Ilyin, V. I.; Musza, L. L.; Blake, P. R.; Kyle, D. J., *J. Med. Chem.*, **57**, 6623-6631 (2014). Copyright 2014 American Chemical Society
- ⁵⁰ Norton, R. S., *Amino Acids, Peptides and Proteins in Organic Chemistry*, ed: Hughes, A. B., Wiley-VCH, **5**, (2010)
- ⁵¹ Armishaw, C. J.; Daly, N. L.; Nevin, S. T.; Adams, D. J.; Craik, D. J.; Alewood, P. F., *J. Biol. Chem.*, **281**, 14136-14143 (2006)
- ⁵² Muttenthaler, M.; Nevin, S. T.; Grishin, A. A.; Ngo, S. T.; Choy, P. T.; Daly, N. L.; Hu, S. H.; Armishaw, C. J.; Wang, C. I.; Lewis, R. J.; Martin, J. L.; Noakes, P. G.; Craik, D. J.; Adams, D. J.; Alewood, P. F., *J. Am. Chem. Soc.*, **132**, 3514-3522 (2010)
- ⁵³ MacRaid, C. A.; Illesginhe, J.; van Lierop, B. J.; Townsend, A. L.; Chebib, M.; Livett, B. G.; Robinson, A. J.; Norton, R. S., *J. Med. Chem.*, **52**, 755-762 (2009)
- ⁵⁴ Derksen, D. J.; Stymiest, J. L.; Vederas, J. C., *J. Am. Chem. Soc.*, **128**, 14252-14253 (2006)
- ⁵⁵ Stymiest, J. L.; Mitchell, B. F.; Wong, S.; Vederas, J. C., *J. Org. Chem.*, **70**, 7799-7809 (2005)
- ⁵⁶ Elaridi, J.; Patel, J.; Jackson, W. R.; Robinson, A. J., *J. Org. Chem.*, **71**, 7538-7545 (2006)
- ⁵⁷ Hargittai, B.; Solé, N. A.; Groebe, D. R.; Abramson, S. N.; Barany, G., *J. Med. Chem.*, **43**, 4787-4792 (2000)
- ⁵⁸ Hidaka, Y.; Ohmori, K.; Wada, A.; Ozaki, H.; Ito, H.; Hirayama, T.; Takeda, Y.; Shimonishi, Y., *Biochem. Biophys. Res. Commun.*, **176**, 958-965 (1991)
- ⁵⁹ Cui, H.-K.; Guo, Y.; Wang, F.-L.; Chang, H.-N.; Wang, Y.-J.; Wu, F.-M.; Tian, C.-L.; Liu, L., *Angew. Chem. Int. Ed.*, **52**, 9558-9562 (2013)
- ⁶⁰ Knerr, P. J.; Tzekou, A.; Ricklin, D.; Qu, H.; Chen, H.; van der Donk, W. A.; Lambris, J. D., *ACS Chem. Biol.*, **6**, 753-760 (2011)
- ⁶¹ Dekan, Z.; Vetter, I.; Daly, D. L.; Craik, D. J.; Lewis, R. J.; Alewood, P. F., *J. Am. Chem. Soc.*, **133**, 15866-15869 (2011)
- ⁶² Ösapay, G.; Prokai, L.; Kim, H.-S.; Medzihradszky, K. F.; Coy, D. H.; Liapakis, G.; Reisine, T.; Melacini, G.; Zhi, Q.; Wang, S. H.-H.; Mattern, R.-H.; Goodman, M., *J. Med. Chem.*, **40**, 2241-2251 (1997)
- ⁶³ Chatterjee, C.; Paul, M.; Xie, L.; van der Donk, W. A., *Chem Rev.*, **105**, 633-684 (2005)
- ⁶⁴ Hasper, H. E.; Kramer, N. E.; Smith, J. L.; Hillman, J. D.; Zachariah, C.; Kuipers, O. P.; de Kruijff, B.; Breukink, E., *Science*, **313**, 1636-1637 (2006)
- ⁶⁵ Cortés, J.; Appleyard, A. N.; Dawson, M. J., *Methods Enzymol.*, **458**, 559-574 (2009)
- ⁶⁶ Field, D.; Connor, P. M. O.; Cotter, P. D.; Hill, C.; Ross, R. P., *Mol. Microbiol.*, **69**, 1, 218-230 (2008)
- ⁶⁷ Levengood, M. R.; Knerr, P. J.; Oman, T. J.; van der Donk, W. A., *J. Am. Chem. Soc.*, **131**, 12024-12025 (2009)
- ⁶⁸ Levengood, M. R.; Kerwood, C. C.; Chatterjee, C.; van der Donk, W. A., *ChemBioChem.*, **10**, 911-919 (2009)
- ⁶⁹ Tabor, A. B., *Org. Biomol. Chem.*, **9**, 7606-7628 (2011)
- ⁷⁰ Probert, J. M.; Rennex, D.; Bradley, M., *Tetrahedron Lett.*, **37**, 1101-1104 (1996)
- ⁷¹ Brown, G. B.; du Vigneaud, V., *J. Biol. Chem.*, **140**, 767-771 (1941)
- ⁷² Bregant, S.; Tabor, A. B., *J. Org. Chem.*, **70**, 2430-2438 (2005)
- ⁷³ Zhu, X.; Schmidt, R. R., *Eur J Org Chem*, **20**, 4069-4072 (2003)
- ⁷⁴ Mustapa, M. F.; Harris, R.; Esposito, D.; Chubb, N. A. L.; Mould, J.; Schultz, D.; Driscoll, P. C.; Tabor, A. B., *J. Org. Chem.*, **68**, 8193-8198 (2003)

-
- ⁷⁵ Mustapa, M. F. M.; Harris, R.; Subanovic, N. B.; Elliot, S. L.; Bregant, S.; Groussier, M. F. A.; Mould, J.; Schultz, D.; Chubb, N. A. L.; Gaffney, P. R. J.; Driscoll, P. C.; Tabor, A. B., *J. Org. Chem.*, **68**, 8185-8192 (2003)
- ⁷⁶ Harpp, D. J.; Gleason, D. G., *J. Org. Chem.*, **36**, 73-80 (1971)
- ⁷⁷ Olsen, R. J.; Kini, G. D.; Hennen, W. J., *J. Org. Chem.*, **50**, 4332-4336 (1985)
- ⁷⁸ Ösapay, G.; Goodman, M., *J. Chem. Soc., Chem. Commun.*, 1599-1600 (1993)
- ⁷⁹ Fukase, K.; Kitazawa, M.; Sano, A.; Shimbo, K.; Fujita, H.; Horimoto, S.; Wakamiya, S.; Shiba, T., *Tetrahedron Lett.*, **29**, 795-798 (1988)
- ⁸⁰ Zhou, H.; van der Donk, W. A., *Org. Lett.*, **4**, 1335-1338 (2002)
- ⁸¹ Ross, A. C.; Liu, H.; Pattabiraman, V. R.; Vederas, J. C., *J. Am. Chem. Soc.*, **132**, 462-463 (2010)
- ⁸² Pattabiraman, V. R.; McKinnie, S. M. K.; Vederas, J. C., *Angew. Chem. Int. Ed.*, **47**, 9472-9475 (2008)
- ⁸³ Liu, W.; Chan, A. S. H.; Liu, H.; Cochrane, S. A.; Vederas, J. C., *J. Am. Chem. Soc.*, **133**, 14216-14219 (2011)
- ⁸⁴ Mothia, B.; Appleyard, A. N.; Wadman, S.; Tabor, A. B., *Org. Lett.*, **13**, 16, 4216-4219 (2011)

2. Chapter 2: Synthesis of Orthogonally Protected Lanthionine for Use in Solid Phase Peptide Synthesis

2.1 Introduction

This chapter describes attempts to synthesise a novel diastereoisomer of orthogonally protected lanthionine. The original ProTX-II peptide (**22**) was shown to have good inhibitory effects of the Na_v1.7 channel *in vitro* but showed comparatively poor results *in vivo*, owing to difficulties in crossing the blood-nerve barrier.¹ To investigate which part of the peptide was important for binding, it was decided to synthesise shorter analogues of ProTX-II (**22**). As shown in Figure 2.1, it has three disulfide-linking bridges:

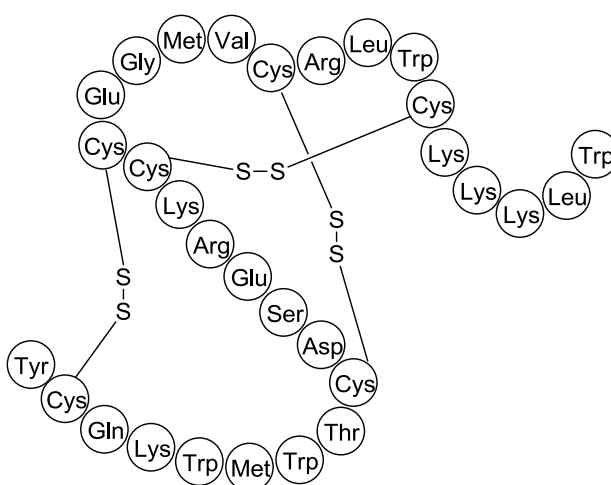


Figure 2.1: Structure of ProTX-II (**22**)

As part of the research, it was decided to investigate the effect of the disulfide link on the efficacy of the compound by replacing it with a monosulfide link formed from the incorporation of the non-proteinogenic amino acid lanthionine (**132**, Figure 2.2). This has the dual effect of decreasing the size of the ring by one atom and increasing the stability of the peptide towards disulfide bond opening *in vivo*.

In order to control the primary sequence of the lanthionine-containing peptides, it was necessary to use an orthogonally protected lanthionine, which could be used in conjunction with an automated Fmoc solid phase peptide synthesis (SPPS) protocol. In all lantibiotics, lanthionine exists in the meso *S,R* form (**49**, Figure 2.2) and is formed from the protected forms of L-cysteine and D-serine.^{2,4} However, in ProTX-II (**22**), all constituent amino acids in the sequence are the naturally occurring L-amino acids. Hence, in order to investigate the effect of the thioether bridge on the structure-activity relationship, it will be necessary to synthesise the *R,R* form **132** (Figure 2.2).

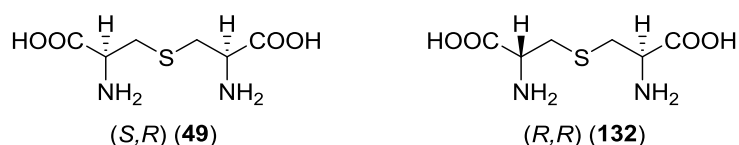


Figure 2.2: Structure of Lanthionine in *S,R* (**49**) and *R,R* (**132**) Forms

2.2 Small Scale Synthesis

2.2.1 Overview of the Small Scale Synthesis

In order to carry out multiple peptide syntheses for a comprehensive investigation into the structural activity relationship of the Na_v1.7 channel, multi-gram quantities of lanthionine were required. However, before this could be achieved, it was decided to establish the synthesis on a small scale, to highlight any problematic steps.

Figure 2.3 shows the synthesis of lanthionine **142** investigated. The procedure began with the esterification of L-cystine (**133**) using *tert*-butyl acetate in the presence of perchloric acid, followed by Fmoc protection using Fmoc succinamide and *N*-methyl morpholine to produce the dimer in reasonable yield. The disulfide bond was then cleaved using tributylphosphine³ to afford the Fmoc protected cysteine (**62**) in 61% yield.

Concurrently, L-serine (**136**) was first reacted with trimethylsilyl chloride before protection with trityl chloride in triethylamine to give the product (**137**) in 90% yield.⁴ The carboxylic acid was then protected using allyl bromide before a Mitsunobu reaction was used to convert the alcohol to an iodo group to give **139**.

The products from these first two stages were then coupled together in the presence of cesium carbonate to give **140** in moderate yield,⁴ before a series of deprotection and re-protection steps afforded the final orthogonally protected lanthionine **142**.

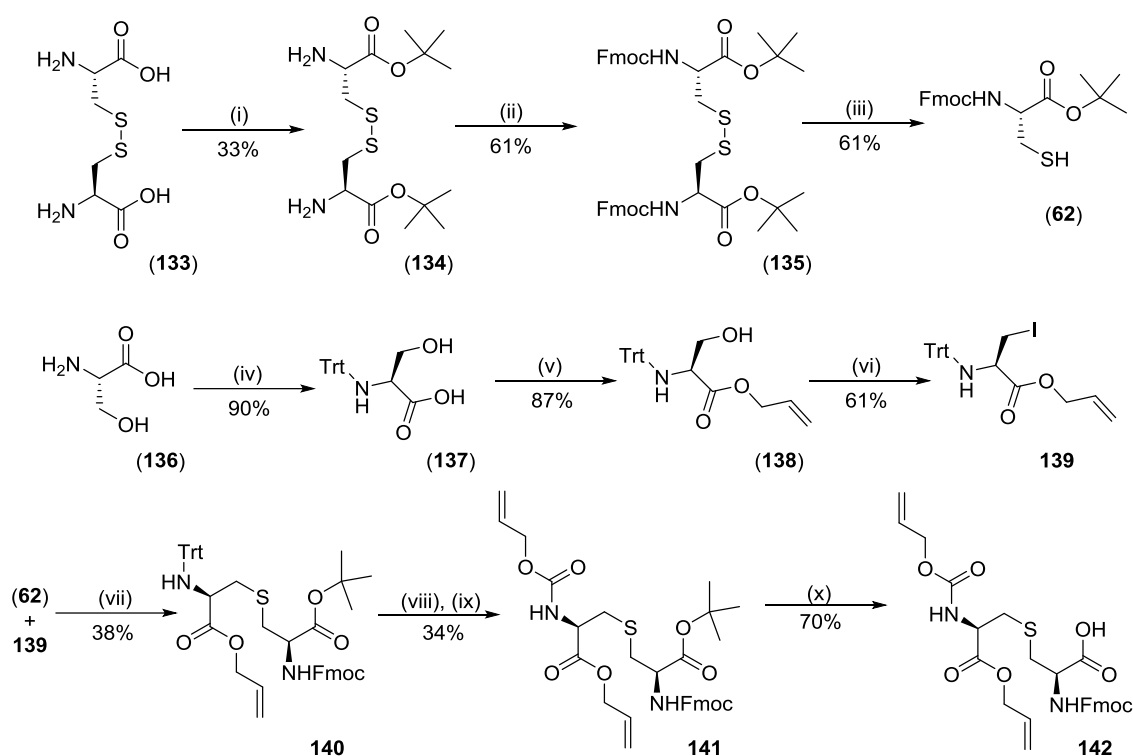


Figure 2.3: Synthesis of Orthogonally Protected Lanthionine **142**

Reagents and Conditions: (i) $t\text{BuOAc}$, HClO_4 , (ii) FmocOSu , NMM , THF (iii) P^nBu_3 , THF (iv) 1. trimethylsilyl chloride, CH_2Cl_2 2. MeOH 3. Et_3N , Ph_3CCl (v) 1. MeOH , Cs_2CO_3 2. DMF , allyl bromide (vi) PPh_3 , DEAD , CH_3I , CH_2Cl_2 (vii) Cs_2CO_3 , DMF (viii) trifluoroacetic acid, triethylsilane (ix) Na_2CO_3 , allyl chloroformate, 1,4-dioxane (x) trifluoroacetic acid, CH_2Cl_2

The overall yield for the seven step synthesis starting from L-Serine was 4% and resulted in the formation of 40 mg of **142**, which was enough for one attempt at peptide synthesis.

2.2.2 Optimisation of the Synthesis

Although the initial synthesis of lanthionine (**142**) worked reasonably well, there were several low yielding steps, including the coupling of the protected iodoalanine and cysteine residues, as well as the trityl deprotection and Alloc re-protection steps. This led to the production of a small quantity of the final product, which allowed for just one attempt at peptide synthesis. Thus, as well as synthesising a novel diastereoisomer, it was important to find a more robust route which could be scaled up to produce multi-gram quantities for optimisation of the peptide synthesis conditions and production of multiple peptide analogues.

2.2.2a Preparation of the Protected Amino Acid Intermediates

The *tert*-butyl protection of L-cystine (**133**) proceeded well on scale-up and afforded a yield of 94% of the desired cystine (**134**). For the Fmoc protection step, two trial reactions were carried out using Fmoc chloride³ and succinimide,⁵ which gave yields of 35% and 61% respectively and it was thus decided to continue with the use of the Fmoc succinimide. In the small scale synthesis, column chromatography had been used to purify the doubly protected

cystine residue (**135**). However, due to the size of column required for large scale purification, investigations into purification *via* recrystallisation were carried out. A number of different solvent systems were tried and it was found that the best yield of the product was obtained from a solution of 10% ethyl acetate in petrol, to give an overall yield of 60%, which was comparable to that obtained by column chromatography.

Unfortunately, on a large scale, it was found that reaction of the doubly protected cystine (**135**) with tributylphosphine to give cysteine (**62**) gave incomplete cleavage and led to difficulties in the separation of the starting material from the product. For this reason, it was decided to try using dithiothreitol, which is commonly used to cleave disulfide bonds in peptides and proteins,⁶ for the cleavage instead. The new reaction methodology both gave an increase in yield from 61% to 80% and was also much faster; while the phosphine reaction required 14 hours, the reaction with dithiothreitol could be carried out in 45 minutes and purification simply required washing, which meant that a large quantity of the doubly protected cystine could be produced from the starting cystine in less than an hour. Overall, the improvements to this route (Figure 2.4) helped to increase the yield from 12% to 45% over three steps, shortened the synthesis by two days and gave a robust method for the production of large quantities of the required cysteine residue (**62**) without the need for purification by column chromatography.

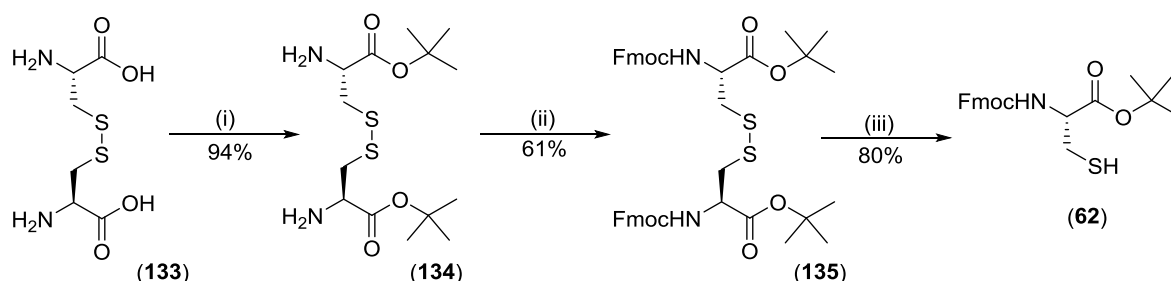


Figure 2.4: Large Scale Synthesis of the Doubly Protected Cysteine (**62**)

Reagents and Conditions: (i) $t\text{BuOAc}$, HClO_4 (ii) FmocOSu , NMM , THF (iii) dithiothreitol, Et_3N , CH_2Cl_2

Synthesis of the doubly-protected iodoalanine **139** unfortunately proved far more challenging on a large scale. The first step involving the trityl protection of serine initially proceeded in a 90% yield to give the product but upon repetition of this reaction, it was not possible to achieve such a high yield again. Whilst trying to solve this problem, another synthesis was published which involved first protecting the carboxylic acid with the allyl group and then trityl protecting the product.⁷ This one-pot procedure was particularly appealing as it required a shorter work-up and 24 hours less reaction time. For this reason, it was decided to swap to this procedure, which gave the doubly protected serine in excellent purity with an overall yield of 91%, which is an improvement on the 78% achieved over the previous two

step process (Figure 2.5). From here, the Mitsunobu reaction used during the initial synthesis produced the iodoalanine in 71% yield and was ready for the coupling reaction.

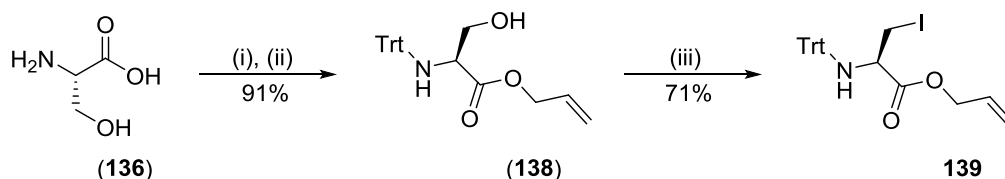


Figure 2.5: Synthesis of Doubly Protected Iodoalanine **139**

Reagents and Conditions: (i) allyl alcohol, para-toluene sulfonic acid, toluene, Dean-Stark Apparatus (ii) trityl chloride, Et₃N, DMF (iii) PPh₃, DEAD, CH₃I, CH₂Cl₂

2.2.2b Optimisation of the Coupling Procedure

Although the literature reports high yields for the coupling step (70%),⁴ a yield of only 38% was achieved for this step on a small scale. However, during the scale-up of the procedure, none of the desired product was formed. It is known that the reaction only proceeds under anhydrous conditions as the presence of water in the reaction can cause the loss of the Fmoc protecting group but no loss was observed. Analysis of the crude NMR spectra showed the presence of cystine, which brought into question the new reduction conditions. However, both NMR spectroscopy and mass spectrometry results showed that it was the cysteine not the cystine that was used in the coupling reaction. This was confirmed by testing the reagent with Ellmann's reagent⁸ (5,5'-dithiobis-(2-nitrobenzoic acid)) prior to addition, which turns vivid orange in the presence of a free thiol but does not react with a disulfide bond. The purity of the iodoalanine **139** was also confirmed by both NMR spectroscopy and mass spectrometry.

On closer inspection of the crude NMR spectrum obtained from the reaction mixture, it was found that in all cases, the iodoalanine **139** was rearranging in solution to give the aziridine **143**. This meant that the cysteine was then effectively stirring in solution with no other reactants present, which explains the oxidation to the corresponding cystine. It is known that the iodoalanine **139** easily rearranges in solution and this has in the past led to problems with the formation of the wrong regioisomer of lanthionine (Figure 2.6).³

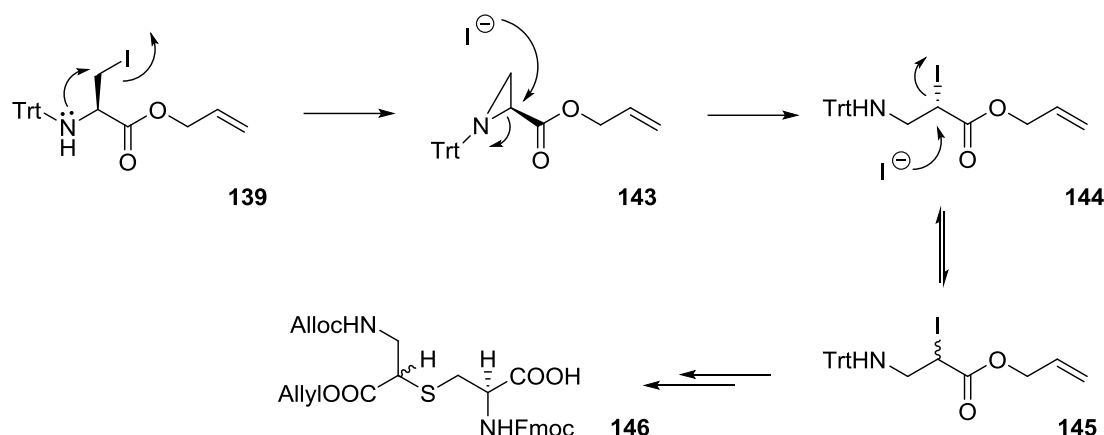


Figure 2.6: Formation of α -iodo- β -alanine Derivative **145** via the Aziridine **143** and Subsequent Reaction to Give Norlanthionine (**146**)

However, it was not immediately obvious why a reaction which had once proceeded in good yield would now no longer occur at all and instead produce large quantities of an unwanted side product. Thus, it was decided to investigate a number of different coupling strategies.

In 2003, Zhu and Schmidt⁹ reported phase transfer conditions using a bromoalanine derivative (**147**) to give the protected lanthionine (**149**) using tetrabutylammonium hydrogen sulfate in ethyl acetate and sodium hydrogencarbonate in water at pH 8.5 (Figure 2.7).

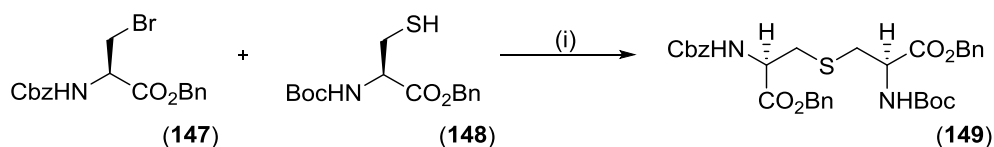


Figure 2.7: Phase Transfer Coupling Conditions
Reagents and Conditions: (i) pH 8.5 solution of NaHCO₃, tetrabutylammonium hydrogen sulfate, ethyl acetate

The disadvantage of this coupling method is that a competing elimination reaction forming the dehydroalanine causes formation of some of the other diastereoisomer (**151**, Figure 2.8).

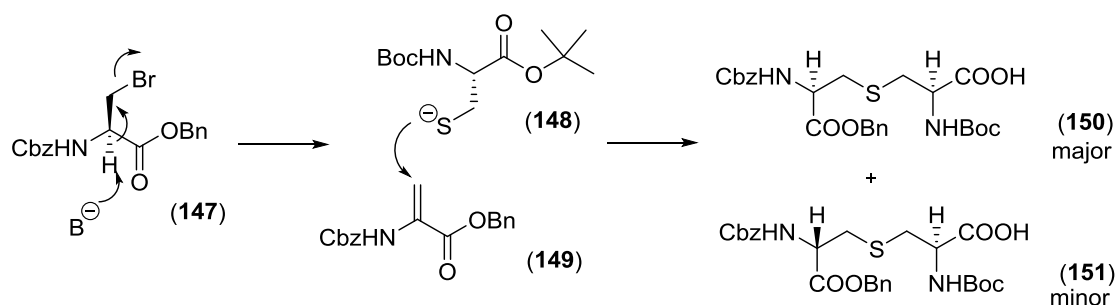


Figure 2.8: Formation of Diastereoisomers via Competing Elimination Reaction

In 2008, Vederas and co-workers¹⁰ published their own route to lanthionine which was two steps shorter than the Bregant and Tabor 2005 method,⁴ utilising the Zhu and Schmidt phase transfer method⁹ but again produced two diastereoisomers of lanthionine with a diastereoisomeric excess of 80%.

It was decided that the optimisation of the coupling step would involve three separate avenues of research:

- Investigations into the Vederas phase-transfer route,
- Combining the phase-transfer methodology with the Bregant and Tabor route,
- Optimisation of the Bregant and Tabor route.

i) Investigation into the Vederas Route¹⁰

The Vederas method uses the same doubly protected cysteine (**62**) described above. This was reacted with the allyl/Alloc protected bromoalanine derivative **153** in ethyl acetate in the presence of an aqueous solution of tetrabutylammonium bromide at pH 8.5 (Figure 2.9). In a similar manner to the iodoalanine **139**, **153** was produced by first carrying out a one-pot allyl/Alloc protection of serine to give the intermediate **152** in reasonable yield. This was then reacted in the presence of carbon tetrabromide and triphenylphosphine to give the product in 60% yield.

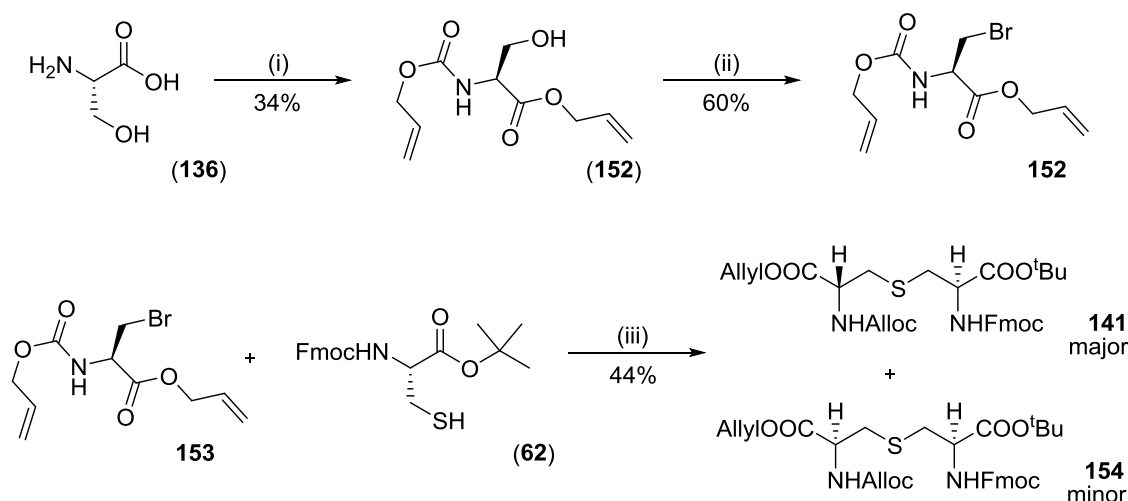


Figure 2.9: Vederas Route to Orthogonally Protected Lanthionine **141**

Reagents and Conditions: (i) 1. allyl alcohol, p-toluenesulfonic acid, toluene, Dean-Stark apparatus 2. allylchloroformate, Et₃N, ethyl acetate (ii) carbon tetrabromide, triphenylphosphine, dichloromethane (iii) NaHCO₃ (pH 8.5), tetrabutylammonium bromide, ethyl acetate

The coupling reaction gave the desired product in a 44% yield but, as with Vederas, a mixture of diastereoisomers was produced (83:17 ratio), which could not be separated. As it was also not possible to separate the diastereoisomers after the final deprotection step, it was decided not to carry this material on further.

ii) Hybrid Route Investigations

It was next decided to investigate combining the phase transfer conditions with the protected iodoalanine used by Bregant and Tabor (Figure 2.10).^{4,9} This has the advantage of avoiding

the elimination *in situ* and consequent diastereoisomer production observed in the Vederas method and could potentially eliminate some of the problems associated with the cesium carbonate coupling procedure.

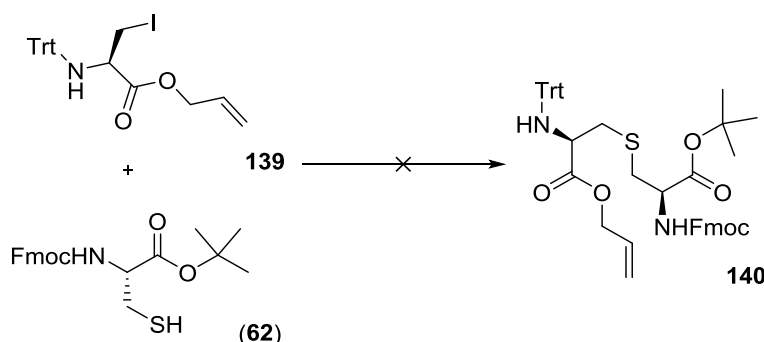


Figure 2.10: Hybrid Route to Formation of Lanthionine

Reagents and Conditions: aq. NaHCO_3 (pH 8.5), tetrabutylammonium bromide, ethyl acetate

However, in practice it was found that the conditions were too harsh for iodoalanine **139** and that the aziridine formed before any of the desired product could be obtained. The stability of **139** in pure water was next investigated and it was found that after just a few hours, the aziridine had already formed. It was thus decided to abandon this line of investigation.

iii) Optimisation of the Bregant and Tabor Route⁴

Whilst carrying out these reactions, it was realised that there had been a great discrepancy in the ambient temperature of the laboratory; in a given one year period, the temperature had varied over a 30 °C range. The best results for the coupling reaction had been achieved when the laboratory temperature was lower and so it was decided to trial the reaction at 4 °C rather than the previously reported room temperature. Reassuringly, it was found that the reaction once again proceeded as expected and that formation of the first protected lanthionine compound **140** could be achieved, albeit still in a low yield of 35%.

It was found that if the iodoalanine **139** is left to stir at 20 °C, the formation of aziridine **143** occurred faster than the desired coupling reaction. This explains the sudden apparent change in reactivity of the molecules and highlights the instability of the iodoalanine **139**. As it is less stable in solution than previously thought, it was decided to see if a more robust coupling procedure could be used before large scale coupling was attempted. All further investigations were carried out at 4 °C.

The first line of investigation was into the possibility of forming the iodo compound *in situ* by using a Finkelstein reaction to convert the allyl/trityl bromoalanine **155** (Figure 2.11).¹¹ It was hoped that decreasing the amount of time the iodoalanine was in solution could help to increase the overall yield of the coupling reaction. To form the bromo compound, the

chemistry used to form the allyl/Alloc protected bromoalanine **153** was again employed¹⁰ and produced the desired product from the allyl trityl serine (**138**) in 71% yield.

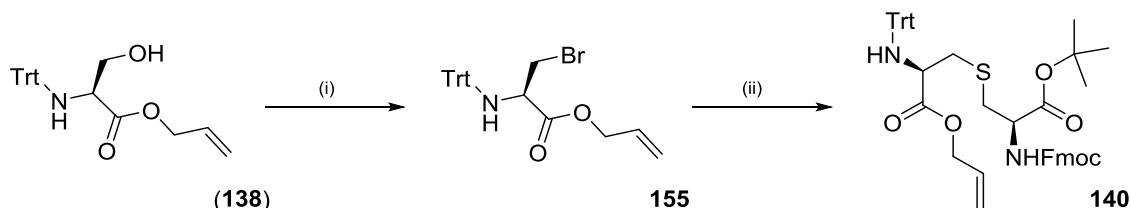


Figure 2.11: Formation of Doubly Protected Bromoalanine **155** and in situ Finkelstein Reaction Reagents and Conditions: (i) carbon tetrabromide, triphenylphosphine, CH_2Cl_2 (ii) 1 eq. (**62**), 10% sodium iodide, Cs_2CO_3 , DMF

In the first attempt, the sodium iodide was added before the cysteine (**62**). Crude NMR spectra showed that the aziridine had been formed during the reaction and this suggested that the Finkelstein reaction was occurring faster than expected. For this reason, the reaction was repeated with addition of the sodium iodide left until last, which gave the desired product in a 50% yield (Figure 2.12, entry 3). A series of reactions were then carried out trialling different amounts of sodium iodide both with the Bregant and Tabor⁴ allyl/trityl compound **139** and also with the Vederas¹⁰ allyl/Alloc **153** compound (Figure 2.12, Table 2.1).

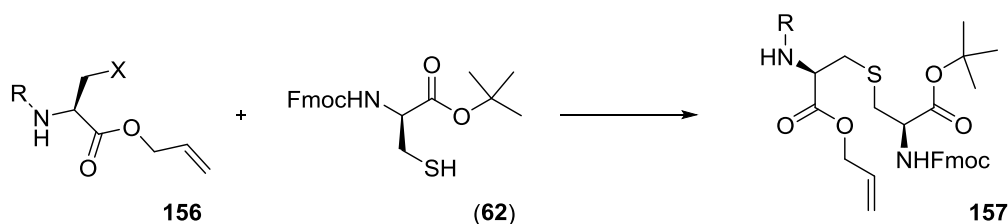


Figure 2.12: Summary of Results from Coupling Investigations

Entry	R	X	Method	Results
1	Alloc	Br	50 mg scale, 1 eq. Cs_2CO_3 then 10 mol% NaI	32% (83:17)*
2	Alloc	Br	200 mg scale, 1 eq. Cs_2CO_3 then 10 mol% NaI	27% (73:22)*
3	Trityl	Br	1 eq. Cs_2CO_3 then 20 mol% NaI	35%
4	Trityl	Br	1 eq. Cs_2CO_3 then 5 mol% NaI	48%
5	Trityl	Br	1 eq. Cs_2CO_3 only	39%
6	Trityl	I	1 eq. Cs_2CO_3 only	38%
7	Trityl	Br	10 mol% NaI then 1 eq. Cs_2CO_3	Aziridine formation
8	Trityl	Br	1 eq. Cs_2CO_3 then 10 mol% NaI	50%
9	Alloc	Br	1 eq. Cs_2CO_3 only	No reaction

Table 2.1: Summary of Results from Coupling Investigations (* indicates diastereoisomeric ratio, as determined by NMR)

As shown in table 2.1, coupling with the Alloc protected bromoalanine **153** gave a mixture of diastereoisomers, with more elimination occurring on a larger scale (Table 2.1, entries 8 and 9). Although the use of allyl/Alloc protected alanine does save two steps in the overall synthesis, the formation of both isomers prevents the use of this method, as they cannot be separated and would therefore be carried all the way through to the peptide synthesis stage.

Thus, it was decided to use the trityl protecting group and change to the Alloc group once the coupling step had been completed.

On increasing the amount of sodium iodide used from 10 to 20 mol%, the overall yield of the desired product decreased and more aziridine formation was observed (Table 2.1, entry 4). A decrease in sodium iodide to 5 mol% showed no change in the overall yield (Table 2.1, entry 5). Reaction of the bromoalanine **155** without the addition of sodium iodide also gave the desired product, showing that the bromoalanine on its own is sufficiently reactive at this scale (Table 2.1, entry 6).

For large scale synthesis, the bromoalanine compound **155** presents a far better choice of reagent for two reasons; firstly, it is stable at room temperature and does not form the aziridine by-product as readily and secondly, the synthesis is both quicker and easier and gives a greater yield (Table 2.1, entries 1 and 3). To form the bromoalanine, the protected serine was reacted with carbon tetrabromide and triphenylphosphine for 1 h at 0 °C.⁹ Purification *via* column chromatography gave **155** in high purity with a yield typically between 70% and 75%, while the iodoalanine Mitsunobu reaction conversely took 3 h at -10 °C and requires a more complicated column.

Hence, for the multi-gram scale coupling reaction, it was envisaged that bromoalanine **155** would be used in place of iodoalanine **139** (Figure 2.13).

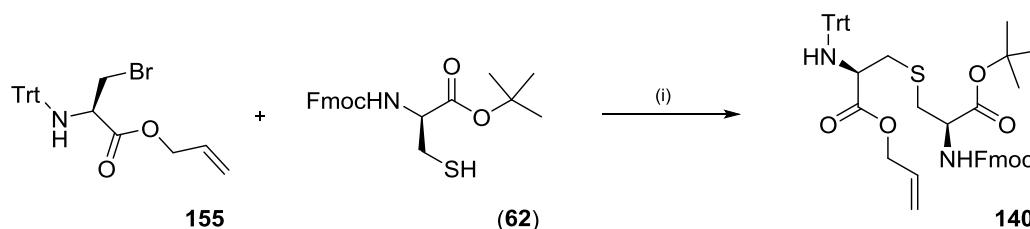


Figure 2.13: Proposed Large Scale Coupling Procedure
Reagents and Conditions: (i) 1 eq. Cs₂CO₃, 0.1 eq. I₂, DMF, 4°C, 4 h

Unfortunately, although this reaction proceeded well on a small scale, on a 1 g scale no reaction occurred, presumably because the S_N2 reaction with the bromoalanine **155** occurred at too slow a rate for a meaningful amount of product to be made in 4 h. Thus it was decided not to use **155** but rather to use the iodoalanine **139** for large scale coupling reactions.

It had already been established that the iodoalanine **139** was not stable in solution at room temperature. For this reason, a second line of investigation was carried out involving the use of *in situ* reactions. The advantage of an *in situ* method is that the iodoalanine would react as soon as it formed without the need for purification, in theory giving more of the desired product and reducing the amount of aziridine **143** produced. As well as testing previously

studied reactions, an alternative to the Mitsunobu reaction using triphenylphosphine and iodine was trialled. This reaction is well-documented within literature^{12,13,14} and provides a safe alternative to the use of DEAD, which carries the risk of explosion when used in larger quantities.

A trial reaction in which trityl allyl serine **138** was reacted with the iodine (Figure 2.14) was first performed. This resulted in a 4:1 ratio of product **139** to aziridine **143** in 80% yield.

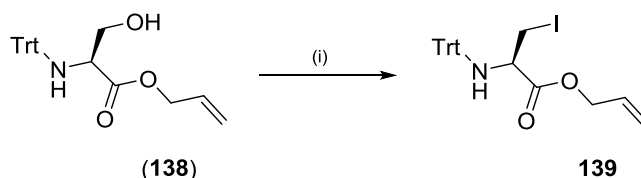


Figure 2.14: New Mitsunobu Conditions to give Iodoalanine **139**
Reagents and Conditions: (i) 1.25 eq. PPh_3 , 1.3 eq. Imidazole, 1 eq. I_2 , CH_2Cl_2

An *in situ* reaction in which the iodoalanine **139** produced was then reacted directly with cysteine (**62**) without intermediate purification was also trialled, to see if this could avoid the high proportion of aziridine formed. The results of this and all the other *in situ* experiments are summarised in the table below (Figure 2.15, Table 2.2).

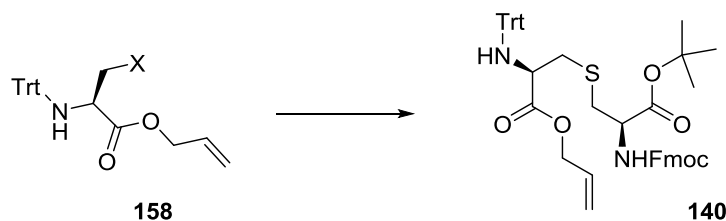


Figure 2.15: Summary of the *in situ* Investigations into Coupling Reactions

Entry	X	Conditions	Results
1	Br	1 eq. cysteine (62), 1 eq. Cs_2CO_3 then 10 mol% NaI	No product formed
2	OH	1) DEAD/ PPh_3 /MeI 2) 1 eq. cysteine (62), 1 eq. Cs_2CO_3	No product formed
3	OH	1) Imidazole/ PPh_3 / I_2 2) 1 eq. cysteine (62), 1 eq. Cs_2CO_3	27% over 2 steps

Table 2.2: Summary of the *in situ* Investigations into Coupling Reactions
All reactions were carried out on a 1 g scale.

As shown in table 2.2, both the scale-up of the *in situ* Finkelstein method (Table 2.2, entry 1) and the reaction of the iodoalanine **139** without intermediate purification (Table 2.2, entry 2) unfortunately yielded none of the desired product. It is possible no reaction occurred in the *in situ* Mitsunobu reaction because the phosphine and DEAD side products interfered with the reaction causing more aziridine **143** to form. The use of the alternative iodination conditions (Table 2.2, entry 3) gave rise to the formation of the desired product. The yield over the two steps is the same as that achieved with the original method. It was decided to compare this method to the improved original method of coupling the iodoalanine **139** at

4 °C to the protected cysteine (**62**) after purification. On a 1 g scale, 895 mg of product was produced, corresponding to a yield of 58% which was a great improvement in yield and far closer to the literature reported yield of 70%. Comparing like-for-like, the yield over 2 steps on a 1 g scale was 42% for this method, compared with 27% using the new iodination conditions.

In conclusion, after initial problems with scale-up of the coupling reaction, three possible routes were investigated. Use of the phase transfer conditions pioneered by Zhu and Schmidt⁹ gave rise to the formation of two diastereoisomers which could not be separated by column chromatography or recrystallization. Extensive investigations into the coupling reaction used by Bregant and Tabor⁴ showed that although the iodoalanine **139** is much less stable than previously thought, good yields can be achieved in this reaction providing the temperature of the reaction is controlled. Attempts to improve the yield through a variety of *in situ* one pot reactions unfortunately did not increase the efficiency of the reaction but did highlight the need for clean starting materials and decreased reaction temperatures (Figure 2.16).

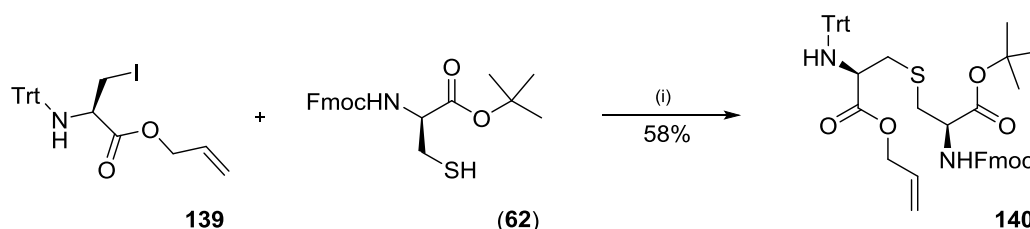


Figure 2.16: Large Scale Coupling Procedure
Reagents and Conditions: (i) 1 eq. Cs_2CO_3 , DMF, 4°C, 4h

2.2.2c Optimisation of the Trityl Deprotection and Alloc Protection Steps

In the original synthesis used in the Tabor group,⁴ a one-pot procedure involving removal of the trityl group and subsequent replacement with the Alloc protecting group was employed. However, on following this strategy, a low yield of 34% was obtained (Figure 2.17 and Table 2.3, entry 1). In order to produce multi-gram quantities of the orthogonally protected lanthionine **142**, it was also necessary to optimise this step. The reaction was repeated and the pH of the second step was monitored during the reaction. It was found to have dropped to pH 4 over the course of the first hour but the addition of extra base and allyl chloroformate showed a slight decrease in yield to 26% (Table 2.3, entry 2).

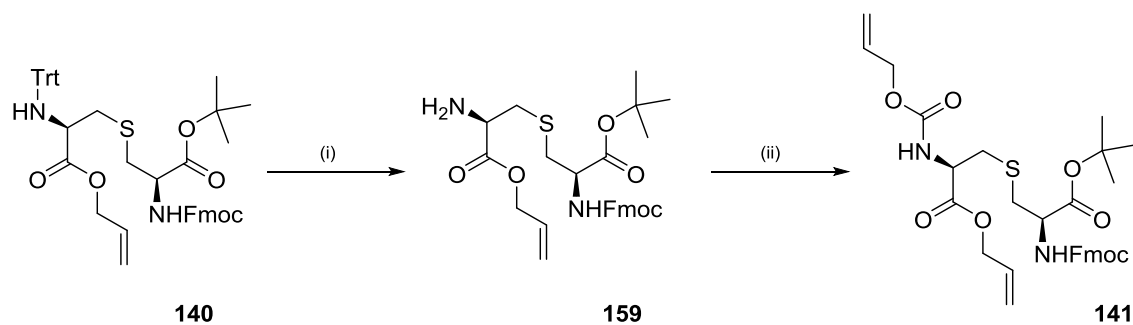


Figure 2.17: Reaction Conditions for Trityl Deprotection and Alloc Protection Steps

Entry	Reaction Conditions	Yield (i) (%)	Yield (ii) (%)	Overall Yield (%)
1	i) 10% TFA, 5% TES, CH ₂ Cl ₂ ii) 4 eq. NaHCO ₃ , 2 eq. allyl chloroformate, 1,4-dioxane	-	-	34
2	i) 10% TFA, 5% TES, CH ₂ Cl ₂ ii) 8 eq. NaHCO ₃ , 4 eq. allyl chloroformate, 1,4-dioxane	Crude = 91	Crude = 72	26
3	i) 10% TFA, 5% TES, CH ₂ Cl ₂ ii) 4 eq. NaHCO ₃ , 2 eq. allyl chloroformate, 1,4-dioxane	Column = 49	Crude = 99	49

Table 2.3: Reaction Conditions for Trityl Deprotection and Alloc Protection Steps

TES = triethylsilane, Overall Yield refers to yield after purification by column chromatography

It was observed that there was a significant drop in yield upon purification after the second step. Intermediate purification after the removal of the trityl group yielded the free amine **159** in 49% yield and Alloc protection gave the desired product in quantitative yield (Table 2.3, entry 3).

It was also found that yields of the first stage were quite low and further optimisation was required before large scale work could be carried out.

Waldmann and co-workers¹⁵ showed that changing the quantities of triethylsilane and trifluoroacetic acid used could help improve the yield. A series of trial reactions were carried out in which the quantities of these two reagents were varied (Figure 2.18 and Table 2.4).

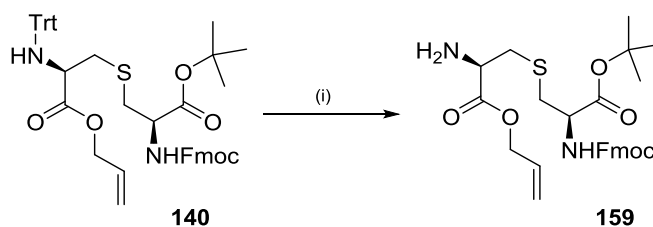


Figure 2.18: Results from Trial Deprotection Reactions

Entry	Amount of TFA (v/v, %)	Amount of Triethylsilane (v/v, %)	Conversion (%)*
1	10	5	49
2	1	3	70
3	10	10	63
4	5	10	100

Table 2.4: Results from Trial Deprotection Reactions (* conversion determined by NMR)

As the results show, the best yield was from using an excess of triethylsilane compared with trifluoroacetic acid. A large scale reaction using the conditions from entry 4 gave the desired product in a 64% yield (Figure 2.19).

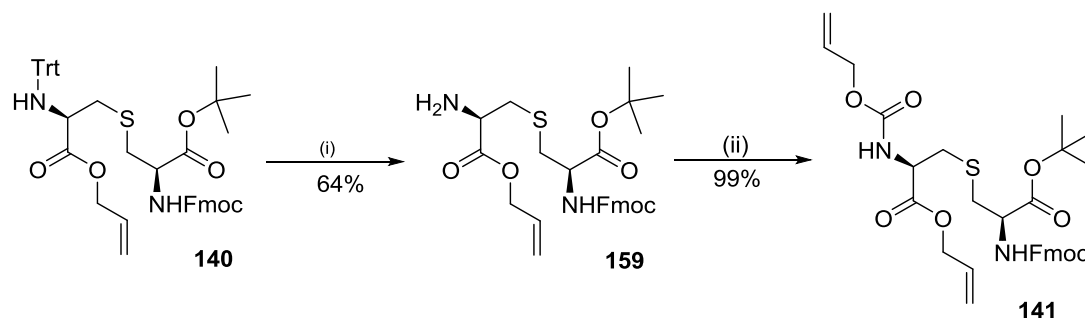


Figure 2.19: Summary of the Trityl to Alloc Protecting Group Reaction

Reagents and Conditions: (i) 5 mol% trifluoroacetic acid, 10 mol% triethylsilane (ii) Na_2CO_3 , allyl chloroformate, 1,4-dioxane

In conclusion, the breakdown of the one pot trityl deprotection and Alloc protection into two separate steps doubled the yield and resulted in the production of 500 mg of **141**.

2.2.2d Optimisation of the ^tBu Deprotection Step

Although the final deprotection progressed well with a yield of 70%, the work-up procedure was very involved and it was necessary to find an alternative purification procedure. The original procedure required the use of basic reverse phase column chromatography, followed by acidification of the aqueous layer and extraction with chloroform, before drying the organic layer and removing the solvent *in vacuo*. Although this method is adequate for small scale syntheses, this would become extremely cumbersome when using larger quantities of material.

In 2008, Vederas and co-workers¹⁰ published an alternative method for the production of orthogonally protected lanthionine in which purification of the final stage was carried out using recrystallisation from toluene. Pleasingly, this purification method worked with comparable yields (76% against 71% for the reverse phase column).

2.2.2e Conclusions from the Small Scale Synthesis Work

In order to produce multi-gram quantities of the orthogonally protected lanthionine **142** for peptide synthesis, it was necessary to spend time optimising each step to ensure the greatest

possible efficiency of the synthesis on a large scale. Improvements were made in the formation of the protected amino acid intermediates, which allowed for production of large quantities (over 100 g) of iodoalanine **139** and doubly protected cysteine (**62**).

In the case of iodoalanine **139**, the one-pot procedure to form trityl allyl serine (**138**) saves time and provides an easier purification procedure, whilst increasing the yield from 78% over two steps to 91% in a single step procedure. For the production of doubly protected cysteine (**62**), both the purification of the doubly protected cystine (**135**) *via* recrystallisation and the alternative cleavage procedure helped to increase the yield over three steps from 12% to 45%.

The greatest challenge was in improving the coupling of these two intermediates to form protected lanthionine **140**. A series of trial reactions were carried out using phase-transfer techniques and a variety of *in situ* methods. It was concluded that carrying out the reaction at reduced temperature gave the desired product in good yield (58%).

The trityl deprotection and Alloc protection steps were originally carried out in a one-pot process, giving an overall yield of 34%. Investigation into purification techniques showed that a higher yield was obtained by breaking the reaction into two steps and purifying at the intermediate stage. Subsequent investigations into the trityl deprotection step showed that changing the ratio of trifluoroacetic acid to triethylsilane significantly improved the yield of the first step. The new procedure gave a yield of 64% over the two steps, which was almost double the previous result.

Finally, investigations into an alternative purification for the production of the final product have found a recrystallisation technique which will save time and produce the desired product as white solid ready for solid phase peptide synthesis. The overall yield for the seven step synthesis starting from L-serine was 18% and resulted in the production of 120 mg of **142** (Figure 2.20).

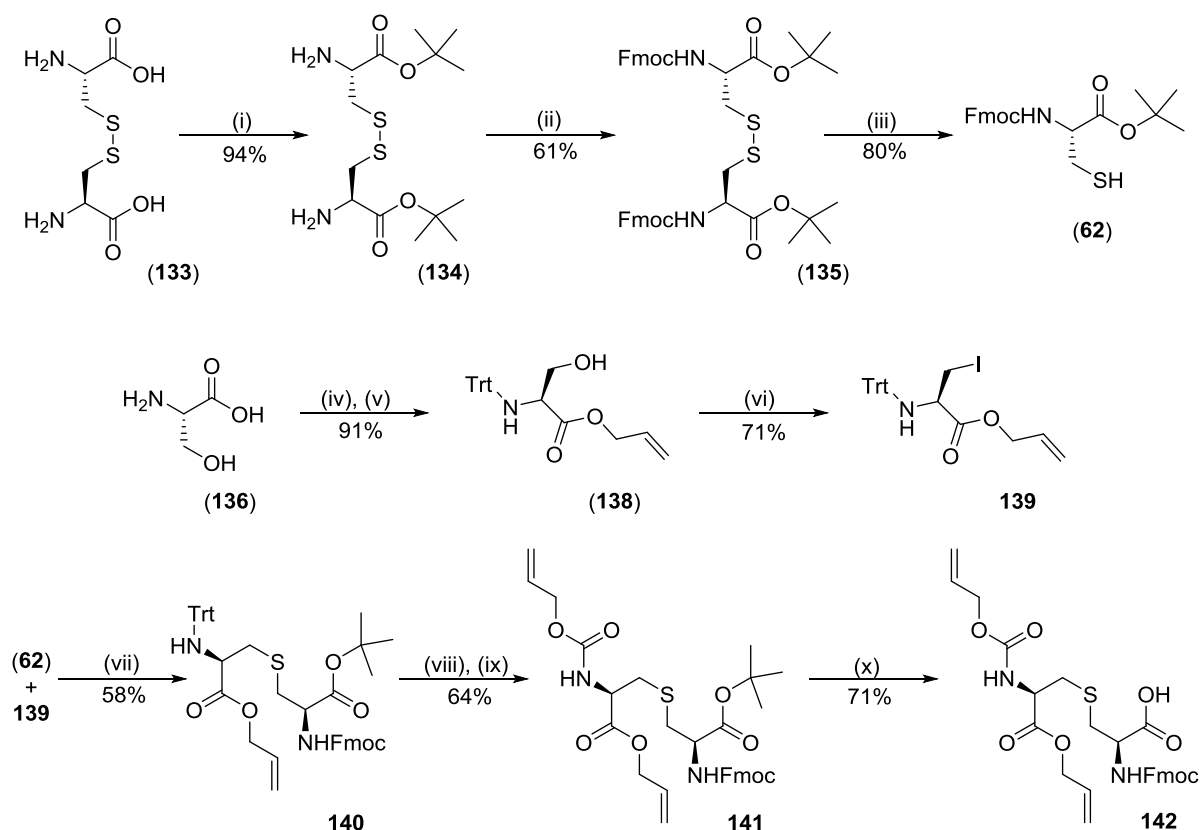


Figure 2.20: New Synthesis for the Production of Orthogonally Protected Lanthionine **142**
 Reagents and Conditions: (i) *t*BuOAc, HClO₄, (ii) FmocOSu, NMM, THF (iii) dithiothreitol, Et₃N, CH₂Cl₂ (iv) allyl alcohol, *para*-toluene sulfonic acid, toluene, Dean-Stark Apparatus (v) trityl chloride, Et₃N, DMF (vi) PPh₃, DEAD, CH₃I, CH₂Cl₂ (vii) Cs₂CO₃, DMF, 4°C (viii) 5 mol% trifluoroacetic acid, 10 mol% triethylsilane (ix) Na₂CO₃, allyl chloroformate, 1,4-dioxane (x) trifluoroacetic acid, triethylsilane, CH₂Cl₂

2.3 Large Scale Synthesis

The large scale synthesis was carried out at the European Knowledge Centre of Eisai Ltd. in Hatfield, UK. Preparation of trityl allyl serine (**138**) and doubly protected cystine (**135**) was outsourced to Oxygen Healthcare, Cambridge, UK, which is part of Piramal Enterprises Ltd, Mumbai, India, who produced 100 g of each compound following the procedures developed during the small scale investigations.

2.3.1 Reaction Monitoring and Safety Concerns^{16,17}

When scaling up reactions, a number of problems can be encountered; with large solution volumes, it is possible to have localised exotherms, which can arise from non-uniform stirring and can contribute to unwanted side reactions occurring in the reaction vessel. A second problem occurs with the overall volume: on a small scale, reactions tend to be more dilute to allow for meaningful volumes of solvent to be used. However, upon scaling up, these volumes can rapidly become too large to handle easily and so a more concentrated reaction mixture is often used. This again brings into question the possibility of unwanted side

reactions and exotherms. Before large scale synthesis could be carried out, it was important to carry out the synthesis on a medium scale to monitor all the temperature changes within the reaction vessel and to ensure all the steps behaved as expected.

This was particularly important for the Mitsunobu step to form iodoalanine **139** because the use of DEAD carries with it a risk of explosion. Although the replacement of DEAD with DIAD was investigated at this stage, none of the desired product formed, possibly due to the increased size of the ligand preventing the reaction occurring with the starting material.

The order of addition was also investigated. The generally accepted reaction is believed to proceed *via* the formation of a quaternary phosphonium salt (**162**). Attack by the alcohol (**163**) leads to formation of an alkoxy phosphonium intermediate (**165**), which is followed by an S_N2 displacement of the triphenylphosphine by an iodide nucleophile (**166**) to give the product (**167**, Figure 2.21).

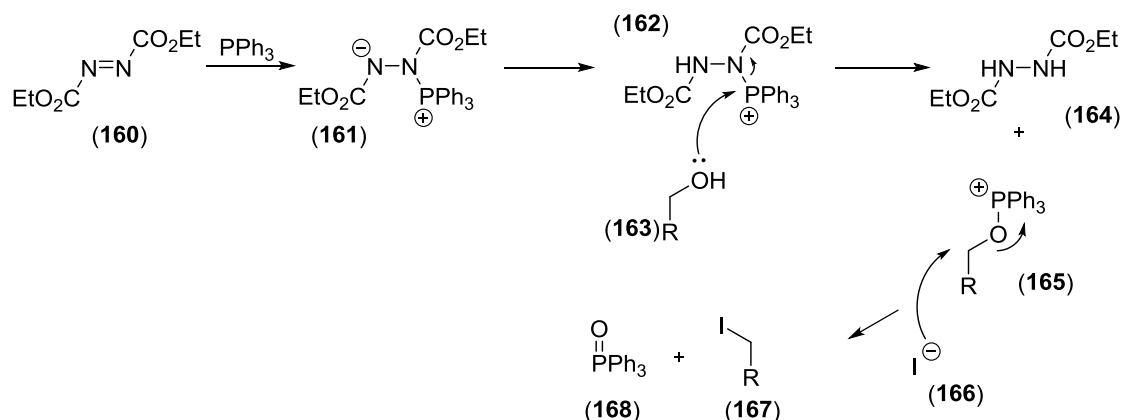


Figure 2.21: Generally Accepted Mechanism for a Mitsunobu Reaction¹⁸

In line with this procedure, the DEAD was added slowly to a stirred solution of PPh_3 in dichloromethane, followed by addition of methyl iodide and lastly addition of allyl trityl serine (**138**). The reaction was carried out on a 10 g scale to allow meaningful monitoring of the changes in temperature. A large spike was observed upon initial addition of DEAD from $-9.4\text{ }^\circ\text{C}$ to $+12.0\text{ }^\circ\text{C}$ and consequently addition was carried out slowly over 40 minutes. Similarly, the addition of methyl iodide triggered another rapid increase in temperature. Addition of allyl trityl serine (**138**) did not produce any significant change in temperature. Unfortunately, after the requisite 3 h, none of the desired product was formed and only unreacted starting material was retrieved from the reaction mixture. This was in line with previous observations within the group¹⁹ suggesting that the reaction did not follow the generally accepted mechanistic pathway. As the addition of DEAD caused a large increase in temperature, it was decided to try adding it in as a solution in dichloromethane.

The original method for forming the iodoalanine **139** involved dissolving the allyl trityl serine (**138**) and triphenylphosphine in dichloromethane and adding DEAD dropwise to the solution before adding methyl iodide. This reaction was repeated on a 10 g scale and the temperature and progress of the reaction was monitored. Again, the addition of DEAD in dichloromethane caused a large increase in temperature but careful slow addition ensured the temperature inside the vessel never exceeded 12.0 °C. Addition of methyl iodide also caused a sudden increase in temperature and it was decided to add the rest in a solution of dichloromethane as well. This again led to easier control of the temperature.

The reaction was followed by LC-MS (please see Appendix 1) and peaks corresponding to an allyl trityl serine-triphenylphosphine adduct **169** and both methylated **170** and non-methylated **164** DEAD side products were observed (Figure 2.22).

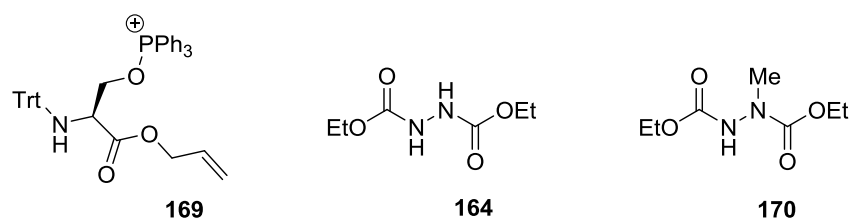


Figure 2.22: Possible Structures of Intermediates and Side Products Observed by LC-MS during the Mitsunobu Iodination Reaction

Current understanding of the Mitsunobu mechanism suggests that multiple pathways are at play, not just the one detailed in (Figure 2.21) above.^{20,21} Observations have shown other DEAD side products resulting from reaction with the nucleophile, which is in agreement with the formation of (**170**). As well as degradation pathways, it is also thought that a second phosphorous species (**172**) forms from reaction of triphenylphosphine with two alcohol molecules (Figure 2.23). In this case, two S_N2 displacements occur to give the desired product (**167**) and triphenylphosphine oxide (**168**).

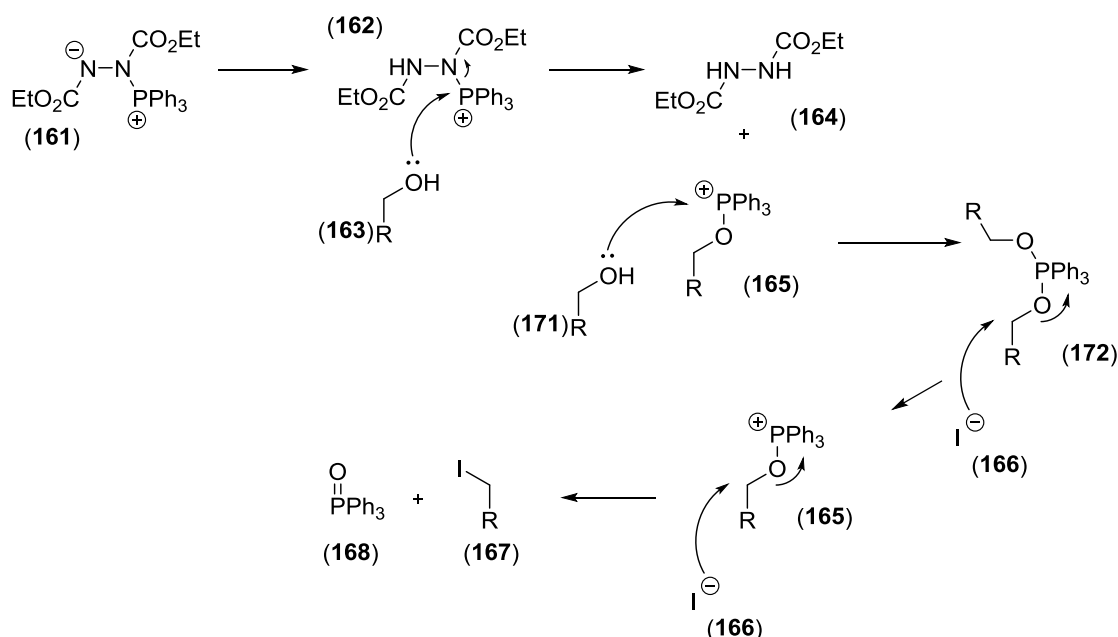


Figure 2.23: A Second Mechanistic Pathway for the Mitsunobu Reaction^{20,21}

The double addition product (**172**) was not observed in the LC-MS data collected during these reactions and the order of addition clearly plays an important role in this reaction. This suggests that perhaps the “traditional” Mitsunobu reaction is not occurring and that the role of the DEAD is actually that of an organic base. This is in agreement with the observation in the optimisation work that the reaction also works well when DEAD is replaced with imidazole, albeit giving a higher proportion of aziridine **143** formation. One reaction omitting the DEAD entirely and using just triphenylphosphine and iodine¹² was also tried but this did not lead to formation of any of the desired product, presumably due to the large amount of HI present, causing side reactions to occur.

A possible reaction mechanism for the iodination is detailed below (Figure 2.24). The presence of a triphenylphosphine-serine adduct (**163**) is confirmed. It is possible that this activated phosphine then reacts with the DEAD to give intermediate (**173**). Here the adduct can either methylate or protonate as shown (Figure 2.24, paths a and b). A final S_N2 displacement then gives the desired product, triphenylphosphine and the observed side products (**164**) and (**170**).

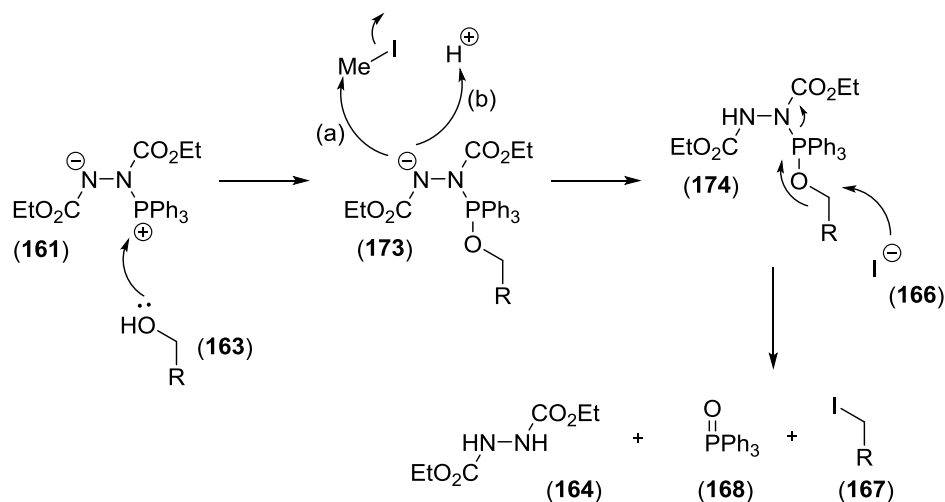


Figure 2.24: A Possible Mechanistic Pathway for the Iodination Reaction

Unfortunately, it was beyond the scope of this project to investigate this mechanism any further but this certainly suggests that the reaction is following an alternative mechanistic pathway.

The large scale reactions were carried out according to the original method described by Bregant and Tabor.⁴ The reaction proceeded to completion in 3 h, as observed when carried out on small scale and produced 8.4 g (65%) of the iodoalanine **139**. When carried out on a 30 g scale, 18.1 g of the desired product were formed. This was a slightly reduced yield of 47% but provided sufficient material to carry on with the synthesis.

2.3.2 Results and Summary of the Large Scale Synthesis Work

The Mitsunobu reaction provided the greatest safety concerns and although the temperature of all other reactions was monitored, no significant changes in temperature were observed.

The reduction of the doubly protected cystine (**135**) to produce cysteine (**62**) proceeded smoothly and produced 9.5 g from 10 g of starting material (95%). The improved reaction and work up meant that no further purification was required. This translated exactly on scale-up to produce 28.7 g from 30 g of starting material, which was again a yield of 95% and did not require further purification.

A trial coupling reaction using 7.36 g of iodoalanine **139** gave 6.84 g of the trityl protected lanthionine **140**, which was a yield of 61%. Scaling up the coupling reaction saw a slight decrease in yield to 48% but a total of 30 g of **140** was produced. Trityl deprotection saw a slight drop in yield to 55% and Alloc protection also saw a slight drop to 85%. Overall, 10.3 g of **142** was produced (Figure 2.25).

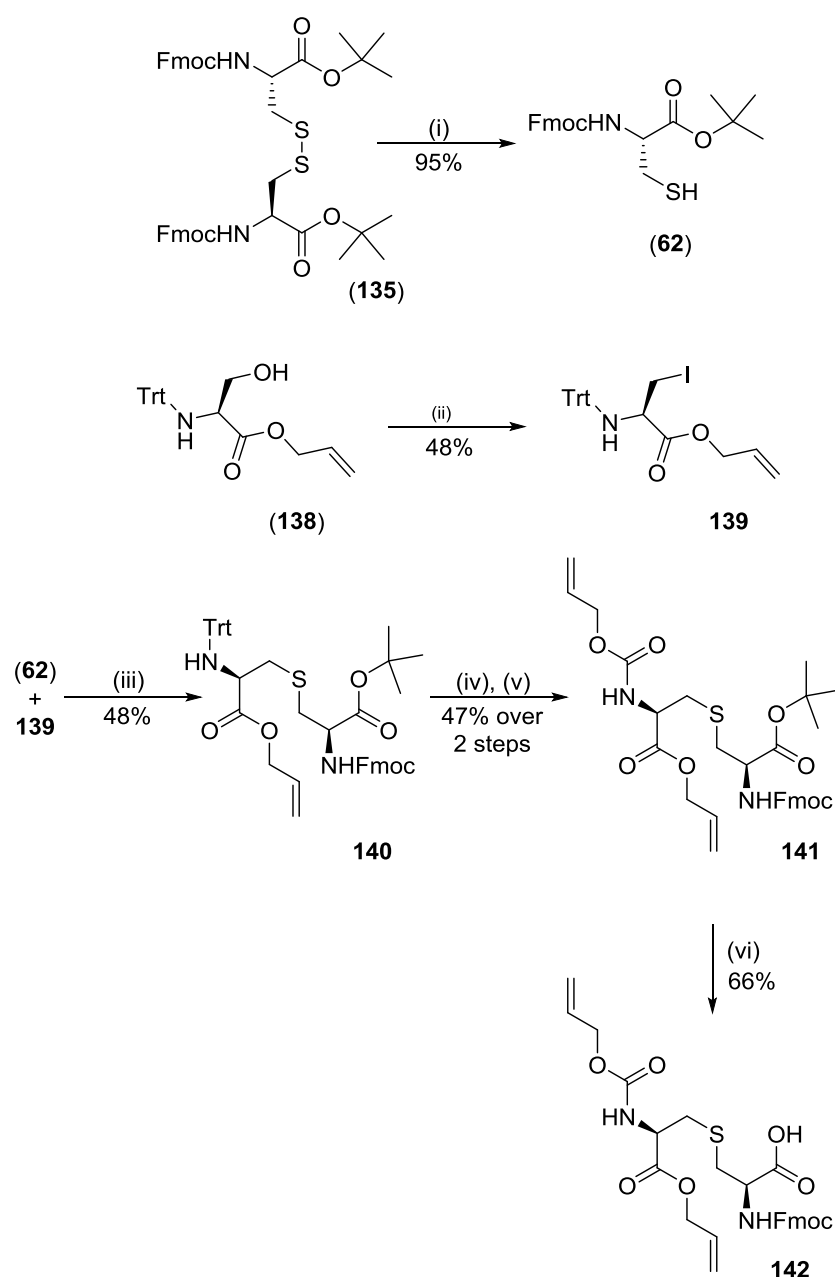


Figure 2.25: Summary of the Large Scale Synthesis

Reagents and Conditions: (i) dithiothreitol, Et_3N , CH_2Cl_2 (ii) PPh_3 , DEAD, CH_3I , CH_2Cl_2 (iii) Cs_2CO_3 , DMF, 4°C (iv) 5 mol% trifluoroacetic acid, 10 mol% triethylsilane (v) Na_2CO_3 , allyl chloroformate, 1,4-dioxane (vi) trifluoroacetic acid, triethylsilane, CH_2Cl_2

The aim of this work was to produce approximately 10 g of **141**. It was not known whether or not the removal of the ^tBu affected the stability of the compound and so only half of this material was used in the final step. The rest was stored as **141** for use at a later point. The large scale recrystallisation proceeded well with 3.00 g (66%) of white crystals produced. Starting from trityl allyl serine (**138**), the yield was 10% over 4 steps at large scale and 18% on a 10 g scale, which provided enough material to carry out multiple peptide syntheses.

2.4 Conclusions

Extensive research into the synthesis of orthogonally protected lanthionine resulted in the design of an improved, more robust route which worked well on a small scale. Improvements were made in the protection of the constituent amino acids both in the reaction and purification procedures, which allowed the synthesis of the intermediates to be outsourced. Re-evaluation of the coupling procedure highlighted the instability of the iodoalanine intermediate **139** and showed that reducing the temperature of the reaction could help control the reaction and prevent unwanted side reactions from occurring. A change in reactant ratio improved the efficiency of the trityl deprotection reaction. Breaking the one-pot deprotection and subsequent Alloc re-protection into a two-step process increased the yield. Finally, a change in purification procedure of the final deprotection decreased the time taken to produce the final product and also gave the product in higher purity.

Pleasingly, this route also translated well to large scale processing and it was possible to use this method in an industrial setting to produce multi-gram quantities of the desired novel diastereoisomer of lanthionine **142**. Investigations into the large scale Mitsunobu reaction showed that the reaction occurred by a non-conventional mechanism which could be controlled by careful addition of the reactants in solution with dichloromethane, thereby decreasing the risk of unexpected exotherms and explosions. The synthesis progressed well and produced 3.00 g of orthogonally protected lanthionine **142**, which can now be incorporated into peptides and allows a full and thorough investigation of the structure-activity relationship of the Na_v1.7 ion channel to be carried out.

¹Schmalhofer, W. A.; Calhoun, J.; Burrows, R.; Bailey, T.; Kohler, M. G.; Weinglass, A. B.; Kaczorowski, G. J.; Garcia, M. L.; Koltzenburg, M.; Priest, B. T., *Mol. Pharmacol.*, **74**, 1476-1484 (2008)

²Tabor, A. B., *Org. Biomol. Chem.*, **9**, 7606-7628 (2011)

³Mustapa, M. F.; Harris, R.; Esposito, D.; Chubb, N. A. L.; Mould, J.; Schultz, D.; Driscoll, P. C.; Tabor, A. B., *J. Org. Chem.*, **68**, 8193-8198 (2003)

⁴Bregant, S.; Tabor, A. B., *J. Org. Chem.*, **70**, 2430-2438 (2005)

⁵Swali, V.; Matteucci, M.; Elliot, R.; Bradley, M., *Tetrahedron*, **58**, 44, 9101-9109 (2002)

⁶Muttenthaler, M.; Andersson, A.; de Araujo, A. D.; Dekan, Z.; Lewis, R. J.; Alewood, P.F., *J Med Chem.*, **53**, 8585-8596 (2010)

⁷Liu, W.; Chan, A.S.H.; Liu, H.; Cochrane, S.A.; and Vederas, J.C., *J. Am. Chem. Soc.*, **133**, 14216-14219 (2011)

⁸Ellman, G. L, *Arch. Biochem. Biophys.*, **82**, 1, 70-77 (1959)

⁹Zhu, X.; Schmidt, R. R., *Eur J Org Chem*, **20**, 4069-4072 (2003)

¹⁰Pattabiraman, V. R.; McKinnie, S. M. K.; Vederas, J. C., *Angew. Chem. Int. Ed.*, **47**, 9472-9475 (2008)

¹¹Finkelstein, H., *Eur. J. Inorg. Chem.*, **43** (2), 1528-1532 (1910)

¹²Donohoe, T. J.; Winship, P. C. M.; Tatton, M. R.; Szeto, P., *Angew. Chem. Int. Ed.*, **50**, 7604-7606 (2011)

¹³Trost, B. M.; Rudd, M. T., *Org. Lett.*, **5** (24), 4599-4602 (2003)

¹⁴Hattori, Y.; Asano, T.; Kirihaata, M.; Yamaguchi, Y.; Wakamiva, T., *Tet. Lett.*, **49** (33), 4977-4980 (2008)

-
- ¹⁵ Kadereit, D.; Deck, P.; Heinemann, I.; Waldmann, H., *Chem. Eur. J.*, **7**, 6, 1184-1193 (2001).
- ¹⁶ EHSC note on Scale up of Chem reactions v2, Royal Society of Chemistry,
<http://www.rsc.org/ScienceAndTechnology/Policy/EHSC/ScaleUp.asp> (last accessed 08/02/2015)
- ¹⁷ Stoessel, F., *Curr. Opin. Drug Discov. Devel.*, **4** (6), 834-839 (2001).
- ¹⁸ Mitsunobu, O., *Synthesis*, **1**, 1-28 (1981)
- ¹⁹ Mustapa, M. F. M., *Synthesis of Lanthionine-Containing Peptides on Solid Phase via an Orthogonal Protecting Group Strategy*, PhD Thesis, University College London (2002)
- ²⁰ But, T. Y. S.; Toy, P. H., *Chem. Asian J.*, **2**, 1340-1355 (2007)
- ²¹ Schenk, S.; Weston, J.; Anders, E., *J. Am. Chem. Soc.*, **127**, 12566-12576 (2005)

3. Chapter 3: Synthesis of ProTx-II (22) and Truncated Analogues

This chapter details the attempts to synthesise ProTx-II (22) and a group of truncated analogues which were tested for their ability to bind to the Na_v1.7 ion channel. To begin with, a group of analogues were synthesised based on truncated sections of the original peptide by dividing it into units as determined by the disulfide rings. This gave a total of three single and two double ring analogues (compounds 175 – 179, Figure 3.1).

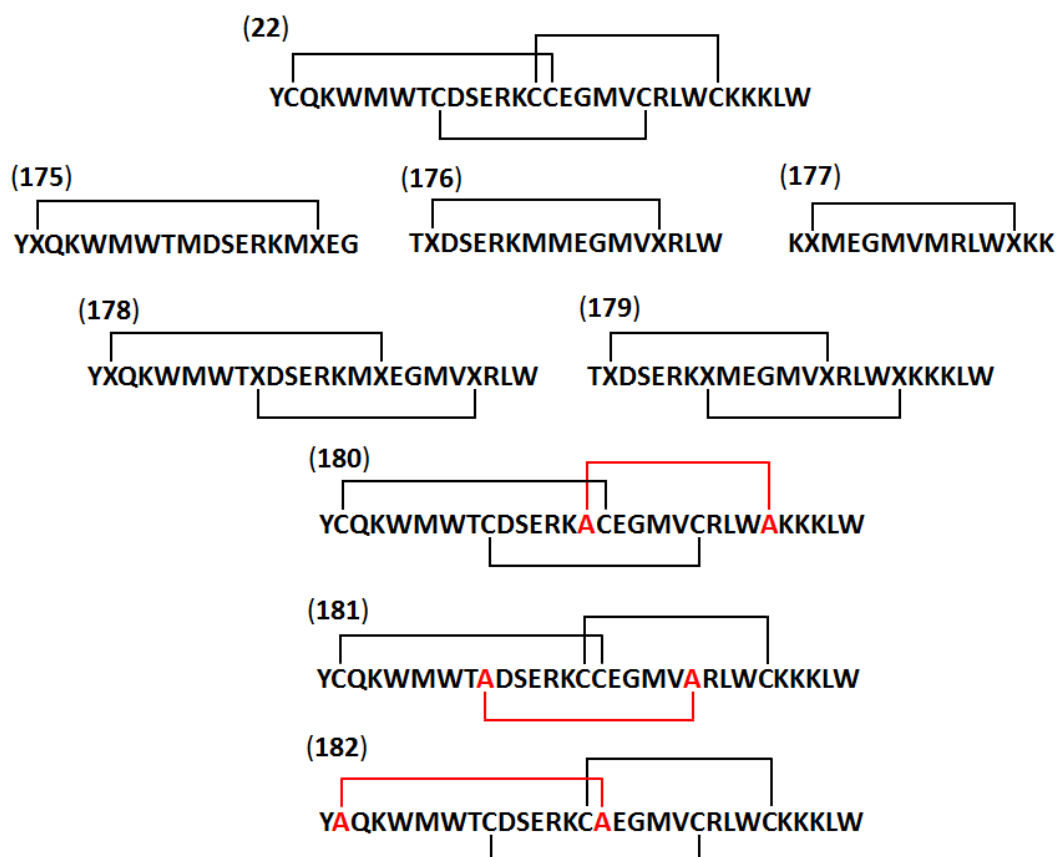


Figure 3.1: Structure of ProTx-II (22) and Suggested Analogues for Synthesis
X = either cysteine or lanthionine to give a disulfide or thioether bond, A = lanthionine bond

The next group of analogues investigated the effect of replacing one of the disulfide bonds in the ProTx-II (22) structure with a thioether linkage by the addition of an orthogonally protected lanthionine moiety. This had the dual advantage of both preventing the degradation of the peptide ring by disulfide cleavage and decreasing the ring size to see if this subtle alteration has an influence on binding affinity. To investigate the incorporation of a thioether linkage in to the SPPS protocol, a methodology study was carried out using a single ring structure for simplicity before attention was focussed on the full analogues of ProTx-II (22).

3.1 Synthesis of ProTx-II (22)

ProTx-II (22) is extracted from the venom of the Peruvian Green Velvet Tarantula¹ (*Thrixopelma pruriens*). Although it is possible to purchase the venom commercially, it is very expensive (£109 for 100 µg on Sigma Aldrich) so it was first necessary to investigate the chemical synthesis.

To make the straight chain sequence (YCQKWMWTCDSEKCCGMCRLWCKKKLW), standard Fmoc SPPS protocols were used. The initial synthesis provided a low yield of the crude peptide, which prompted a short investigation into peptide cleavage times (Table 3.1).

Standard cleavage of the peptide from an acid labile resin uses a cocktail of TFA, ethanedithiol, triisopropylsilane and water in the ratio 95:2.5:1:1.² Traditionally, this is left for 3 h before collecting the cleavage solution² and precipitating it into diethyl ether. In this case, it was found that two shorter cleavage times (Table 3.1, Entries 2 and 3) gave a higher yield of crude peptide.

Entry	Cleavage Time 1 (min)	Cleavage Time 2 (min)	Cleavage Time 3 (min)	Yield
1	180	-	-	11%
2	30	60	90	22%
3	30	70	-	23%

Table 3.1: Short Investigation into Cleavage Times

It is known that tryptophan can re-attach to the resin³ if left for a long period of time and so it is likely that the shorter reaction time allows for cleavage of the peptide from the resin but does not allow time for the counter reaction to occur. For the rest of this work, this double cleavage procedure was followed.

3.1.1 Cyclisation and Structure Determination of ProTx-II (22)

In 2002, Middleton *et al.*¹ published the chemical synthesis of ProTx-II (22). They also employed standard SPPS protocols to make the straight chain sequence of ProTx-II (22) and claimed that upon cleavage from the resin, the peptide could be cyclised by dissolving the peptide in a solution containing 2 M Urea, 0.1 M Tris buffer (pH 8.0) and a mixture of reduced and oxidised glutathione. However, attempts to re-create these conditions did not yield any of the desired product (Table 3.2, Entry 1). A change in concentration also did not produce the cyclised peptide (Table 3.2, Entry 2). After investigating another buffer, it was found that the peptide could easily be cyclised in pure water at a concentration of 0.1 mg/mL. This method has the advantage of not requiring dialysis to

remove the peptide from the buffer solution and instead the volume of solvent can be reduced *in vacuo* and then purified directly by HPLC.

Entry	Conditions	Results
1	Water, Urea, Tris, Glutathione (peptide conc. - 0.1 mg/mL)	No product or starting material
2	Water, Urea, Tris, Glutathione (peptide conc. - 0.02 mg/mL)	No product or starting material
3	Phosphate Buffer	Starting material only
4	Water (rt, 2 days)	No product or starting material
5	Water – 3 days (~10 °C)	Inseparable mixture of cyclised and uncyclised peptide
6	Water – 7 days (~10 °C)	Cyclised peptide
7	Water – 14 days (4 °C)	Cyclised peptide

Table 3.2: Investigation into Cyclisation Conditions

The cyclised peptide loses six protons from the sulfhydryl side chains on the cysteines to form three disulfide bonds, giving the native peptide mass of 3826 Da. Although the reaction can be followed by observing the decrease in mass using an LC-MS machine, this method does not give information on the connectivity of the disulfide bonds. There are 15 possible combinations for bonding the six cysteine residues and Middleton *et al.*¹ determined the connectivity using a double digestion protocol in conjunction with MALDI analysis (Figure 3.2). Firstly, the peptide was dissolved in Tris buffer and subjected to trypsin digestion to cleave in six places (Figure 3.2). This was followed by the addition of the Glu-C enzyme to cleave between the glutamate and glycine residues. Assuming the correct connectivity, this should give rise to two major fragments: the first containing the 2–5 disulfide bond and the second containing the other four cysteine residues with masses of 1776 and 1438 amu respectively.

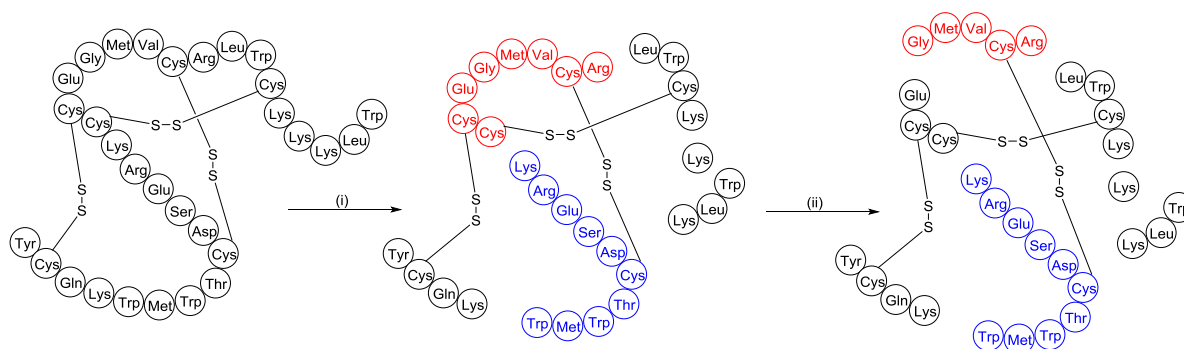


Figure 3.2: Double Digestion of ProTx-II

Reagents and Conditions: (i) Trypsin Digestion (ii) Glu-C Digestion

On repetition of this protocol, the mass of 1438 was observed but a number of problems were also encountered. In the case of a system as tightly bound together as an ICK peptide, it was difficult to cleave with trypsin at all six sites on the peptide. This led to a complex mass spectrum, comprised of many fragments of ProTx-II as well as the trypsin

and Glu-C enzymes. To add to this difficulty, some oxidation of ProTx-II was also observed. Attempts to decrease complexity of the spectrum by using resin-bound trypsin removed the trypsin peaks from the data but did not prevent the incomplete cleavage and oxidation problems previously observed.

Middleton *et al.* continued with the structure determination by using post-source decay (PSD) experiments to show the final connectivity; it was claimed that the PSD experiment cleaved the amide bond between the two cysteine residues to give the two separated fragments, each containing a disulfide bond. The difference in mass in this case will be determined by which fragment contains the glutamate residue, which will in turn conclude the connectivity (Figure 3.3).

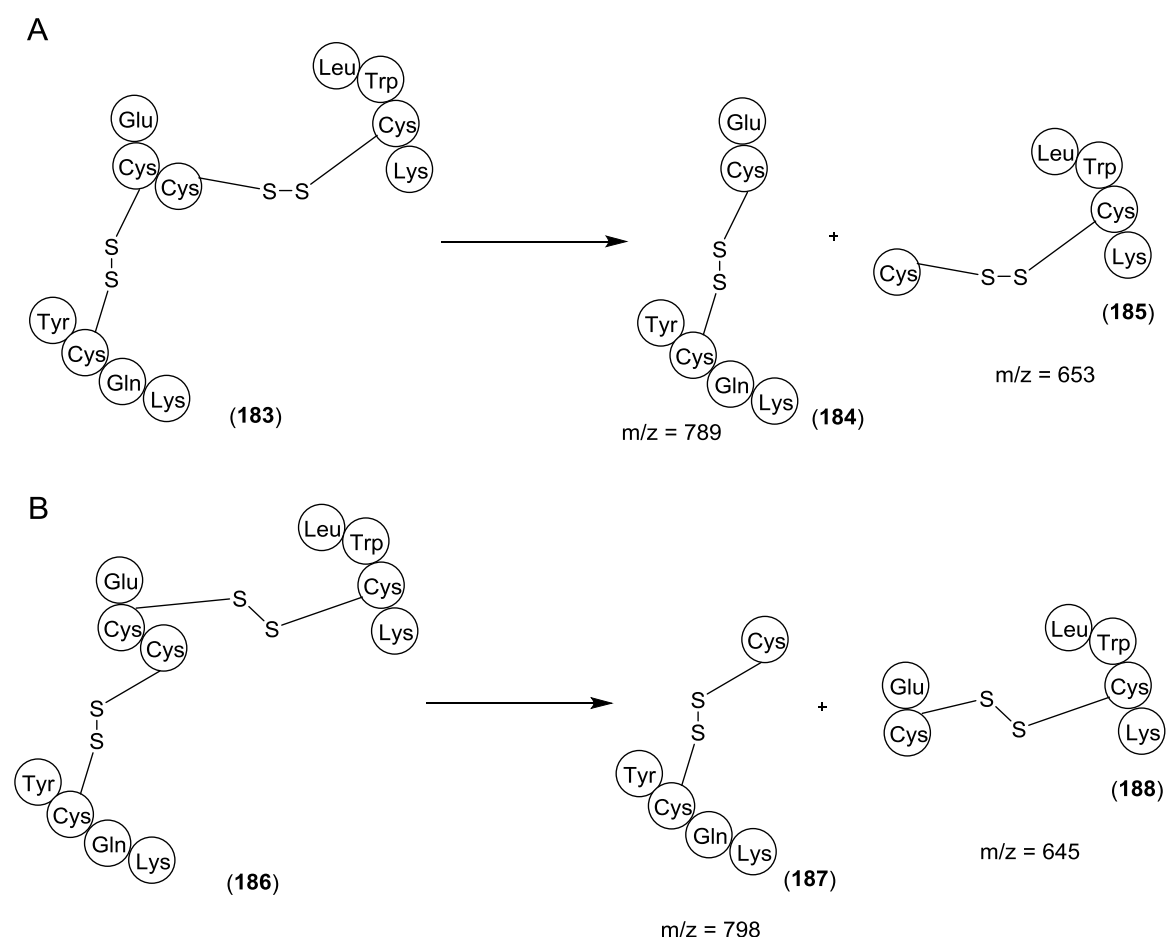


Figure 3.3: PSD Experimental Results
A – correct connectivity, B – incorrect connectivity

As the name suggests, fragmentation in a post source decay experiment occurs after the acceleration region of the mass spectrometer. The fragmentation observed is due to metastable ions breaking down as a result of the excess energy they possess as they leave the source but before they reach the detector. In general, the efficiency of this type of fragmentation is low and tends to result in a high level of background noise.⁴

When using metastable ions as the source for an experiment, it is difficult to control exactly which bonds are broken during post source decay and it was not possible to reproduce the experimental data from the PSD experiments.^a Thus, using this method, the connectivity was narrowed down to two possible structures, containing either 1-3 and 4-6 disulfide bonds or the desired 1-4, 3-6 disulfide bonds (Figure 3.4).

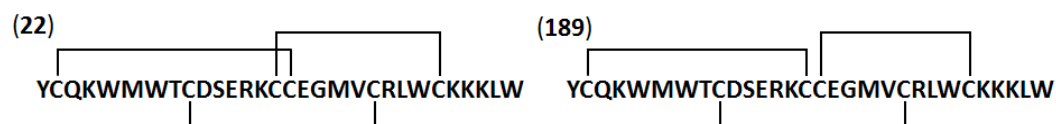


Figure 3.4: Possible Connectivity in Synthesised ProTx-II
A – correct connectivity, B – incorrect connectivity

In 2004, Chagot *et al.*⁵ published structural NMR data on the related peptide PaTx-I, which shares 83% homology with ProTx-II (Figure 3.5).

ProTx-II (22): YCQKW MWTCD **SER**KC CEG**MV** CRLWC **KKKLW**
PaTx-I (190): YCQKW MWTCD **SAR**KC CEG**LV** CRLWC **KKII**

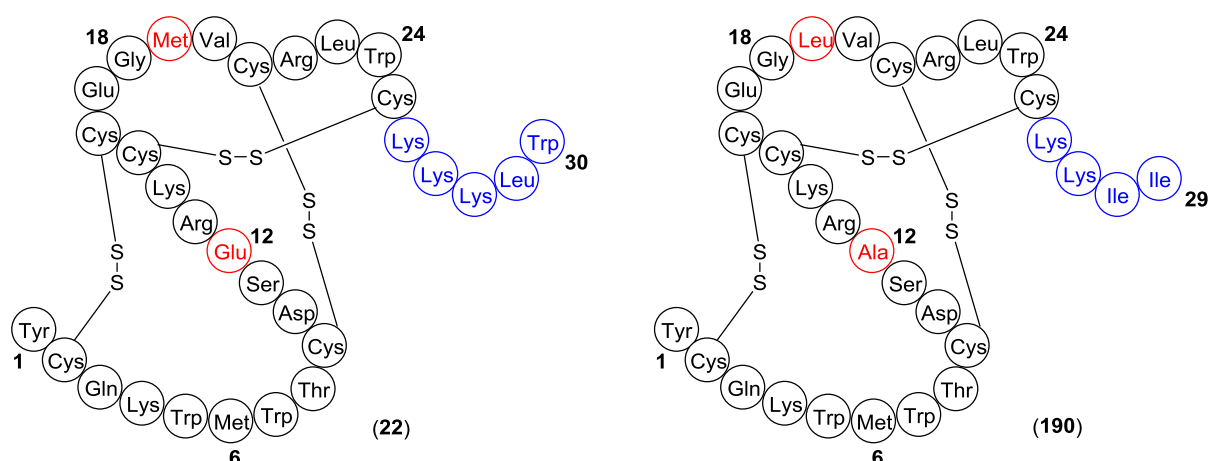


Figure 3.5: Structures of ProTx-II (22) and PaTx-I (190)

Aside from the flexible C-terminal, PaTx-I and ProTx-II share only two differences in amino acids at positions 12 and 19. From this data, it was reasonable to assume that, although the PSD experiments described by Middleton *et al.* could not be repeated, the correct connectivity could be assigned as the desired 1 – 4, 2 – 5, 3 – 6 binding observed in all reported ICK peptides. This structure was finally confirmed with the release of a solution NMR structure of ProTx-II by Park *et al.*⁶ in 2014 (Chapter 5).

As mentioned previously, it is possible to purchase ProTx-II from commercial sources. In almost all cases, it is made synthetically rather than isolated directly from the tarantula, due to the low quantities obtained from venom and the large degree of purification required. To add to the body of evidence that the ProTx-II synthesised in-house was the

^a Post-Source Decay Experiments were carried out by Dr. C. Hyde, University College London

same as that purchased commercially, analytical HPLC analysis was run using a gradient of 5 – 95% acetonitrile (0.1% TFA) in water (0.1% TFA) (Figures 3.6 - 3.8).

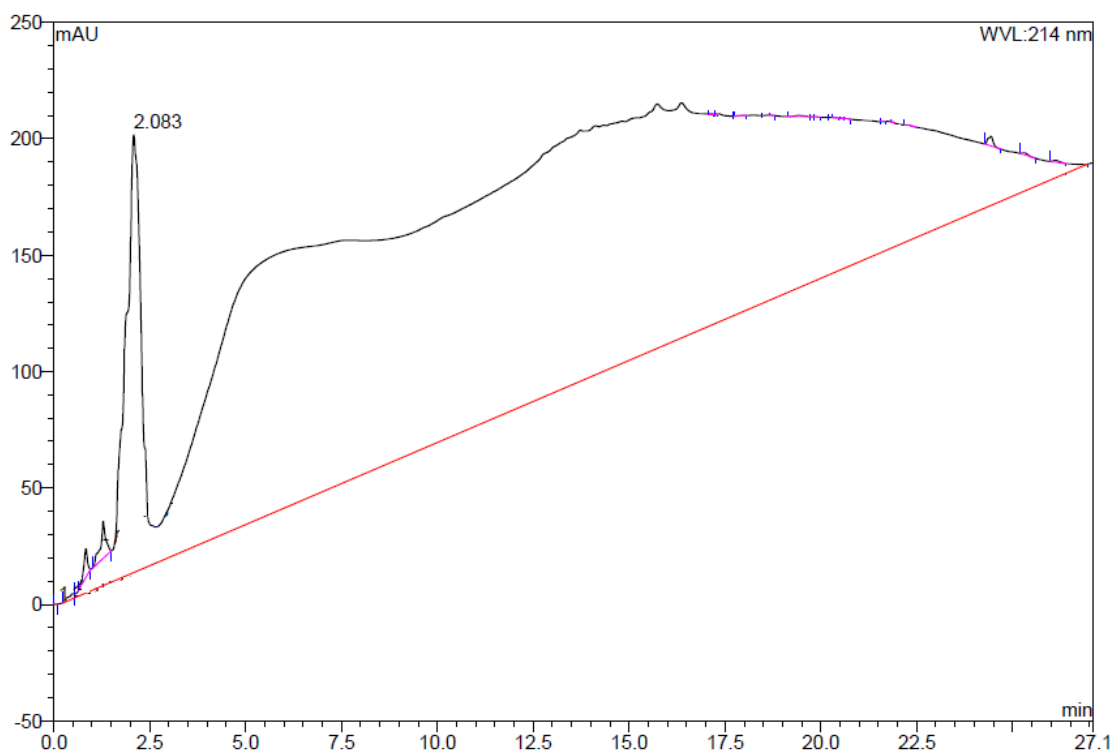


Figure 3.6 HPLC Trace Showing Injection of Synthesised ProTx-II

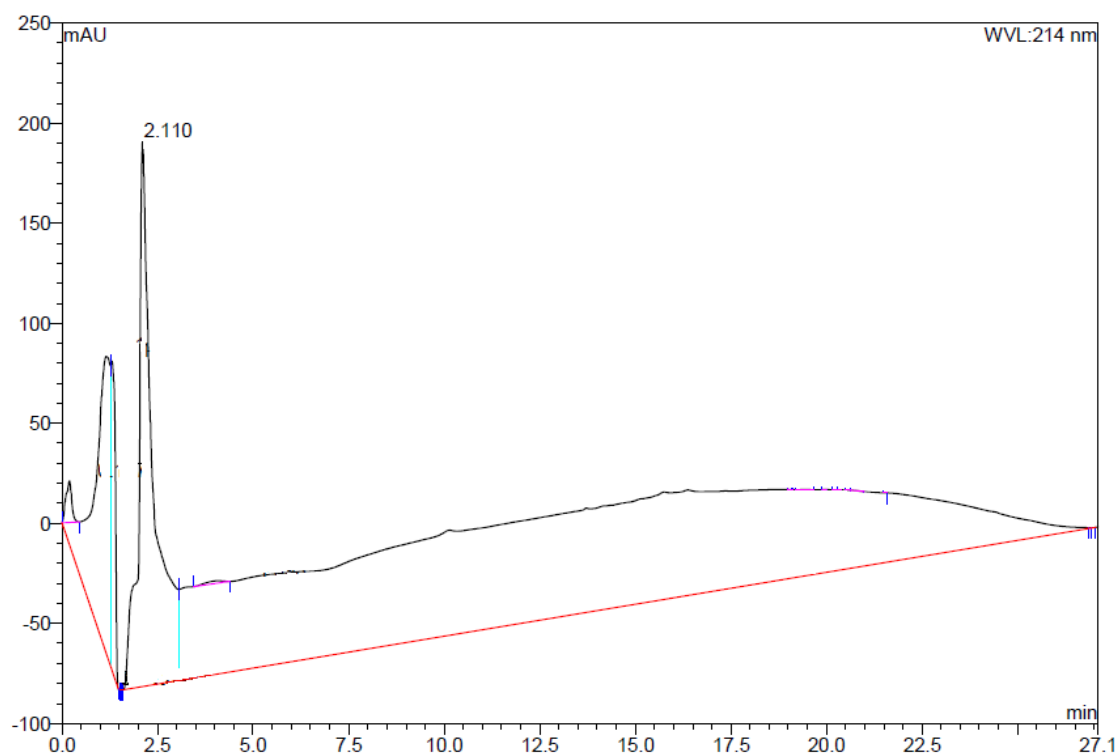


Figure 3.7: HPLC Trace Showing Injection of Purchased ProTx-II

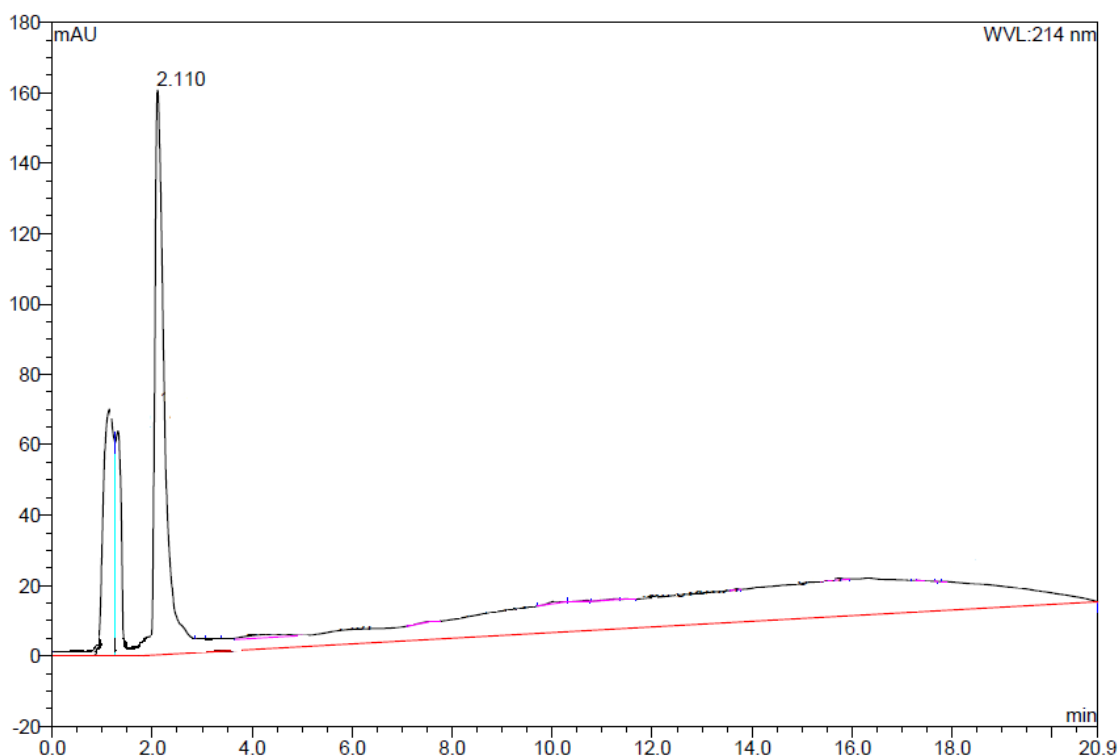


Figure 3.8: HPLC Trace Showing Combined Injection of Synthesised and Purchased ProTx-II

HPLC data has shown that the traces of commercially available peptide purchased from Tocris and that synthesised in house overlap, which suggests that the connectivity of these peptides is likely to be the same.

3.2 Synthesis of Disulfide Bridge Truncated Analogues

ProTx-II (**22**) was shown to have good inhibitory effects of the $\text{Na}_v1.7$ channel *in vitro* but showed comparatively poor results *in vivo*, owing to difficulties in crossing the blood-nerve barrier.⁷ With no crystal structure of the ion channel currently available, it is difficult to know which part of the peptide is important in binding. To investigate this, a series of smaller analogues based on truncated sections of the original peptide were synthesised.

3.2.1 Synthesis of Single Ring Disulfide Analogues

The simplest compounds investigated in this thesis are the single ring disulfide analogues of ProTx-II (**22**). The structures of these compounds are determined by the disulfide bonds in the original peptide to give small cyclic peptides of 14 – 18 amino acids in length (Figure 3.9). A recent publication by Park *et al.*⁶ has shown that the tail fragment KKKLW is important in binding. To test this theory, two versions of the C-terminal ring were made with and without the tail fragment.

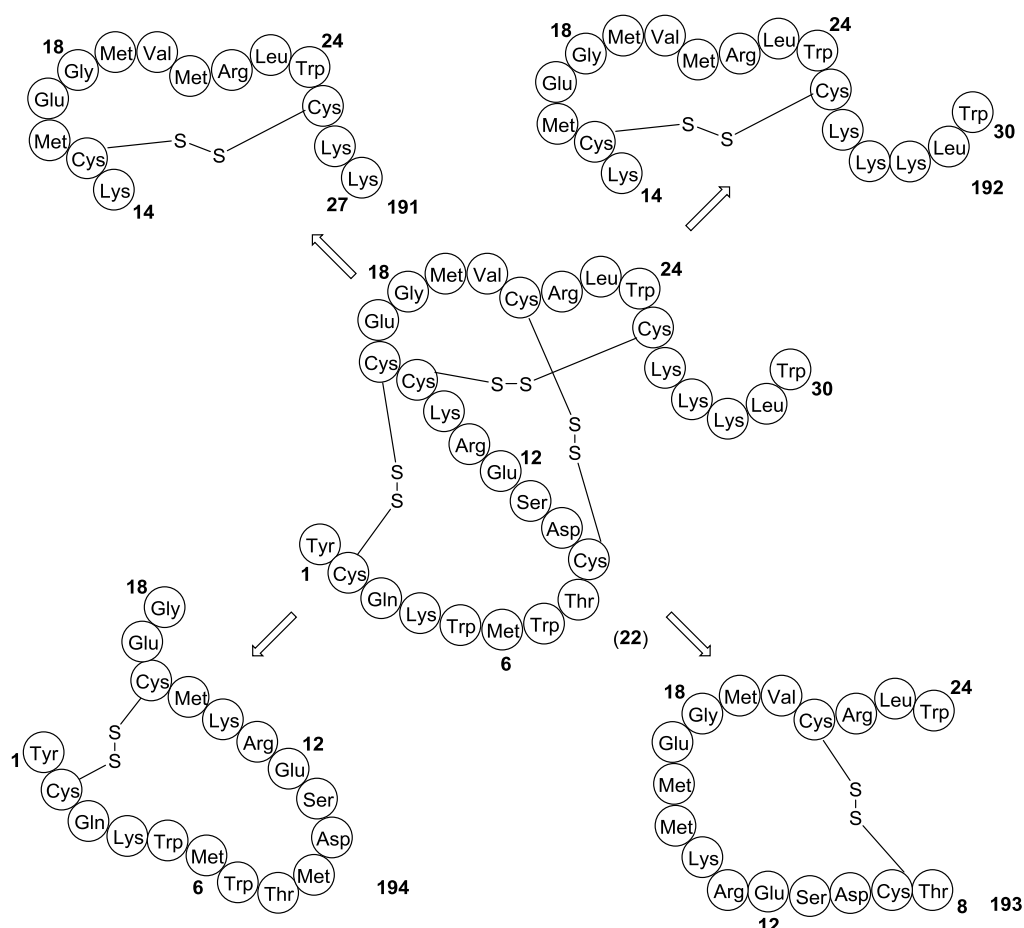


Figure 3.9: Single Ring Disulfide Analogues

To synthesise these analogues, standard Fmoc SPPS protocols were again used, as well as the cleavage and cyclisation procedures detailed in section 3.1. Peptide **191** was used to investigate the use of different resins to see if this had an effect on the overall yield of the product (Table 3.3).

Entry	Resin	Loading (mmol/g)	Yield (%)
1	NovaSyn TGA	0.2	49
2	NovaSyn TGT	0.19	55
3	LL-Wang	0.24	38
4	Cl-Trt	0.73	53
5	Low Loading Cl-Trt	0.11	52

Table 3.3: Summary of Investigations into the Effect of Resin on Yield

The best result used the highly acid sensitive TGT resin (Table 3.3, Entry 2), which gave the product in high yield and good purity. The synthesis of the other analogues **192**, **193** and **194** were thus carried out using the appropriately loaded TGT resins to give them in yields of 16%, 14% and 26% respectively. It is interesting to note that although it was easy to form both **192** and **193**, it was far more difficult to form **194**. Although the latter was eventually formed in good yield, a number of failed attempts were first recorded, where either uncyclised strands of a peptide of incorrect mass were formed or the peptide

would not fold to give the desired product but instead decomposed. As the protocol for forming the ring did not change from that employed to form the previous two structures, it was postulated that the increased size of the ring could make cyclisation more difficult, leading to a low yield and a less reliable reaction. It is also possible that this specific sequence could potentially have problems with stability, which again would lead to difficulties in synthesis of the peptide.

3.2.2 Synthesis of Double Ring Disulfide Analogues

Having synthesised the four single disulfide rings, the level of complexity was increased to form the interlocking double ring analogues (Figure 3.10).

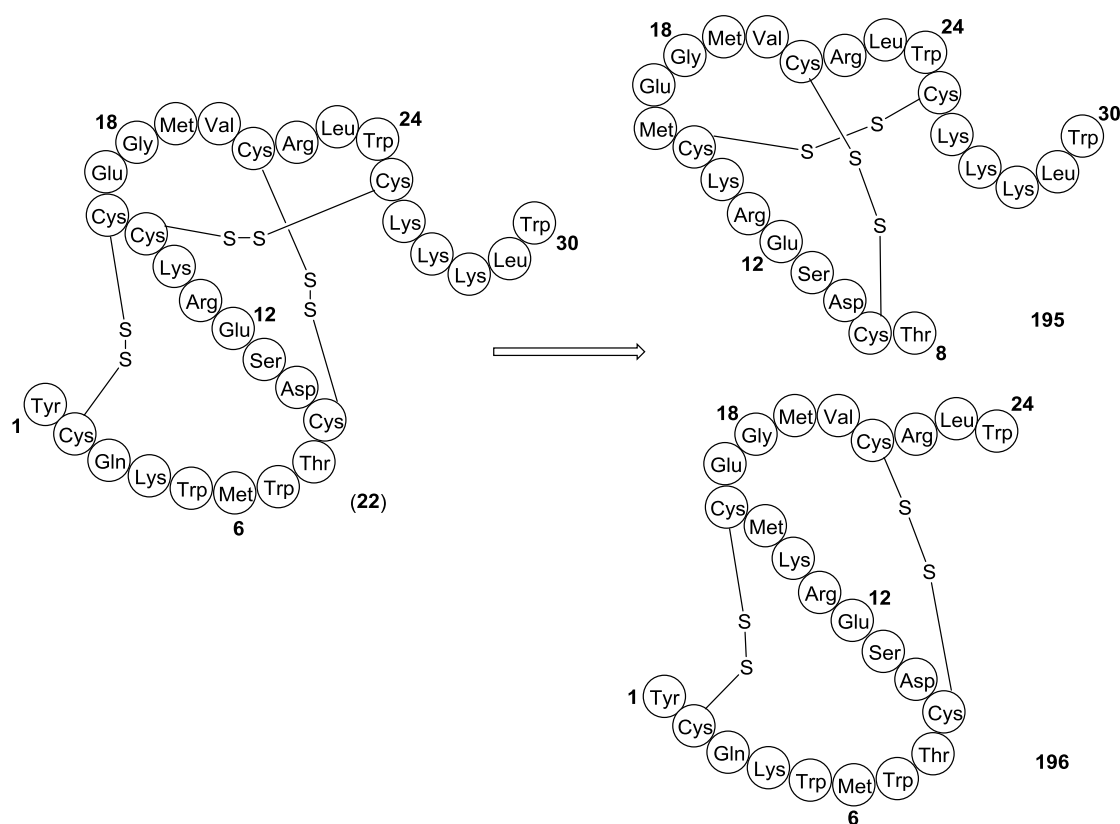


Figure 3.10: Double Ring Disulfide Analogues

In order to control the connectivity of the disulfide bonds, it was necessary to employ orthogonal protecting groups on the cysteine side chains. A number of different orthogonal protecting groups were employed to form both compound **195** and **196** (Table 3.4).

Entry	Structure	Protecting Group Combination	Result
1	195	Trt/Acm	Mixture of Cyclised and Uncyclised
2	195	Trt/MMT	Product
3	195	Trt x 4	Product
4	196	Trt/MMT (TGA and TGT resins)	Decomposition
5	196	Trt/ ^t Bu	Decomposition
6	196	Trt/S ^t Bu	Decomposition
7	196	Trt x 4	Decomposition

Table 3.4: Summary of Investigations into the Use of Orthogonal Protecting Groups

The synthesis of **196** proved particularly difficult. Although it was possible to make the uncyclised peptide with protected cysteine side chains, as soon as attempts at deprotection and folding took place, the peptide appeared to break down often leading to the formation of a black solid. To test to see if the structure was inherently unstable, all four cysteines were protected using the trityl group and then simultaneously deprotected along with cleavage from the resin (Table 3.4, Entry 7). Although the uncyclised peptide could be formed, once the peptide was left to stir in water, decomposition was again observed, suggesting that the third disulfide bond is required in order to form a stable peptide. Conversely, for compound **195**, the deprotection and subsequent cyclisation of the tetra-trityl protected peptide did yield the required product (Table 3.4, Entry 3), although without the control over the deprotection step, no guarantee of correct regioselectivity could be given. This finding is consistent with the formation of the single rings, where considerable difficulty in forming **194** was also observed, suggesting that the increase in size makes it more difficult to form or that this end of the peptide structure could be inherently unstable on its own.

In contrast with the findings for structure **196**, peptide **195** was found to form under a number of different conditions. However, upon scale up of the synthesis, it was found that although the uncyclised peptide was again observed by LC-MS, the cyclisation and subsequent purification did not yield any of the desired product. Prior to purification, small amounts of the desired peptide were observed but could never be isolated. Cyclisation on resin followed by cleavage was also attempted but again resulted in the decomposition of the peptide.

It was postulated that, as with peptide **196**, the structure is inherently unstable without the third disulfide bond for stability, which would account for the observation of several smaller fragments of the peptide by LC-MS.

3.2.3 Conclusions

A total of four different disulfide-containing single ring analogues of ProTx-II (**22**) were successfully synthesised and purified for testing on the Na_v1.7 ion channel. Despite numerous attempts to produce the double ring analogues, involving the use of various protecting groups, deprotection chemistries and cyclisation procedures, only the straight chain analogues could be formed. These were found to be inherently unstable in solution and decomposed rapidly before isolation could be carried out, leading to the conclusion that the double ring analogues were not stable enough to be submitted for further analysis or testing on the Na_v1.7 ion channel.

3.3 Synthesis of Thioether Bridge Truncated Analogues

3.3.1 Introduction

Having successfully synthesised the library of single ring disulfide-containing analogues, investigations into the incorporation of a thioether bridge into the peptide sequence were begun. The work began with the introduction of the orthogonally protected Lanthionine moiety **142** produced in Chapter 2.

Previous work in the Tabor group⁸ has shown that lanthionine could be added in to an SPPS sequence (Figure 3.11). To begin, the chain is built up using the standard Fmoc SPPS protocol (Fmoc deprotection using 40% piperidine, followed by amino acid addition using HBTU and DIPEA) to give **197**. The lanthionine moiety is incorporated using the non-uronium based coupling reagents HOAt and PyAOP in the presence of DIPEA to generate **198**.

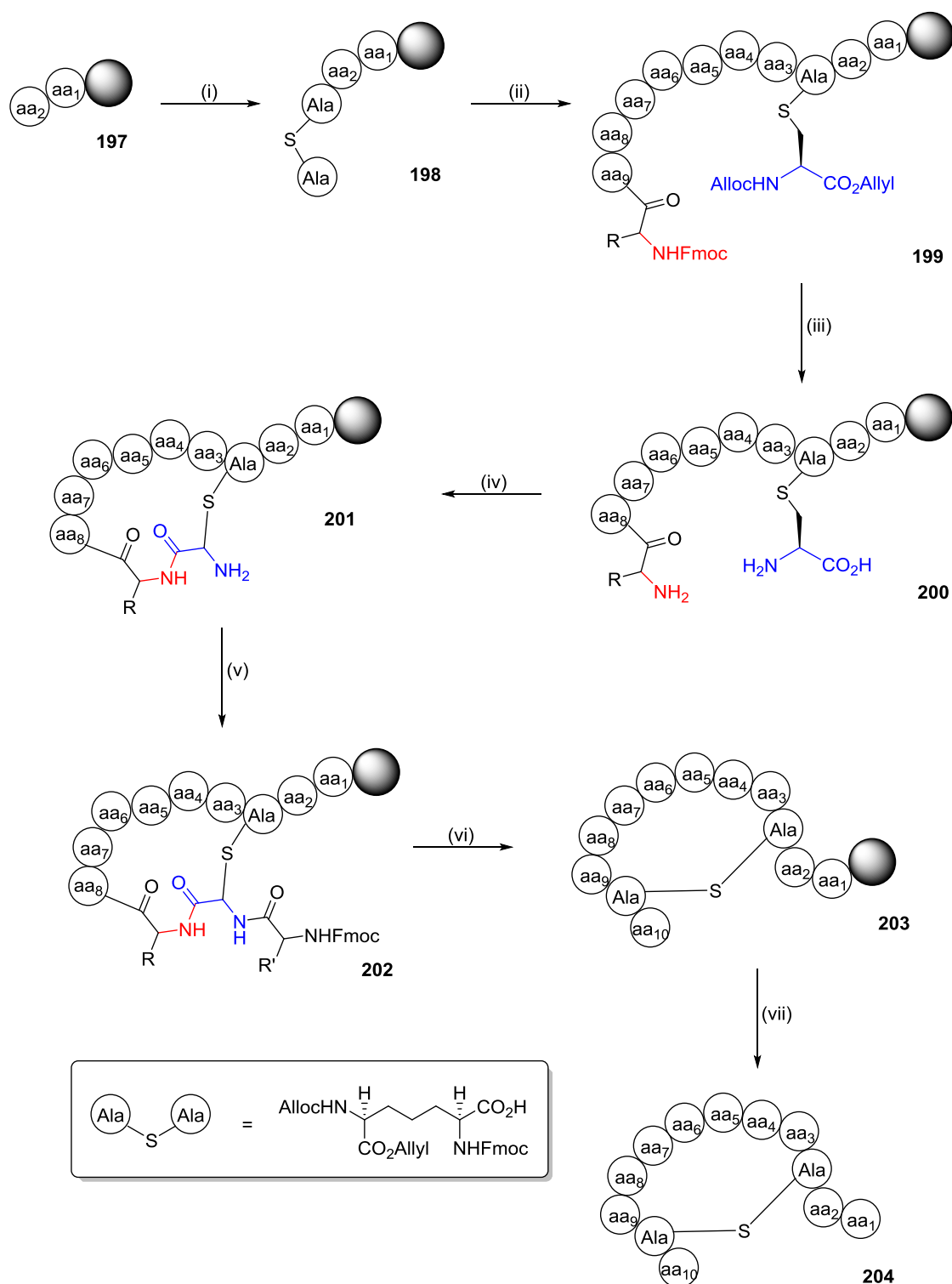


Figure 3.11: Methodology for the Incorporation and Cyclisation of Orthogonally Protected Lanthionine (142) into a Peptide Sequence

Reagents and Conditions: (i) HOAt, PyAOP, DIPEA, lanthionine (**142**), DMF (ii) 40% piperidine in DMF, then amino acid, HBTU, DIPEA, DMF (iii) 40% piperidine in DMF, then Pd(PPh₃)₄, 1,3-dimethylbarbituric acid, DMF, CH₂Cl₂ (iv) HOAt, PyAOP, DIPEA, DMF (v) FmocLysOH, HBTU, DIPEA, DMF (vi) 40% piperidine in DMF (vii) TFA, ethanedithiol, triisopropylsilane, water

Once the lanthionine moiety was successfully installed, the classical Fmoc SPPS protocol was used to build up the amino acid chain to the desired length **199**. To cyclise the peptide, the Fmoc group was again removed using piperidine and the allyl and Alloc groups are then removed using tetrakis(triphenylphosphine) palladium and 1,3-dimethylbarbituric acid to give the fully deprotected peptide **200**. Cyclisation again employed the HOAt and PyAOP conditions to give **201**. These reagents were used because it has been shown that uronium based coupling reagents such as HBTU can react with the free amine after Alloc deprotection in an irreversible guanylation reaction,⁹ which then could not be used to continue the peptide synthesis. Use of PyAOP prevents this from occurring. The free amino group was then ready to react with the next Fmoc protected amino acid to give **202**. To complete the synthesis, one last Fmoc deprotection using 40% piperidine was carried out followed by TFA-mediated cleavage from the resin with simultaneous side chain deprotection to give **204**, which can be purified by HPLC.

Previous work within the Tabor group^{8,10} has focussed on the SPPS synthesis of sections of the antibiotic Nisin, a lantibiotic peptide containing 34 amino acids and five lanthionine bridges. The orthogonal protecting groups allowed for control of the regiochemistry and cyclisation to give the desired product. However, yields of the lanthionine containing rings were typically low and required extensive, difficult purification. The largest ring in Nisin contains five amino acids between the two stereocentres of lanthionine, whereas the smallest ring in this work contains nine residues. Combining the increased ring size and a novel diastereomer of lanthionine with low yields and difficult purification procedures meant a greater challenge for the established protocol and provided an opportunity for new methodology studies.

3.3.2 Synthesis of Single Ring Lanthionine Analogues

As a direct comparison to the single ring disulfide analogues, the first compounds to be synthesised were the single ring lanthionine-containing thioether analogues (Figure 3.12).

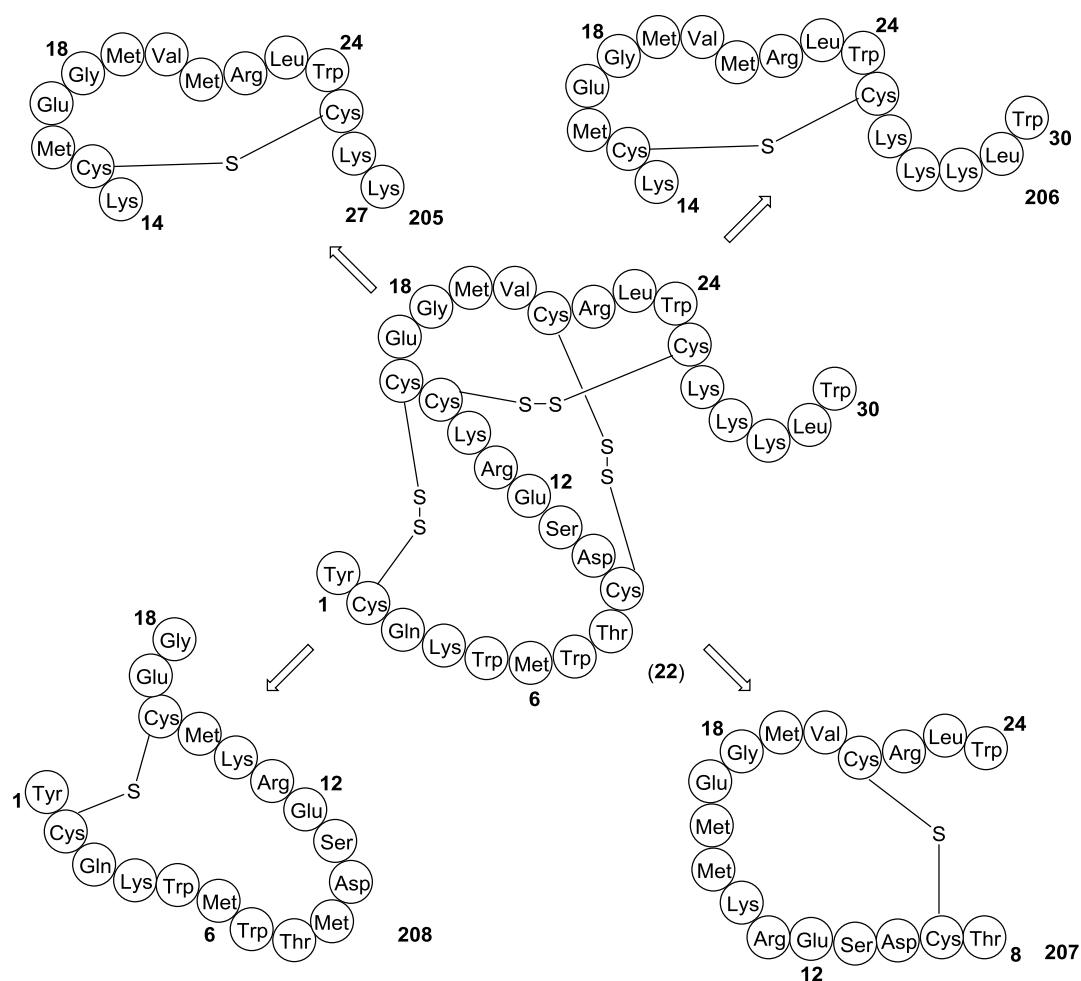


Figure 3.12: Single Ring Thioether Analogues

A trial synthesis of compound **205** showed that the product could be formed using the orthogonal peptide synthesis protocol described above but that, as well as forming the desired product, some of the peptide sequence minus lanthionine **209** was also formed (Figure 3.13).

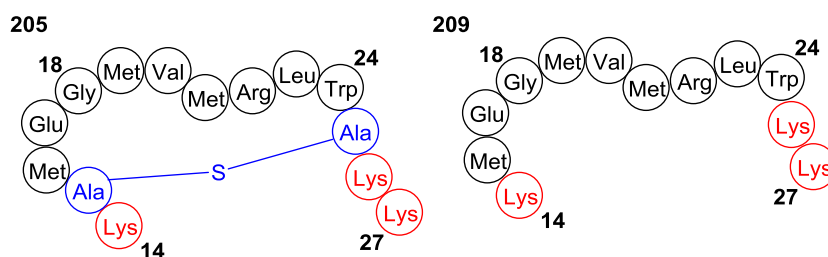


Figure 3.13: Structure of the Desired Peptide **205** and the Peptide Without Lanthionine Incorporation **209**

Separation of these two compounds was difficult by HPLC and led to a very low amount of the pure desired product (less than 1 mg). It was decided to investigate the use of a microwave for the incorporation and cyclisation of the lanthionine to see if this could improve the yield of the reaction and ease the purification difficulties.

In 1991, Yu *et al.*^{11,12} reported that using the microwave could significantly increase the coupling efficiency of a reaction, particularly with those amino acids containing bulky side chain groups. Their experiments were performed in a standard kitchen microwave, which was adapted to allow a stream of nitrogen to pass through a vessel in the centre of the machine. Although the kitchen equipment has now been replaced by specially designed apparatus in which temperature and duration of the microwaves can be carefully controlled, the principles of microwave-assisted peptide synthesis remain unchanged. Since its initial conception, it has gone from strength to strength and can now be employed for both the coupling and deprotection steps, with optimised reaction times decreasing from 120 minutes to as low as 2 minutes.¹³

Further investigations into the use of a microwave have shown that cysteine is susceptible to racemisation at higher temperatures. This is thought to occur as a result of abstraction of the α -proton by a tertiary amine such as diisopropylethylamine in solution. This can be reduced by decreasing the temperature of the reaction from 80 °C to 50 °C.¹⁴

Thus the advantages to the microwave are two-fold: it not only gives a more reliable coupling procedure but also decreases the time required to make a peptide chain, allowing longer peptides to be synthesised quickly and efficiently. Microwave assisted SPPS has shown great improvements in the efficiency of reactions involving amino acids with bulky side chains. It was therefore hoped that employing the use of a microwave reactor for the addition of orthogonally protected lanthionine (**142**) would decrease the amount of peptide produced which did not contain the lanthionine moiety and ease some of the purification problems encountered.

Previous investigations with the single disulfide rings had shown good overall yields for many types of resin. To see which type of resin would give the best results, trial microwave syntheses were set up using the three resins which showed the highest yields for the equivalent disulfide compound, namely the NovaSyn TGT resin and Cl-Trt resin. It was postulated that higher loading resins like the Cl-Trt resin could result in polymerisation instead of cyclisation of the lanthionine bridge. For this reason, it was decided to trial both the normal and the knock-down (low-loading, LL) Cl-Trt resin.^{15,16}

The standard SPPS protocol was then followed to form the peptide, with the lanthionine addition step using the microwave at a given temperature for a pre-determined duration (Table 3.5).

Entry	Resin	Loading (mmol/g)	Temp (°C)	Time (mins)	Peptide Formed
1	NovaSyn TGT	0.2	60	5	✓
2	NovaSyn TGT	0.2	60	7	✓
3	NovaSyn TGT	0.2	70	5	✓
4	LL Cl-Trt	0.11	60	5	✓
5	LL Cl-Trt	0.11	60	7	✓
6	LL Cl-Trt	0.11	70	5	✓
7	Cl-Trt	0.73	60	5	polymerisation
8	Cl-Trt	0.73	60	7	polymerisation
9	Cl-Trt	0.73	70	5	Polymerisation

Table 3.5: Summary of Preliminary Investigations into the Use of the Microwave for Incorporation of Lanthionine (142) into the Peptide Sequence

The initial small-scale reactions showed promise, proving it was possible to incorporate a thioether linkage into the peptide synthesis using the microwave. The results also show that low loading resins are preferred, as the use of a high loading resin led to polymerisation rather than formation of the desired single ring peptide (Table 3.5, Entries 7 – 9). It was found that the resins could tolerate temperatures of up to 70 °C and could be subjected to microwaves for at least seven minutes. For the next set of experiments, it was decided to increase the time of the reactions from seven to ten minutes, to see if this could be tolerated and if it would increase the yield of the reaction (Table 3.6). Having ascertained that low loading resins were preferred, these reactions were carried out using the NovaSyn TGT and low loading chlorotrityl resins only.

Entry	Resin	Temp (°C)	Time (mins)	Yield (%)
1	NovaSyn TGT	60	5	8
2	NovaSyn TGT	60	10	2
3	NovaSyn TGT	70	5	4
4	LL Cl-Trt	60	5	0
5	LL Cl-Trt	60	10	0
6	LL Cl-Trt	70	5	0
7	NovaSyn TGT	RT, no μ W	120	8 (+ 3 peptide – lanthionine)

Table 3.6: Summary of Further Investigations into the Use of the Microwave for Incorporation of Lanthionine (142) into the Peptide Sequence

The most surprising result was that on scaling up the synthesis, the reactions using low loading chlorotrityl resin no longer produced peptides at the end of the synthesis (Table 3.6, Entries 4 – 6). The resin was modified by partially capping the resin with acetic anhydride and then calculating the loading by measuring the UV absorption (see Chapter 7.3.3 for details). However, it was found that, despite careful procedures, it was difficult to achieve reproducible results with this resin and that loading could differ greatly from batch to batch, with full end-capping occurring despite using fewer than the required number of equivalents of acetic anhydride. This accounted for the 0% yield for this resin

(Table 3.6, Entries 4 – 6) and as the process proved so unreliable, it was decided to focus on the NovaSyn TGT resin, which gave the best results for the disulfide analogues as well.

The results showed that although both 60 °C and 70 °C were tolerated by the resin (Table 3.6, Entries 1 and 3), the higher temperature did start to show a decrease in yield for the peptide synthesis. Similarly, prolonged exposure to microwaves (Table 3.6, Entries 1 and 2) was also found to have a detrimental effect on the yield, which decreased by a factor of four to just 2%. Therefore, it was concluded that milder conditions gave the best yield.

Finally, the best microwave condition was compared with the non-microwave conditions pioneered by Bregant and Tabor,⁸ in which the reaction was left to agitate at room temperature for 2 h. As the results show (Table 3.6, Entries 1 and 8) both methods yielded the same amount of peptide; however, the use of the microwave for the installation of orthogonally protected lanthionine (**142**) into the peptide sequence has the dual advantages of saving time and easing purification, as no peptide chain minus lanthionine was observed in the crude LC-MS results, thus making purification by HPLC both quicker and simpler. The new reaction conditions yielded 3 mg of **205** after purification by HPLC, which could then be tested directly on the Na_v1.7 ion channel.

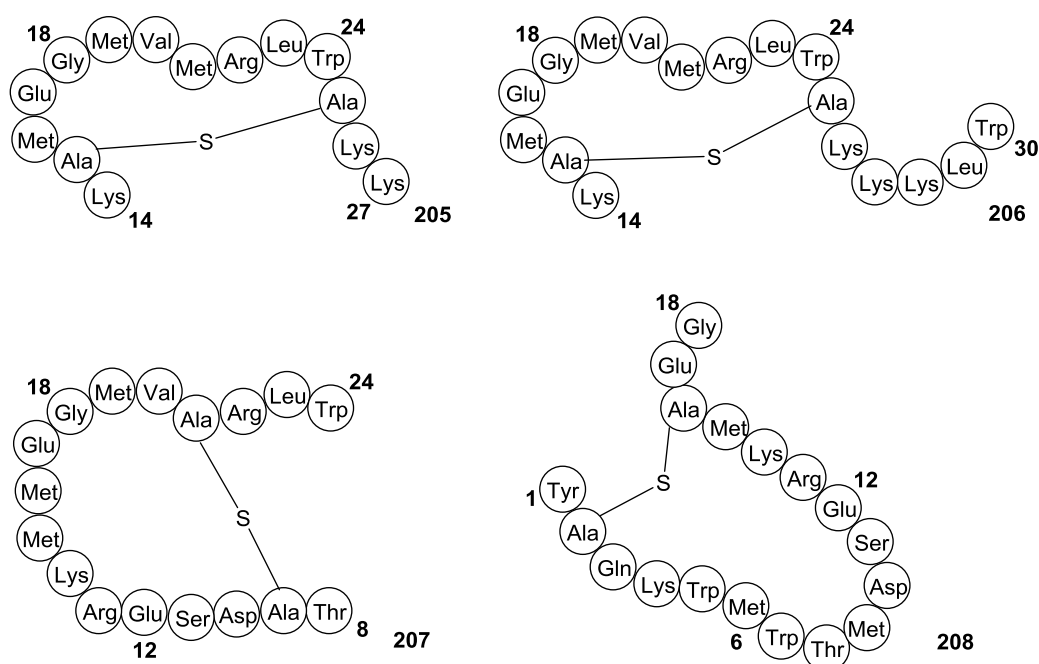


Figure 3.14: Structures of the Single Ring Thioether Analogues

Having successfully synthesised one analogue using the new methodology, attention was turned to the other rings **206**, **207** and **208** (Figure 3.14). Pleasingly, the protocol was found to work for **206** and **207**, producing 4 mg and 0.5 mg respectively after HPLC purification. However, the synthesis of **208** proved far more challenging; as with the disulfide analogue **194**, many truncated versions of the straight-chain peptide were

observed, with none of the desired product, despite many repetitions of the synthesis. It was again concluded that this was due to the large size of the ring making it difficult for the peptide to cyclise.

3.3.3 Synthesis of Double Ring Lanthionine Analogues

Having synthesised the single thioether rings, the level of complexity was increased to form the interlocking double ring analogues (Figure 3.15). Prior to the microwave methodology experiments, investigations into the formation of these compounds were carried out in parallel with the research into the single ring lanthionine containing analogues. However, as with the disulfide analogues, it was found that none of the desired straight chain analogues were formed. Instead many shorter peptides were formed, which did not contain the thioether bridge.

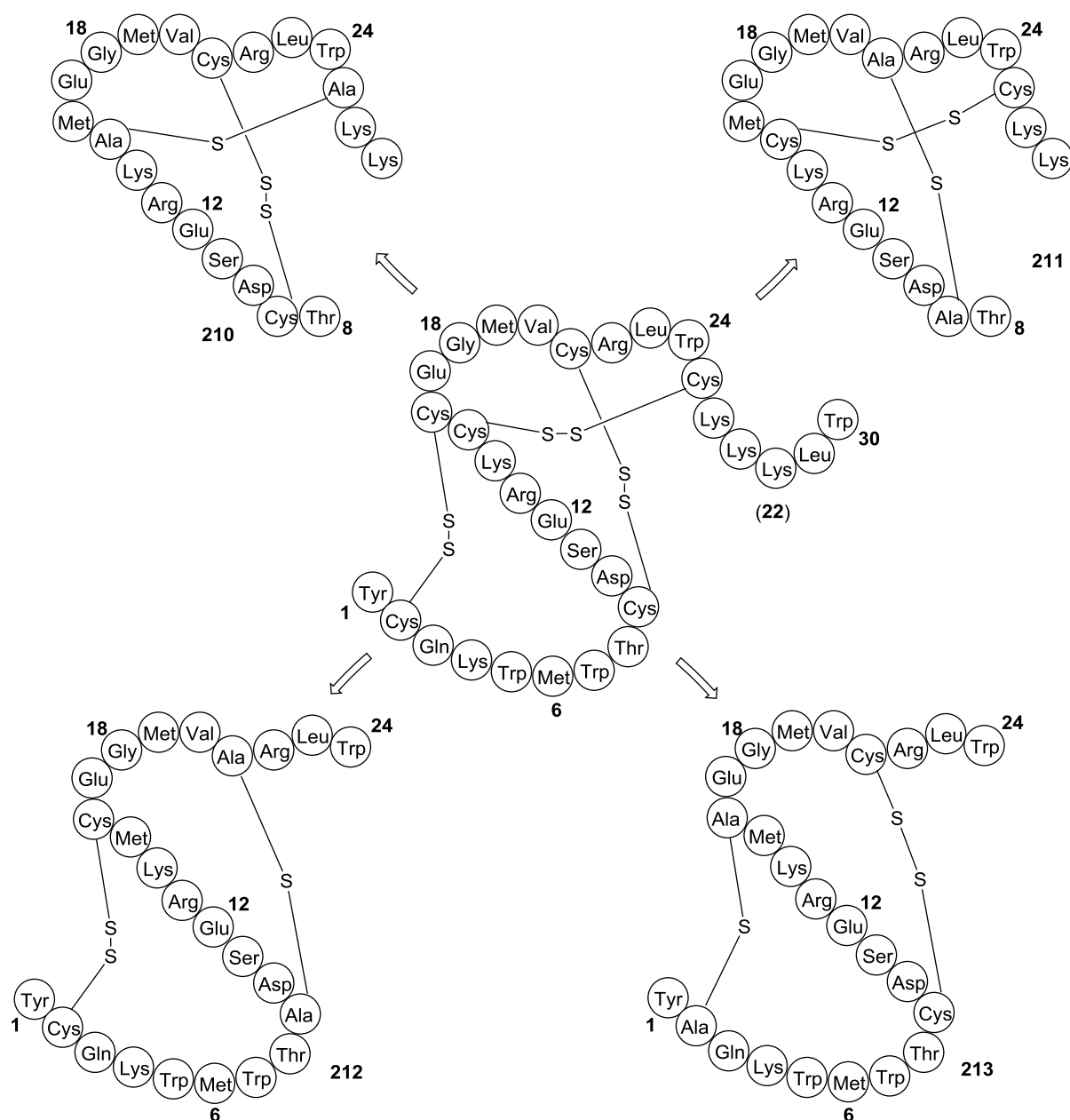


Figure 3.15: Double Ring Thioether Analogues

These larger, more complicated structures were the first real test of the versatility of the new methodology and it was hoped that the complex structures could be synthesised by employing the microwave-assisted protocol. Given the trouble encountered with the double disulfide ring analogues, it was perhaps not surprising to discover that although traces of some of the peptides were seen in crude LC-MS analysis, upon purification, none of the desired products were observed. As initial analysis showed that the compounds were present, it was decided that the microwave protocol itself was not the problem but again the inherent stability of the compounds was called into question. As the peptides did not stay in solution long enough for purification to occur, these analogues were also

not submitted for biological testing and instead it was decided to focus on the synthesis of the full length analogues.

3.4 Synthesis of Triple Ring Lanthionine Analogues

The final lanthionine analogues to be added to the library were those based on the full structure of ProTx-II (**22**). In these molecules, one disulfide bond is replaced by a lanthionine moiety to give two disulfide bonds and one thioether linkage (Figure 3.16). The triple ring analogues are the most interesting compounds from the lanthionine-containing analogues as they are closest in shape and size to the naturally occurring ProTx-II (**22**).

Previous work carried out by other groups had suggested that by changing the disulfide bond in a peptide to a thioether linkage, the relative stability of the peptide *in vivo* could be increased whilst still maintaining good levels of activity;^{17,18} Cui *et al.*¹⁷ tested thioether and biscalba linked analogues of tachyplesin I (TPI-1) which were stable to reducing agents and disulfide isomerases but maintained good activity as measured by the minimal inhibitory concentration values. Similarly, Dekan *et al.*¹⁸ showed that activity was also maintained when one of the disulfide bonds in α -conotoxin IMI was replaced by a thioether bridge. With this in mind, it was decided to try replacing each disulfide bond in turn with a thioether bridge (Figure 3.16).

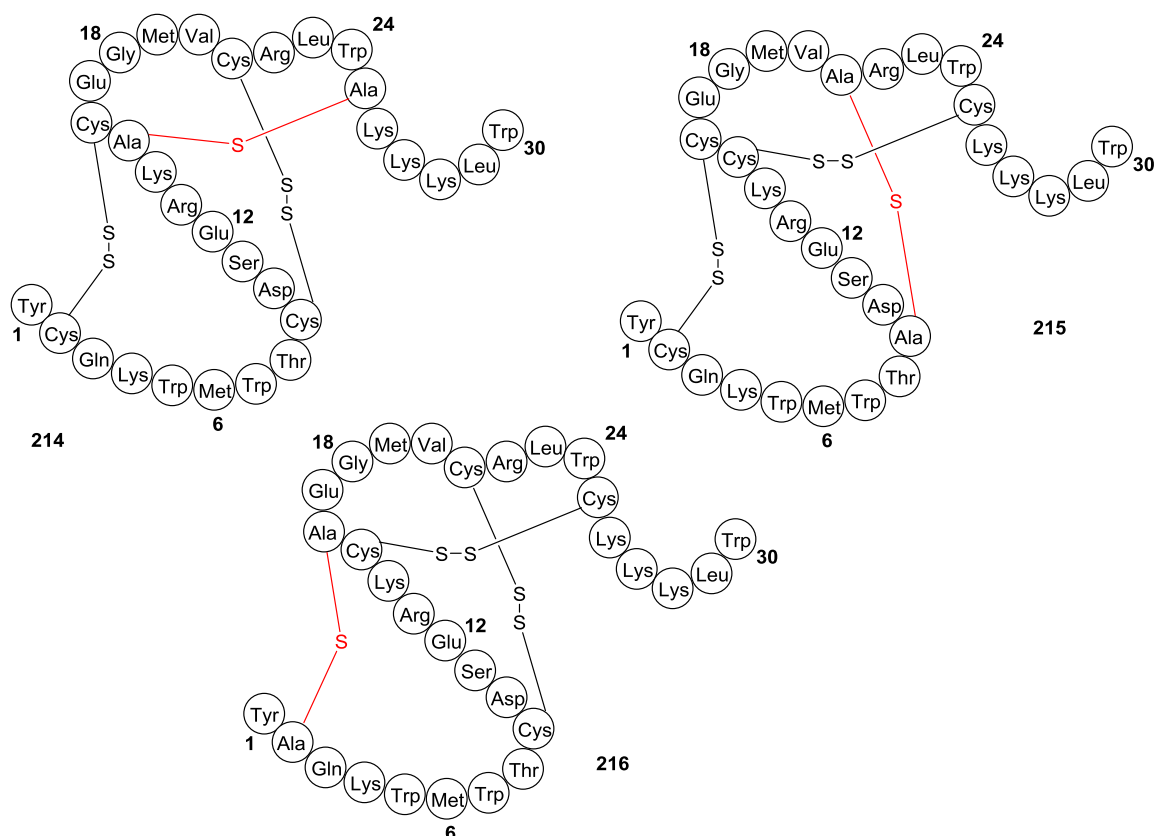


Figure 3.16: Triple Ring Thioether Analogues

The syntheses of the full analogues of ProTx-II (**22**) were the most challenging use of the methodology thus far, due to the increased size of the compounds and the intricate connectivity of the disulfide bonds and the thioether linkage.

Two major problems were envisaged before synthesis began: firstly there was a concern that after cyclisation, it was possible that the growing peptide chain could fold in on itself meaning the unprotected amino group could become inaccessible. This would be especially relevant when the lanthionine moiety was replacing the first disulfide bond as a further 14 amino acids needed to be added after the cyclisation step. Secondly, there was the concern that the lanthionine could oxidise whilst forming the other disulfide bonds. To a certain extent, the latter could be avoided by minimising the amount of time the peptide remained in solution, as, the oxidation of lanthionine is relatively slow.

However, the question of the inaccessible free amino group was less easily solved and could only be addressed once trial reactions had been carried out. To this end, all three of the peptides were synthesised on a small scale. It was decided to first synthesise analogues using trityl protected cysteine for all four residues. The reasons for this were twofold; firstly, this would allow investigation of the effect of the lanthionine on disulfide regioselectivity and secondly, it makes the synthesis simpler – with fewer factors to control in the first instance, it was easier to locate the problem steps.

The first experiment was thus designed to omit the orthogonal protecting group chemistry and focus on the insertion of the lanthionine moiety and subsequent cyclisation in order to form one of the rings in the inhibitory cysteine knot peptide analogues. However, on the first attempt at full synthesis, none of the desired masses were observed for any of the three peptides by crude LC-MS and the traces themselves were extremely complicated with multiple peaks present.

It was decided to re-start the syntheses and to check each step individually in an attempt to locate the source of the problem. After each coupling step, a small amount of resin was removed and cleaved in TFA before dilution in water. The crude LC-MS traces were then recorded and compared with the expected masses. It was quickly found that the Fmoc protected chains did not give very good mass spectra and so the protocol was amended to include a mini Fmoc deprotection, using 40% piperidine in DMF, prior to cleavage from the resin. Unexpectedly the first problems were encountered after the chain length had reached just six amino acids in length (corresponding to CKKKLW or LanKKKLW) with multiple peaks observed in the LC-MS traces for all three peptides. As the syntheses progressed, the spectra rapidly became more complicated until it was no longer possible to see the correct mass.

The spectra for all the peptides were dominated by masses corresponding to smaller peptides. At this point, it was not immediately obvious whether this was due to the mini-cleavage procedure from the resin or another factor. As mentioned previously, tryptophan has been found to re-attach to the resin³ during the cleavage procedure, which could have complicated the spectra and led to the observation of the smaller peptides. Thus, it was decided to try the synthesis again from lysine-28, which would avoid these problems. The results from this second attempt at synthesis are summarised in Figure 3.17.

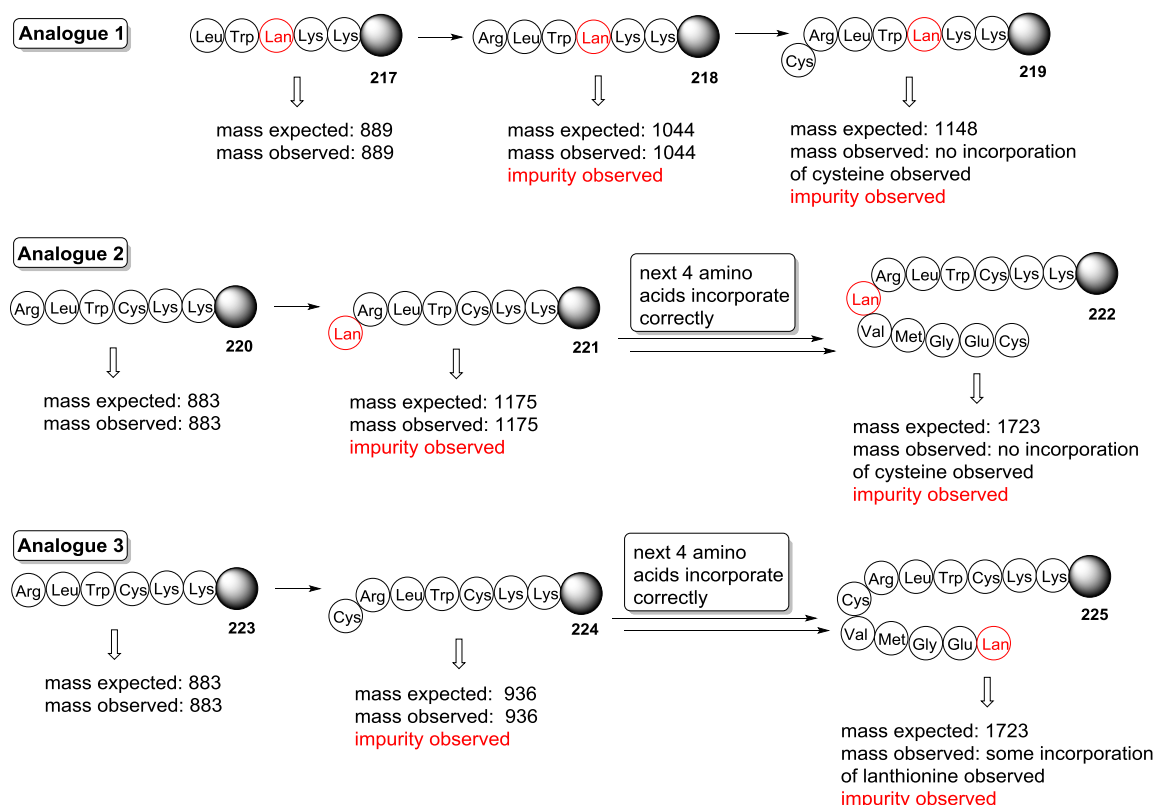


Figure 3.17: Step-wise Insertion of Amino Acids into the Peptide Sequence

Interestingly, the same problems began to occur once the peptide reached five to six amino acids in length. For peptide **214**, the secondary products dominated the LC-MS trace after addition of arginine (**218**) and despite the double coupling of the amino acid, none of the desired product from the addition of lanthionine was observed (**218**, Figure 3.17). The addition of cysteine in place of lanthionine for peptides **215** and **216** was more successful but the traces were already quite messy, with many smaller fragments of peptide detected. As the synthesis progressed along the sequence, the spectra became less and less clear and were dominated by peaks corresponding to peptides of unknown sequences. The addition of the cysteine to peptide **222** could not be achieved, despite attempting double coupling and the synthesis was not continued any further. Some product was observed when lanthionine was added to **224** but attempts to add the next cysteine again did not yield the desired product. At this point all further sequence additions were suspended.

In all of the traces, masses corresponding to unknown peptide sequences dominated the spectra. This phenomenon had been observed in previous syntheses of shorter peptides but until this point had not been considered detrimental as they were only present in small amounts. It was postulated that these masses could have arisen from peptide aggregation on resin, leading to unwanted side products.

From these experiments, evidence suggested that peptide aggregation¹⁹ was preventing the peptide chain from growing in length as would be expected. This is in direct contrast with the formation of the native ProTx-II peptide (**22**), which did contain some peptides of unknown masses but did not seem to impinge on the overall synthesis of the peptide chain. Secondly, as predicted at the beginning, it appeared that aggregation was causing the peptide to fold in on itself and that the growing chain quickly made the free amino group inaccessible, preventing further coupling reactions from occurring. For each peptide, it would appear that the addition of the large orthogonally protected lanthionine had a direct effect on the growth of the peptide chain; when lanthionine was added into the first cysteine position (cysteine 24 in ProTx-II **22**) to form peptide **214**, it was found that the peptide chain could not increase in length past six amino acids. Similarly, when adding lanthionine into cysteine positions 21 and 16 (peptides **215** and **216** respectively), the ability to continue the peptide chain rapidly decreased. It is postulated that the large size of the lanthionine moiety exacerbated the aggregation problem, potentially by shielding the free amino group and preventing the subsequent coupling reactions to increase the amino acid chain from occurring. This would account for the observation that although some small peptide lengths were observed in the straight chain synthesis of ProTx-II (**22**), it was still possible to reach the end of the synthesis and form the desired product.

The next step in the investigations was thus to investigate the ways to minimise the amount of aggregation that occurred. In the 1990s, Hmb-protected amino acids¹⁹ were introduced into difficult peptide syntheses to counteract this problem by replacing the hydrogen atoms in the peptide backbone with the Hmb group, thus disrupting the hydrogen bonding and preventing aggregation (Figure 3.18). The Hmb group also aids peptide synthesis by enabling acyl capture to form intermediate **228** followed by intramolecular acyl transfer to give the desired product (**229**, Figure 3.18). Peptide synthesis can then continue using the standard Fmoc protected amino acids and SPPS protocol to build up the chain.

The three peptides were again synthesised incorporating the Hmb protection and followed by LC-MS after every step (Figure 3.20). The Hmb protected amino acids were installed into the peptide chain in the same manner as the standard Fmoc amino acids, namely by using HBTU and DIPEA and agitating for 40 min. Piperidine was then used to remove the Fmoc group as normal to allow the peptide chain to grow further.

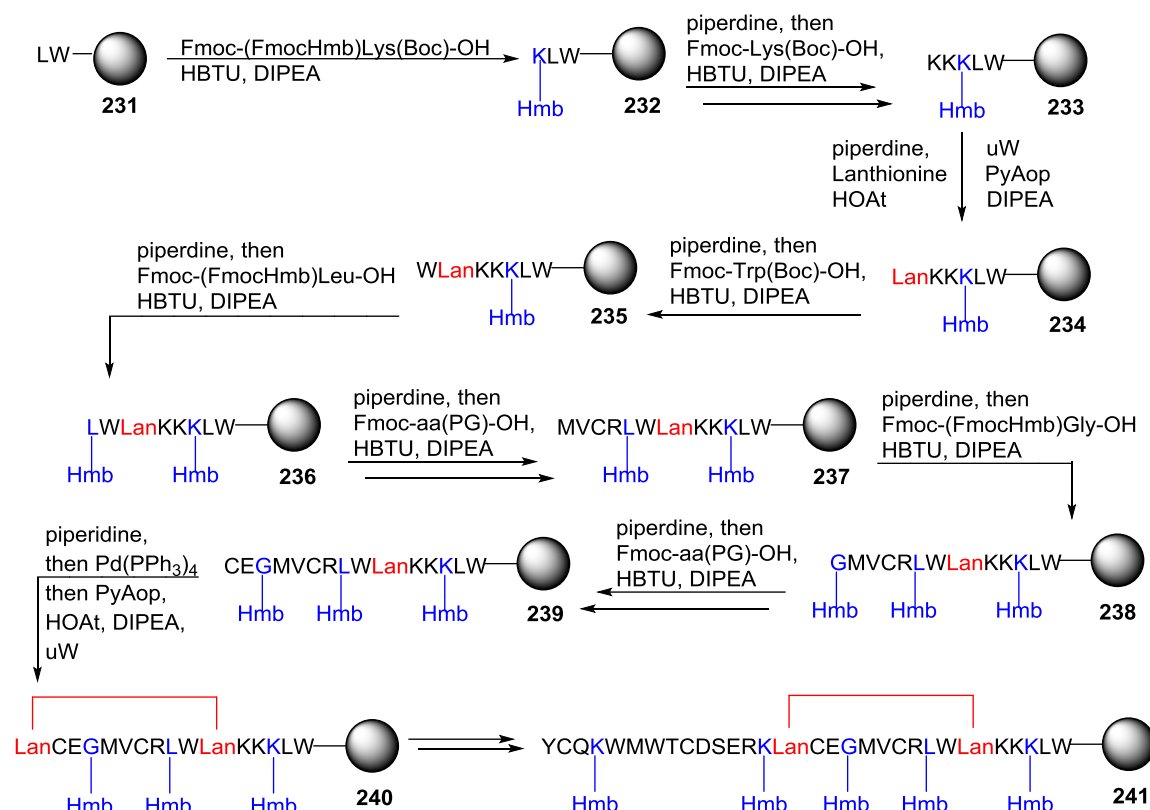


Figure 3.20: Synthetic Strategy for Formation of the Triple Ring Analogues Incorporating Hmb Protection and Addition of Lanthionine Using the Microwave Protocol

As the synthesis progressed, it was noted that the additions required a double coupling; after an Fmoc deprotection, the amino acid was added along with HBTU and DIPEA and allowed to react for 40 minutes. After this time, the peptide syringe was evacuated before repeating the coupling step with fresh activated amino acid solution. This was shown to guarantee the addition of each amino acid and for this reason, this became the standard protocol for these experiments.

At the end of the experiments, the crude LC-MS results showed a much reduced level of peptides of unknown mass and the +5 and +6 ions ($m/z = 760$ and 634 respectively) of the full length peptides for analogues (**214** and **216**) with the lanthionine bridge at either terminus were observed. However, analogue **215** with the thioether bridge in the middle ring was not observed.

The syntheses of **214** and **216** were then scaled up to produce 0.3 mg and 0.8 mg respectively after purification, which were then ready for biological testing. A serendipitous omission of EDT from the cleavage solution was found to give the cyclised product upon immediate cleavage from the resin, suggesting that the partially folded structure aided the cyclisation of the disulfide bonds during the cleavage and side chain deprotection procedure.

Upon successful production of these two analogues, attention was turned to the final peptide in this sequence. As the third and fourth cysteine residues are next to each other in this sequence (Figure 3.16), it was decided to employ orthogonal protecting group chemistry to guarantee the 1 – 4, 3 – 6 connectivity. As had been shown in the synthesis of ProTx-II (**22**), the cyclisation in water produced the desired 2 – 5 connectivity but it was difficult to ascertain if 1 – 4, 3 – 6 or 1 – 3, 4 – 6 connectivity or a mixture of the two was achieved. In analogues **214** and **216**, this was not such a great problem as one of the cysteine-15 and cysteine-16 residues was replaced by the lanthionine to give the thioether linkage. However, in the case of the final analogue, this became more critical.

Since the original protecting group investigations were carried out, a new protecting group was brought to market by Merck. The S(Tmp) protected cysteine^{21,22} (**242**, Figure 3.21) is stable to piperidine but very labile in mild thiolysis conditions, for example in the presence of DTT. The problem with using combinations of the trityl, MMT and Acn protecting groups is that the deprotection relied on graduated acidolysis, which meant that there was always a risk of accidental deprotection. Mild thiolysis is truly orthogonal to trityl deprotection making control of the regiochemistry more reliable.

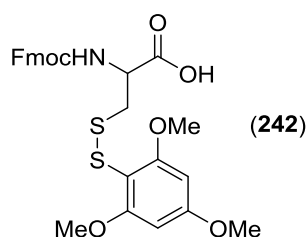


Figure 3.21: Structure of the S(Tmp) protected Cysteine (**242**)

Once all the amino acids had been added in the peptide sequence, the S(Tmp) protecting group was removed on resin using DTT and cyclised using NCS. Simultaneous cleavage from the resin and removal of all the protecting groups using the TFA cocktail thus deprotected the last pair of cysteines and allowed for formation of the final disulfide bond (Figure 3.22).

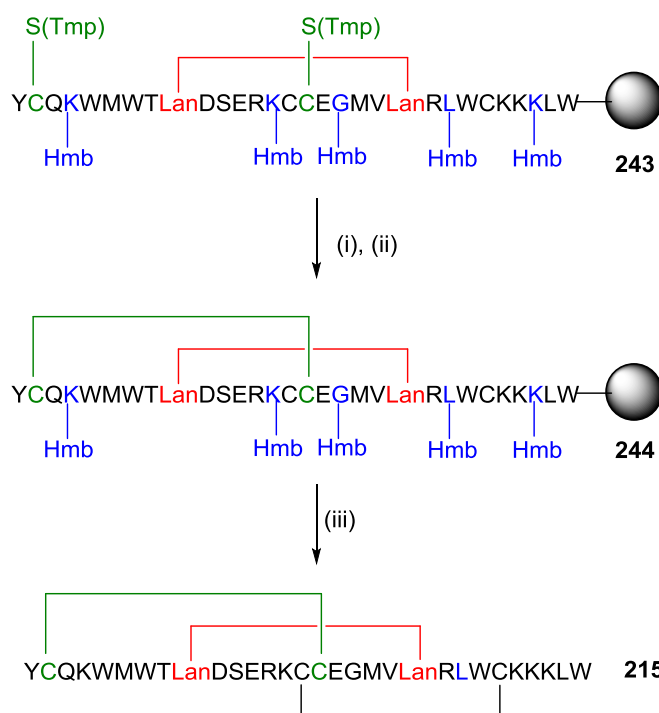


Figure 3.22: Formation of Peptide **215**

Reagents and Conditions: (i) 5% DTT in 0.1M NMM in DMF (ii) 2 eq. NCS, DMF (iii) TFA, triisopropylsilane, water

This procedure allowed for the production of 5 mg of the desired product after purification, which along with the other two triple ring analogues was submitted for testing against the Na_v1.7 ion channel.

In conclusion, the synthesis of the three interlocking triple ring analogues proved the versatility of the microwave protocol and allowed for the formation of the most complicated lanthionine-containing structures synthesised to date. The protocol was modified slightly to include the use of the Hmb protecting group to prevent aggregation on resin and double coupling of each amino acid to ensure each amino acid in the sequence was added in correctly. In addition, the introduction of the S(Tmp) protecting group allowed for the use of truly orthogonal cysteine side chain protection which allowed for control of the connectivity of the structure.

3.5 Conclusions

Research has allowed for the production of a total of 10 analogues of ProTx-II (**22**) as well as synthesis of the native peptide. Investigations into the synthesis and cyclisation of ProTx-II (**22**) have allowed for the production of multiple milligram quantities for use in digestion experiments to determine connectivity and as a control for the biological testing against the Na_v1.7 ion channel.

A total of seven single ring analogues were synthesised to probe the SAR by finding out which parts of the peptide are important for binding within the active site of the ion channel. By designing a novel microwave methodology for the incorporation of lanthionine into a peptide, three analogues containing a thioether bridge were formed. This methodology allowed for the synthesis of the largest known lanthionine-containing single ring structures made to date. Research showed that although it was possible to observe the double ring analogues both with and without a lanthionine bridge, these proved to have inherently unstable structures which could not be subjected to purification by conventional means as they did not appear to be stable in water for long periods of time.

Using the novel microwave-based protocol, together with the inclusion of Hmb protection to prevent aggregation on resin and the use of orthogonal protecting groups, three further analogues were synthesised which all contained one thioether bridge interlocking with two disulfide bridges. These are the first known examples of such structures produced to date and show the versatility of the synthetic strategy.

These 10 analogues and the native peptide were purified by reverse-phase HPLC and were then ready for testing on an automated patch clamp platform against the Na_v1.7 ion channel (Chapter 5).

¹ Middleton, R. E.; Warren, V. A.; Kraus, R. L.; Hwang, J. C.; Liu, C. J.; Dai, G.; Brochu, R. M.; Kohler, M. G.; Gao, Y.-D.; Garsky, V. M.; Bogusky, M. J.; Mehl, J. T.; Cohen, C. J.; Smith, M. M., *Biochemistry*, **41**, 14734-14747 (2002)

² Chan, W. C.; White, P. D., *Fmoc Solid Phases Peptide Synthesis: a Practical Approach*, Oxford University Press, Oxford (2000)

³ Atherton, E.; Sheppard, R. C., *Solid Phase Peptide Synthesis A Practical Approach*, IRL Press, Oxford (1989)

⁴ de Hoffmann, E.; Stroobant, V., *Mass Spectrometry Principles and Applications*, **3rd Edition**, 138, Wiley (2007)

⁵ Chagot, B.; Escoubas, P.; Villegas, E.; Bernard, C.; Ferrat, G.; Corzo, G.; Lazdunski, M.; Darbon, H., *Protein Sci.*, **13**, 1197-1208 (2004)

⁶ Park, J. H.; Carlin, K. P.; Wu, G.; Ilyin, V. I.; Musza, L. L.; Blake, P. R.; Kyle, D. J., *J. Med. Chem.*, **57**, 6623-6631 (2014)

⁷ Schmalhofer, W. A.; Calhoun, J.; Burrows, R.; Bailey, T.; Kohler, M. G.; Weinglass, A. B.; Kaczorowski, G. J.; Garcia, M. L.; Koltzenburg, M.; Priest, B. T., *Mol. Pharmacol.*, **74**, 1476-1484 (2008)

⁸ Bregant, S.; Tabor, A. B.; *J. Org. Chem.*, **70**, 2430-2438 (2005)

⁹ Alberico, F.; Cases, M.; Alsina, J.; Triolo, S. A.; Carpino, L. A.; Kates, S. A., *Tetrahedron Lett.*, **38**, 4853-4856 (1997)

¹⁰ Mustapa, M. F.; Harris, R.; Esposito, D.; Chubb, N. A. L.; Mould, J.; Schultz, D.; Driscoll, P. C.; Tabor, A. B., *J. Org. Chem.*, **68**, 8193-8198 (2003)

¹¹ Yu, H.-M.; Chen, S.-T.; Wang, K.-T., *J. Org. Chem.*, **57**, 4781-4784 (1992)

¹² Chen, S.-T.; Chiou, S.-H.; Wang, K.-T., *J. Chin. Chem. Soc.*, **38**, 85 (1991)

¹³ Erdélyi, M.; Gogoll, A., *Synthesis*, **11**, 1592-1596 (2002)

-
- ¹⁴ Palasek, S. A.; Cox, Z. J.; Collins, J. M., *J. Pept. Sci.*, **13**, 143–148 (2007)
- ¹⁵ Gude, M.; Ryf, J.; White, P. D., *Lett. Pept. Sci.*, **9**, 203-206 (2003)
- ¹⁶ Simon, M. L.; *Methods in Enzymology: Constitutive Activity in Receptors and Other Proteins, Part B*, **485**, 110 (2010)
- ¹⁷ Cui, H.-K.; Guo, Y.; He, Y.; Wang, F.-L.; Chang, H.-N.; Wang, Y.-J.; Wu, F.-M.; Tian, C.-L.; Liu, L., *Angew. Chem. Int. Ed.*, **52**, 9558-9562 (2013)
- ¹⁸ Dekan, Z.; Vetter, I.; Daly, N. L.; Craik, D. J.; Lewis, R. J.; Alewood, P. F., *J. Am. Chem. Soc.*, **133**, 15866 – 15869 (2011)
- ¹⁹ Hyde, C.; Johnson, T.; Owen, D.; Quibell, M.; Sheppard, R. C., *Int. J. Peptide Protein Res.*, **43**, 431-440 (1994)
- ²⁰ Johnson, T.; Quibell, M.; Sheppard, R. C., *J. Pept. Sci.*, **1**, 11-25 (1995)
- ²¹ Postma, T. M.; Giraud, M.; Albericio, F., *Org. Lett.*, **14**, 21, 5468-5471 (2012)
- ²² Postma, T. M.; Albericio, F., *Org. Lett.*, **15**, 3, 616-619 (2013)

4 Chapter 4: Towards the Synthesis of Orthogonally Protected Cystathionine for Use in Solid Phase Peptide Synthesis

4.1 Introduction

Thioether bridged peptides containing a lanthionine moiety have one atom less in the ring than their disulfide counterparts. These analogues have the dual advantages of preventing ring opening by breaking the disulfide bond and of subtly changing the ring size and conformation. However, for a true comparison study, it would also be interesting to replace one of the sulfur atoms in the disulfide bond with a carbon to give compounds with the same ring size, to see if this had any advantages to selectivity and potency.

Recently, work by van der Donk *et al.*¹ has shown that cystathionine, a thioether linked amino acid in which one sulfur in a traditional disulfide bond is replaced by a CH₂ linkage, is a good replacement for a disulfide bond. Their work focussed on the synthesis of analogues of the 13 amino acid peptide compstatin, which contains one disulfide bond between residues 2 and 12 and is found to have a dramatic decrease in potency in reducing conditions. Compstatin is used to treat problems with the human complement system, which is a biochemical cascade involved in attack of the surfaces of foreign cells in conjunction with antibodies. By replacing the disulfide bond with a thioether linkage obtained from insertion of a cystathionine moiety, it was found that the peptide maintained the binding and inhibitory properties of the parent peptide but was no longer susceptible to reduction. It was also found that the effect of oxidation of the thioether bridge had a far less significant effect on binding and potency, meaning that the cystathionine substitution was of great benefit in this instance.

Cystathionine can be thought of as a disulfide in which one sulfur atom is replaced by a carbon, or a lanthionine with one extra carbon in the ring structure, giving rise to two possible regioisomers (Figure 4.1).

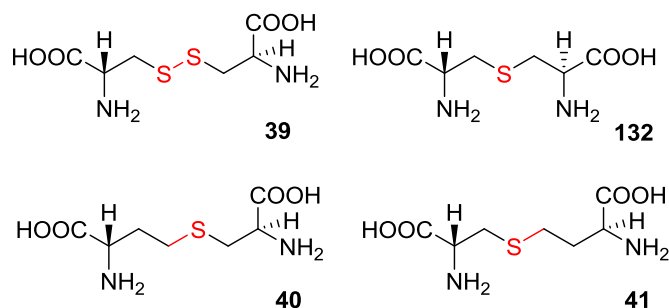


Figure 4.1: Structural Comparison of Disulfide and Thioether Linkages
39 – Disulfide Bond, **132** – Lanthionine Bond, **40** – Cystathionine Bond, Regioisomer 1,
41 – Cystathionine Bond, Regioisomer 2

The work by van der Donk and co-workers¹ showed that the position of the thioether linker had a significant effect on potency; in the case of compstatin, the δ -cystathionine analogues maintained the activity of the disulfide parent peptide, while the γ -cystathionine analogues showed a drop in inhibition and binding ability (Figure 4.2). As with the synthesis of lanthionine, in order to incorporate cystathionine into a peptide synthesis strategy, it was necessary to synthesise the orthogonally protected versions. As it was not known which regioisomer would prove to be more potent in this instance, it was decided to synthesise both regioisomers.

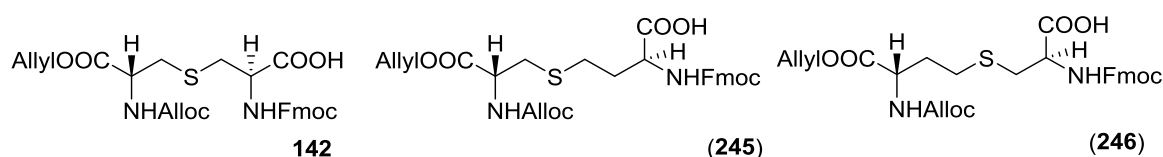


Figure 4.2: Orthogonally Protected Thioether Moieties for Use in Peptide Synthesis
142 – Lanthionine, **(245)** – δ -Cystathionine, Regioisomer 1, **(246)** – γ -Cystathionine, Regioisomer 2

Van der Donk and co-workers synthesised both regioisomers of cystathionine using the phase transfer conditions pioneered by Zhu and Schmidt² and used by Vederas³ to form orthogonally protected lanthionine (Figure 4.3).

The published synthesis¹ began with the formation of allyl/Alloc protected homoserine (**248**) which was then brominated using CBr_4 and triphenylphosphine to give desired intermediate (**249**). This was then reacted with doubly protected cysteine (**62**) to give the fully protected cystathionine (**250**). Similarly, the other regioisomer was formed by first doubly protecting homoserine (**247**) to give (**254**) which was again brominated to give intermediate (**255**). Concurrently, *S*-trityl-L-cysteine (**251**) was doubly protected to give (**252**) before removing the trityl group to give the corresponding cysteine (**253**). These were again reacted using the phase transfer conditions to give fully protected cystathionine (**256**). In both cases, the $t\text{Bu}$ protecting group could then be removed using TFA to give the desired products **245** and **246** for peptide synthesis.

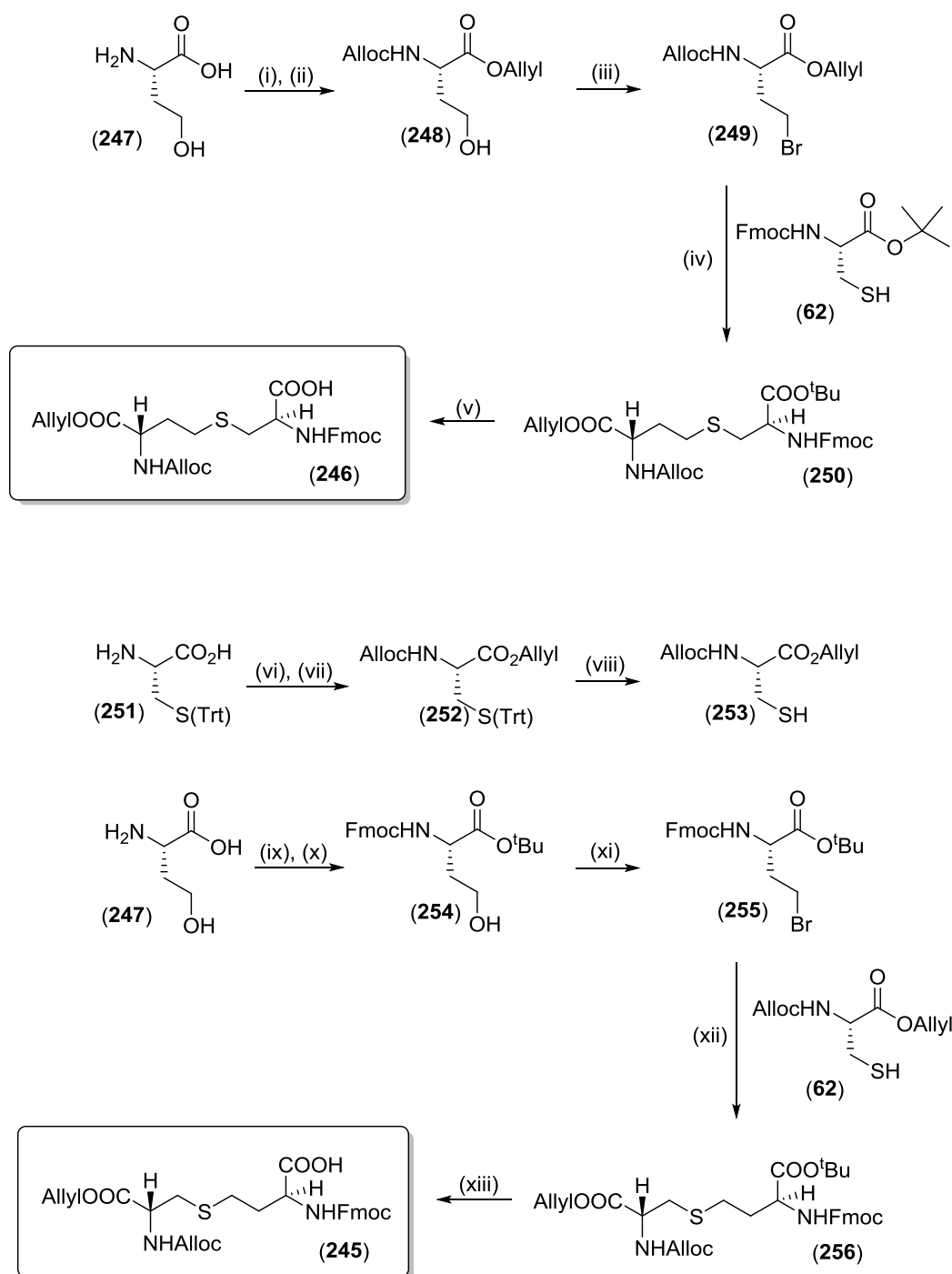


Figure 4.3: Van der Donk Synthesis of Cystathionines (**245**) and (**246**)¹

Reagents and Conditions: (i) allyl chloroformate, Na_2CO_3 , CH_2Cl_2 (ii) allyl bromide, NaHCO_3 , DMF (iii) PPh_3 , CBr_4 , CH_2Cl_2 (iv) Bu_4NBr , NaHCO_3 , H_2O , EtOAc (v) TFA, triethylsilane, CH_2Cl_2 (vi) allyl chloroformate, Na_2CO_3 , CH_2Cl_2 (vii) allyl bromide, NaHCO_3 , DMF (viii) TFA, triethylsilane, CH_2Cl_2 (ix) Fmoc-OSu, 1,4-dioxane, Na_2CO_3 , water (x) tert-butyl-2,2,2-trichloroacetimidate, CH_2Cl_2 , THF (xi) PPh_3 , CBr_4 , CH_2Cl_2 (xii) Bu_4NBr , NaHCO_3 , H_2O , EtOAc (xiii) TFA, triethylsilane, CH_2Cl_2

Previous work^a with the synthesis of lanthionine had shown the phase transfer conditions to be unreliable, not only with forming the unwanted diastereoisomers of the product but also

^a See Chapter 2, Section 2.2.2b

with stability of the compounds in water. For this reason, it was decided to try a new route which would hopefully alleviate the problems with stability and isomerisation.

The synthetic strategy used in this work for the synthesis of both regioisomers of cystathionine was based on the synthesis of lanthionine; to form the cystathionine bond, an S_N2 reaction will take place between a sulfur atom and an iodine atom, with the amino and carboxy residues protected by the orthogonal protecting groups employed previously. For each regioisomer, it is possible to break the thioether bond in two places, giving rise to two possible synthetic routes for each isomer using either a protected homoserine and a protected cysteine derivative or a protected serine and a protected homocysteine derivative (Figure 4.4).

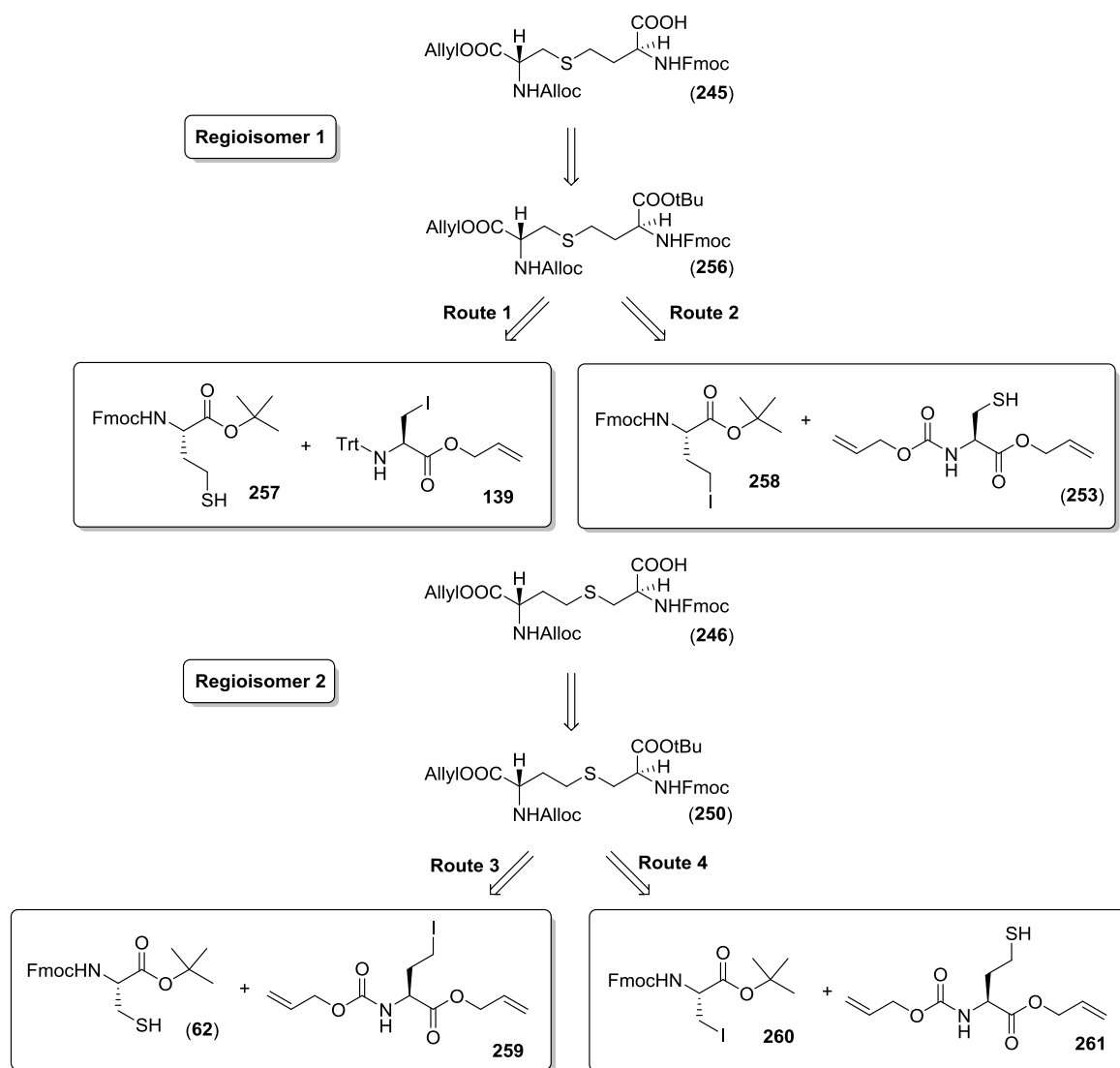


Figure 4.4: Possible Synthetic Strategies for the Synthesis of Cystathionines (245) and (246)

As with the synthesis of lanthionine, a series of protecting steps would be needed to give rise to the required intermediates. These could then be reacted together in the presence of

cesium carbonate to give the desired coupled products (**250**) and (**256**), which could be deprotected to give the desired compounds for inclusion in a peptide synthesis strategy.

The large scale synthesis of orthogonally protected lanthionine **142** had produced large quantities of trityl allyl alcohol **138** and protected cystine (**62**), so it was decided to first try synthetic routes 1 and 3 to minimise the number of steps required to make the desired products.

4.2 Synthesis of Regioisomer 1 (**245**)

As mentioned above, large quantities of trityl allyl alcohol **138** were already available for use, so it was decided to first try synthetic strategy 1 to synthesise cystathionine (**245**). Thus, the forward strategy involves the preparation of an Fmoc and ^tBu protected homocysteine residue **257**, which can then be reacted with the iodinated serine **138**. It is difficult to buy homocysteine or homocysteine commercially, however, fortuitously, Fmoc and trityl protected homocysteine (**262**) is available to buy. The proposed forward synthetic scheme (Figure 4.5) uses many of the reactions used in the synthesis of orthogonally protected lanthionine and thus has the advantage of being a known route.

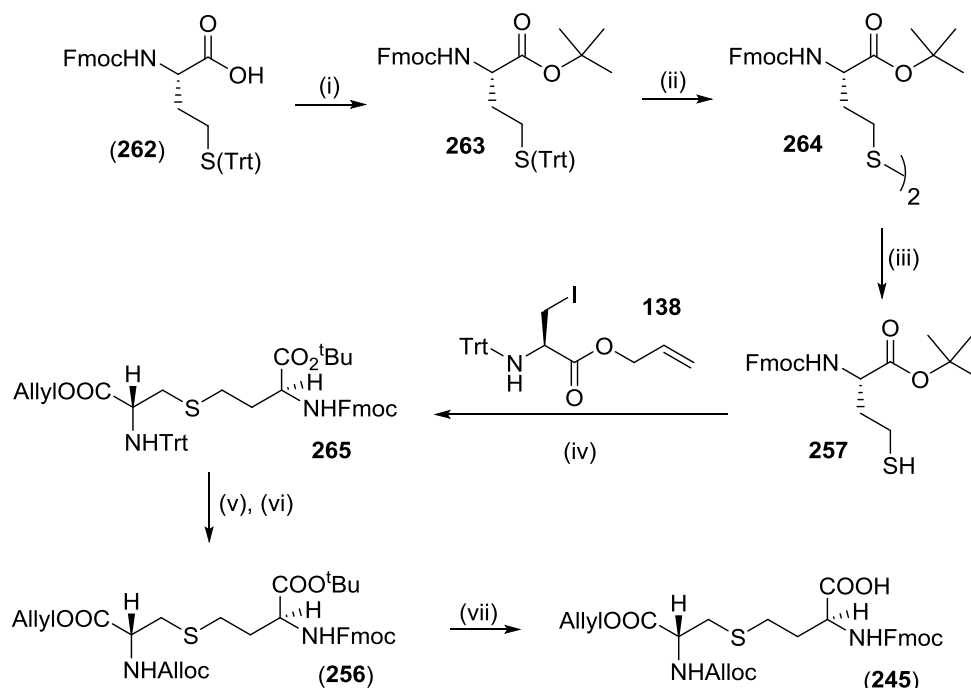


Figure 4.5: Proposed Synthetic Strategy for Synthesis of Cystathionine (**245**)

Reagents and Conditions: (i) *tert*-butyl-2,2,2-trichloroacetimidate, CH₂Cl₂ (ii) TFA, triethylsilane, CH₂Cl₂ (iii) dithiothreitol, Et₃N, CH₂Cl₂ (iv) Cs₂CO₃, DMF (v) 10% TFA, 5% triethylsilane, CH₂Cl₂ (vi) allyl chloroformate, Na₂CO₃, CH₂Cl₂ (vii) TFA, triethylsilane, CH₂Cl₂

Firstly, the commercially available homocysteine (**262**) was *tert*-butyl protected using *tert*-butyl-2,2,2-trichloroacetimidate to give **263** in quantitative yield. The trityl group was then removed in the presence of trifluoroacetic acid to give the homocysteine **264**, which could be

cleaved to give the desired homocysteine **257**. The first three steps proceeded well and gave an overall yield of 39% of the double protected homocysteine ready for coupling. Unfortunately, using the same conditions used to form the coupled lanthionine product **140**, that is, 4 h stirring on ice, did not yield any of the desired product (Figure 4.6, Table 4.1, Entry 1) with the column instead yielding only starting material. Although longer reactions were tried (Table 4.1, Entries 2 and 3), the predominant reaction seemed to be production of the aziridine **143**. The major problem appeared to be that the S_N2 reaction to produce the coupled product **265** was very slow and that the competing reaction to form the aziridine was occurring much faster. This is in agreement with earlier work carried out on the synthesis of lanthionine, which showed that when left in solution for too long, the iodoalanine product **143** tends to form the aziridine.

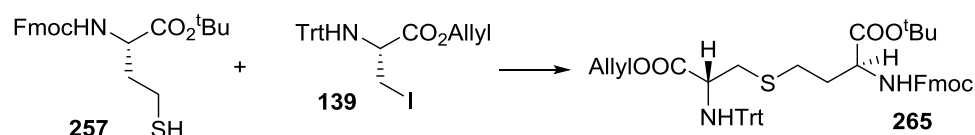


Figure 4.6: Attempts to Couple Iodoalanine **139** and Protected Homocysteine **257** to form Cystathionine

Entry	Reaction Conditions	Results
1	0.5 eq. Cs ₂ CO ₃ at 0 h, 0.5 eq. Cs ₂ CO ₃ at 2 h, total reaction time – 4 h	No Reaction – starting materials isolated
2	1 eq. Cs ₂ CO ₃ at 0 h, total reaction time – 21 h	5 % product, aziridine formation predominated
3	1 eq. Cs ₂ CO ₃ at 0 h, total reaction time – 38 h	21 % product, aziridine formation predominated

Table 4.1: Attempts to Couple Iodoalanine **139** and Protected Homocysteine **257** to form Cystathionine

All reactions used 1 eq. Iodoalanine **139** and 1 eq. Homocysteine **257** in DMF.

As the coupling step did not give a good yield of the cystathionine **265**, it was not possible to continue with this route as the yield of the final product would have been too low to allow multiple attempts at solid phase peptide synthesis.

As this reaction was so unreliable, it was decided not to continue with this synthesis but to try the alternative route (Route 2, Figure 4.2) to see if this could improve the yield of the final product. The second route has the advantage of only requiring the removal of the *tert*-butyl group after the coupling reaction, as opposed to the three steps required in route one (Figure 4.7).

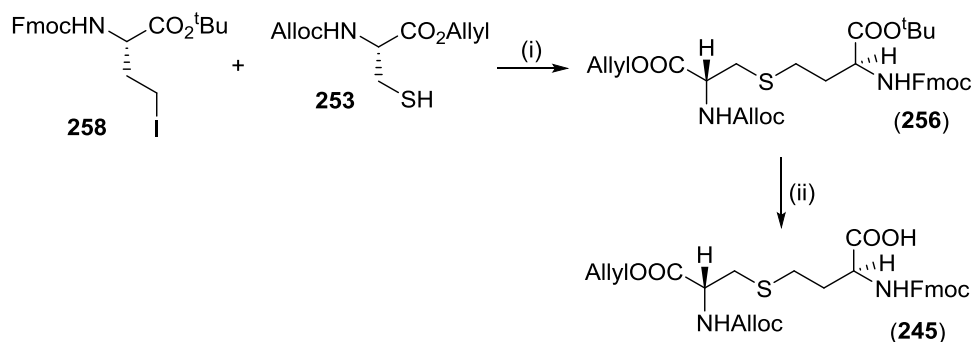


Figure 4.7: Alternative Synthetic Strategy for Synthesis of Cystathionine (**245**)

Reagents and Conditions: (i) Cs₂CO₃, DMF (ii) TFA, triethylsilane, CH₂Cl₂

Using the same S_N2 strategy, it was predicted that the coupled product (**256**) could be formed in the presence of cesium carbonate, with careful control of the temperature. Using this reaction as a starting point, it was necessary to find a strategy to quickly and easily form the two doubly protected amino acids. Work began with the production of the allyl/Alloc protected cysteine **253** (Figure 4.8).

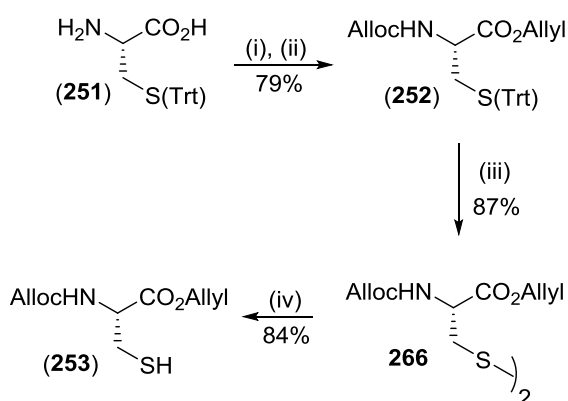


Figure 4.8: Alternative Synthetic Strategy for Synthesis of Protected Cysteine (**253**)

Reagents and Conditions: (i) allyl chloroformate, Na₂CO₃, CH₂Cl₂ (ii) allyl bromide, NaHCO₃, DMF (iii) TFA, triethylsilane, CH₂Cl₂ (iv) dithiothreitol, triethylamine, CH₂Cl₂

Following the work of van der Donk,¹ commercially available trityl cysteine (**251**) was first allyl and Alloc protected in a clean one pot reaction to give the product (**252**) in good yield without the need for purification. According to the paper, the desired cysteine product could then be formed directly by removal of the trityl group using trifluoroacetic acid. However, in all cases, the dimer **266** was formed instead. This was confirmed by using Ellman's reagent which did not change colour, indicating that no free SH group was present.

Using the previously established method with dithiothreitol, it was found that the dimer could be cleaved easily to provide the required cysteine (**253**) for the coupling reaction. These reactions gave an overall yield of (**253**) of 58%, starting from the commercially available trityl cysteine (**251**). As this procedure only required one column after the removal of the trityl protecting group, it was envisaged that this reaction could be scaled up quickly

and easily. Indeed, on a 2 g scale, the method allowed for the production of 753 mg of the desired product, which equates to a slightly reduced yield of 37%.

With the synthesis of the cysteine complete, attention turned to the formation of the protected homoserine. The Fmoc and *tert*-butyl protecting groups were installed in a one pot reaction to give the monomer (**254**). Unfortunately, this reaction also produced some of the Fmoc protected lactone **268**, which was difficult to remove by column chromatography and decreased the overall yield of the reaction. However, careful purification resulted in a 60% yield of the desired double protected product (**254**, Figure 4.9).

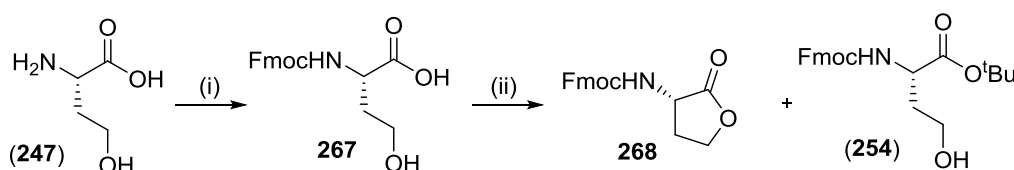


Figure 4.9: Attempts to Synthesise allyl/Alloc Homoserine (**254**)
Reagents and Conditions: (i) allyl chloroformate, Na_2CO_3 , CH_2Cl_2 (ii) see table

Incorporation of the iodine into the compound proved to be more difficult (Table 4.2).

Entry	Reaction Conditions	Results
1	1.5 eq. triphenylphosphine, 1.5 eq. methyl iodide, DEAD, CH_2Cl_2	No Reaction
2	1 eq. mesyl chloride, CH_2Cl_2 , then 1.1 eq. NaI in acetone	No Reaction
3	1.2 eq. triphenylphosphine, 1.2 eq. imidazole, 1.2 eq. iodine, CH_2Cl_2	53%

Table 4.2: Summary of Attempts to Iodinate Homoserine (**254**)

The first attempt using the Mitsunobu reaction conditions employed in the synthesis of lanthionine did not yield any of the desired product. For the next attempt, the alcohol was first mesylated using mesyl chloride before reaction with sodium iodide but this again did not produce any of the desired product. Finally, it was found that the iodinated product could be made using triphenylphosphine, imidazole and iodine, which gave the product with a yield of 53% (Figure 4.10).

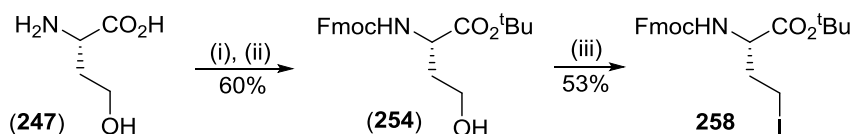


Figure 4.10: Alternative Synthetic Strategy for Synthesis of Protected Homoserine **258**
Reagents and Conditions: (i) Fmoc-OSu, 1,4-dioxane, Na_2CO_3 , water (ii) *tert*-butyl-2,2,2-trichloroacetimidate, CH_2Cl_2 :THF 5:1 (iii) triphenylphosphine, imidazole, iodine, CH_2Cl_2

Once the synthesis of the intermediates was completed, attention turned to the coupling reaction to form (**256**). The major problem with the previous synthetic route was the slow speed of the $\text{S}_{\text{N}}2$ reaction in the coupling step, which could in part have been due to the large size of the trityl and allyl groups on the serine **138** making the iodo group less accessible to the bulky cysteine derivative for nucleophilic attack. The advantages of using the iodinated homoserine **258** are two-fold; firstly with one extra carbon atom in the chain, it is not

possible to form the aziridine and secondly, the extra carbon also places the iodine further away from the bulky protecting groups on the amino acid, which makes it more accessible for attack by the nucleophile and should increase the rate of reaction. To form the equivalent lanthionine product **142**, the reaction is left to stir for a total of 4 h. After this point, no further reaction is observed and instead any excess iodinated serine **138** turns into aziridine. The reaction to form cystathionine (**256**) is noticeably more capricious (Figure 4.11). Initial observations with both routes had shown that the reaction appeared to be noticeably slower than the equivalent lanthionine coupling reaction. However, despite trying a number of different timings for the reaction and ensuring the reaction was kept cold, none of the desired product was observed in any case.

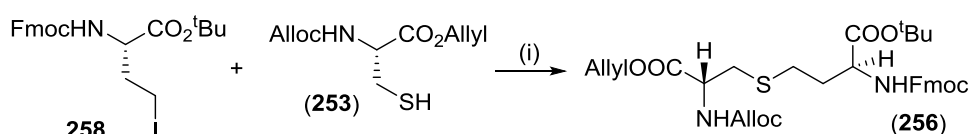


Figure 4.11: Synthesis of Cystathionine (**256**)

Entry	Reaction Time (h)	Results
1	4 h	No Reaction
2	21 h	Potentially a small amount of product without Fmoc observed
3	8 h	Potentially a small amount of product without Fmoc observed

Table 4.3: Synthesis of Cystathionine (**256**)

Reagents and Conditions: (i) Cs_2CO_3 , DMF

In two cases, it was thought that potentially the desired product without the Fmoc protecting group was observed (Table 4.3, Entries 2 and 3) but attempts to reinstate the Fmoc group using both Fmoc chloride and Fmoc succinimide did not yield any of the desired product. From the three reactions, it is not clear exactly why the reaction has not proceeded as expected and further investigations will be required to draw definite conclusions. Unfortunately it was beyond the scope of this work to investigate this any further.

4.3 Conclusions from the Synthesis of Regioisomer 1 (**245**)

This new synthetic strategy, based on the work carried out to form an orthogonally protected lanthionine **142**, should lead to the production of cystathionine (**245**), which could be used in solid phase peptide synthesis to form another group of ProTx-II analogues. Two routes were originally proposed for this synthesis and it was found that the most promising route was between the protected homoserine **258** and the protected cysteine (**253**). Preliminary work has shown that both monomers can be formed quickly and easily on a medium scale and should be amenable to scale-up work in the future. The coupling reaction to form the desired fully protected product (**256**) needs further work and alternatives could include using the bromo compound in place of the iodinated homoserine. Work could also focus on the use of

the phase-transfer conditions used by Vederas³ and van der Donk,¹ as in this case, racemisation at the α -centre would not be a concern.

4.4 Synthesis of Regioisomer 2 (**246**)

As large quantities of the doubly protected cystine (**62**) were available for use, the first synthesis attempted was that shown in route 3 (Figure 4.4). In order to carry out the coupling step, it was first necessary to form the allyl/Alloc protected homoserine (**248**), which could then be iodinated and coupled to the doubly protected cystine (**62**) to produce cystathionine (**250**). As with route 2, the advantage of this route is that after the coupling reaction, only one reaction is required to make the final product ready for peptide synthesis. In the synthesis of lanthionine, it was not possible to use the equivalent iodinated allyl/Alloc protected serine, as the iodine could eliminate leaving the dehydroalanine, which in turn led to racemisation at the stereocentre and a mixture of diastereomers was produced. The advantage of using the homoserine equivalent **259** is that if elimination occurs, racemisation does not occur at the α -centre as the iodine atom is one further carbon atom away. This removes the need for the trityl deprotection and re-protection steps, which shortens the synthesis and makes it more efficient. The proposed synthesis (Figure 4.12) thus began with the allyl/Alloc protection of homoserine (**247**), to give (**248**). It was envisaged that this could then be iodinated using the Mitsunobu conditions employed in the synthesis of the iodoalanine **139**, before coupling in the presence of cesium carbonate and removal of the *tert*-butyl protecting group gave the desired product.

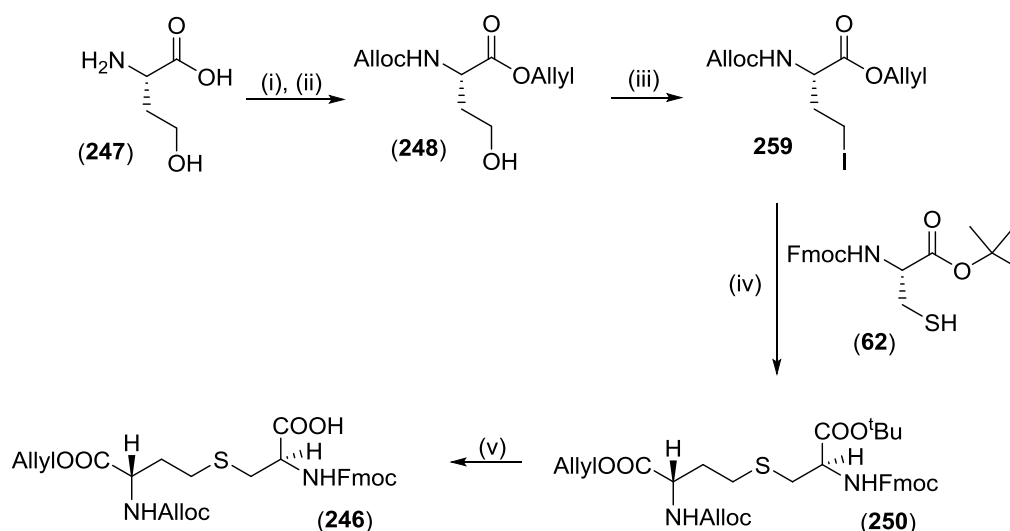


Figure 4.12: Proposed Synthetic Strategy for Synthesis of Cystathionine (246**)**
Reagents and Conditions: (i) allyl chloroformate, Na_2CO_3 , CH_2Cl_2 (ii) allyl bromide, NaHCO_3 , CH_2Cl_2 (iii) triphenylphosphine, methyl iodide, DEAD, CH_2Cl_2 (iv) Cs_2CO_3 , DMF (v) TFA, triethylsilane, CH_2Cl_2

According to the work published by van der Donk and coworkers¹, the desired homoserine (**248**) could be easily formed in a one pot reaction starting from the commercially available homoserine (**247**) by first Alloc protecting with allyl chloroformate and then protecting the carboxylic acid moiety with allyl bromide (Table 4.4, Entry 1). Unfortunately, it was found that the majority product formed was always the Alloc protected lactone **270**. This product could not be iodinated directly to make the desired **259**, so the double protection strategy was researched in more detail. It was found that the reaction to form Alloc homoserine **269** proceeded cleanly to give the desired product without need for further purification. However, upon addition of allyl bromide, lactonization began to occur. This is unsurprising, as the 5-*exo-trig* reaction for cyclisation is favoured by Baldwin's rules^{4,5} as the OAllyl moiety can act as a good leaving group. Thus, work focussed on the allyl protection reaction to see if lactonization could be circumvented to give the desired product (**248**, Figure 4.13).

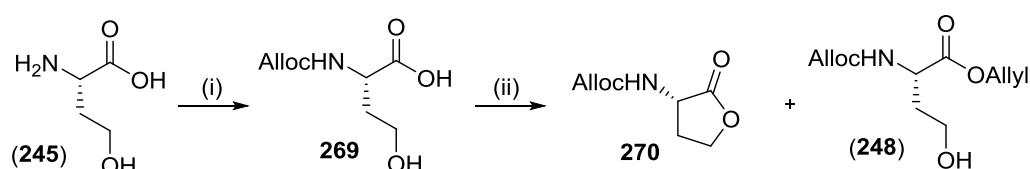


Figure 4.13: Attempts to Synthesise allyl/Alloc Homoserine (**248**)

Entry	Reaction Conditions (ii)	Results
1	1.1 eq. allyl bromide, NaHCO ₃ , 24 h	100% lactone 270
2	allyl alcohol, <i>para</i> -toluene sulfonic acid, 5 h	100% lactone 270
3	1.1 eq. allyl bromide, NaHCO ₃ , 65 h	100% lactone 270
4	1.1 eq. allyl bromide, NaHCO ₃ , then additional 0.6 eq. allyl bromide after 24 h. total stirring time =36 h	100% lactone 270
5	1.1 eq. allyl bromide, NaHCO ₃ , 8 h, on ice	1:1 lactone 270 and homoserine (248) mix, 20% yield
6	1.1 eq. allyl bromide, NaHCO ₃ , 24 h, no work up	2:3 lactone 270 and homoserine (248) mix, 25% yield

Table 4.4: Attempts to Synthesise allyl/Alloc Homoserine (**248**)

Reagents and Conditions: (i) allyl chloroformate, Na₂CO₃, CH₂Cl₂ (ii) see table

Firstly, it was decided to try using the conditions to make the allyl/Alloc serine **152** discussed in Chapter 2,⁶ using allyl alcohol and Dean-Stark apparatus in the presence of *para*-toluene sulfonic acid (Table 4.4, Entry 2). These conditions promoted the formation of the lactone and so this reaction was not pursued any further. It was then decided to see if the lactonization process could be reversed by leaving the allylation for longer and by adding an additional portion of allyl bromide (Table 4.4, Entries 3 and 4) but this again did not lead to any of the desired product. The next step was to try a shorter reaction time at a reduced temperature (Table 4.4, Entry 5). This finally saw production of the desired homoserine product (**248**) in a 1:1 ratio with the unwanted lactone **270** which was difficult to remove *via*

column chromatography. Lastly, attention turned to the work-up procedure: it was feared that the use of a basic aqueous work-up could enhance the lactonization process, so a small scale reaction was carried out where the reaction was simply concentrated *in vacuo* before re-dissolving in chloroform and washing once with water to remove the bicarbonate salt, before purification *via* column chromatography (Table 4.4, Entry 6). This also had some success leading to isolation of a mixture containing a higher proportion of the desired homoserine (**248**) but was still difficult to purify. Although a limited amount of the desired product was accessible, this was not enough to carry through to produce large quantities of the cystathionine end product.

Given that the products were so difficult to separate, research next turned to attempts to re-open the lactone to see if the desired product could be isolated in a greater yield. Following this strategy, attempts to re-open the lactone under both acidic and basic conditions were attempted with equally disappointing outcomes (Figure 4.14).

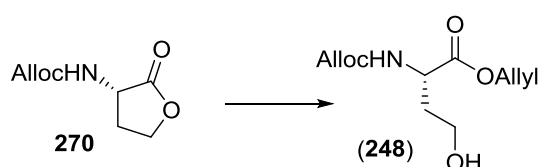


Figure 4.14: Attempts to Open Alloc Lactone **270**
Reagents and Conditions: see table

Entry	Reaction Conditions	Results
1	allyl alcohol as solvent, few drops of HCl	100% lactone 270
2	(i) 1 eq. NaOH, EtOH, 30 min (ii) 1.2 eq. allyl bromide, DMF, 8 h	100% lactone 270
3	(i) 1 eq. NaOH, EtOH, 30 min (ii) 1.2 eq. allyl bromide, DMF, 21 h	100% lactone 270

Table 4.5: Attempts to Open Alloc Lactone **270**

Dissolving in allyl alcohol and adding concentrated HCl showed no reaction (Table 4.5, Entry 1). Ozinskas and Rosenthal⁷ claim that the lactone can be opened in base using 1.2 equivalents of allyl bromide to give the desired homoserine (**248**). Unfortunately, the reaction was carried out twice for both 8 and 21 h but no reaction was observed in either case (Table 4.5, Entries 2 and 3).

As the products were so difficult to separate, it was decided to try iodinating the mixture of lactone and homoserine to get the desired iodinated compound **259**. It was found that the Mitsunobu conditions employed previously did not work in this instance but that the product could be formed if the alcohol was first mesylated and then reacted with iodine. This allowed for the production of 60 mg of **259**, which was found to be very unstable in solution and to purification by column chromatography, leading to rapid decomposition. The small amount isolated was reacted with the doubly protected cysteine (**62**) to give the second regioisomer

of cystathionine (**250**), in reasonable yield. However, not enough of the product was made to carry out the final deprotection step and obtain a meaningful amount of cystathionine (**246**) for peptide synthesis (Figure 4.15).

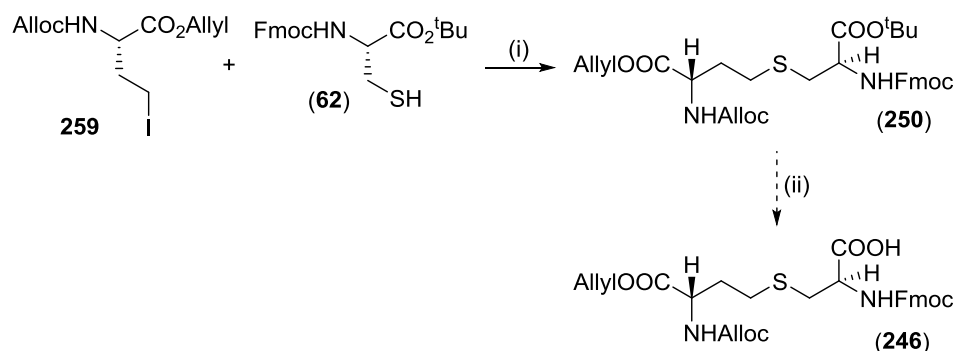


Figure 4.15: Attempted Synthesis of Cystathionine (**246**)

Reagents and Conditions: (i) Cs₂CO₃, DMF (ii) TFA, triethylsilane, CH₂Cl₂

Given the major difficulties with lactonization, it became clear that this route was not going to be suitable for large scale work and so attention turned to route 4 to see if this could produce the desired cystathionine (**246**) in better yield.

This route is in fact the most cumbersome of the four as homocysteine and homocystine are not available to buy commercially. Instead, the route had to begin with the Fmoc/Trt protected homocysteine (**262**) used in the synthesis of the other regioisomer of cystathionine (**245**). To begin, it was decided to try removing the Fmoc group and then to do a one pot allyl/Alloc protection to form **274**. The Fmoc deprotection proceeded well but unfortunately gave the product as a barely soluble white solid. The next reaction to Alloc protect the homocysteine did not proceed, probably due to the lack of solubility (Figure 4.16).

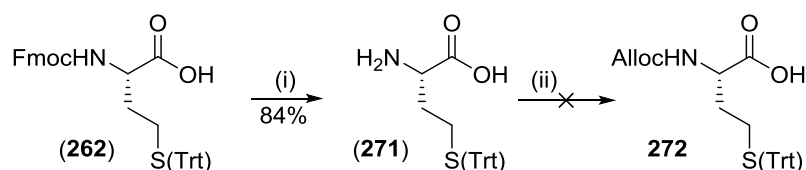


Figure 4.16: Attempts to Synthesise allyl/Alloc Protected Homocysteine **274**

Reagents and Conditions: (i) piperidine, DMF (ii) allyl chloroformate, Na₂CO₃, CH₂Cl₂

As an alternative, it was decided to first allyl protect the homocysteine before removing the Fmoc group to see if this would improve the solubility problems. Pleasingly, this reaction proceeded well and the Fmoc/allyl protected homocysteine **273** was produced in 42% yield. From here, the Fmoc group was removed using piperidine in DMF before addition of the Alloc group using allyl chloroformate to produce **274** in good yield. The trityl group was then left as the corresponding dimer until the desired homocysteine **261** was required in the coupling step. Overall, this route required 4 steps and had an overall yield of 8% (Figure 4.17).

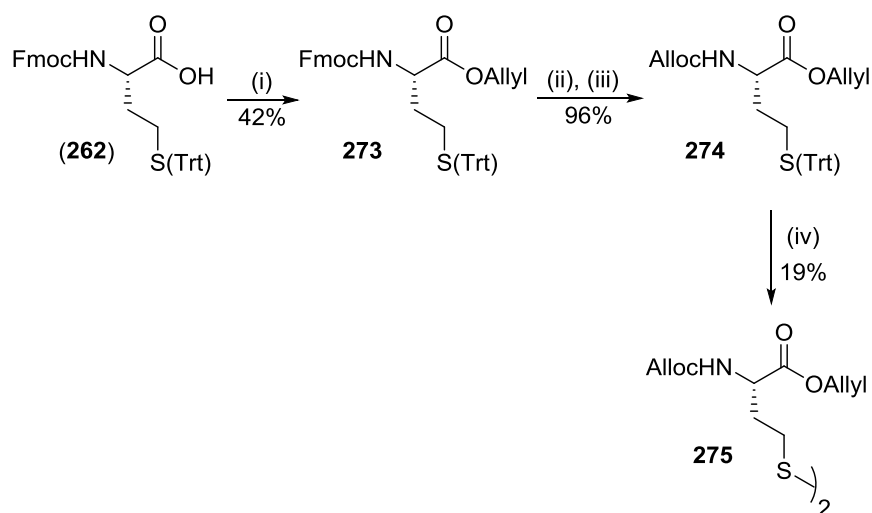


Figure 4.17: Synthesis of Homocysteine **275**

Reagents and Conditions: (i) allyl bromide, methanol, Cs_2CO_3 , DMF (ii) 40% piperidine in DMF (iii) allyl chloroformate, acetonitrile, Na_2CO_3 , CH_2Cl_2 (iv) TFA, triethylsilane, CH_2Cl_2

With this synthesis complete, attention turned to the formation of Fmoc/^tBu protected serine (**258**), which it was envisaged would then be iodinated before coupling with the allyl/Alloc homocysteine **261** to form the desired regioisomer of cystathionine (**250**, Figure 4.18).

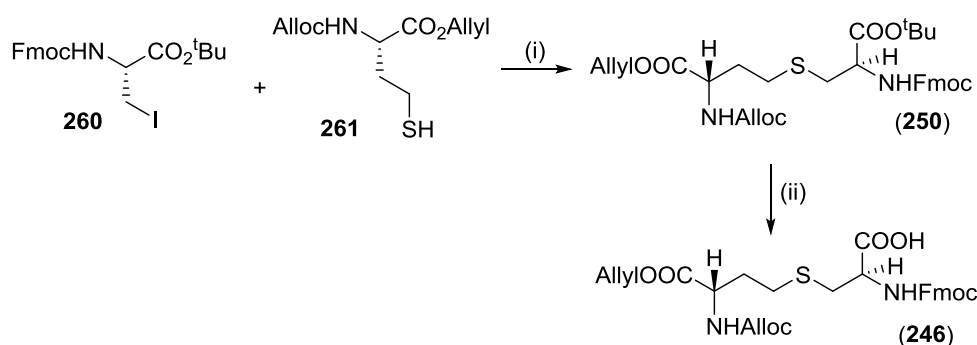


Figure 4.18: Alternative Strategy for the Synthesis of Cystathionine (**246**)

Reagents and Conditions: (i) Cs_2CO_3 , DMF (ii) TFA, triethylsilane, CH_2Cl_2

Unfortunately, the iodination of the doubly protected serine **276** proved elusive; both the Mitsunobu conditions used to form trityl allyl iodoalanine **139** and the attempt to mesylate the alcohol, followed by reaction with sodium iodide used to form the iodinated allyl/Alloc homoserine **248** did not yield any of the desired product.

Previous work carried out by others within the group showed that when the iodination of this serine was successful,⁸ the subsequent coupling reaction did not proceed as expected but lead to a mixture of diastereoisomers of the product. This occurred as some of the serine formed the unwanted dehydroalanine side product, which could then undergo a Michael addition to form either diastereoisomer of the product (Figure 4.19).

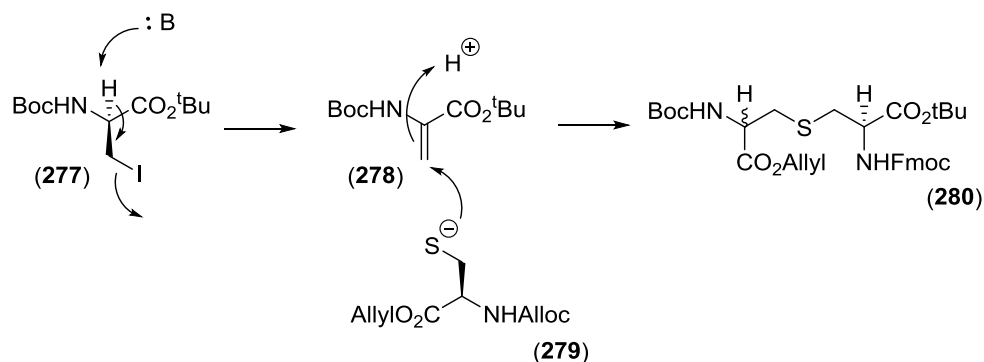


Figure 4.19: Formation of Dehydroalanine (278) and the Subsequent Coupling Reaction⁸

When the nitrogen atom is attached to an electron withdrawing group such as Fmoc or Cbz, the acidity of the α-proton increases and is easily abstracted, leading to elimination of the iodine and formation of the double bond in (278).

In the synthesis of lanthionine, this is circumvented by the use of the trityl protected serine **139**,⁸ which does not lead to diastereoisomers as dehydroalanine formation is not promoted. However, the electron donating group does favour elimination of iodine to form the corresponding aziridine, and indeed, in all cases some aziridine formation was observed. It was beyond the scope of the current work to investigate this further but this could be a potential avenue for future work.

4.5 Conclusions from the Synthesis of Regioisomer 2 (246)

The synthesis of the second regioisomer of cystathionine proved to be as elusive as the first, due to the instability of the iodinated homoserine and the great propensity for lactonization. Although an alternative route *via* the protected homocysteine **261** and protected serine **260** analogues was investigated, it was not possible to form any of the desired product using this method. Although beyond the scope of this piece of work, future work would need to focus on either the synthesis of the allyl/Alloc homoserine (248) or the synthesis of a trityl serine derivative for reaction with the allyl/Alloc homocysteine **261**. Preliminary investigations using the homoserine pathway have shown it is possible to make a combination of the lactone **270** and the desired product and further work would surely improve upon this. The synthesis attempts allowed for the production of 110 mg of the desired product (250), showing the coupling conditions work, although more work will be required. The iodinated homoserine product **259** was found to be particularly unstable and it may be that the bromo derivative may be better suited to large scale production of cystathionine. Future work should focus on both this and ways to prevent lactonization.

4.6 Conclusions

Preliminary investigations into the synthesis of both regioisomers of the orthogonally protected cystathionines (**245**) and (**246**), have shown that the syntheses will require further optimisation before any large scale work can be carried out. However, work thus far has shown that it is possible to form the required monomers in the synthesis of regioisomer (**245**) in high yield on reasonably large scale. To finish the synthesis, a significant amount of work on the coupling reaction is required but with greater amounts of the monomers available, the final two steps should be easily achieved. Possible routes to investigate for the coupling reaction include using the bromo-derivative with the cesium carbonate coupling conditions or using the phase-transfer conditions used in the van der Donk group. With regards to the second regioisomer (**246**), more work needs to be done to prevent lactonization of the allyl/Alloc homoserine (**246**). With that complete and the work on the coupling reaction to form the other regioisomer, it should again prove easy to form the final product.

¹ Knerr, P. J.; Tzekou, A.; Ricklin, D.; Qu, H.; Chen, H.; van der Donk, W. A.; Lambris, J. D., *ACS Chem. Biol.*, **6**, 753-760 (2011)

² Zhu, X.; Schmidt, R. R., *Eur J Org Chem*, **20**, 4069-4072 (2003)

³ Pattabiraman, V. R.; McKinnie, S. M. K.; Vederas, J. C., *Angew. Chem. Int. Ed.*, **47**, 9472-9475 (2008)

⁴ Baldwin, J. E., *J. Chem. Soc., Chem. Commun.*, **18**, 734-736 (1976)

⁵ Baldwin, J. E.; Thomas, R. C.; Kruse, L. I.; Silberman, L., *J. Org. Chem.*, **42**, 24, 3846-3852 (1977)

⁶ Liu, W.; Chan, A.S.H.; Liu, H.; Cochrane, S.A.; and Vederas, J.C., *J. Am. Chem. Soc.*, **133**, 14216-14219 (2011)

⁷ Ozinskas, A. J.; Rosenthal, G. A., *J. Org. Chem.*, **51**, 26, 5047-5050 (1986)

⁸ Bregant, S.; Tabor, A. B., *J. Org. Chem.*, **70**, 2430-2438 (2005)

5. Chapter 5: Biological and *in silico* Evaluation of the Analogues of ProTx-II

ProTx-II (**22**) was previously shown to have good inhibitory effects of the Na_v1.7 ion channel with an IC₅₀ value of 0.3 nM *in vitro*.¹ However, comparatively poorer results were observed *in vivo*, suggesting the peptide was too large to cross the blood-nerve barrier. A number of analogues of ProTx-II were synthesised (see Chapter 3). The first set were truncated to probe the structure-activity relationship of ProTx-II by investigating which parts of the peptide were important for binding to the channel and the second set of analogues were designed to be more resistant to enzymatic degradation *in vivo* through replacement of a disulfide bond with a thioether linkage. Having synthesised a set of 10 analogues, along with the native peptide, the next step was to investigate the effects of these analogues on the Na_v1.7 ion channel. This work consisted of two separate experimental approaches; in the first, evaluation of the structures of the compounds was carried out using homology modelling *in silico*. In the second line of investigation, the biological effect on the ion channel was assessed using an automated patch clamp assay. The patch clamp experiments were carried out in collaboration with two commercial companies, Essen Bioscience from Welwyn Garden City, UK and B'Sys from Witterswil, Switzerland.

5.1 *In Silico* Analysis of Structures

As mentioned in the introduction (Section 1.5) prior to release of the structure of ProTx-II by Park *et al.* in 2014,² the only structural information available came from homology modelling carried out by Smith and co-workers.³ In their work, the initial model was based on the structure of HpTx-II, another ICK peptide containing the same secondary structure as ProTx-II. However, the primary sequences differed significantly, with the peptides only sharing 50% similarity^a (Figure 1.20). Ideally, it would be possible to evaluate the structures of the analogues of ProTx-II using the coordinates from the solution phase NMR published by Park and co-workers. Unfortunately, at the time of writing, it was not possible to obtain this information as it was not uploaded to the Protein Data Bank and attempts to contact the group directly proved unsuccessful.

Given the large discrepancy in structure between HpTx-II and ProTx-II, it was decided to investigate the structure of ProTx-II using a different structure as the basis for molecular modelling. In 2004, the solution phase NMR structure of PaTx-I was released⁴ which shares 83% identity^a with ProTx-II and is also an ICK peptide (Figure 5.1). This peptide was first isolated from the *Phrixotrichus auratus* spider and is 29 amino acids in length. Although the

^a as calculated by the clustal W2 software available at www.ebi.ac.uk

C-terminii of the peptides are non-homologous, only two amino acids differ between the two peptides within the core structure, making PaTx-I the ideal candidate for the basic structure for homology modelling.

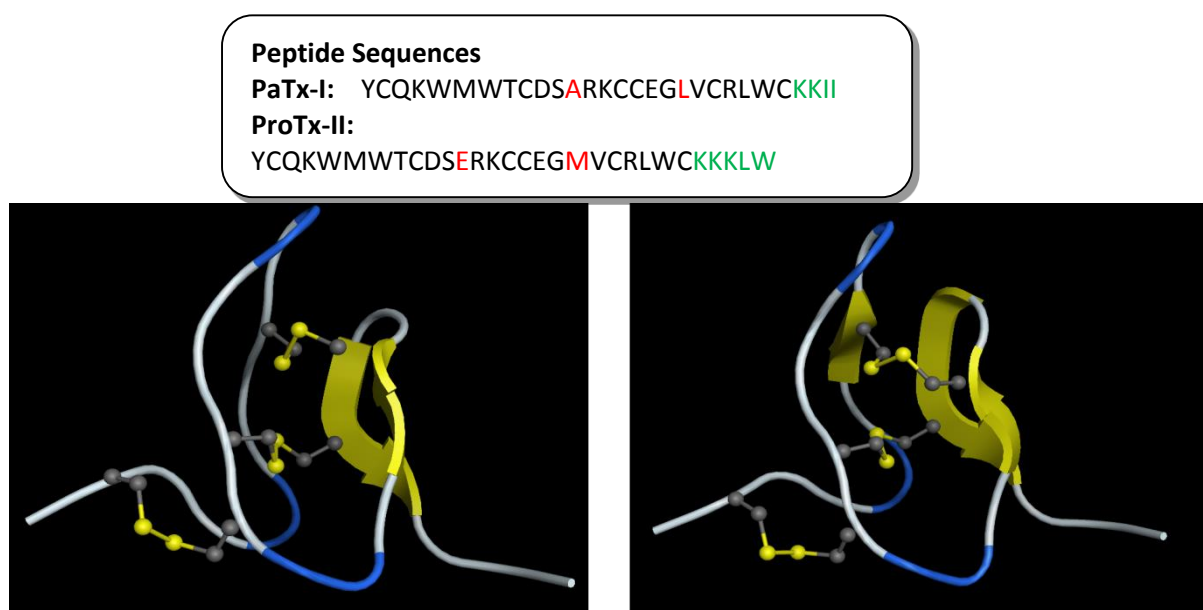


Figure 5.1: Comparison of PaTx-I (left) and ProTx-II (right) Structure Generated by MOE™ Software

To create the model of ProTx-II, the coordinates of PaTx-I were first uploaded to the Molecular Operating Environment (MOE™) software before the amino acids were altered *in silico* to give the correct structure for ProTx-II. The Amber94 forcefield and Born solvation conditions were then applied and a quick molecular dynamics calculation performed to give the structure above. The diagram shows that PaTx-I and ProTx-II are both predicted to be tightly bound molecules with a well-defined backbone structure and small area of β -sheet ordering within each of the peptides (indicated by the arrows).

The predicted structure created by the MOE™ software agrees closely with the previously published model by Park *et al.* (Figure 5.2). The only difference is that the software predicts a slightly more ordered structure with an extended β -sheet region around Cys-25 with respect to that found in the solution NMR structure, with an additional two areas of ordering predicted around the disulfide bond connecting Cys-9 to Cys-25.

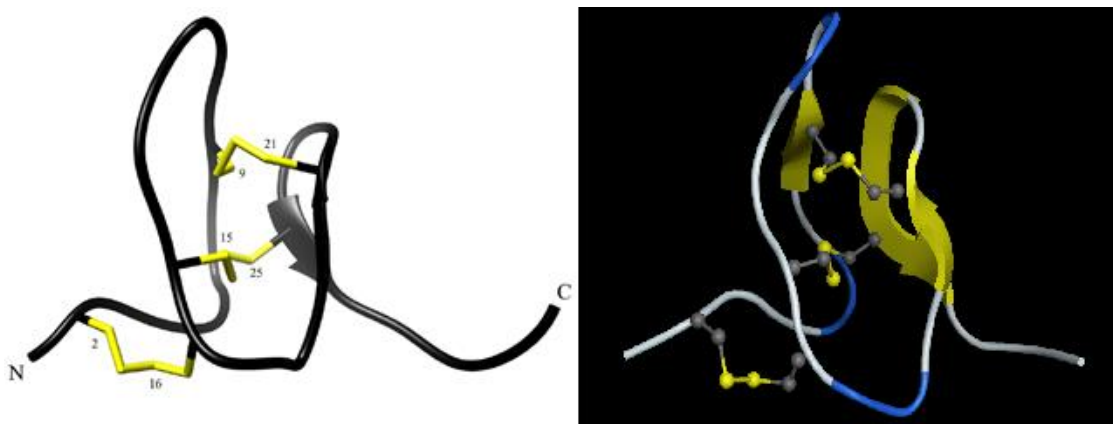


Figure 5.2: Comparison of Solution NMR Structure of ProTx-II (left) With Structure Predicted by MOE™ Software (right)⁵

Park and co-workers found that the C-terminal motif (KKKLW) was structurally undefined and found to form a flexible tail region. As the flexible tail region is also observed in the C-terminal motif of PaTx-I (KKII), it can be assumed that the tail region in the structure generated by the MOE™ software also shows a high degree of flexibility.

5.1.1 Modelling of the Single Ring Analogues of ProTx-II

Having generated the structure of the parent peptide, the next step was to model the three disulfide single ring analogues using the same calculations (Figures 5.3 – 5.5). To model the single ring analogues, the residues not present in the parent peptide were removed from the sequence and the cysteines no longer involved in disulfide bond formation were altered to methionine, to reflect the structures synthesised in the laboratory. To model the lanthionine bond, the equivalent structure containing the disulfide bond was first generated. One sulfur atom was then removed from the structure and the structure was re-minimised to generate an approximation of the lanthionine bond. An energy minimising calculation was then performed for each of the peptides to generate the structures shown below.

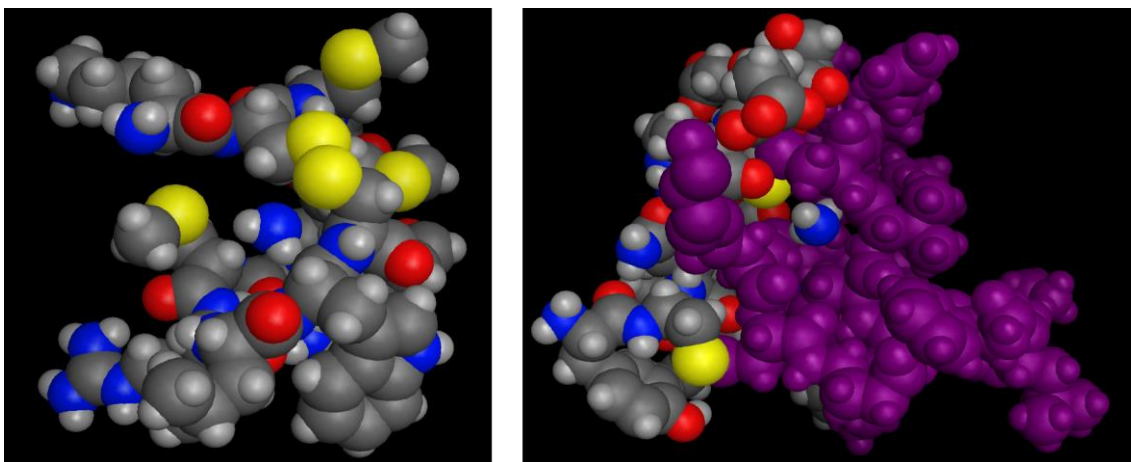


Figure 5.3: Structure of C-terminal Single Ring (**192**) and Location of the Residues Within ProTx-II (**22**, purple)

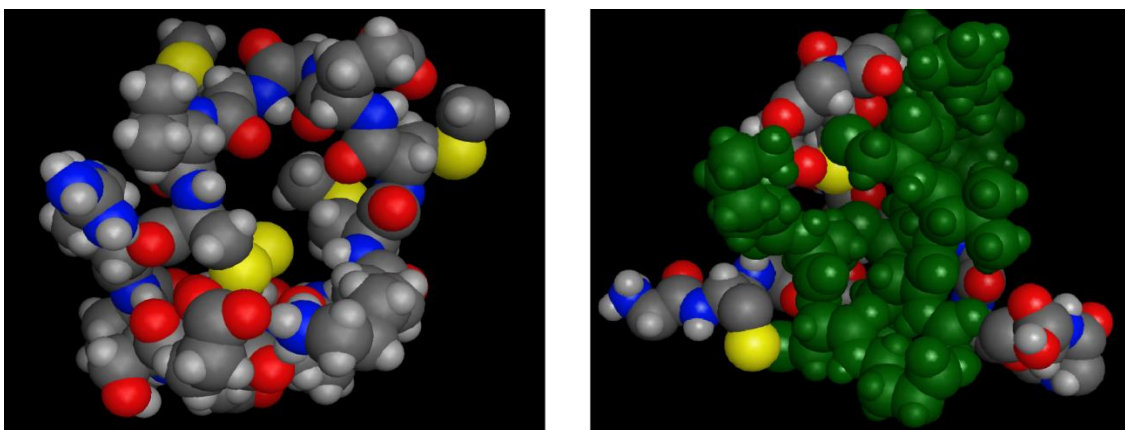


Figure 5.4: Structure of Middle Single Ring (**193**) and Location of the Residues Within ProTx-II (**22**, green)

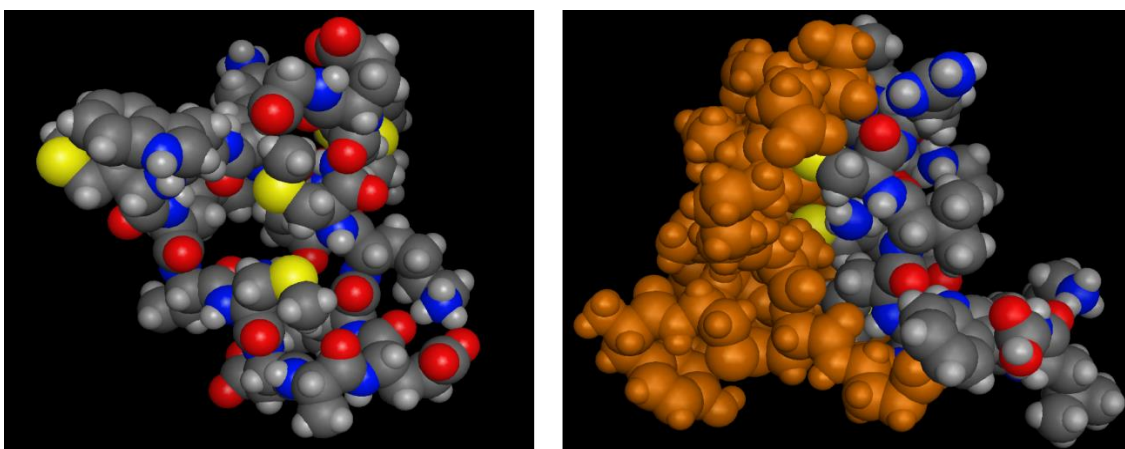


Figure 5.5: Structure of N-terminal Single Ring (**194**) and Location of the Residues Within ProTx-II (**22**, orange)

The most striking aspect from the three predicted structures is that the single ring analogues are far less tightly held together than each of the equivalent rings in the parent structure. This is unsurprising as the ICK structure is very tightly bound thanks to the presence of three interlocking disulfide bridges; if two of these bridges are removed then the constraint on the system will be greatly reduced leading to a more open and flexible structure.

As well as being more flexible, the single ring structures show a general decrease in organisation, with no predicted secondary structure (Figures 5.6 – 5.8). In the case of the single ring structures based on the disulfide ring closest to the C-terminal (Figure 5.6), the β -sheet present predicted in ProTx-II around Cys-25 is no longer present in the single ring structures containing either a lanthionine or disulfide bond.

The decrease in size when changing from the disulfide to the lanthionine bond is reflected in the slight contraction observed in the overall structure (compare Figure 5.6, A to B and C to D). This is particularly noticeable when the C-terminal KKLW motif is removed (C and D,

Figure 5.6) as the lanthionine containing analogue (D) shows a more disordered overall structure than the disulfide counterpart (C).

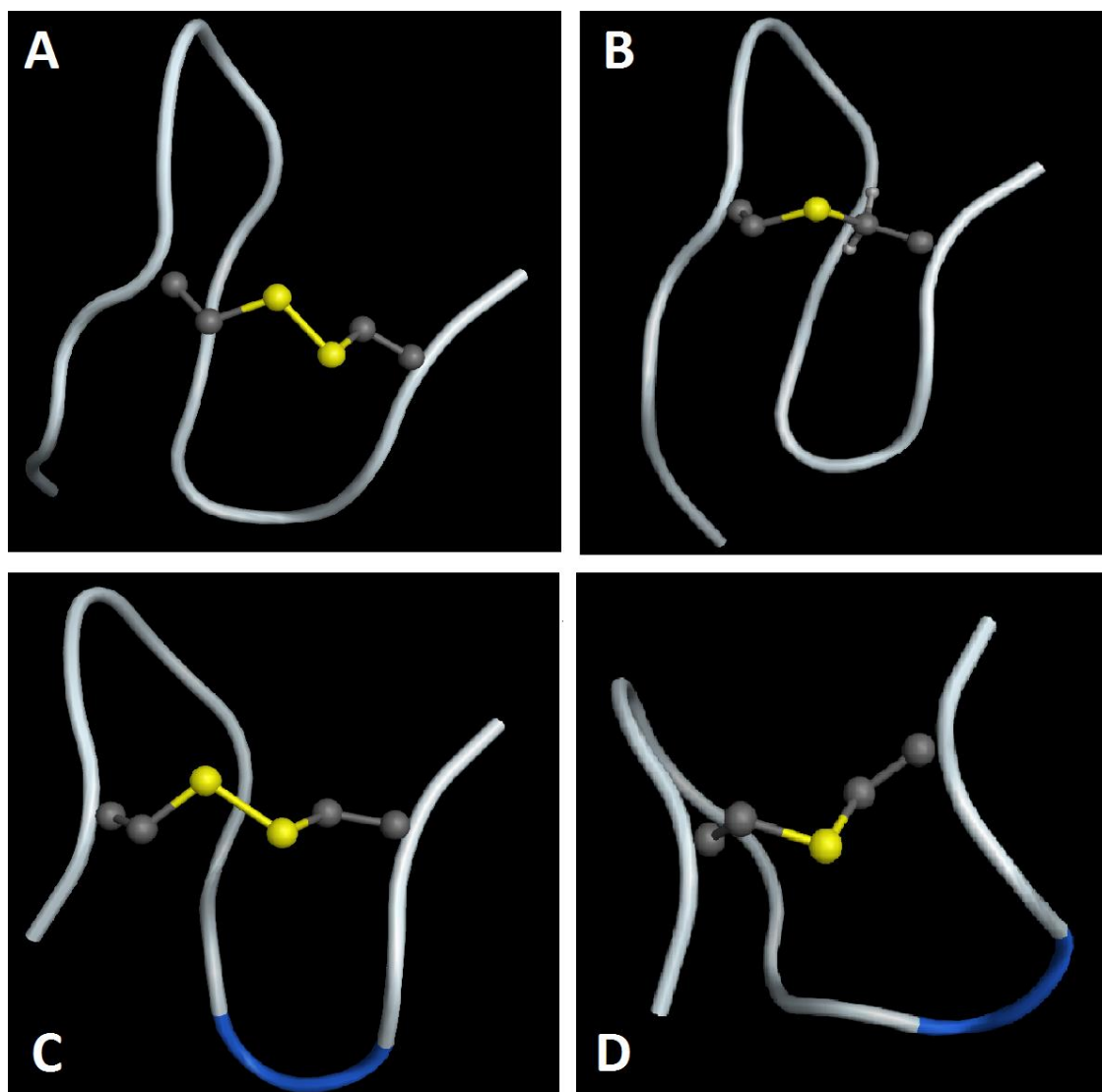


*Figure 5.6: Comparison of the Structures of the C-Terminal Single Ring
A – C-terminal Disulfide Single Ring with KKLW motif (**192**) B – C-terminal Lanthionine Single Ring with KKLW motif (**206**) C – C-terminal Disulfide Single Ring without KKLW motif (**191**) D – C-terminal Lanthionine Single Ring without KKLW motif (**205**)*

When modelling the single ring analogues based on the middle ring of ProTx-II (**193** and **207**), it became obvious that on its own, this part of the molecule is far less well ordered than in the parent peptide (Figure 5.7). This supports the hypothesis that the system requires all three disulfide bonds in order to form the well-defined structure characterised by Park and co-workers, and also observed in the structure of PaTx-I.

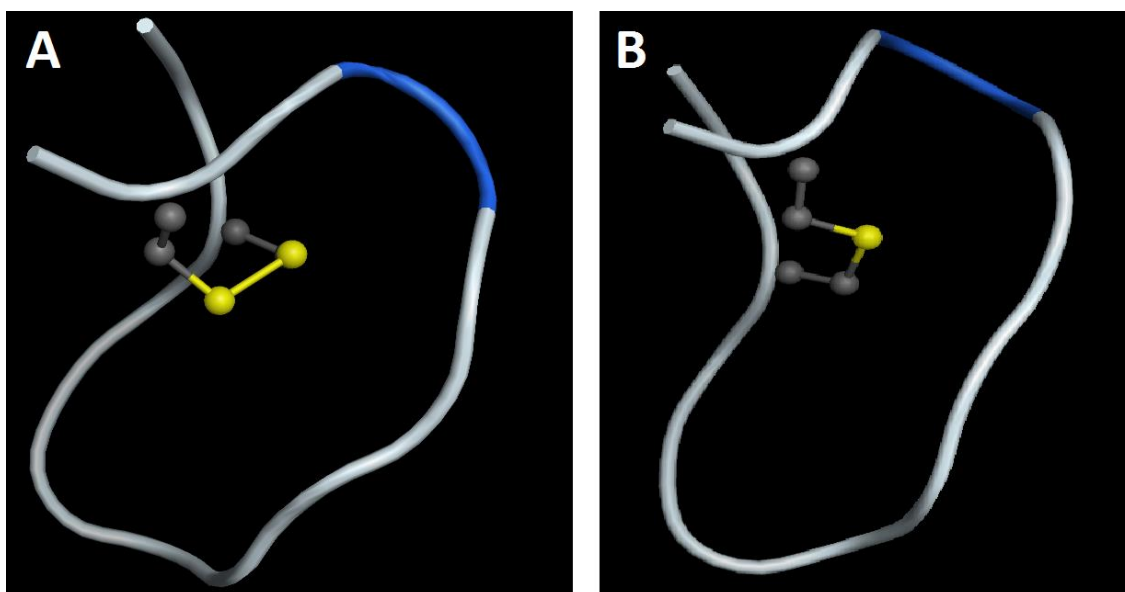


Figure 5.7: Comparison of the Structures of the Middle Single Ring
A – Middle Ring with Disulfide Bond (193) B – Middle Ring with Lanthionine Bond (207)

Conversely, the single ring structure based on the N-terminal disulfide bond (**194** and **208**) appears to show a more complex structure than that observed in the solution phase NMR. The calculations predict that while the end of the ring containing either a lanthionine or disulfide bond is still fairly undefined, the opposite side is far more twisted than in the parent peptide.

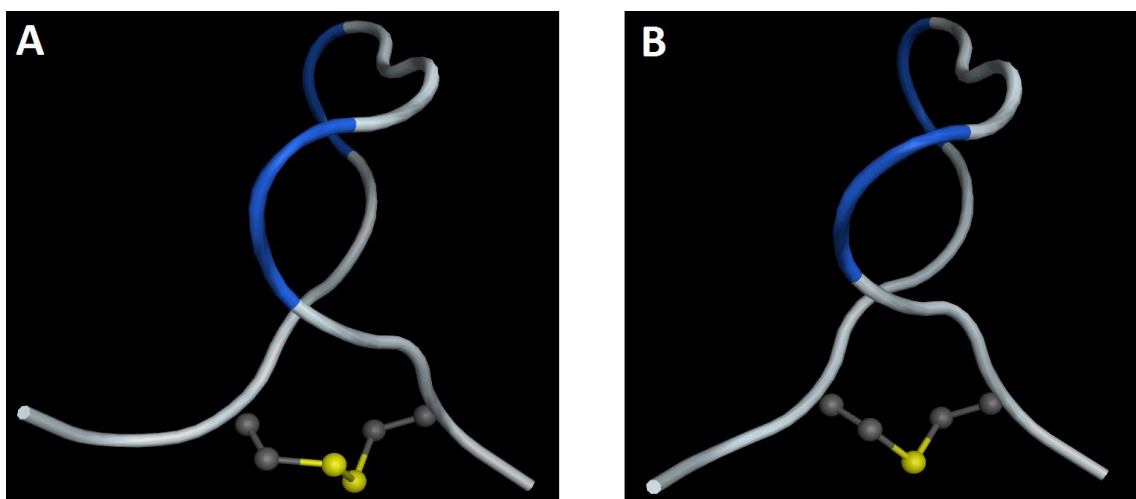


Figure 5.8: Comparison of the Structures of the N-Terminal Single Ring
A – N-terminal Disulfide Single Ring (194) B – N-terminal Lanthionine Single Ring (208)

5.1.2 Modelling of the Double Ring Analogues of ProTx-II

In total, six double ring analogues were modelled containing either two disulfide bonds or one lanthionine and one disulfide bridge (Figures 5.9 – 5.11). The structures were generated using the same method as described in section 5.1.1.

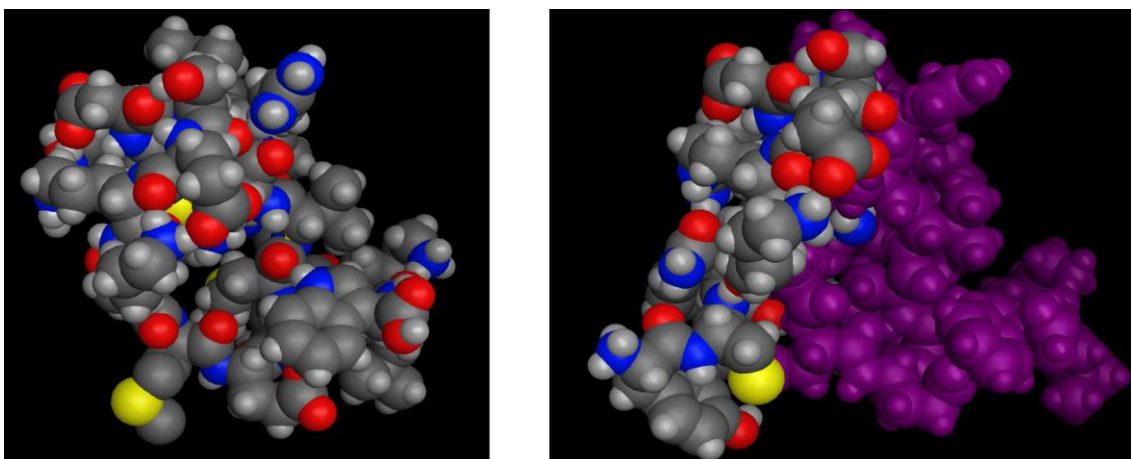


Figure 5.9: Structure of C-Terminal Double Ring (195) and Location of the Residues Within ProTx-II (22)

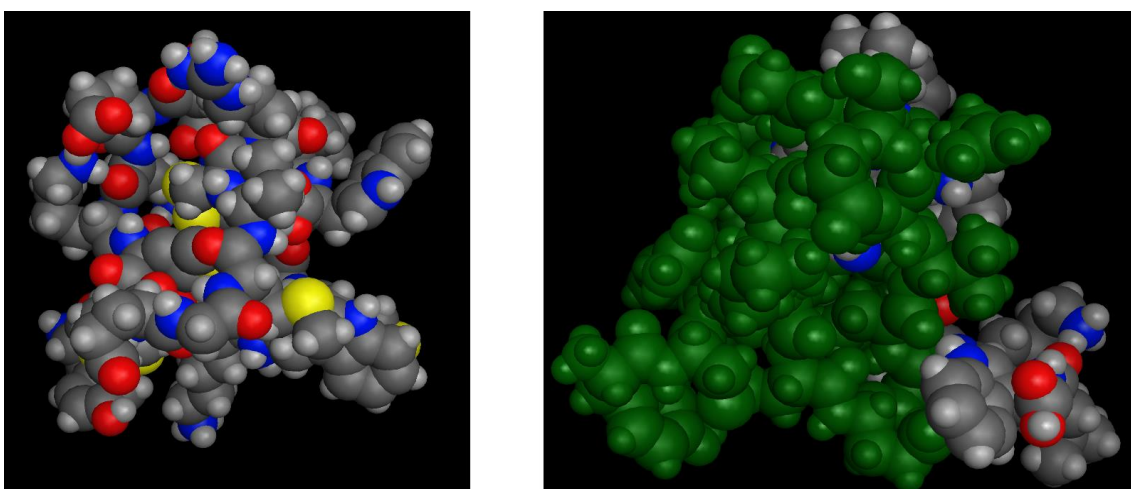


Figure 5.10: Structure of N-Terminal Double Ring (196) and Location of the Residues Within ProTx-II (22)

As with the single ring analogues, the double ring analogues exhibit a more flexible structure than the parent peptide. The C-terminal double ring analogues (Figure 5.9) are quite differing structures depending on whether or not a lanthionine bridge is present in the structure. The structures containing the KKLW tail motif (Structures A, C, and E, Figure 5.11) all maintain the β -sheet motif observed in the parent structure. However, without the final motif present, the structures appear to be less ordered (Structures B, D and F, Figure 5.11) possibly due to a loss of interaction between the disordered tail motif and residues within the core of the peptide. The replacement of the C-terminal disulfide bond with the lanthionine thioether bridge does not appear to cause any major structural difference to the peptide (A against C and B against D, Figure 5.11). However, the replacement of the middle disulfide bond with a thioether linkage has major structural implications (Structures E and F, Figure 5.11).

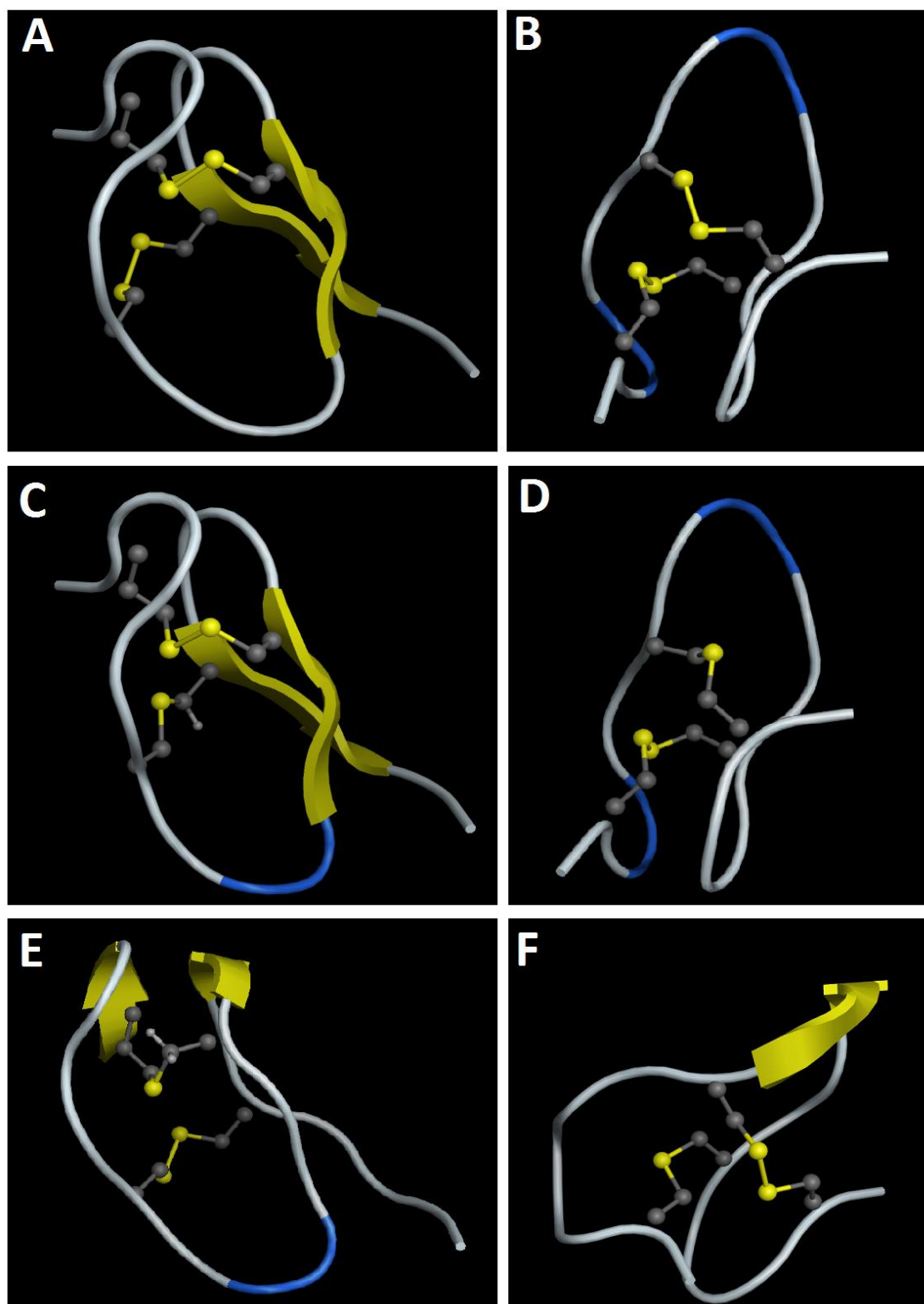


Figure 5.11: Structure of C-Terminal Double Ring Analogues

A – Double Disulfide Bond with KKLW motif (195) B – Double Disulfide Bond without KKLW motif (281) C – C-terminal Lanthionine with KKLW motif (282) D – C-terminal Lanthionine without KKLW motif (210) E – Middle Ring Lanthionine with KKLW motif (283) F – Middle Ring Lanthionine without KKLW motif (211)

With the tail motif intact (Structure E, Figure 5.11) some β -sheet ordering is maintained. However, these sections are in fact in different positions to those observed in either the

parent peptide or the other four double ring analogues; instead of the peptide exhibiting ordering around Cys-25, the folding appears to be around Cys-9 and Cys-21, or rather directly around the thioether linkage which forms the middle ring of the peptide.

Aside from this small defined structure however, the peptide does not show any strongly defined areas of structure and neither resembles the structures exhibited by the other four analogues, nor resembles the solution phase structure of the parent peptide (Figure 5.12).

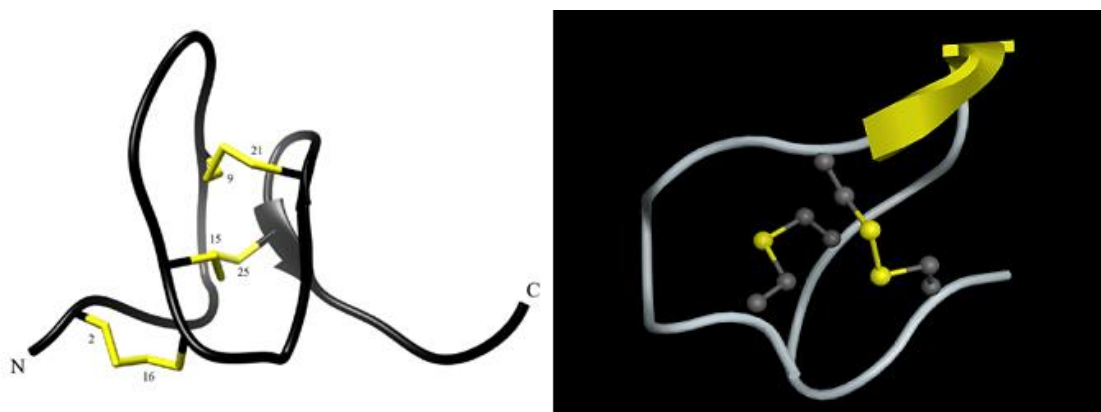


*Figure 5.12: Comparison of Solution Phase NMR of ProTx-II (**22**, left) Against Predicted Structure for C-Terminal Double Ring Analogue with the Middle Ring Containing the Thioether Bridge (**211**)⁵*

As with the C-terminal double ring analogues, replacement of the N-terminal disulfide with a lanthionine bridge (Structure D, Figure 5.13) does not appear to alter the structure too dramatically from either the double disulfide analogue (Structure B, Figure 5.13) or the parent peptide (Structure A, Figure 5.13). However, replacement of the middle ring again shows a dramatic difference in structure, with almost complete loss of the loops defined in the other three structures. From these predicted structures, it is clear that the middle disulfide bond contains a key interaction which holds the peptide together and that even a slight change in size of this ring causes a dramatic change in the conformation of the truncated peptides.

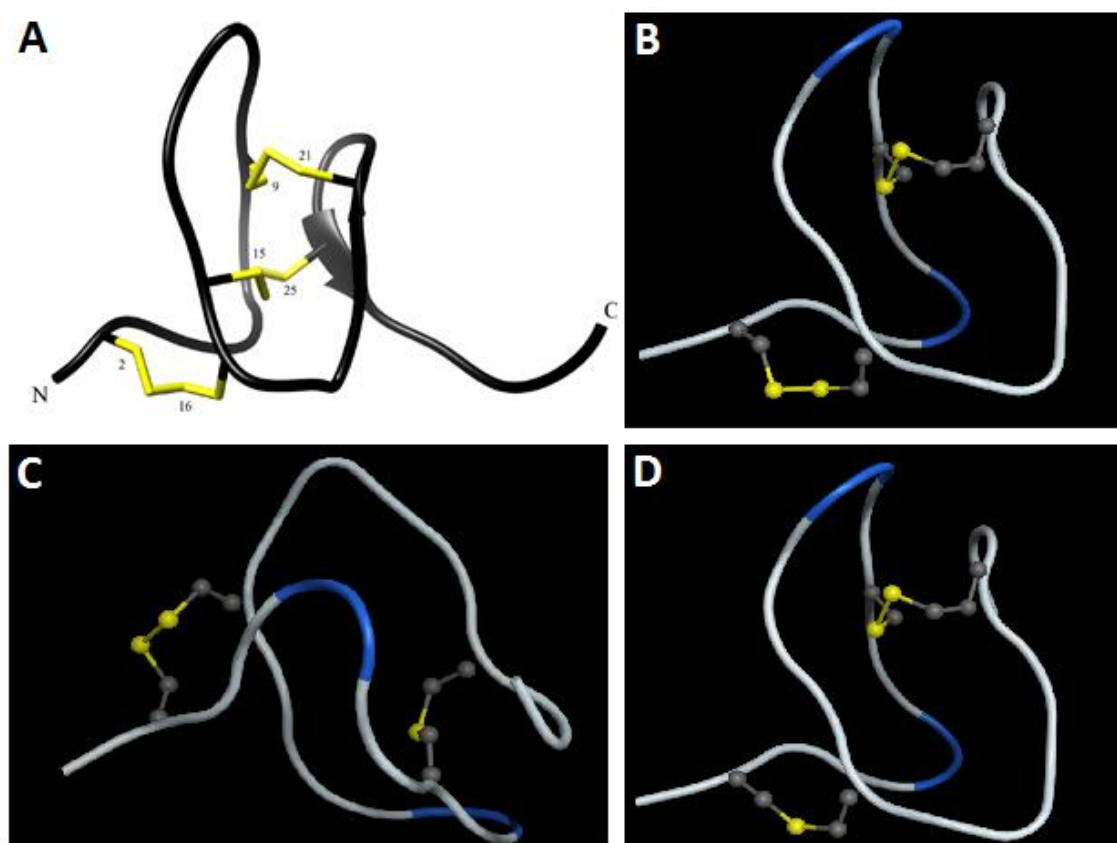


Figure 5.13: Structure of the N-Terminal Double Ring Analogues⁵

A – Solution Phase NMR Structure of ProTx-II B – Double Disulfide Analogue (**196**) C – Middle Ring with Lanthionine Replacement (**212**) D – N-Terminal Lanthionine Replacement (**213**)

Although the difference in structure when the middle disulfide ring is replaced with Lanthionine shows the most significant departure from the parent structure, none of the C-terminal double ring structures show the same conformation as the original structure. This is likely to be due to the third disulfide bond providing an extra level of constraint to the structure and thus preventing the peptide from forming certain conformations. Given that the predicted structures are quite different from the parent peptide, this could explain why it was not possible to isolate the double ring analogues during synthesis and does suggest that without the third disulfide bond these peptides are inherently unstable.

However, with the exception of the N-terminal analogue where the middle ring is replaced by a Lanthionine, the other two N-terminal double ring structures do closely resemble the parent structure. From the computer modelling, it could therefore be concluded that it should be possible to form both the double disulfide analogue and the analogue where the N-terminal disulfide is replaced with a Lanthionine moiety (Structures B and D, Figure 5.13). However, direct experimental evidence showed that the N-terminal double ring analogues were in fact more difficult to isolate than the C-terminal counterparts; whereas traces of the N-terminal

analogues were observed on just one occasion each, the C-terminal analogues were all observed multiple times, although could still never be isolated.

These observations support work published by the King group, which showed that the N-terminal disulfide bond is not essential to formation of the basic ICK fold and does not contribute to the hydrophobic core.⁶ This finding corroborated work by Heitz *et al.*, who showed that removal of the N-terminal disulfide bond did not affect the thermal stability or tertiary structure of the peptidic trypsin inhibitor EETI II.^{7,8} Thus, it is unsurprising that the modelling also predicts that the truncated analogues will show a similar structure to the original peptide. However, structural similarity to the original peptide does not necessarily equate with ease of synthesis, as the practical results showed.

5.1.3 Modelling of the Triple Ring Analogues of ProTx-II

The last analogues to be modelled were the triple ring analogues in which each disulfide bond in turn was replaced with a thioether linkage (Figures 5.14 – 5.17).

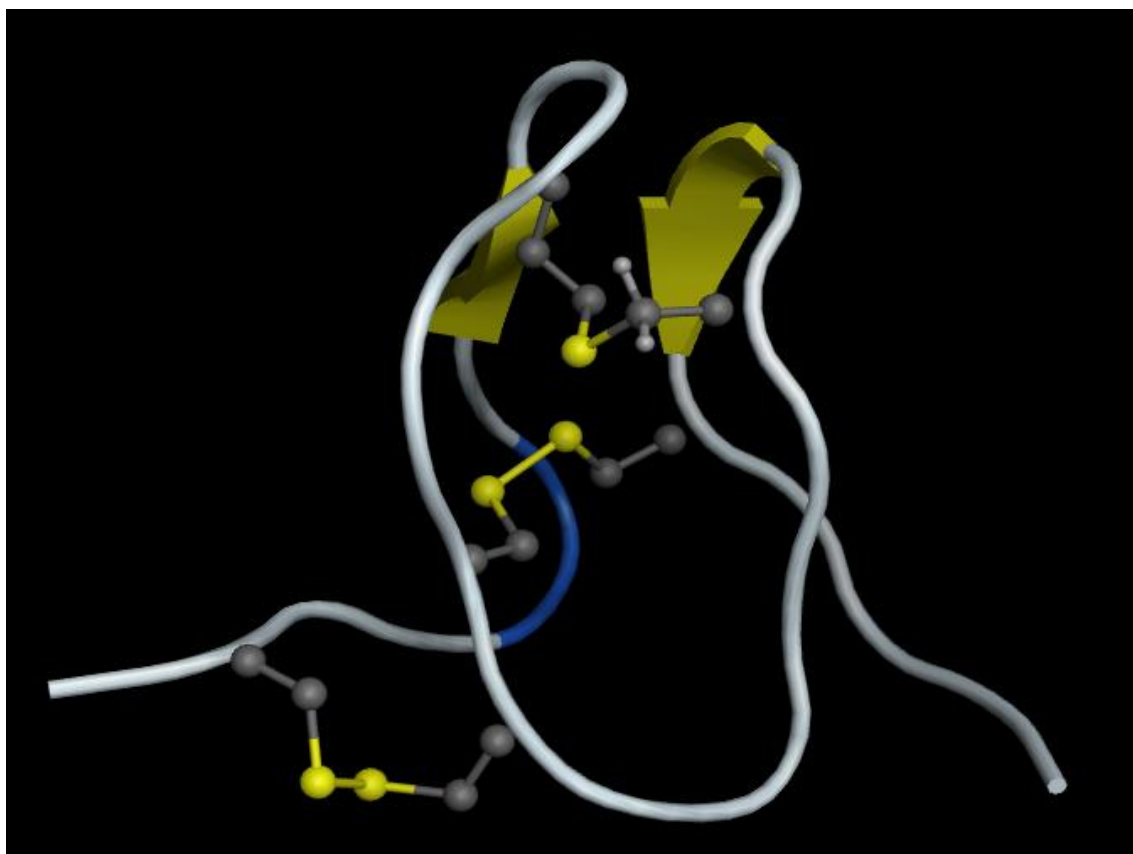


Figure 5.14: Structure of Triple Ring Analogue with C-Terminal Lanthionine Bridge (214)

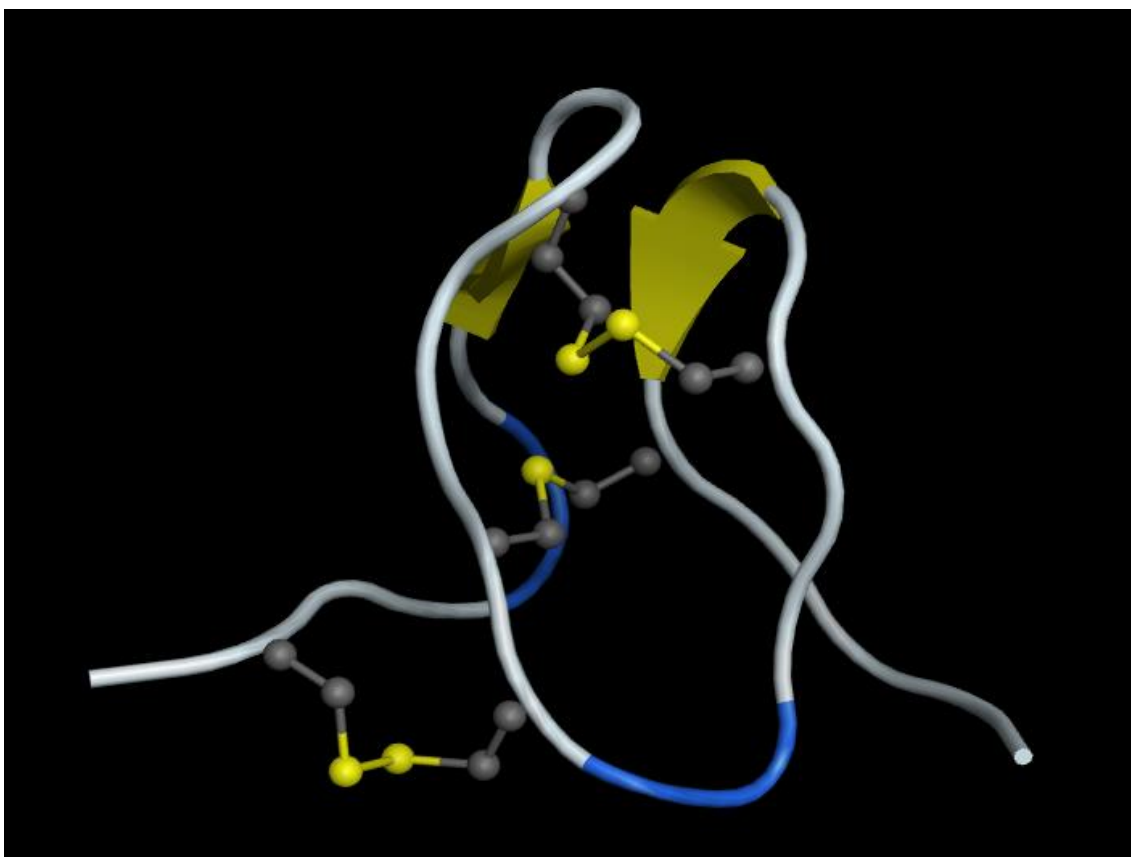


Figure 5.15: Structure of Triple Ring Analogue with Middle Lanthionine Bridge (**215**)

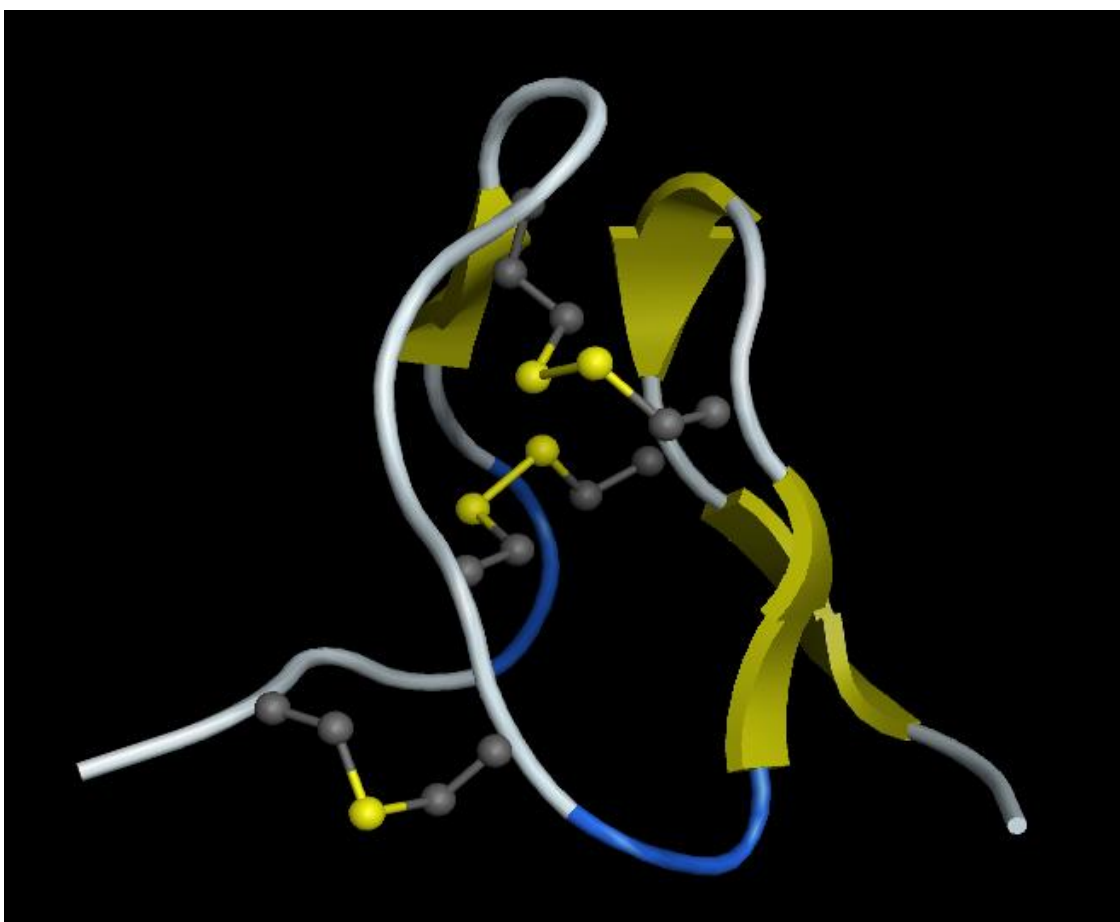


Figure 5.16: Structure of Triple Ring Analogue with N-Terminal Lanthionine Bridge (**216**)

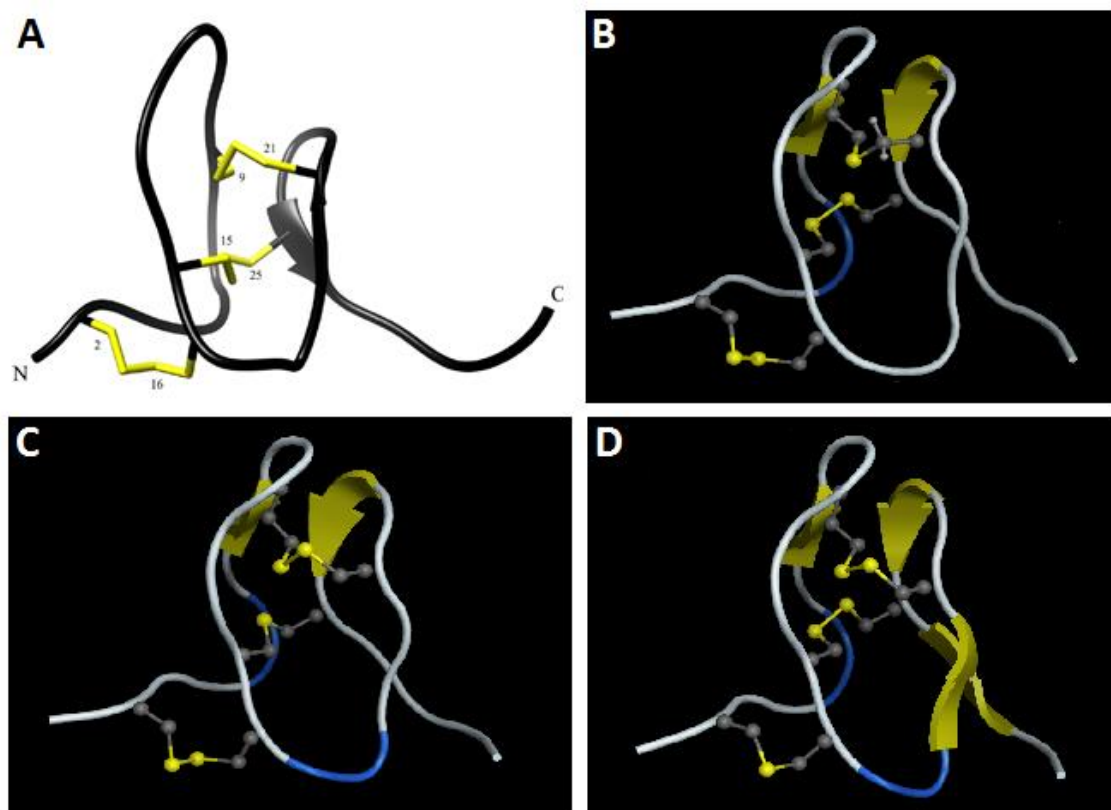


Figure 5.17: Comparison of the Triple Ring Structures with the Solution Phase NMR Structure⁵
 A – Solution Phase NMR of ProTx-II (**22**) B – Triple Ring Analogue with C-Terminal Lanthionine (**214**) C – Triple Ring Analogue with Middle Ring Lanthionine (**215**) D – Triple Ring Analogue with N-Terminal Lanthionine (**216**)

As predicted, the replacement of a disulfide bond with a thioether linkage in the triple ring analogues does not cause a great change in the overall structure of the peptides. When the lanthionine bridge replaces either the middle or C-terminal disulfide bonds, the peptide maintains the structure of the parent peptide with only slight changes in the backbone structure. It is interesting to note that when all three disulfide bonds are present, the effect of the replacement of the middle disulfide bond by lanthionine appears to be negated, corroborating the argument that all three disulfide bonds are required to give the structure stability. Interestingly, the calculations predict an increase in the ordering of the system when the N-terminal disulfide is replaced by lanthionine, with two extra β -sheet areas predicted around Met-19 (Structure D, Figure 5.17). The second more ordered region is located in the KKLW C-terminal motif. The work by Park *et al.* shows that the C-terminus is flexible with no defined conformation, so although it is predicted to have a more defined structure in this calculation, it is likely that it adopts a number of different conformations in solution. However, it is entirely possible that by constraining the N-terminal ring slightly, more order is forced upon the core of the peptide giving the β -sheet conformation around Met-19.

5.1.4 Conclusions from the Modelling Calculations

As it was not possible to obtain the co-ordinates for the recently published solution NMR structure of ProTx-II, the structure of ProTx-II was first generated from the solution NMR structure of PaTx-I, a peptide showing a high degree of similarity to ProTx-II. Using the homology modelling software from MOE™, it was possible to build a structure which was shown to be very close to that published by Park and co-workers, which gave a good degree of confidence in the calculations. Using this structure, a total of 20 analogues of ProTx-II were generated and evaluated.

A total of eight analogues of the single ring structures were produced, which all showed different structures from that adopted by the parent peptide. This was unsurprising as it was predicted that all three disulfide bonds were required to form the defined tightly bound core of the peptide and so once two of these three constraints were removed, the structure was unlikely to display such a great degree of ordering. Given the vastly differing structures, it is unlikely that any of these single ring structures will display activity on their own.

Similarly, the six analogues generated from the C-terminal double ring structure did not show structural similarity to the parent peptide and were also unlikely to show any activity *in vitro*. Conversely, of the three analogues of the N-terminal double ring which were modelled, both the analogues containing the double disulfide bond and the N-terminal lanthionine bond did show structural similarity to the parent peptide. This observation is in line with work published by other groups, who showed that changing the N-terminal ring did not have any great structural effect on the peptide.^{6, 7, 8} However, as it was not possible to synthesise and isolate these analogues, it will not be possible to find out if these structures show any biological activity.

Finally, as predicted, all three of the triple ring analogues closely resemble the structure of the parent peptide. This is unsurprising as replacing a disulfide bond with a lanthionine bridge results in only a mild change in the constraint on each of the rings; as the structure is already highly constrained, this small difference appears to have little effect on the overall structure of the peptides and, as such, all three analogues are predicted to have similar levels of activity *in vitro*.

5.2 An Introduction to Patch Clamping

Modelling the structure of each of the compounds can give confidence in the predictions on the activity of the compounds. However, in order to assess whether a lanthionine bridge could truly provide an alternative to a disulfide bond in a peptide, the compounds needed to

be tested in a biological system, albeit *in vitro*. For this work, it was decided to test the compounds against the Na_v1.7 ion channel using an automated patch clamp assay. This assay uses Na_v1.7 ion channels generated in stably transfected cells, isolated from the membrane using a patch clamp and then changes in current and voltage across the channel are recorded to give a measure of activity. In a stably transfected cell, the DNA of the receptor becomes encoded in the genome of the host cell. Although the DNA was not originally endogenous to the host cell, upon replication, this new DNA is also replicated. For this work, the gene for the Na_v1.7 ion channel was cloned and functionally expressed in either Human Embryonic Kidney (HEK) or Chinese Hamster Ovary (CHO) cells. The cell lines were tested for expression and correct membrane integration of the Na_v1.7 ion channel.

5.2.1 Manual Patch Clamping

The patch clamping technique was pioneered by Neher and Sakmann⁹ in the 1970s as a novel method of conductance measurement over a cell membrane, which has allowed for the evaluation of individual ion channels.

As discussed in Chapter 1, an action potential occurs as a result of the movement of ions across the cell membrane. There are more positive ions outside of a cell and the charge imbalance gives rise to an electric potential across the membrane potential typically in the range of -50 to -80 mV.¹⁰ Sodium ion channels are involved in the propagation of a nerve impulse along the axon (Section 1.2 and Figure 5.18). In unmyelinated axons, action potentials move as a cascade of voltage-gated ion channels open, resulting in the passive spread of voltage change along the axon (Figure 5.19).

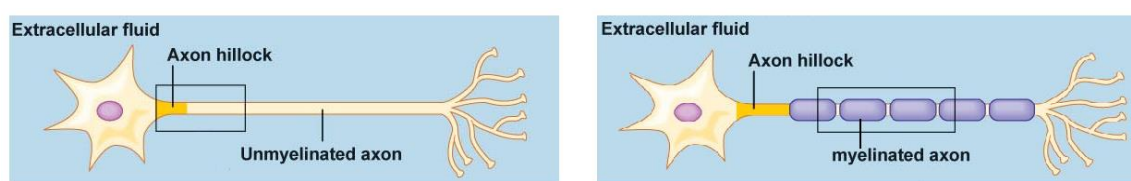


Figure 5.18: Unmyelinated vs Myelinated Neurons¹¹

When an action potential occurs at the axon hillock, positive charges (both Na⁺ and K⁺) move into the cell creating a change in the local charge and rapid depolarisation. Once this has occurred, the cell needs time to recover before it can signal again (Figures 1.2 and 1.3). This is known as the refractory period and ensures that the action potential always moves in the forward direction. As a general rule, a larger diameter axon has a faster propagation rate due to the decreased resistance to current flow within the neuron.

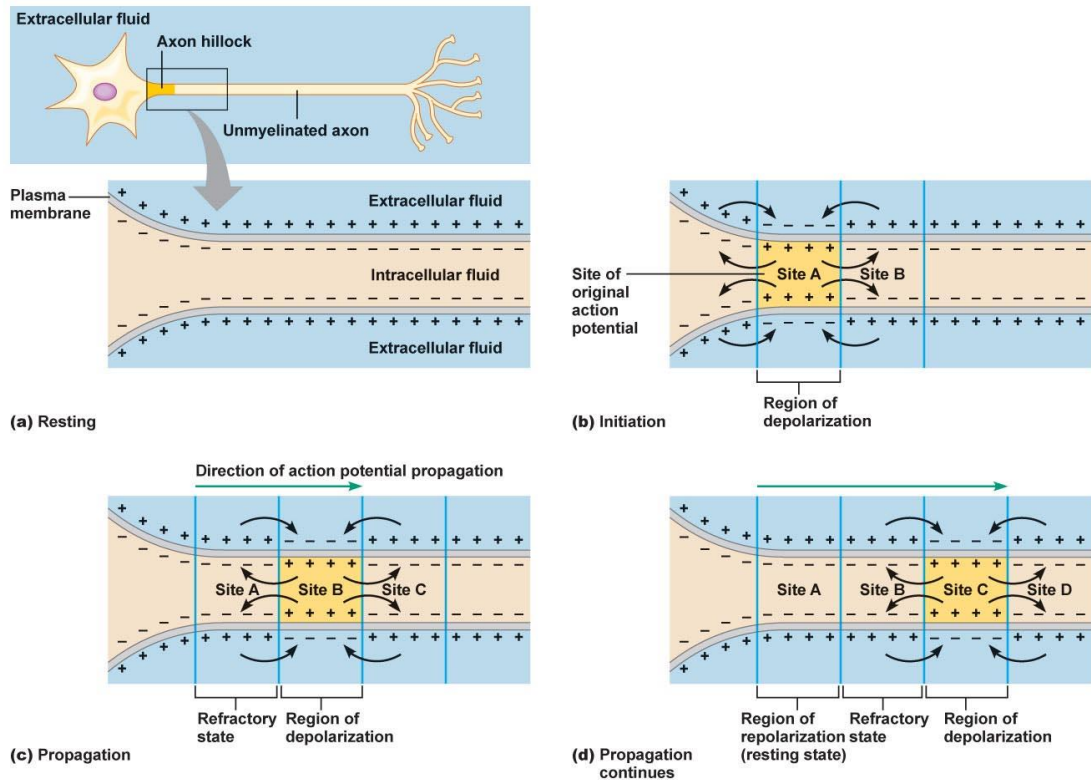


Figure 5.19: Propagation of the Nerve Impulse in an Unmyelinated Neuron¹¹

Myelinated axons propagate nerve impulses faster. This is due to the myelin providing high resistance to ion flow, preventing the movement of ions. This resistance is only absent at the points where no myelin covers the neuron at gaps known as Nodes of Ranvier, which contain a high concentration of both Na_v and K_v channels. In the case of myelinated axons, the action potential jumps from one node to the next. This is known as saltatory conduction and results in an increased speed of propagation (Figure 5.20).

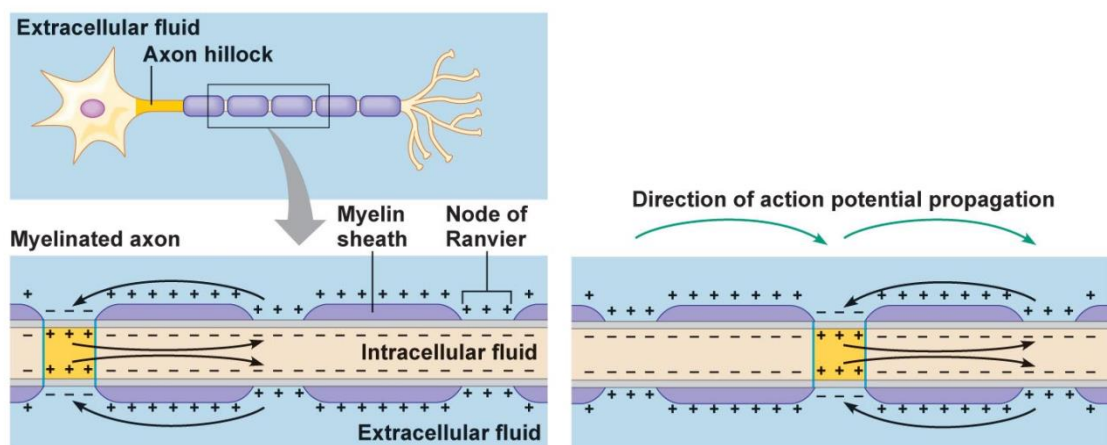


Figure 5.20: Propagation of the Nerve Impulse in a Myelinated Neuron¹¹

Prior to the work by Neher and Sakmann, it was necessary to base all calculations on conductance on macroscopic variations with a system,^{9,12,13} which did not give such a high degree of accuracy.

Patch clamp experiments work by keeping either the voltage or current constant and then measuring the changes in the other variable. This work is concerned with voltage clamp experiments in which the membrane potential is controlled and the current measured directly. To do this, the measured potential is compared with a holding potential set by the experimenter through an electronic feedback system. Deviation from the holding potential is corrected by a compensatory current injection, which corresponds to the ionic current over the membrane at that moment. The current and voltage are measured using a single electrode voltage clamp within a micropipette, which switches quickly between injecting current and measuring potential difference (Figure 5.21).

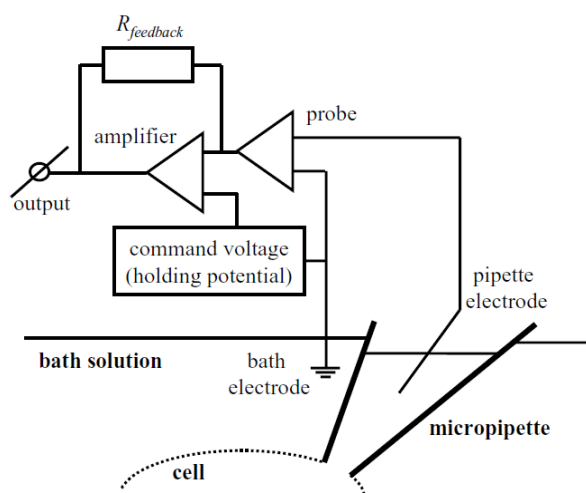


Figure 5.21: Schematic Diagram of a Patch Clamp Experiment¹⁴

The work in this thesis uses whole cell patch clamping. In this scenario, the patch of membrane under the pipette tip is ruptured allowing the pipette solution and electrode to make direct contact with the cytoplasm. The pipette tip is wide enough to permit “washout” of the cytoplasm, which is then replaced by the pipette-filling solution. To maintain “physiological situation” within the cell, the pipette is filled with an ionic solution resembling the cytoplasm as closely as possible. In this case, the following composition was used (Table 5.1):

Compound	Amount
Cesium Fluoride	135 mM
Sodium Chloride	10 mM
HEPES	10 mM (pH = 7.3)
EGTA	5 mM

Table 5.1: Composition of the Pipette Solution

5.2.2 Automated Patch Clamping

Although manual patch clamping gives accurate readings, it is also time consuming as experiments can only be carried out one at a time. However, it is possible to use an

automated system in which multiple readings can be taken simultaneously. The principle is the same as that employed for manual whole cell patch clamping but the cells are put into microtitre plates with multiple cells present in each well. By using continuous flow and recording, more data points can be collected in a shorter time frame, which allows for faster production of data.

All the patch clamping results presented in this chapter come from automated patch clamp experiments carried out by Essen Bioscience and B'Sys.

5.3 Preliminary Patch Clamping Results

In collaboration with both Essen Bioscience and B'Sys, the following compounds were tested (Table 5.2). All compounds were tested using either the hNa_v1.7-HEK cell IonWorks Population Patch Clamp Assay, as designed by Essen Bioscience or the Sophion QPatch™ Patch Clamp Assay as designed by B'Sys. The compounds tested at Essen Bioscience were tested at 11 different points to make an IC₅₀ curve using threefold dilution from 1 μM – 0.000001 μM in triplicate, using tetracaine as the control molecule. The samples were allowed to incubate for 5 – 7 min before testing occurred and were tested in the presence of 0.1% Bovine Serum Albumin to prevent the samples adhering to the side of the microtitre plate. The percentage inhibition between the 1st and 20th pulses was then analysed and plotted on a graph.

Unfortunately, although the lidocaine performed as expected in these experiments, no activity was recorded with any of the truncated or full size analogues of ProTx-II (Table 5.2). In addition, the ProTx-II made in the laboratory did not show any activity and neither did commercially sourced ProTx-II from either Sigma Aldrich or Tocris.

Structure	Company	Result
(191) KCMEGMVMRLWCKK	Essen Bioscience	No Activity
(192) TCDSEKMMEGMVCRLW	Essen Bioscience	No Activity
(193) YCQKWMWTMDSEKMCCEG	Essen Bioscience	No Activity
(205) KAMEGMVMRLWAKK	Essen Bioscience	No Activity
(207) TADSEKMMEGMVARLW	Essen Bioscience	No Activity
(22) YCQKWMWTCDSEKCCCEGMVCRLWCKKKLW	Essen Bioscience and B'Sys	No Activity
(214) YCQKWMWTCDSEKACEGMVCRLWCKKKLW	Essen Bioscience	No Activity
(215) YCQKWMWTADSEKCCCEGMVARLWCKKKLW	Essen Bioscience	No Activity
(216) Y AQKWMWTCDSEKCAEGMVCRLWCKKKLW	Essen Bioscience AND B'Sys	No Activity
(206) KAMEGMVMRLWAKKKLW	B'Sys	No Activity
(194) KCMEGMVMRLWCKKKLW	B'Sys	No Activity

Table 5.2: Structures of Peptides Submitted for the First Round of Testing
Key: black = disulfide bond, red = lanthionine bond

The purity of all the compounds was checked by both analytical HPLC and LC-MS but the compounds were found to be unchanged. It was therefore initially concluded that there was a problem with the testing platform at Essen. Although the company spent some time investigating possible problems such as the electrics within the system and transfection errors, it was not possible to draw any firm conclusions about the cause of failure. Unfortunately, the same problem was found when the samples were sent to B'Sys in Switzerland with no activity recorded for either the ProTx-II or the single ring analogues.

5.4 Further Results from B'Sys

As no activity was recorded for both the compounds synthesised in-house and the parent peptide made by two separate companies, it was decided to investigate ProTx-II (**22**) activity further. A series of samples both synthesised in-house and purchased from a variety of commercial sources were then tested in an attempt to locate the source of the problem (Table 5.3).

Entry	Source of ProTx-II	Result
1	Made in-house, cyclised	No Activity
2	Sigma Aldrich	No Activity
3	Tocris	No Activity
4	Made in-house, uncyclised	No Activity
5	Smartox	97.6% drop in activity

Table 5.3: Summary of Testing Results from B'Sys

As the table shows, no activity was observed for either the Sigma Aldrich or the Tocris samples of ProTx-II (Table 5.3, Entries 2 and 3). Given that activity has been reported multiple times in the literature^{1,2} and that Essen Bioscience has also previously seen activity with ProTx-II in their assay,¹⁵ it was clear that there were discrepancies with either the methods used in the testing or the peptides themselves. To ensure that the problem had not occurred due to disulfide bond opening in previous experiments, it was next decided to test an uncyclised sample of the peptide. As expected, this form of the peptide did not show any activity (Table 5.3, Entry 4). However, upon testing a final sample of ProTx-II obtained from Smartox, a peptide company based in France, the expected activity was observed.

However, having ascertained that the procedure for carrying out the testing worked, it was clear that the nature of the peptide was the cause of the problem. This could be as a result of one of several factors:

- Did ProTx-II show activity in the first place or was it an, as yet unidentified, side product causing the activity?
- Do all of the peptides have the same molecular weight or do they have different primary structures?
- Is the peptide fully cyclised or has only partial cyclisation occurred in the Smartox peptide? Has partial cyclisation led to the observed activity?
- If the peptide is fully cyclised, do the peptides all have the same disulfide bond connectivity?

The first question, although the most concerning, is also the least likely option as activity has been reported in the literature many times since the initial isolation of the peptide.^{16,1,2,15}

However, the next three could only be determined by further analysis of the structure of ProTx-II.

5.5 Analysis of the Structure of ProTx-II

The data in Table 5.3 shows there is clearly a difference between the commercially available sources of ProTx-II. To investigate the possibility of differences in structure, the peptides were first submitted for LC-MS analysis.

As well as testing the in-house peptide against samples from both Sigma Aldrich and Smartox, a second in-house sample of the peptide was prepared using the cyclisation conditions as detailed by Park *et al.*² The cyclisation procedure detailed in their work was a more thorough version of that used by Middleton *et al.*¹⁶ for the initial studies in to the structure of the peptide (Chapter 3). In this procedure, GSH (0.15 mM) and GSSG (0.3 mM) were added to a solution of 2 M Urea and 0.1 M Tris-HCl in water. The pH was adjusted to 8 using saturated aqueous NaHCO₃ before addition of the crude linear peptide (0.1 mg/mL). The reaction was left to stir for 24 h before the pH of the reaction mixture was adjusted to 3 and the crude product was analysed by analytical HPLC. It is curious to note that although the cyclisation worked when using crude linear peptide, attempts to cyclise the pure linear peptide did not yield any of the desired product. This unexpected observation is in line with results from Chapter 3 which showed that it was not possible to cyclise the pure linear peptide using the Middleton conditions or other buffering conditions.

All of the samples tested show the same molecular weight by LC-MS, which indicates that they all have the same primary sequence and that any difference in activity must be caused by a difference in disulfide bond connectivity.

As the LC-MS machine used only gives masses between 100 and 2000 Daltons, the molecular ion is not observed. Instead, the +5, +6 and +7 ions are the most commonly observed masses of ProTx-II. However, the difference between the fully cyclised, partially cyclised and completely uncyclised peptide is very small and so the first experiments were designed to make sure all of the peptide samples were fully cyclised. To do this, 2,3-dibromomaleimide was added to each of the peptide samples, which reacts with a free sulfhydryl group to give a maleimide-conjugated moiety thereby end-capping the peptide (Figure 5.22).¹⁷

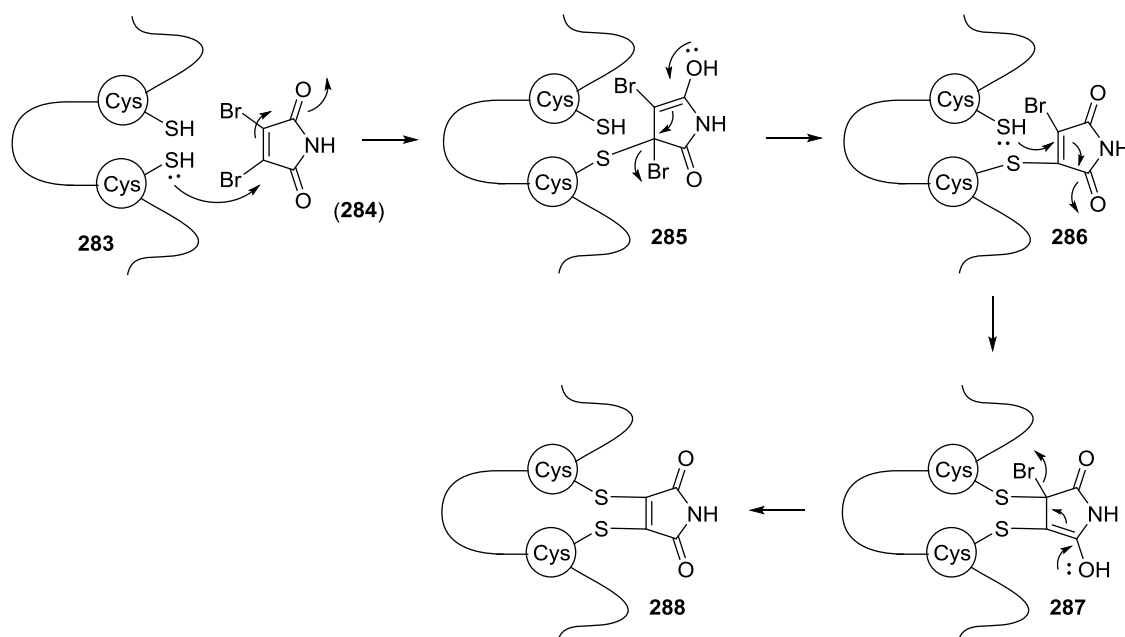


Figure 5.22: Reaction of a Free Sulfhydryl Group with 2,3-Dibromomaleimide (284)

To compare the samples, the peptides were then left in the presence of TCEP for 1 h to break all the disulfide bonds before again adding the maleimide, which should in theory add three maleimide residues to the peptide increasing the mass by 285 Daltons. The results from these experiments are summarised in Table 5.4.

Entry	Experiment	Mass Recorded	Result
1	In-house ProTx-II	3826	Control
2	In-house ProTx-II, Park Cyclisation conditions	3826	Control
3	Smartox Peptide	3826	Control
4	In-house ProTx-II + Maleimide (284)	3826	No Maleimide addition
5	In-house ProTx-II, Park Cyclisation conditions + Maleimide (284)	3826	No Maleimide addition
6	Smartox Peptide + Maleimide (284)	3826	No Maleimide addition
7	In-house ProTx-II + TCEP + Maleimide (284)	4111	Peptide + 3 maleimides
8	In-house ProTx-II, Park Cyclisation conditions + TCEP + Maleimide (284)	3826	No Maleimide addition
9	Smartox Peptide + TCEP + Maleimide (284)	3826	No Maleimide addition

Table 5.4: Results from the Maleimide End-Capping Experiments

Before the experiments began, each peptide was submitted for LC-MS analysis to ensure the correct mass (3826 Da) was present (Table 5.4, Entries 1 – 3). With this condition satisfied, maleimide was added (Table 5.4, Entries 4 – 6). In all three cases, no addition of maleimide was observed which confirmed that there were no free sulfhydryl groups present and

corroborates the work by Middleton *et al.*¹⁶ that all six cysteines are involved in disulfide bonds.

The addition of TCEP (Table 5.4, Entries 7 – 9) was designed to act as a control; the TCEP should fully reduce the peptide thereby giving 6 free sulfhydryl groups which will then be able to react with the maleimide reagent. A step-wise protocol was adopted as described by Smith *et al.*¹⁷ in which the peptide is first left to reduce in the presence of TCEP for 1 h before the addition of maleimide. After incubation with TCEP, the peptide produced in-house by leaving it to cyclise in water for 7 days was fully reduced and showed a mass of 3832 as expected. Upon addition of maleimide, the mass increased to 4111, which corresponds to the addition of 3 maleimide bridges, that is, reaction with all six free sulfhydryl bridges occurred as expected (Table 5.4, Entry 7). Interestingly, after 1 h in the reducing conditions, neither the peptide produced in house using the Park cyclisation conditions nor that synthesised by Smartox showed any reduction (Table 5.4, Entries 8 and 9). As no reduction was observed, it is also not surprising that no maleimide addition could occur.

The LC-MS data shows that no free sulfhydryl groups are present and that all six cysteines are involved in disulfide bonds, which is in line with the work reported by Middleton *et al.*¹⁶ However, the difference in reactivity with the TCEP and in the patch clamping experiments suggests that there are discrepancies between the peptides. To probe this, the peptides were next submitted for analysis by analytical HPLC (Table 5.5).

Entry	Peptide	Retention Time (min)
1	Original In-house Cyclisation	2.08
2	Tocris	2.11
3	Smartox	2.32
4	In-house using Park Cyclisation	1.99 and 2.25
5	Tocris + In-house	2.11
6	Smartox + In-house	2.15 and 2.47
7	Smartox + In-house using Park Cyclisation	1.90 and 2.32

Table 5.5: Summary of Analytical HPLC Results

From the analytical HPLC data, it is clear that two separate peptide species with different retention times are present. As previous data have shown, the cyclisation in pure water for 7 days gives the same peptide as that formed by Tocris (Table 5.5, Entries 1, 2 and 5). However, it is clear that this differs from the peptide produced by Smartox (Table 5.5, Entries 1, 3 and 6). By far the most interesting result is the peptide cyclised in-house using the Park cyclisation method (Table 5.5, Entry 4). The results show that two peptides have formed – one with the same retention time as that shown by the Tocris peptide and one with the same retention time as that shown by the Smartox peptide. Unfortunately, attempts to separate

the two peptides were not successful as analysis by HPLC after purification revealed that only one peptide with a retention time of 2.06 (that is, the same as the Tocris peptide) was found to be present.

The difference in reactivity between the peptides and the different analytical HPLC traces both strongly suggest that two separate disulfide bond connectivities have been synthesised in the laboratory. This strongly suggests that whilst the original peptide method for cyclisation in-house gives the thermodynamic product, the park cyclisation peptide and the peptide produced by Smartox are both the kinetic product. This was confirmed by the fact that the Park cyclisation product could be turned into the thermodynamic, TCEP-sensitive, product if left in pure water. As all the peptides tested were shown to have the same mass by LC-MS, it is highly likely that the difference in the products comes from the disulfide bond connectivity.

5.6 Probing Disulfide Bond Connectivity

In Chapter 3 it was shown that although the connectivity between Cys-2 and Cys-5 was confirmed, it was not possible to determine the other two cysteine bonds. The well-documented ICK structure contains three overlapping disulfide bonds in the pattern 1-4, 2-5, 3-6. However, another connectivity pattern known as the disulfide-directed β -hairpin (DDH) motif in which the disulfide bonds are found in the pattern 1-3, 2-5, 4-6 could also be present in the system. Work by Shu *et al.*¹⁸ has shown that HwTx-II (**289**), a peptide isolated from the *Selenocosmia huwena* spider has this DDH motif, which is characterised by two β -turns and a double-stranded antiparallel β -sheet (Figure 5.23). The 2-5 bond is the only conserved link between the ICK and DDH motifs and the group propose that the DDH motif is a structural ancestor to the more complex ICK binding pattern. It is thought that the 2-5 bond contributes to the stability of the β -sheet structure¹⁹ and that this explains the conservation of the bond between the two motifs. The DDH motif was first identified by the King group,⁶ who found the fold to be present in a peptide isolated from the *Hadronyche versuta* spider.

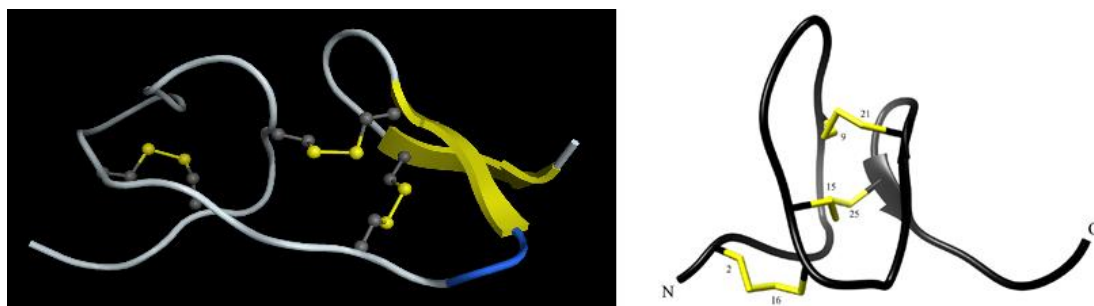


Figure 5.23: Comparison of the Solution Phase NMR Structures of the DDH motif in HwTx-II (**289**)¹⁸ against the ICK motif of ProTx-II (**22**)^{2,5}

To investigate the disulfide connectivity of the two ProTx-II structures, a sample of the peptide produced in-house by cyclising in water for 7 days and a sample of the peptide from Smartox were again subjected to the double digestion procedure detailed in Chapter 3 (Figure 5.24).

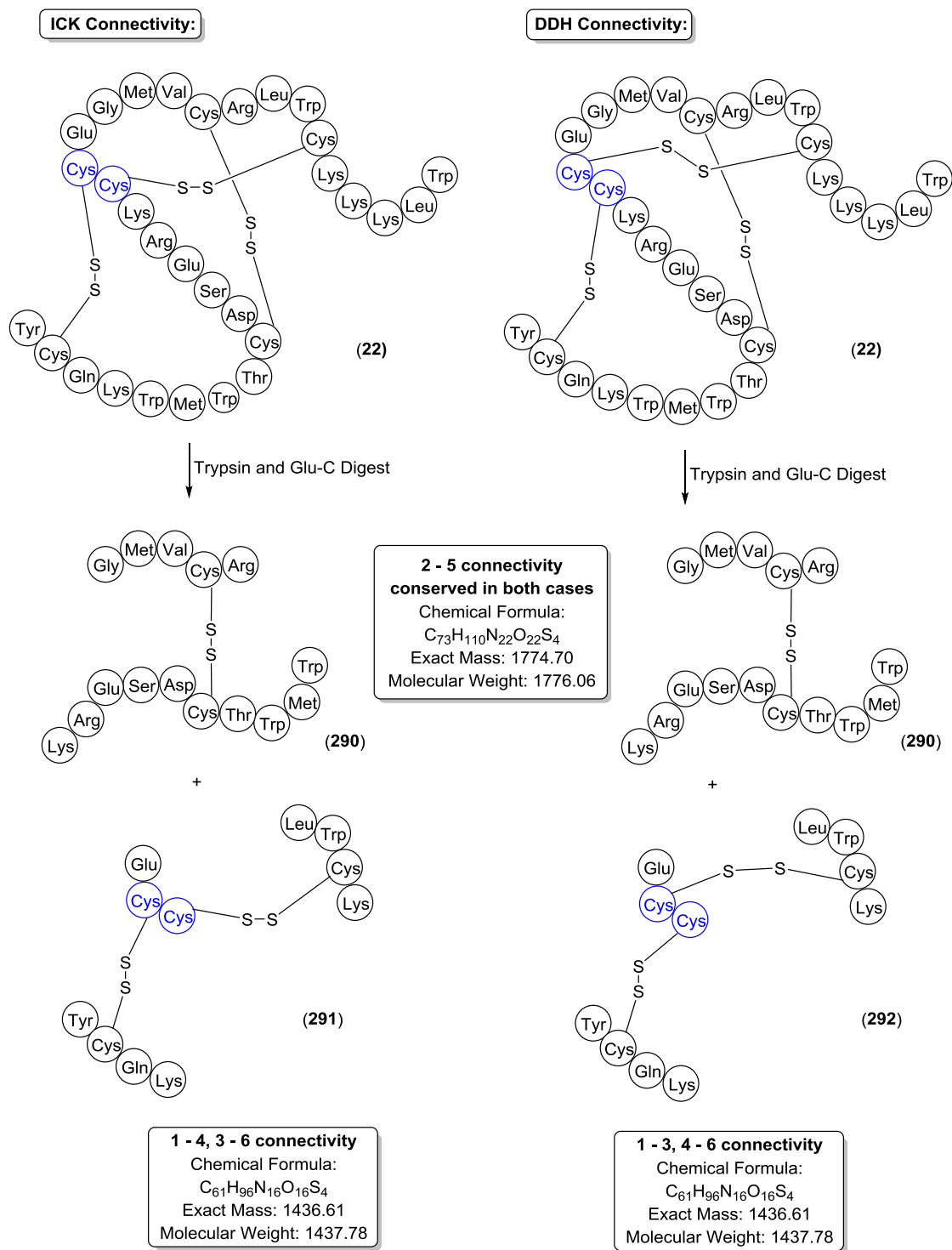


Figure 5.24: Products from the Digestion of ProTx-II using Trypsin and Glu-C

Having digested the peptide with both Trypsin and Glu-C, the peptides were submitted for MS/MS analysis.^b The peptide should theoretically be cleaved in five places by the Trypsin and then between Glu-17 and Gly-18 by the Glu-C enzyme to give fragments (**290**) and either (**291**) or (**292**) (Figure 5.24).

In Chapter 3, it was shown that the post-source decay experiments carried out by Middleton and co-workers could not be replicated and that it was not possible to differentiate between a 1-3, 4-6 connectivity and a 1-4, 3-6 connectivity. This meant that only the presence of the 2-5 disulfide bond had been previously confirmed and that the question of ICK or DDH connectivity had not been answered.

By leaving the peptides to cyclise in water for seven days, the thermodynamic minimum was reached. The triple ring analogues **214** – **216** are also likely to have the same thermodynamic minimum structure as the parent peptide, given the use of the same cyclisation procedure and the control of the connectivity by virtue of the insertion of a thioether bond. It is highly likely that the structures all share the ICK pattern, in common with the Sigma Aldrich and Tocris samples of ProTx-II. The kinetic product structure exhibited by the Smartox and Park cyclisation peptides is therefore likely to have the DDH connectivity of 1-3, 2-5, 4-6.

A preliminary MS/MS experiment was carried out to try to ascertain if this theory was correct. Unfortunately, it was found that no fragment with a mass of 1436 amu was found in either peptide sample. However, in the Smartox sample, a peptide with a mass of 1566 amu was discovered. This corresponds to the expected fragment plus an extra lysine and was also observed by Middleton and co-workers. Given the tight structures of both the ICK and DDH motifs, it is unsurprising that the trypsin was unable to cleave at all five sites on the peptide, which is in line with observations outlined in Chapter 3 and those published in the Middleton paper. There are two possibilities for the position of the lysine - Lys-14 or Lys-27. As two lysines next to each other must be cleaved at the tail end of the molecule, it is more likely to be Lys-27 which has not been removed by the trypsin. This would give **293** or **294** (Figure 5.25).

^b This work was carried out by Adam Cryar in the Thalassinos Laboratory at UCL.

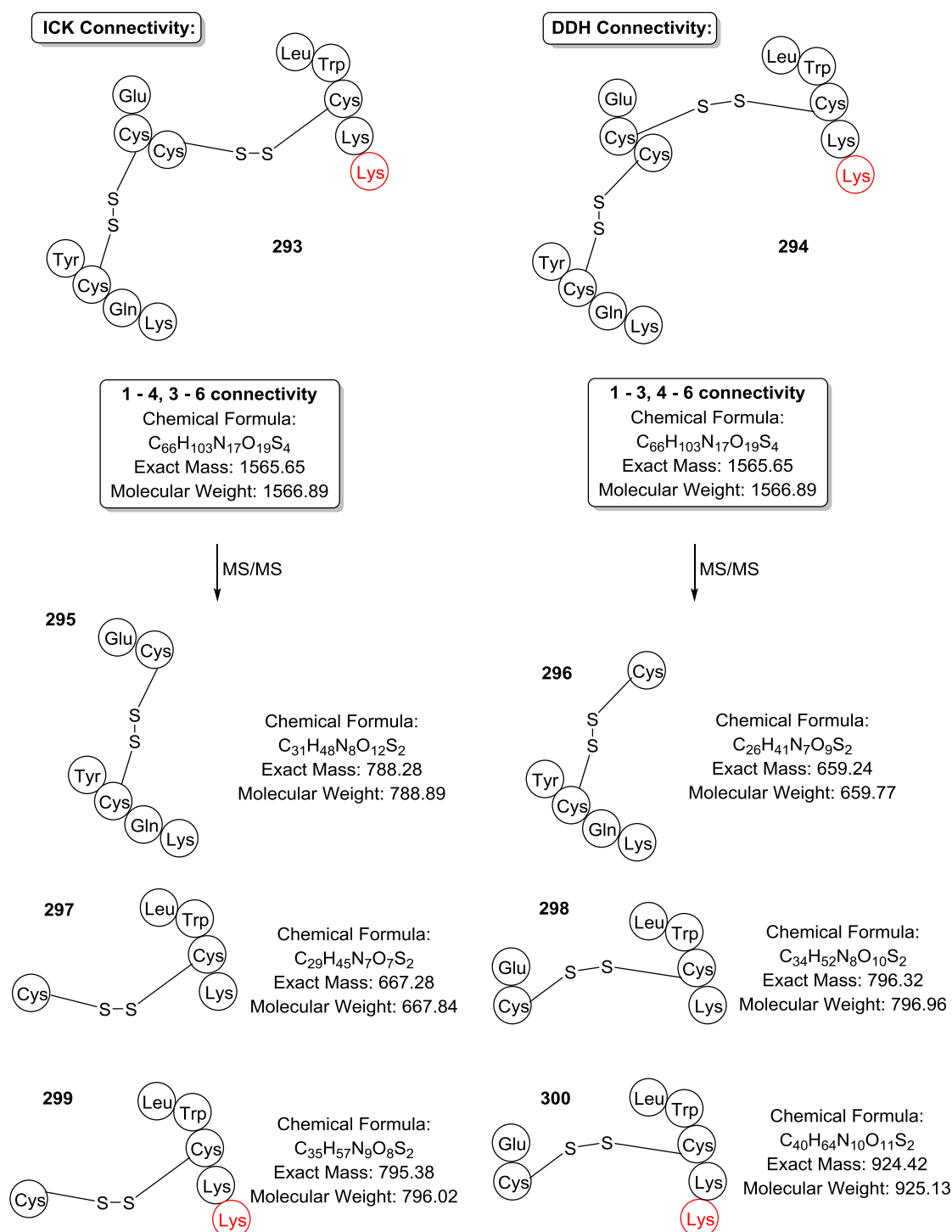


Figure 5.25: Possible Products from the MS/MS Experiments
Position of Extra Lysine Resulting from Incomplete Cleavage Highlighted in Red.

Bombardment of the 1566 amu fragment gave masses close to those for **296** and **298**. However, in both cases, the desired mass was 1 amu out. This data is not conclusive but could be used to tentatively suggest the naturally occurring ProTx-II peptide in fact displays the DDH and not the ICK structure previously published. Unfortunately, in this set of preliminary experiments, the peptide sample cyclised using pure water for 7 days did not digest correctly using the double digestion method. Neither the 1436 nor 1566 amu

fragments corresponding to the peptides containing cysteines 1, 3, 4 and 6 nor the 1776 amu fragment containing the 2-5 connectivity were observed. Thus, no further analysis could be carried out on this sample.

However, given that the Park cyclisation structure could be easily converted into the thermodynamic minimum structure by leaving in water, it is possible that the Middleton group unwittingly carried out the same experiment and thus analysed the non-naturally occurring structure of ProTx-II. As the experimental details for their trypsin digest involved leaving the peptide in water for 2 – 5 days, it is highly likely that this experiment did cause the peptide to interconvert. As the trypsin digest was longer than that performed in this thesis (18 h for the trypsin digest, followed by 24 h for the Glu-C digest), this would account for the differences in peptide structure observed in both experiments.

Therefore, tentative data from the peptide digestions carried out in the Middleton paper and in this thesis could be combined to postulate that the naturally occurring ProTx-II peptide in fact displays DDH and not the previously stated ICK connectivity. Further MS/MS analysis will need to be carried out before this can be conclusively decided but the body of evidence presented here clearly shows that two separate structures are present and can be differentiated by analytical HPLC (although they have the same mass by LCMS).

5.7 Conclusions

Through the use of homology modelling software, it was possible to build a structure of ProTx-II (**22**) close to that determined experimentally by Park and co-workers in 2014. Using this structure, a total of 20 analogues of ProTx-II were generated and evaluated. These comprised of eight single ring structural analogues, which adopted different structures from the parent peptide, as well as nine double ring and three triple ring analogues. As with the single ring analogues, the double ring structures generated from the C-terminal end of the parent peptide also did not show similarity to the parent peptide and were deemed unlikely to show any activity *in vitro*. However, two of the N-terminal double ring analogues modelled did show similarity to the parent peptide. Although this observation was in line with work published by other groups, who showed that changing the N-terminal ring did not have any great structural effect on the peptide,⁶⁻⁸ it was not possible to synthesise and isolate these analogues. This could be due to instability within the structure, which was not apparent from the modelling calculations and prevented the peptides from cyclising to give the desired products.

Finally, as predicted, all three of the triple ring analogues closely resemble the structure of the parent peptide. This is unsurprising as replacing a disulfide bond with a lanthionine bridge results in only a mild change in the constraint on each of the rings; as the structure is already highly constrained, this small difference appears to have little effect on the overall structure of the peptides and as such all three analogues are predicted to have similar levels of activity *in vitro*.

Unexpectedly, none of the compounds synthesised, including the parent peptide, showed any activity when tested against the hNav1.7 ion channel. The use of two separate companies for testing indicated that the problem was with the peptides themselves rather than the testing platform used by the company. This led to work on a new structural characterisation of ProTx-II (**22**) and the identification of a discrepancy between commercial sources of the peptide. Analysis by LC-MS including the use of maleimide end-capping experiments confirmed that all sources of ProTx-II (**22**) contained a peptide of the same mass and that all six cysteines were involved in disulfide bonds. However, analysis by analytical HPLC showed that the peptides gave two peaks differing in retention time by 0.2 min. These peptides were predicted to differ in their cysteine cross-linking patterns and to be the thermodynamic and kinetic products of cyclisation of ProTx-II. To investigate this further, one sample of each of the peptides was submitted for digestion and re-analysis by MS/MS. Although further work will need to be carried out, the evidence has started to suggest that ProTx-II itself can be found in two forms displaying the previously reported ICK connectivity and the evolutionary precursor DDH structure, with the naturally occurring peptide displaying the DDH motif.

¹ Schmalhofer, W. A.; Calhoun, J.; Burrows, R.; Bailey, T.; Kohler, M. G.; Weinglass, A. B.; Kaczorowski, G. J.; Garcia, M. L.; Koltzenburg, M.; Priest, B. T., *Mol. Pharmacol.*, **74**, 1476-1484 (2008)

² Park, J. H.; Carlin, K. P.; Wu, G.; Ilyin, V. I.; Musza, L. L.; Blake, P. R.; Kyle, D. J., *J. Med. Chem.*, **57**, 6623-6631 (2014)

³ Smith, J. J.; Cummins, T. R.; Alphy, S.; Blumenthal, K. M., *J. Biol. Chem.*, **282**, 17, 12687-12697 (2007)

⁴ Chagot, B.; Escoubas, P.; Villegas, E.; Bernard, C.; Ferrat, G.; Corzo, G.; Lazdunski, M.; Darbon, H., *Prot. Sci.*, **13**, 1197-1208 (2004)

⁵ Adapted with permission from Park, J. H.; Carlin, K. P.; Wu, G.; Ilyin, V. I.; Musza, L. L.; Blake, P. R.; Kyle, D. J., *J. Med. Chem.*, **57**, 6623-6631 (2014). Copyright 2014 American Chemical Society

⁶ Wang, X.-H.; Connor, M.; Smith, R.; Maciejewski, M. W.; Howden, M. E. H.; Nicholson, G. M.; Christie, M. J.; King, G. F., *Nature Structural Biology*, **7**, 6, 505-513 (2000)

⁷ Heitz, A.; Le-Nguyen, D.; Chiche, L., *Biochemistry*, **38**, 10615-10625 (1999)

⁸ Le-Nguyen, D.; Heitz, A.; Chiche, L.; El Hajji, M.; Castro, B., *Protein Sci.*, **2**, 165-174 (1993)

⁹ Neher, E.; Sakmann, B., *Nature*, **260**, 799-802 (1976)

¹⁰ Stanfield, C. L., *Principles of Human Physiology*, **5th Edition**, Ed: Pearson Education Inc. (2013)

¹¹ Stanfield, C. L., *Principles of Human Physiology*, **5th Edition** (2013). Reprinted by permission of Pearson Education, Inc., New York, New York

¹² Katz, B.; Miledi, R., *J. Physiol.*, **224**, 665-699 (1972)

-
- ¹³ Anderson, C. R.; Stevens, C. F., *J. Physiol.*, **235**, 655-691 (1973)
- ¹⁴ Molleman, A., *Patch Clamping: An Introductory Guide to Patch Clamp Electrophysiology*, Ed: Wiley and Co (2003)
- ¹⁵ Personal Communication with Dr. S. Kanumilli, Essen Bioscience (17/11/2014)
- ¹⁶ Middleton, R. E.; Warren, V. A.; Kraus, R. L.; Hwang, J. C.; Liu, C. J.; Dai, G.; Brochu, R. M.; Kohler, M. G.; Gao, Y-D.; Garsky, V. M.; Bogusky, M. J.; Mehl, J. T.; Cohen, C. J.; Smith, M. M., *Biochemistry*, **41**, 14734-14747 (2002)
- ¹⁷ Smith, M. E. B.; Schumacher, F. F.; Ryan, C. P.; Tedaldi, L. M.; Papaioannou, D.; Waksman, G.; Caddick, S.; Baker, J. R., *J. Am. Chem. Soc.*, **132**, 1960-1965 (2010)
- ¹⁸ Shu, Q.; Lu, S.-Y.; Gu, X.-C.; Liang, S.-P., *Protein Science*, **11**, 245-252 (2002)
- ¹⁹ Shu, Q.; Huang, R.; Liang, S.-P., *Eur. J. Biochem.*, **268**, 2301-2307 (2001)

6. Chapter 6: Conclusions and Future Work

The aim of this thesis was to investigate the synthesis of truncated analogues of an active parent peptide containing both disulfide and thioether bridges, with the aim of probing the structure-activity relationship of the hNa_v1.7 ion channel. In order to form the thioether bridged peptides, it was first necessary to synthesise a large quantity of diastereomerically pure, orthogonally protected lanthionine. Extensive research into the synthesis resulted in the design of an improved, more robust methodology which worked well on both small and large scales. Improvements were made in the protection of the constituent amino acids both with the reaction themselves and in the purification procedures, which allowed the large scale synthesis of the intermediates to be outsourced. Improvements in the coupling and deprotection steps helped improve the overall yield to 18% over seven steps on small scale. This route also translated well to large scale processing and it was possible to use this method in an industrial setting to produce multi-gram quantities of the desired novel diastereoisomer of lanthionine **142**.

Using this procedure, preliminary investigations into the synthesis of both regioisomers of the orthogonally protected cystathionines (**245**) and (**246**) were also carried out. The work has thus far shown that it is possible to form the required monomers in the synthesis of regioisomer (**245**) in high yield on a reasonably large scale. To finish the synthesis, a significant amount of optimisation of the coupling reaction is required but with greater amounts of the monomers available, the final two steps should be easily achieved. Possible routes to investigate the coupling reaction further include using the bromo-derivative with the cesium carbonate coupling conditions or using the phase-transfer conditions used in the van der Donk group. With regards to the second regioisomer (**246**), more work needs to be done to prevent lactonization of the allyl/Alloc homoserine (**246**). With the complete protection of the homoserine and the work on the coupling reaction to form the other regioisomer, it should again prove easy to form the final product.

Having synthesised large quantities of lanthionine **142**, research began on the synthesis of lanthionine-containing analogues of ProTx-II (**22**) as well as the disulfide-containing equivalents. In total, 10 analogues of ProTx-II (**22**) were synthesised as well as two forms of the native peptide. A total of seven single ring analogues were synthesised to probe the SAR by finding out which parts of the peptide are important for binding within the active site of the ion channel. By designing a novel microwave methodology for the incorporation of lanthionine into a peptide, three analogues containing a thioether bridge were formed. This methodology allowed for the synthesis of the largest known lanthionine-containing single

ring structures made to date. Research showed that although it was possible to observe the double ring analogues both with and without a lanthionine bridge, these proved to have inherently unstable structures, which could not be subjected to purification by conventional means as they did not appear to be stable in water for long periods of time.

Using the novel microwave-based protocol, together with the inclusion of Hmb protection to prevent aggregation on resin and the use of orthogonal protecting groups, three further analogues were synthesised which all contained one thioether bridge interlocking with two disulfide bridges. These are the first known examples of such structures produced to date and show the versatility of the synthetic strategy.

The use of the Hmb protecting group could help with the synthesis of the double ring analogues and future work should include investigation into the incorporation of these amino acids into the synthetic strategy. An alternative method could use pseudo-proline structures in the synthesis; this would increase the amount of constraint in a system and could encourage the cyclisation step. Use of a pseudo-proline could also theoretically increase the maximum ring size beyond the 11 amino acids between the two halves of the lanthionine moiety, which may allow for the synthesis of the N-terminal lanthionine-containing single ring.

Having synthesised the peptides, all the structures were modelled to allow for prediction of activity. As expected, the triple ring analogues exhibited structures closely related to the parent peptide. Unexpectedly, none of the compounds synthesised, nor the parent peptide showed any activity against the hNa_v1.7 ion channel. Having ruled out the possibility of a problem with the testing platform by using two companies, investigations into the nature of the parent peptide were begun. Although LC-MS analysis confirmed that all sources of ProTx-II (**22**) shared the same mass, analytical HPLC showed that two forms of the peptide, with differing retention times, were present. These peptides display differing products of cyclisation and one product can be converted into the other product by leaving in water. Further MS/MS experiments need to be carried out but preliminary data suggests that contrary to the published literature, naturally occurring ProTx-II actually has the DDH motif and not the previously assumed ICK structure. The peptides designed and synthesised in this thesis were based on an original paper claiming that the parent peptide displayed an ICK connectivity motif. The ICK structure has been shown to likely be the inactive conformation of the peptide and so it would be interesting to form DDH analogues of ProTx-II to see if these displayed any activity. It might be interesting to make the single ring disulfide and thioether analogues to probe the structure-activity relationship between the peptide and the

ion channel, but more intriguing would be the formation of the triple ring analogues. The most interesting peptide would contain a thioether bridge in place of either the 1-3 or 4-6 disulfide bond, as this should guarantee a DDH motif. These peptides would then need to be tested against the hNa_v1.7 ion channel assay to see if activity could be restored.

As it has been found to be facile to convert between the DDH and ICK connectivities for this system, it would be interesting to see if other ICK peptides can also form the DDH structures. If this turns out to be the case, it will need to be determined on a case-by-case basis which peptide structure is isolated from a particular source. Given the wide use of ICK peptides within literature for probing a variety of ion channels, this could have far-reaching consequences on investigations into the use of ICK peptides within research as both probes and therapeutics.

7. Chapter 7: Experimental

7.1 General Experimental

Unless otherwise indicated, all reagents were obtained from chemical suppliers with no further purification. Dry DMF, THF and CH₂Cl₂ were dried over anhydrous alumina columns,¹ with moisture levels typically below 15 ppm by Karl Fischer titration. Brine refers to a saturated solution of sodium chloride in water and sodium bicarbonate refers to a saturated solution of sodium hydrogen carbonate in water. Ether refers to diethyl ether and petrol to petroleum ether fractions boiling between 40 and 60 °C. All water used was either distilled using an Elga Purelab Option R 7 water purifier or used directly from a bottle of HPLC-grade water. All reactions were carried out in closed systems under Argon.

NMR spectra were recorded using a Bruker AC300, AV400, AC500 or AC600 spectrometer (300 MHz, 400 MHz, 500 MHz and 600 MHz respectively) and all samples were dissolved in deuterated chloroform unless otherwise stated. Chemical shifts (δ) are given in ppm units relative to tetramethylsilane and coupling constants (J) are measured in Hertz. Proton (¹H) NMR multiplicities are shown as s (singlet), d (doublet), t (triplet), q (quartet), m (multiplet), dd (double doublet), dt (double triplet), dq (doublet of quartets), dt (doublet of triplets), tt (triplet of triplets), br s (broad singlet), br d (broad doublet), ddt (doublet of doublet of triplets), dddd (doublet of doublet of doublet of triplets), dddd (doublet of doublet of doublet of doublets). ¹H and ¹³C NMRs were assigned using COSY, DEPT, HMBC and HSQC spectra.

MS refers to low resolution mass spectrometry and HRMS refers to high resolution mass spectrometry. MS was performed on a Waters Acquity UPLC SQD using HPLC grade water and acetonitrile (both with 0.1% formic acid) as the solvents. Electrospray ionization (ESI) accurate mass was determined using a Waters LCT Premier XE.

Infrared spectra were recorded using a Perkin Elmer 100 FT-IR spectrometer and Optical Rotations were recorded using a Perkin Elmer 343 polarimeter and are reported in 10⁻¹ deg cm² g⁻¹. Melting points were recorded on a Gallenkamp Hot Stage apparatus and are uncorrected.

Flash column chromatography was carried out using silica gel with particle size <60 μ m and reverse phase column chromatography was carried out using silica gel 60 silanized (53-200 μ m). Thin layer chromatography (TLC) was performed on aluminium backed Sigma-Aldrich TLC plates with F₂₅₄ fluorescent indicator. Developed plates were air dried and analysed under a UV light or by staining with the appropriate indicator.

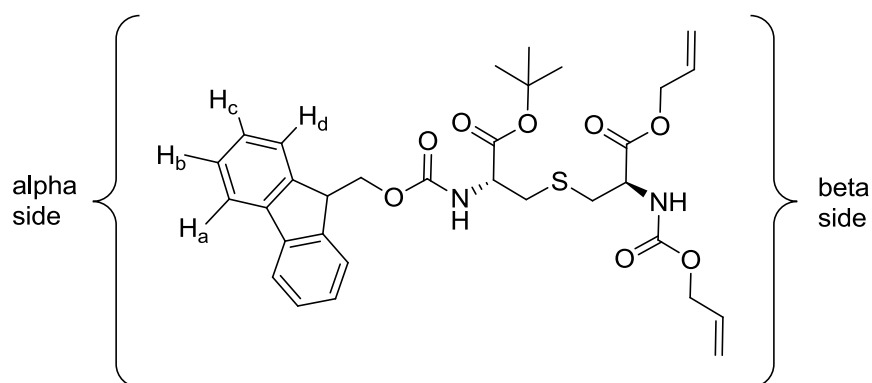
Large scale column chromatography was carried out using a Biotage Isolera 4 with either Biotage 340 g KP-Sil Snap Cartridges filled with 50 μm silica or Biotage 375 g KP-NH Snap Cartridges filled with amine-bonded silica.

7.2 Experimental for the Synthesis of Lanthionine (Chapter 2)

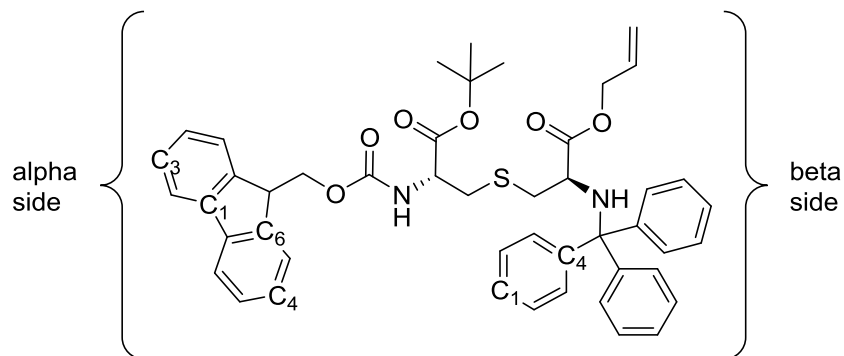
7.2.1 Key to NMR Assignments:

The following nomenclature is used throughout this chapter when assigning NMRs:

^1H NMR:

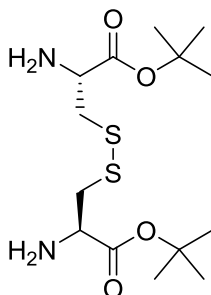


^{13}C NMR:



7.2.2 Experimental for Small Scale Synthesis

(2*R*,2'*R*)-*tert*-Butyl 3,3'-disulfanediylbis(2-aminopropanoate) (**134**)



Tert-butyl acetate (200 mL, 1.49 mol) was added dropwise to a mechanically stirred solution of L-cystine (**133**) (20.0 g, 83.2 mmol) and 70% perchloric acid (33.2 mL, 0.550 mol) behind a blast shield to form two immiscible layers, which dispersed on stirring. The reaction was left to stir for 18 h and a viscous white paste was formed. The reaction was then cooled on ice for 15 min before adding water (200 mL) and ethyl acetate (200 mL). The aqueous layer was then adjusted to pH 9 using 10 M sodium hydroxide before separating the organic layer and extracting the aqueous layer with ethyl acetate (3 x 150 mL). The combined organic layers were dried over MgSO₄ and concentrated *in vacuo* to yield a pale yellow oil (27.6 g, 78.2 mmol, 94%) which was used without further purification.

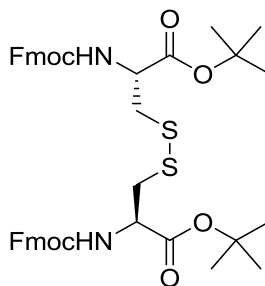
NMR: δ_{H} (500 MHz CDCl₃) 3.71 (2H, dd, *J* 7.3, 4.4 Hz, SCH₂CH), 3.16 (2H, dd, *J* 13.5, 4.4 Hz, SCHH'H), 2.88 16 (2H, dd, *J* 13.5, 7.3 Hz, SCHH'H), 2.20 (2H, br s, NH), 1.47 (18H, s, *t*Bu).

δ_{C} (125 MHz CDCl₃) 169.8 (COO^{*t*}Bu), 84.0 (C(CH₃)₃), 53.9 (CHNH₂), 40.9 (CH₂SH), 28.0 (C(CH₃)₃).

MS: *m/z* (Cl⁺) 353 ([M+H]⁺, 25%), 304 ([M+Na-O^{*t*}Bu]⁺, 100%); HRMS C₁₄H₂₉O₄N₂S₂ ([M+H]⁺) requires 353.1569, found 353.1572.

Spectroscopic data are in agreement with the literature values.²

(2*R*,2'*R*)-tert-Butyl 3,3'-disulfanediylbis(2-(9(fluorenylmethoxycarbonyl)) aminopropanoate) (135)



N-methylmorpholine (8.16 mL, 74.3 mmol, 2 eq.) was added to a stirred solution of (2*R*,2'*R*)-*tert*-butyl 3,3'-disulfanediylbis(2-aminopropanoate) (**134**) (14.0 g, 37.1 mmol, 1 eq.) at room temperature in THF (100 mL). To this, a solution of *N*-(9-Fluorenylmethoxycarbonyloxy)succinimide (25.0 g, 74.3 mmol, 2 eq.) in THF (100 mL) was added dropwise and the resulting mixture was left to stir overnight.

The THF was removed *in vacuo* and the residue was re-dissolved in ethyl acetate (125 mL) and washed with water (2 x 100 mL) and brine (2 x 100 mL). The organic layer was dried over MgSO₄, filtered and concentrated *in vacuo*. Purification by recrystallisation (petrol : ethyl acetate 90 : 10) yielded a pale yellow solid (18.0 g, 22.6 mmol, 61%).

NMR: δ_{H} (500 MHz CDCl₃) 7.74 (4H, d, *J* 7.3 Hz, Fmoc H_a) 7.58 (4H, d, *J* 7.3 Hz, Fmoc H_d), 7.38 (4H, t, *J* 7.3 Hz, Fmoc H_b), 7.28 (4H, t, *J* 7.3 Hz, Fmoc H_c) 5.72 (2H, d, *J* 7.0 Hz, NH), 4.57 (2H, m, SCH₂CH), 4.36 (4H, d, *J* 7.1 Hz, CH₂Fmoc), 4.19 (2H, t, *J* 7.1 Hz, CHFmoc), 3.20 (4H, m, SCH₂CH), 1.48 (18H, s, *t*Bu).

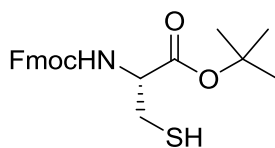
δ_{C} (125 MHz CDCl₃) 169.5 (COO^{*t*}Bu), 155.8 (NHCOO), 143.9 (C-1 Fmoc), 143.8 (C-6 Fmoc), 127.8 (C-4 Fmoc), 127.2 (C-3 Fmoc), 125.3 (C-2 Fmoc), 125.1 (C-5 Fmoc), 83.4 (C(CH₃)₃), 67.3 (CH₂ Fmoc), 54.2 (CHNH₂), 47.1 (CH Fmoc), 42.0 (CH₂S), 28.1 (C(CH₃)₃).

MS: *m/z* (ES⁺) 819.28 ([M+Na]⁺, 100%); HRMS C₄₄H₄₈O₈N₂S₂Na ([M+Na]⁺) requires 819.2750, found 819.2748.

Melting point: 149-152 °C.

Spectroscopic data are in agreement with the literature values.³

(R)-tert-Butyl 2-((9(fluorenylmethoxycarbonyl))amino)-3-mercaptopropanoate (62)



Method 1:

Tributylphosphine (2.60 mL, 10.4 mmol, 2 eq.) was added to a stirred solution of (2*R*,2'*R*)-tert-butyl 3,3'-disulfanediylbis(2-(9(fluorenylmethoxycarbonyl))aminopropanoate) (**135**) (4.00 g, 5.20 mmol, 1 eq.) in dry THF (60 mL) and left to stir for 15 min before the addition of water (6 mL). The reaction was left to stir for a further 19 h before the mixture was concentrated *in vacuo* and re-dissolved in ethyl acetate (90 mL). This was washed with citric acid (5% aq. w/v, 2 x 60 mL), water (60 mL) and brine (60 mL). The organic layer was dried over MgSO₄ and purified by flash chromatography (CH₂Cl₂ : hexane 1 : 1) to yield the title product as a colourless oil (2.56 g, 6.3 mmol, 61%).

R_f = 0.35 (CH₂Cl₂ : hexane 1 : 1)

Method 2:

Dithiothreitol (0.145 g, 0.94 mmol, 1.5 eq.) was added to a stirred solution of (2*R*,2'*R*)-tert-butyl 3,3'-disulfanediylbis(2-(9(fluorenylmethoxycarbonyl))aminopropanoate) (**135**) (0.500 g, 0.630 mmol, 1 eq.) in dry CH₂Cl₂ (10 mL). To this, triethylamine (0.130 mL, 0.940 mmol, 1.5 eq.) was added and the solution was left to stir for 45 min. The solution was then washed with sodium bicarbonate (2 x 20 mL) and water (2 x 20 mL), dried (MgSO₄) and concentrated *in vacuo* to yield the product as a colourless oil (0.400 g, 0.750 mmol, 80%).

NMR: δ_H (600 MHz CDCl₃) 7.77 (2H, d, *J* 7.4 Hz, Fmoc H_a), 7.62 (2H, d, *J* 7.4 Hz, Fmoc H_d), 7.41 (2H, t, *J* 7.4 Hz, Fmoc H_b), 7.33 (2H, t, *J* 7.4 Hz, Fmoc H_c), 5.76 (1H, d, *J* 7.2 Hz, NH), 4.56 (1H, m, SCH₂CH), 4.41 (2H, d, *J* 6.9 Hz, CH₂Fmoc), 4.24 (1H, t, *J* 6.9 Hz, CHFmoc), 3.00 (2H, m, SCH₂CH), 1.51 (9H, s, *t*Bu).

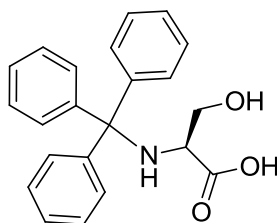
δ_C (125 MHz CDCl₃) 169.1 (COO^{*t*}Bu), 155.8 (NHCOO), 144.0 (C-1 Fmoc), 141.5 (C-6 Fmoc), 127.9 (C-2 Fmoc), 127.2 (C-5 Fmoc), 125.3 (C-4 Fmoc), 120.2 (C-3 Fmoc), 83.2 (C(CH₃)₃), 67.2 (CH₂ Fmoc), 55.6 (CHCH₂SH), 47.3 (CH Fmoc), 28.2 (C(CH₃)₃), 27.5 (CH₂SH).

MS: *m/z* (Cl⁺) 400.2 ([M+H]⁺, 10%), 313 ([M-O^{*t*}Bu]⁺, 50%), 179 ([FmocNHC]⁺, 100%); HRMS C₂₂H₂₆O₂NSH ([M+H]⁺) requires 400.1583, found 400.1587.

[α]_D²⁰ -16.9 (c 1.0, CH₃OH)

Spectroscopic data are in agreement with the literature values.³

(S)-3-Hydroxy-2-(tritylamino)propanoic acid (137**)**



Trimethylsilyl chloride (29.8 mL, 234 mmol, 3.1 eq.) was added to a suspension of L-serine (**136**) (7.95 g, 75.7 mmol, 1 eq.) in CH₂Cl₂ (120 mL). The mixture was refluxed for 20 min and then cooled to room temperature. Triethylamine (32.7 mL, 234 mmol, 3.1 eq.) was then added dropwise and the solution refluxed for a further 45 minutes, before cooling to room temperature again. The reaction was then cooled to 0 °C in an ice bath before the careful addition of anhydrous MeOH (3.07 mL, 75.7 mmol, 1 eq.). The mixture was then allowed to warm to room temperature again before the addition of a further portion of triethylamine (10.4 mL, 75.7 mmol, 1 eq.) followed by trityl chloride (21.1 g, 75.7 mmol, 1 eq.). The reaction was then left to stir for 20 h at room temperature.

After this time, excess triethylamine (30 mL) and MeOH (180 mL) were added and the solvents removed *in vacuo* to leave yellow crystals. These were then dissolved in ethyl acetate (400 mL) and pre-cooled citric acid (4 °C, 5% aq. w/v, 250 mL). The organic layer was extracted with sodium hydroxide (2M, 2 x 50 mL), water (2 x 100 mL) and brine (2 x 100 mL). The combined aqueous layers were then neutralised with a few drops of glacial acetic acid. The precipitated product was extracted with ethyl acetate (4 x 100 mL) and the combined organic layers were dried over MgSO₄ and the solvent removed *in vacuo* to give a pale yellow solid (23.6 g, 211 mmol, 90%).

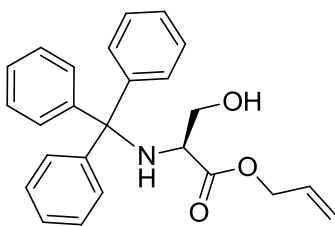
NMR: δ_H (600 MHz CDCl₃) 7.43 (6H, m, trityl) 7.29 (9H, m, trityl), 3.76 (1H, dd, *J* 11.0, 3.0 Hz, CHCHH'OH), 3.53 (1H, dt, *J* 4.3, 3.0 Hz, CHCH₂OH), 2.79 (1H, dd, *J* 11.0, 4.3 Hz, CHCHH'OH).

δ_C (150 MHz CDCl₃) 174.3 (COOH), 144.7 (C-4 trityl), 128.6 (C-1 trityl), 128.5 (C-2 trityl), 127.4 (C-3 trityl), 71.9 (CPh₃), 62.6 (CHCH₂OH), 58.6 (CHCH₂OH).

MS: *m/z* (ES⁻) 346.15 ([M-H]⁻, 100%); HRMS C₂₂H₂₀O₃N ([M-H]⁻) requires 346.1443, found 346.1458.

Spectroscopic data are in agreement with the literature values.⁴

(S)-Allyl 3-hydroxy-2-(tritylamino)propanoate (138)



Method 1:

Cesium carbonate (2.77 g, 8.50 mmol, 0.5 eq.) was added to a stirred solution of (S)-3-hydroxy-2-(tritylamino)propanoic acid (**137**) (6.00 g, 17.0 mmol, 1 eq.) in MeOH (170 mL) and left to stir for 15 min before concentrating *in vacuo*. The resulting cesium salt was then dissolved in anhydrous DMF (170 mL) and allyl bromide (1.40 mL, 16.2 mmol, 0.95 eq.) was added dropwise to the solution. The reaction was left to stir overnight before the addition of ethyl acetate (400 mL). The mixture was washed with pre-cooled citric acid (4 °C, 5% aq. w/v, 5 x 200mL) and the organic layer was dried over MgSO₄, filtered and concentrated *in vacuo* to yield the product as a yellow oil (5.75 g, 7.40 mmol, 87%).

Method 2:

Allyl alcohol (24.3 mL, 0.357 mol, 15 eq.) was added to a solution of L-Serine (**136**) (2.5 g, 23.7 mmol, 1 eq.) and *para*-toluene sulfonic acid (5.43 g, 28.5 mmol, 1.2 eq.) in toluene (75 mL). The mixture was refluxed at 110 °C for 4.5 h using a Dean-Stark apparatus. The toluene was removed *in vacuo* and the product was re-dissolved in anhydrous DMF (50 mL) before addition of triethylamine (13.3 mL, 22.6 mmol, 4 eq.). The solution was cooled to 0 °C before the addition of trityl chloride (6.63 g, 23.7 mmol, 1 eq.) in DMF (20 mL). After complete addition, the reaction was allowed to warm to room temperature and left to stir for 16 h.

Ethyl acetate (70 mL) was then added and the solution washed with 0.5 M HCl (70 mL) and water (2 x 70 mL). The organic layer was dried (Na₂SO₄) and concentrated *in vacuo*. Purification by column chromatography (hexane : ethyl acetate 4:1) yielded the title compound as a colourless oil (8.50 g, 20.7 mmol, 91%).

R_f = 0.35 (hexane : ethyl acetate 4 : 1)

NMR: δ_H (600 MHz CDCl₃) 7.49 (6H, d, *J* 7.4 Hz, trityl), 7.27 (6H, m, trityl), 7.20 (3H, m, trityl), 5.70 (1H, dddd, *J* 17.2, 10.5, 5.9, 1.0 Hz, CH₂CH=CH₂), 5.19 (1H, dd, *J* 17.2, 1.0 Hz, CH₂CH=CHH'), 5.17 (1H, dd, *J* 10.5, 1.0 Hz, CH₂CH=CHH'), 4.21 (1H, ddt, *J* 13.2, 5.9, 1.0 Hz,

$\text{CHH}'\text{CH}=\text{CH}_2$), 4.09 (1H, ddt, J 13.2, 5.9, 1.5 Hz, $\text{CHH}'\text{CH}=\text{CH}_2$), 3.72 (1H, m, CHCH_2OH), 3.56 (2H, m, CHCH_2OH).

δ_{C} (150 MHz CDCl_3) 173.3 (COOallyl), 147.0 (C-4 trityl), 131.7 ($\text{CH}_2\text{CH}=\text{CH}_2$), 128.9 (C-1 trityl), 128.1 (C-2 trityl), 126.8 (C-3 trityl), 118.7 ($\text{CH}_2\text{CH}=\text{CH}_2$), 71.1 (CPh_3), 65.9 ($\text{CH}_2\text{CH}=\text{CH}_2$), 65.1 (CHCH_2OH), 57.9 (CHCH_2OH).

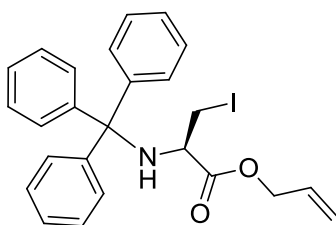
MS: m/z (ES^+) 410.2 ($[\text{M}+\text{Na}]^+$, 35%), 243 ($[\text{CPh}_3]^+$, 100%); HRMS $\text{C}_{25}\text{H}_{25}\text{NO}_3$ ($[\text{M}+\text{Na}]^+$) requires 410.1732, found 410.1733.

ν_{max} (CHCl_3) 3295 (OH stretch, broad), 2941 & 2831 (CH stretch), 1578 (C=O stretch).

$[\alpha]_{\text{D}}^{20} +16.2$ (c 1.0, CH_3OH).

Spectroscopic data are in agreement with the literature values.⁵

***(R)*-Allyl 3-iodo-2-(trimethylphenylamino)propanoate 139**



Method 1:

(*S*)-Allyl 3-hydroxy-2-(trimethylphenylamino)propanoate (**138**) (3.61 g, 9.32 mmol, 1 eq.) was dissolved in dry CH_2Cl_2 (9.4 mL) at room temperature in the presence of triphenylphosphine (3.67 g, 14.0 mmol, 1.5 eq.). After 10 min, the solution was cooled to $-10\text{ }^\circ\text{C}$ using an acetone/ice/water bath. Diethylazodicarboxylate (2.2 mL, 14.0 mmol, 1.5 eq.) was then added dropwise over the course of 1 min. The reaction was left for 5 min before the addition of methyl iodide (0.87 mL, 14.0 mmol, 1.5 eq.). The reaction was left to stir for a further 3 h before the direct addition of silica to the reaction. The solvent was removed *in vacuo* and the mixture purified by column chromatography (20:1 hexane : ethyl acetate) to yield the product as a pale yellow viscous oil (3.26 g, 6.6 mmol, 71%).

Method 2:

Iodine (0.852 g, 3.36 mmol, 1.3 eq.) was added portionwise to a solution of triphenylphosphine (0.846 g, 3.23 mmol, 1.25 eq.) and imidazole (0.228 g, 3.36 mmol, 1.3 eq.) in CH_2Cl_2 (12 mL) to give a yellow solution. To this, a solution of (*S*)-allyl 3-hydroxy-2-(trimethylphenylamino)propanoate (**138**) (1.00 g, 3.23 mmol, 1 eq.) in CH_2Cl_2 (12 mL) was added dropwise. The reaction was left to stir at $0\text{ }^\circ\text{C}$ for 4 h. The solvent was removed *in*

vacuo and the mixture purified by column chromatography (20:1 hexane : ethyl acetate) to yield the product as a pale yellow viscous oil (1.03 g, 4 : 1 ratio of product : aziridine **143** by NMR, 2.07 mmol, 80%).

R_f = 0.35 (hexane : ethyl acetate 20 : 1).

NMR: δ_H (400 MHz $CDCl_3$) 7.50 (6H, m, trityl) 7.27 (9H, m, trityl), 5.77 (1H, ddt, J 17.2, 10.5, 6.0 Hz, $CH_2CH=CH_2$), 5.22 (2H, m, $CH_2CH=CH_2$), 4.27 (1H, dddd, J 13.0, 6.0, 1.5, 1.2 Hz, $CHH'CH=CH_2$), 4.13 (1H, dddd, J 13.0, 6.0, 1.5, 1.2 Hz, $CHH'CH=CH_2$), 3.54 (1H, m, $CHCH_2I$), 3.35 (1H, dd, J 9.8, 3.5 Hz, $CHCHH'I$), 3.23 (1H, dd, J 9.8, 6.0 Hz, $CHCHH'I$), 2.92 (1H, d, J 9.8 Hz, NH).

δ_C (100 MHz $CDCl_3$) 171.9 (COOallyl), 145.6 (C-4 trityl), 131.7 ($CH_2CH=CH_2$), 128.7 (C-1 trityl), 128.1 (C-2 trityl), 126.7 (C-3 trityl), 118.7 ($CH_2CH=CH_2$), 71.2 (CPh_3), 66.0 ($CH_2CH=CH_2$), 56.3 ($CHCH_2I$), 9.8 ($CHCH_2I$).

MS: m/z (Cl^+) 498 ($[M+H]^+$, 15%), 420 ($[M-Ph]^+$, 60%), 243 ($[CPh_3]^+$, 100%);

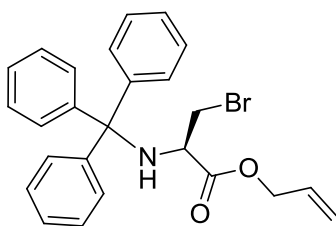
HRMS $C_{25}H_{25}NO_2I$ ($[M+H]^+$) requires 498.0930, found 498.0925.

ν_{max} ($CHCl_3$) 3057 (NH stretch, broad), 1735 (C=O stretch).

$[\alpha]_D^{20}$ +0.8 (c 1.0, CH_3OH).

NMR data is identical to the previously reported (R)-Allyl 3-iodo-2-(trimethylphenylamino)propanoate.⁶

***(R)*-Allyl 3-bromo-2-(trimethylphenylamino)propanoate 155**



Triphenylphosphine (372 mg, 1.42 mmol, 1.1 eq.) was added to a solution of (S)-allyl 3-hydroxy-2-(trimethylphenylamino)propanoate (**138**) (500 mg, 1.29 mmol, 1 eq.) and carbon tetrabromide (471 mg, 1.42 mmol, 1.1 eq.) in CH_2Cl_2 (15 mL) at 0 °C. The reaction was allowed to warm to room temperature and left to stir for 1 h. The solution was then washed with water (30 mL) and the organic layer dried (Na_2SO_4) and concentrated *in vacuo*. Purification by column chromatography (hexane : ethyl acetate 10:1) yielded the title compound as a colourless oil (415 mg, 1.01 mmol, 71%).

R_f = 0.4 (hexane : ethyl acetate 10 : 1)

NMR: δ_H (600 MHz $CDCl_3$) 7.56 (6H, m, trityl), 7.31 (6H, m, trityl), 7.24 (3H, m, trityl), 5.76 (1H, m, $CH_2CH=CH_2$), , 5.24 (2H, m, $CH_2CH=CH_2$), 4.29 (1H, m, $CHH'CH=CH_2$), 4.14 (1H, m, $CHH'CH=CH_2$), 3.76 (1H, br s, NH), 3.61 (1H, m, $CHCHH'Br$), 3.44 (1H, m, $CHCHH'Br$), 2.98 (1H, m, $CHCH_2Br$)

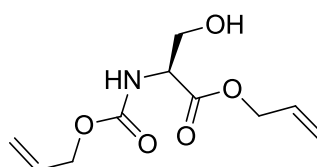
δ_C (150 MHz $CDCl_3$) 171.9 (COOallyl), 145.8 (C-1 trityl), 131.8 ($CH_2CH=CH_2$), 128.8 (trityl), 128.6 (trityl), 128.2 (trityl), 126.9 (trityl), 126.8 (trityl), 118.8 ($CH_2CH=CH_2$), 71.3 (CPh_3), 66.2 ($CH_2CH=CH_2$), 56.9 ($CHCH_2Br$), 35.7 ($CHCH_2Br$).

MS: m/z (Cl^+) 450 : 452 (1 : 1, ^{79}Br : ^{81}Br $[M+H]^+$, 5%), 243 ($[CPh_3]^+$, 100%);

HRMS $C_{25}H_{24}NO_2^{79}Br$ ($[M+H]^+$) requires 450.1069, found 450.1064.

ν_{max} ($CHCl_3$) 3323 (NH stretch, broad), 3058 (C-H stretch, broad), 1736 (C=O stretch), 1490 (NH amide or C=C stretch).

(S)-Allyl 2-(allyloxycarbonylamino)-3-hydroxypropanoate (152)



Allyl alcohol (6.47 mL, 95.2 mmol, 10 eq.) was added to a solution of L-Serine (**136**) (1.00 g, 9.52 mmol, 1 eq.) and *para*-toluene sulfonic acid (1.81 g, 11.4 mmol, 1.2 eq.) in toluene (30 mL). The mixture was refluxed at 110 °C for 4.5 h using a Dean-Stark apparatus. The toluene was removed *in vacuo* and the product was re-dissolved in ethyl acetate (20 mL) before addition of triethylamine (5.3 mL, 38.1 mmol, 4 eq.). The solution was cooled to 0 °C before the slow addition of allyl chloroformate (1.1 mL, 10.5 mmol, 1.1 eq.) in ethyl acetate (10 mL) *via* a dropping funnel. After complete addition, the reaction was allowed to warm to room temperature and left to stir for 14 h.

After this time, the solution was washed with 0.5 M HCl (20 mL), water (20 mL) and brine (20 mL). The organic layer was dried (Na_2SO_4) and concentrated *in vacuo*. Purification by column chromatography (hexane : ethyl acetate 1:1) yielded the title compound as a colourless oil (0.750 g, 3.24 mmol, 34%).

R_f = 0.35 (hexane : ethyl acetate 1 : 1)

NMR: δ_H (600 MHz $CDCl_3$) 5.97 (1H, d, J 7.8 Hz, NH), 5.87 (2H, ddt, J 17.1, 10.4, 5.7 Hz, $CH_2CH=CH_2$ both sides), 5.30 (1H, dd, J 17.1, 1.4 Hz, $CH_2CH=CHH'$ allyl), 5.27 (1H, br d, J 17.1 Hz, $CH_2CH=CHH'$ Alloc), 5.22 (1H, dd, J 10.4, 1.4 Hz, $CH_2CH=CHH'$ allyl), 5.18 (1H, dd, J 10.4, 1.4 Hz, $CH_2CH=CHH'$ Alloc), 4.62 (2H, d, J 5.7 Hz, $CH_2CH=CH_2$ allyl), 4.54 (2H, m, $CH_2CH=CH_2$

Alloc), 4.40 (1H, m, CHCH₂OH), 3.96 (1H, dd, *J* 11.3, 9.7 Hz, CHCHH'OH), 3.86 (1H, dd, *J* 11.3, 3.4 Hz, CHCHH'OH), 3.10 (1H, br s, OH).

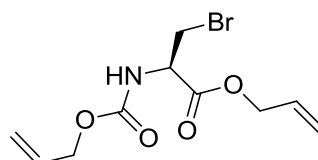
δ_c (150 MHz CDCl₃) 170.6 (COOallyl), 156.4 (COOAlloc), 132.6 (CH₂CH=CH₂ Alloc), 131.5 (CH₂CH=CH₂ allyl), 118.9 (CH₂CH=CH₂ allyl), 118.1 (CH₂CH=CH₂ Alloc), 66.4 (CH₂CH=CH₂ allyl), 66.1 (CH₂CH=CH₂ Alloc), 63.1 (CHCH₂OH), 56.2 (CHCH₂OH).

MS: *m/z* (ES⁺) 230.1 ([M+H]⁺, 100%); HRMS C₁₀H₁₆NO₅ ([M+H]⁺) requires 230.1028, found 230.1034.

ν_{max} (CHCl₃) 3384 (OH stretch, broad), 1700 (C=O stretch), 1520 (NH amide bend).

NMR data is identical to the previously reported (R)-Allyl 2-(allyloxycarbonylamino)-3-hydroxypropanoate.⁷

(R)-Allyl 2-(allyloxycarbonylamino)-3-bromopropanoate (153)



Triphenylphosphine (1.26 g, 4.80 mmol, 1.1 eq.) was added to a solution of (S)-allyl 2-(allyloxycarbonylamino)-3-hydroxypropanoate (**152**) (1.00 g, 4.36 mmol, 1 eq.) and carbon tetrabromide (1.59 g, 4.80 mmol, 1.1 eq.) in CH₂Cl₂ (30 mL) at 0 °C. The reaction was allowed to warm to room temperature and left to stir for 1 h. The solution was then washed with water (30 mL) and the organic layer dried (Na₂SO₄) and concentrated *in vacuo*. Purification by column chromatography (hexane : ethyl acetate 4 : 1) yielded the title compound as a colourless oil (0.84 g, 2.9 mmol, 60%).

R_f = 0.35 (hexane : ethyl acetate 10 : 4)

NMR: δ_H (600 MHz CDCl₃) 5.92 (2H, m, CH₂CH=CH₂ both sides), 5.64 (1H, d, *J* 7.7 Hz, NH), 5.37 (1H, dd, *J* 17.2, 1.4 Hz, CH₂CH=CHH' allyl), 5.33 (1H, dd, *J* 17.3, 1.4 Hz, CH₂CH=CHH' Alloc), 5.29 (1H, dd, *J* 10.5, 1.2 Hz, CH₂CH=CHH' allyl), 5.24 (1H, dd, *J* 10.5, 1.3 Hz, CH₂CH=CHH' Alloc), 4.82 (1H, dt, *J* 7.9, 3.4 Hz, CHCH₂Br), 4.72 (1H, ddt, *J* 13.0, 5.9, 1.2 Hz, CHH'CH=CH₂ allyl), 4.69 (1H, ddt, *J* 13.0, 5.9, 1.2 Hz, CHH'CH=CH₂ allyl), 4.61 (1H, ddt, *J* 13.5, 5.5, 1.3 Hz, CHH'CH=CH₂ Alloc), 4.56 (1H, ddt, *J* 13.5, 5.5, 1.3 Hz, CHH'CH=CH₂ Alloc), 3.86 (1H, dd, *J* 10.6, 3.5 Hz, CHCHH'Br), 3.75 (1H, dd, *J* 10.6, 3.5 Hz, CHCHH'Br).

δ_c (150 MHz CDCl₃) 168.7 (COOallyl), 155.5 (COOAlloc), 132.4 (CH₂CH=CH₂ Alloc), 131.2 (CH₂CH=CH₂ allyl), 119.6 (CH₂CH=CH₂ allyl), 118.3 (CH₂CH=CH₂ Alloc), 66.9 (CH₂CH=CH₂ allyl), 66.3 (CH₂CH=CH₂ Alloc), 54.4 (CHCH₂Br), 33.9 (CHCH₂Br).

MS: m/z (ES^+) 292: 294 (1: 1 ^{79}Br : ^{81}Br $[M+H]^+$, 100%); HRMS $C_{10}H_{15}NO_4^{79}Br$ ($[M+H]^+$) requires 292.0185, found 292.0187.

ν_{max} ($CHCl_3$) 3347 (NH stretch, broad), 2939 (C-H stretch, broad) 1717 (C=O stretch), 1511 (NH amide bend), 1192 (C-Br stretch).

NMR data is identical to the previously reported (S)-Allyl 2-(allyloxycarbonylamino)-3-bromopropanoate.⁷

Optimisation of the Coupling Reaction to form (R)-Allyl 3-((R)-2-((9(fluorenylmethoxycarbonyl))amino-3-tert-butoxy-3-oxopropylthio)-2-(tritylamino)propanoate 140

General Method 1:

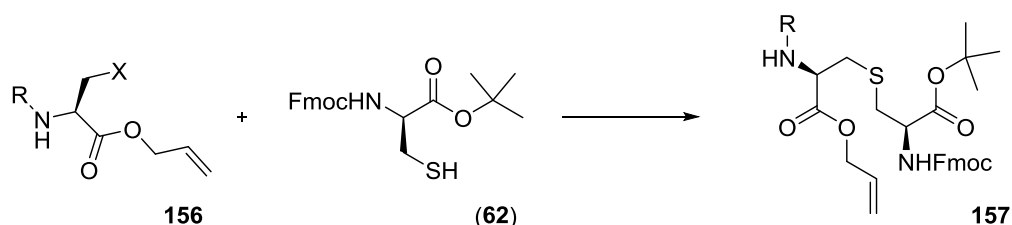


Figure 7.1: Summary of Results from Coupling Investigations (* indicates diastereoisomeric ratio, as determined by NMR)

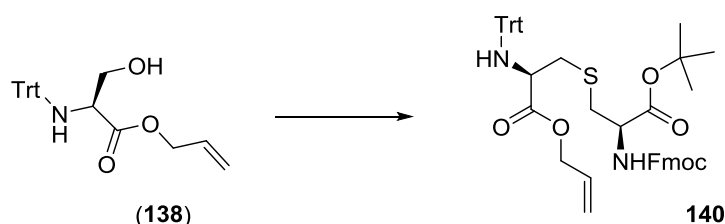
(R)-tert-Butyl 2-((9(fluorenylmethoxycarbonyl))amino)-3-mercaptopropanoate (**62**) (89 mg, 0.220 mmol, 1 eq.) and protected allyl serine derivative (1 eq.) were dissolved in DMF (4 mL) at 0°C. The stated amount of NaI and dry cesium carbonate (see Table 7.1) were added and the reaction stirred for 2 h before the addition of a second portion of cesium carbonate. The reaction was left to stir for a further 2 h and then excess ethyl acetate (10 mL) was added and the mixture washed with cold citric acid (4 °C, 5% aq. w/v, 10 mL) and distilled water (2 x 10 mL). The organic layer was dried over $MgSO_4$ and concentrated *in vacuo*. Purification by column chromatography (hexane : ethyl acetate 4 : 1) yielded the title compound as a white solid (67.9 mg, 0.086 mmol, 39%).

NB: The reaction with brominated trityl serine did not proceed at large scale.

Entry	R	X	Method	Results
1	Alloc	Br	50 mg scale, 1 eq. Cs ₂ CO ₃ then 10 mol% NaI	32% (83:17)*
2	Alloc	Br	200 mg scale, 1 eq. Cs ₂ CO ₃ then 10 mol% NaI	27% (73:22)*
3	Trityl	Br	1 eq. Cs ₂ CO ₃ then 20 mol% NaI	35%
4	Trityl	Br	1 eq. Cs ₂ CO ₃ then 5 mol% NaI	48%
5	Trityl	Br	1 eq. Cs ₂ CO ₃ only	39%
6	Trityl	I	1 eq. Cs ₂ CO ₃ only	38%
7	Trityl	Br	10 mol% NaI then 1 eq. Cs ₂ CO ₃	Aziridine formation
8	Trityl	Br	1 eq. Cs ₂ CO ₃ then 10 mol% NaI	50%
9	Alloc	Br	1 eq. Cs ₂ CO ₃ only	No reaction

Table 7.1: Summary of Results from Coupling Investigations (* indicates diastereoisomeric ratio, as determined by NMR)

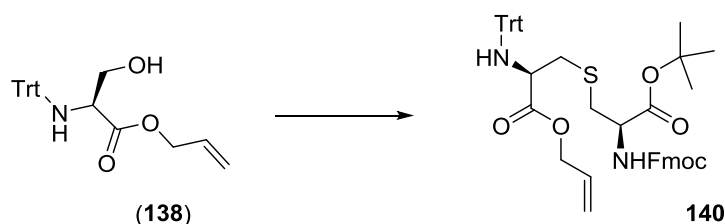
Method 2:



Iodine (0.852 g, 3.36 mmol, 1.3 eq.) was added portionwise to a solution of triphenylphosphine (0.846 g, 3.23 mmol, 1.25 eq.) and imidazole (0.228 g, 3.36 mmol, 1.3 eq.) in CH₂Cl₂ (12 mL) to give a yellow solution. To this a solution of (*S*)-allyl 3-hydroxy-2-(trimethylphenylamino)propanoate (**138**) (1.00 g, 2.58 mmol, 1 eq.) in CH₂Cl₂ (12 mL) was added dropwise. The reaction was left to stir at 0 °C for 2 h before being allowed to warm to room temperature and left to stir for a further hour.

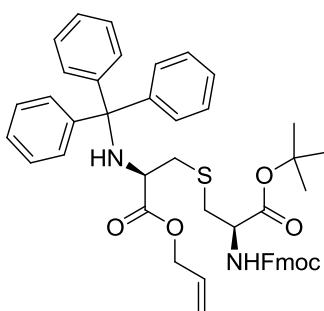
The reaction was then cooled to 0 °C and a solution of (*R*)-*tert*-butyl 2-((9-fluorenylmethoxycarbonyl)amino)-3-mercaptopropanoate (**62**) (0.562 g, 1.41 mmol, 0.7 eq.) in DMF (23 mL) was added. Dry cesium carbonate (0.229 g, 0.703 mmol, 0.35 eq.) was added and the solution turned colourless. The dichloromethane was removed using nitrogen and the reaction was stirred for a further 2 h before the addition of a second portion of cesium carbonate (0.229 g, 0.703 mmol, 0.35 eq.). The reaction was left to stir for 1.5 h before allowing to warm to room temperature. After a further 0.5 h, ethyl acetate (20 mL) was added and the mixture washed with cold citric acid (4 °C, 5% aq. w/v, 3 x 20 mL). The organic layer was dried over Na₂SO₄ and concentrated *in vacuo*. Purification by column chromatography (hexane : ethyl acetate 4 : 1) yielded the title compound as a white solid (0.424 g, 0.551 mmol, 27% over 2 steps).

Method 3



(S)-Allyl 3-hydroxy-2-(trimethylphenylamino)propanoate (**138**) (1.10 g, 2.83 mmol, 1 eq.) was dissolved in dry CH_2Cl_2 (3 mL) at room temperature in the presence of triphenylphosphine (1.114 g, 4.25 mmol, 1.5 eq.). The solution was cooled to $-10\text{ }^\circ\text{C}$ using an acetone/ice/water bath. Diethylazodicarboxylate (0.670 mL, 4.25 mmol, 1.5 eq.) was then added dropwise over the course of 1 min. The reaction was left to stir for 5 min before the addition of methyl iodide (0.260 mL, 4.25 mmol, 1.5 eq.). The reaction was left to stir for a further 3 h before removal of CH_2Cl_2 and excess methyl iodide using nitrogen. The reaction was warmed to $0\text{ }^\circ\text{C}$ and a solution of (*R*)-*tert*-butyl 2-((9-fluorenylmethoxycarbonyl))amino)-3-mercaptopropanoate (**62**) (0.792 g, 1.98 mmol, 0.7 eq.) in DMF (34 mL) was added. A colour change from brown to yellow was observed. Dry cesium carbonate (0.323 g, 0.990 mmol, 0.35 eq.) was added and the reaction stirred for a further 2 h before the addition of a second portion of cesium carbonate (0.323 g, 0.990 mmol, and 0.35 eq.). After a final 2h, ethyl acetate (30 mL) was added and the mixture washed with cold citric acid ($4\text{ }^\circ\text{C}$, 5% aq. w/v, 3 x 30 mL). The organic layer was dried over Na_2SO_4 and concentrated *in vacuo*. Crude NMR showed none of the desired product was formed.

Optimised Synthesis of (*R*)-Allyl 3-((*R*)-2-((9-fluorenylmethoxycarbonyl))amino-3-*tert*-butoxy-3-oxopropylthio)-2-(tritylamino)propanoate **140**



(*R*)-Allyl 3-iodo-2-(trimethylphenylamino)propanoate (1.00 g, 2.01 mmol, 1 eq.) **139** and (*R*)-*tert*-butyl 2-((9-fluorenylmethoxycarbonyl))amino)-3-mercaptopropanoate (**62**) (0.803 mg, 2.01 mmol, 1 eq.) were dissolved in DMF (20 mL) at $4\text{ }^\circ\text{C}$. Dry cesium carbonate (0.328 g, 1.01 mmol, 0.5 eq.) was added and the reaction stirred for 2 h before the addition of a second portion of cesium carbonate (0.328 g, 1.01 mmol, 0.5 eq.). The reaction was left to stir for a further 2 h and then excess ethyl acetate (20 mL) was added and the mixture washed with

cold citric acid (4 °C, 5% aq. w/v, 3 x 20 mL). The organic layer was dried over MgSO₄ and concentrated *in vacuo*. Purification by column chromatography (hexane : ethyl acetate 4 : 1) yielded the title compound as a white solid (0.895 g, 1.16 mmol, 58%).

R_f = 0.4 (hexane : ethyl acetate 4 : 1)

NMR: δ_H (600 MHz CDCl₃) 7.75 (2H, m, Fmoc H_a), 7.60 (2H, m, Fmoc H_d), 7.49 (6H, d, *J* 7.6 Hz, trityl), 7.39 (2H, m, Fmoc H_c), 7.29 (2H, m, Fmoc H_b), 7.24 (6H, t, *J* 7.5 Hz, trityl), 7.17 (3H, t, *J* 7.5 Hz, trityl), 5.70 (1H, ddt, *J* 17.0, 10.7, 7.1 Hz, CH₂CH=CH₂), 5.63 (1H, d, *J* 7.9 Hz, NH), 5.20 (2H, m, CH₂CH=CH₂), 4.49 (1H, m, SCH₂CH α side), 4.35 (2H, m, CH₂Fmoc), 4.21 (1H, t, *J* 7.1 Hz, CHFmoc), 4.14 (1H, dd, *J* 13.1, 7.1 Hz, CHH'CH=CH₂), 3.99 (1H, dd, *J* 13.1, 7.1 Hz, CHH'CH=CH₂), 3.55 (1H, m, SCH₂CH β side), 2.97 (1H, d, *J* 7.4 Hz, SCH₂CH α side), 2.81 (1H, m, SCH₂CH β side), 1.59 (1H, br s, NH), 1.48 (9H, s, *t*Bu).

δ_C (150 MHz CDCl₃) 173.1 (COOtBu), 169.7 (COOFmoc), 155.8 (COOallyl), 145.9 (C-4 trityl), 143.9 (C-1 Fmoc), 141.4 (C-6 Fmoc), 131.8 (CH₂CH=CH₂), 128.9 (trityl), 128.1 (trityl), 127.8 (Fmoc), 127.4 (trityl), 127.2 (Fmoc), 126.7 (trityl), 125.3 (Fmoc), 120.1 (C-5 Fmoc), 118.8 (CH₂CH=CH₂), 83.0 (C*t*Bu), 71.3 (CPh₃), 67.2 (CH₂ Fmoc), 65.9 (CH₂CH=CH₂), 56.6 (CHCOOallyl), 54.4 (CHCOOtBu), 47.2 (CH Fmoc), 38.4 (SCH₂ Fmoc side), 36.1 (SCH₂ trityl side), 28.1 (CH₃).

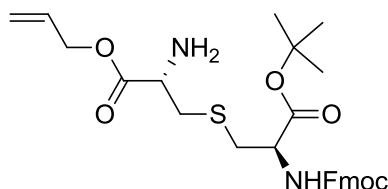
MS: *m/z* (ES⁺) 791.3 ([M+Na]⁺, 10%), 243.1 ([CPh₃]⁺, 100%); HRMS C₄₇H₄₈N₂O₆S ([M+Na]⁺) requires 791.3131, found 791.3148.

ν_{max} (CHCl₃) 3404 (NH stretch, broad), 2978 (CH stretch, broad), 1724 (C=O stretch).

Melting point: 57-59 °C.

$[\alpha]_D^{20}$ +8.0 (c 1.0, CH₃OH).

(*R*)-Allyl 3-((*R*)-2-((9-fluorenylmethoxycarbonyl))amino-3-*tert*-butoxy-3-oxopropylthio)-2-(amino)propanoate 159



A solution of trifluoroacetic acid (1.30 mL) and triethylsilane (2.60 mL) in CH₂Cl₂ (22 mL) was added to (*R*)-allyl 3-((*R*)-2-((9-fluorenylmethoxycarbonyl))amino-3-*tert*-butoxy-3-oxopropylthio)-2-(tritylamino)propanoate **140** (1.30 g, 1.69 mmol) and left to stir at room temperature for 4 h. After this time, CH₂Cl₂ (40 mL) was added and the organic layer was

washed with sodium bicarbonate (2 x 50 mL) and brine (50 mL) before drying over MgSO₄ and concentrating *in vacuo*. The product was then purified by column chromatography (2% MeOH in CH₂Cl₂) to yield the product as a colourless oil (570 mg, 1.08 mmol, 64%).

R_f = 0.25 (2% MeOH in CH₂Cl₂)

NMR: δ_H (600 MHz CDCl₃) 7.76 (2H, m, Fmoc H_a), 7.61 (2H, m, Fmoc H_d), 7.40 (2H, t, *J* 7.4 Hz, Fmoc H_b), 7.31 (2H, t, *J* 7.4 Hz, Fmoc H_c), 6.09 (1H, m, NH), 5.88 (1H, ddt, *J* 17.2, 10.9, 5.7 Hz, CH₂CH=CH₂), 5.28 (2H, m, CH₂CH=CH₂), 4.61 (2H, m, CH₂CH=CH₂), 4.51 (1H, m, CHNH₂), 4.38 (2H, d, *J* 7.1 Hz, CH₂Fmoc), 4.23 (1H, t, *J* 7.1, CHFmoc), 3.71 (1H, m, SCH₂CH β side), 3.02 (3H, m, SCHH'CH α side and SCH₂CH β side), 2.85 (1H, m, SCHH'CH α side), 1.49 (9H, s, tBu).

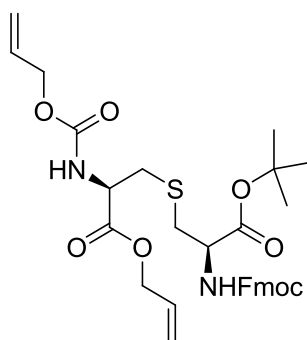
δ_C (150 MHz CDCl₃) 173.0 (COOtBu), 169.5 (COOFmoc), 155.8 (COOallyl), 143.9 (C-1 Fmoc), 141.4 (C-6 Fmoc), 131.5 (CH₂CH=CH₂), 127.9 (C-4 Fmoc), 127.7 (C-3 Fmoc), 125.1 (C-2 Fmoc), 120.0 (C-5 Fmoc), 119.1 (CH₂CH=CH₂), 82.3 (CtBu), 67.1 (CH₂ Fmoc), 66.1 (CH₂CH=CH₂), 54.6 (CHNH₂), 50.1 (CHNHFmoc), 47.1 (CH Fmoc), 37.8 & 35.6 (SCH₂ α and β sides), 28.0 (CH₃).

MS: *m/z* (ES⁺) 527.2 ([M+H]⁺, 85%), 471.2 ([M+H-^tBu]⁺, 100%); HRMS C₂₈H₃₅N₂O₆S ([M+H]⁺) requires 527.2216, found 527.2216.

ν_{max} (CHCl₃) 3347 (NH stretch, broad), 2980 (CH stretch, broad), 1723 (C=O stretch).

$[\alpha]_D^{20}$ -11.0 (c 1.0, CH₃OH).

(*R*)-Allyl 3-((*R*)-2-((9-fluorenylmethoxycarbonyl))amino-3-*tert*-butoxy-3-oxopropylthio)-2-(allyloxycarbonylamino)propanoate 141



Method 1:

A solution of trifluoroacetic acid (0.400 mL) and triethylsilane (0.200 mL) in CH₂Cl₂ (3.40 mL) was added to (*R*)-allyl 3-((*R*)-2-((9-fluorenylmethoxycarbonyl))amino-3-*tert*-butoxy-3-oxopropylthio)-2-(tritylamino)propanoate **140** (200 mg, 0.26 mmol) and left to stir at room temperature for 4 h. After this time, excess CH₂Cl₂ (180 mL) was added and the organic layer

was washed with saturated aqueous sodium bicarbonate (2 x 180 mL) and brine (180 mL) before drying over MgSO_4 and concentrating *in vacuo*.

The product was then re-dissolved in 1,4 dioxane (3.20 mL) and cooled to 0 °C. Allyl chloroformate (0.110 mL, 1.40 mmol, 2 eq.) was added and the reaction was left to stir for 18 h before the addition of excess CH_2Cl_2 (100 mL). The organic layer was washed with saturated sodium bicarbonate (100 mL) and brine (100 mL), dried over MgSO_4 and concentrated *in vacuo* to yield the title product as a colourless oil (26.0 mg, 0.09 mmol, 34%).

Method 2:

Sodium bicarbonate (78.6 mg, 0.940 mmol, 4 eq.) in water (2 mL) was added to a solution of (R)-allyl 3-((R)-2-((9(fluorenylmethoxycarbonyl))amino-3-*tert*-butoxy-3-oxopropylthio)-2-(amino)propanoate **159** (120 mg, 0.230 mmol, 1 eq.) in 1,4-dioxane (2 mL). The reaction was cooled to 0 °C and allyl chloroformate (0.05 mL, 0.44 mmol, 2 eq.) was added. The reaction was left to stir for 18 h before the addition of excess CH_2Cl_2 (100 mL). The organic layer was washed with saturated aqueous sodium bicarbonate (100 mL) and brine (100 mL), dried over MgSO_4 and concentrated *in vacuo* to yield the title product as a colourless oil (156.3 mg, 0.94 mmol, 99%).

NMR: δ_{H} (500 MHz CDCl_3) 7.77 (2H, d, J 7.5 Hz, Fmoc H_a), 7.61 (2H, d, J 7.5 Hz, Fmoc H_d), 7.40 (2H, t, J 7.5 Hz, Fmoc H_b), 7.31 (2H, t, J 7.5 Hz, Fmoc H_c), 5.89 (2H, m, $\text{CH}_2\text{CH}=\text{CH}_2$ allyl and Alloc), 5.64 (1H, m, NH), 5.32 (1H, m, $\text{CH}_2\text{CH}=\text{CHH}'$ allyl), 5.29 (1H, m, $\text{CH}_2\text{CH}=\text{CHH}'$ Alloc), 5.24 (1H, m, $\text{CH}_2\text{CH}=\text{CHH}'$ allyl), 5.19 (1H, m, $\text{CH}_2\text{CH}=\text{CHH}'$ Alloc), 4.64 (2H, d, J 5.7 Hz, $\text{CH}_2\text{CH}=\text{CH}_2$ allyl), 4.57-4.59 (3H, m, CHNH Alloc and $\text{CH}_2\text{CH}=\text{CH}_2$ Alloc), 4.48 (1H, m, CHNH Fmoc), 4.40 (2H, m, CH_2 Fmoc), 4.24 (1H, t, J 7.5 Hz, CH Fmoc), 2.93-3.04 (4H, m, SCH_2CH both sides), 1.48 (9H, s, *t*Bu).

δ_{C} (125 MHz CDCl_3) 170.3 (COOAlloc), 169.5 (COOFmoc), 155.9 (COO*t*Bu), 155.8 (COOallyl), 144.0 (C-1 Fmoc), 141.4 (C-6 Fmoc), 132.6 ($\text{CH}_2\text{CH}=\text{CH}_2$ allyl), 131.4 ($\text{CH}_2\text{CH}=\text{CH}_2$ Alloc), 128.4 (C-3 Fmoc), 127.9 (C-4 Fmoc), 125.3 (C-5 Fmoc), 120.1 (C-2 Fmoc), 119.5 & 118.1 ($\text{CH}_2\text{CH}=\text{CH}_2$ allyl and Alloc), 83.3 (C*t*Bu), 67.3 (CH_2 Fmoc), 66.6 & 66.1 ($\text{CH}_2\text{CH}=\text{CH}_2$ allyl and Alloc), 54.4 (CHNH Fmoc), 53.9 (CHNH Alloc), 47.2 (CH Fmoc), 35.7 & 35.5 (SCH_2 both sides), 28.1 (CH_3).

MS: m/z (ES^+) 633.2 ($[\text{M}+\text{Na}]^+$, 100%), 577.2 ($[\text{M}+\text{Na}-\text{O}^t\text{Bu}]^+$, 50%); HRMS $\text{C}_{32}\text{H}_{38}\text{N}_2\text{O}_8\text{SNa}$ ($[\text{M}+\text{Na}]^+$) requires 633.2247, found 633.2249.

ν_{max} (CHCl_3) 3336 (NH stretch, broad), 2980 (CH stretch, broad), 1714 (C=O stretch).

$[\alpha]_D^{20}$ -27.6 (c 1.0, CH₃OH).

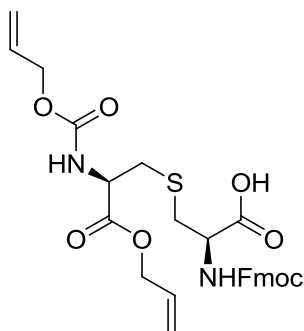
Method 3 (Veders Method):

Tetrabutylammonium bromide (0.287g, 0.889 mmol, 4 eq.) was added to a solution of 0.5M NaHCO₃ in water (2 mL). The solution was left to stir for 5 min before transfer to a solution of (*R*)-allyl 2-(allyloxycarbonylamino)-3-bromopropanoate **153** (0.065 g, 0.223 mmol, 1 eq.) and (*R*)-*tert*-butyl 2-((9(fluorenylmethoxycarbonyl))amino)-3-mercaptopropanoate (**62**) (94.0 mg, 0.223 mmol, 1 eq.) in ethyl acetate (2 mL). The biphasic mixture was left to stir vigorously for 48 h at room temperature before separation of the organic layer, which was washed with water (2 mL), dried (MgSO₄) and concentrated *in vacuo*. Purification by column chromatography (hexane : ethyl acetate 5:1) yielded the product as a colourless oil (60.0 mg, 0.099 mmol, 44%) and as an inseparable mixture of diastereoisomers **141** (Major, M) and **154** (minor, m) in the ratio M : m of 76 : 23.

NMR: δ H (600 MHz CDCl₃ diastereoisomers) 7.77 (2H, d, *J* 7.5 Hz, M Fmoc H_a), 7.74 (2H, d, *J* 7.5 Hz, M Fmoc H_a), 7.61 (2H, d, *J* 7.5 Hz, M Fmoc H_d), 7.58 (2H, d, *J* 7.5 Hz, m Fmoc H_d), 7.40 (2H, t, *J* 7.5 Hz, M Fmoc H_b), 7.37 (2H, m, m Fmoc H_b), 7.31 (2H, t, *J* 7.5 Hz, M Fmoc H_c), 7.28 (2H, m, m Fmoc H_c), 5.89 (4H, m, CH₂CH=CH₂, M and m, allyl and Alloc), 5.74 (2H, d, *J* 7.5, M and m, NH), 5.65 (2H, t, *J* 7.1, M and m, NH), 5.17 – 5.34 (8H, m, M and m, CH₂CH=CH₂ allyl and Alloc), 4.64 (4H, d, *J* 5.5, M and m, CH₂CH=CH₂ allyl), 4.55 – 4.62 (6H, m, M and m, CHNH Alloc and CH₂CH=CH₂ Alloc), 4.46-4.51 (2H, m, M and m, CHNH Fmoc), 4.34-4.44 (2H, m, M and m, CH₂ Fmoc), 4.24 (1H, t, *J* 7.1 Hz, M CH Fmoc), 4.19 (1H, t, *J* 7.3 Hz, M CH Fmoc), 2.94-3.24 (8H, m, M and m, SCH₂CH both sides), 1.49 (9H, s, M *t*Bu), 1.48 (9H, s, m *t*Bu).

δ C (125 MHz CDCl₃ diastereoisomers) 170.3 (M and m, COOAlloc), 169.51 (M COOFmoc), 169.46 (m COOFmoc), 155.9 (M and m, COO*t*Bu), 155.8 (M and m, COOallyl), 144.0 and 143.9 (M and m, C-1 Fmoc), 141.41 and 141.37 (M and m, C-6 Fmoc), 132.6 (M and m, CH₂CH=CH₂ allyl), 131.3 (M and m, CH₂CH=CH₂ Alloc), 128.1 (M C-3 Fmoc), 127.8 (m C-3 Fmoc), 127.2 (M and m, C-4 Fmoc), 125.28 (m C-5 Fmoc), 125.25 (M C-5 Fmoc), 120.11 (M C₂ Fmoc), 120.08 (m C-2 Fmoc), 119.4 & 118.1 (M and m, CH₂CH=CH₂ allyl and Alloc), 83.3 (M and m, C*t*Bu), 67.32 (m, CH₂ Fmoc), 67.27 (M CH₂ Fmoc), 66.60, 66.58 & 66.1 (M and m, CH₂CH=CH₂ allyl and Alloc), 54.4 and 54.2 (M and m, CHNH Fmoc), 54.0 and 53.9 (M and m, CHNH Alloc), 47.21 and 47.17 (M and m, CH Fmoc), 36.0, 35.9, 35.7 & 35.5 (M and m, SCH₂ both sides), 28.1 (M and m, CH₃).

(R)-Allyl 3-((R)-2-((9(fluorenylmethoxycarbonyl))amino-3-*tert*-butoxy-3-oxopropylthio)-2-(allyloxycarbonylamino)propanoic acid **142**



Method 1:

(R)-allyl 3-((R)-2-((9(fluorenylmethoxycarbonyl))amino-3-*tert*-butoxy-3-oxopropylthio)-2-(allyloxycarbonylamino)propanoate **141** (156 mg, 0.260 mmol) was dissolved in a solution of trifluoroacetic acid (0.3 mL) and CH₂Cl₂ (0.3 mL) and stirred for 3 h before concentrating *in vacuo*. Removal of trifluoroacetic acid was aided by the addition of toluene (20 mL). Purification was carried out by reverse phase column chromatography (40% acetonitrile in 20% NaHCO₃ aq. solution, R_f = 0.2).

The acetonitrile was then removed *in vacuo* and concentrated hydrochloric acid was added to bring the aqueous layer to pH 2. Sodium chloride was then added until the solution was saturated and the product was extracted with chloroform (5 x 80 mL). The organic layer was dried over MgSO₄ and concentrated *in vacuo* to yield the title product as a colourless oil (100 mg, 0.18 mmol, 71 %).

Method 2:

(R)-allyl 3-((R)-2-((9(fluorenylmethoxycarbonyl))amino-3-*tert*-butoxy-3-oxopropylthio)-2-(allyloxycarbonylamino)propanoate **141** (180 mg, 0.284 mmol, 1 eq.) was dissolved in a solution of trifluoroacetic acid (1.5 mL), triethylsilane (0.045 mL, 0.284 mmol, 1 eq.) and CH₂Cl₂ (1.5 mL) and stirred for 2 h before concentrating *in vacuo*. Removal of trifluoroacetic acid was aided by the addition of toluene (20 mL). The product was then re-dissolved in toluene whilst heating and left in the freezer for 24 h. After this time, the toluene was decanted off to give the product as a white solid (120 mg, 0.217 mmol, 76 %).

NMR: δ_H (600 MHz CDCl₃) 9.40 (1H, br s, COOH), 7.75 (2H, m, Fmoc H_a) 7.56 (2H, m, Fmoc H_d), 7.38 (2H, m, Fmoc H_b), 7.30 (2H, t, *J* 7.4, Fmoc H_c), 6.86 (1H, d, *J* 6.9, NH Alloc), 5.97 (1H, d, *J* 7.3, NH Fmoc), 5.79-5.89 (2H, m, CH₂CH=CH₂ allyl and Alloc), 5.16-5.35 (4H, m, CH₂CH=CH₂ allyl and Alloc), 4.60-4.63 (2H, m, SCH₂CH both sides), 4.53-4.58 (4H, m, CH₂CH=CH₂ allyl and

Alloc), 4.39 (2H, m, CH₂Fmoc), 4.22 (1H, t, *J* 6.8 CHFmoc), 2.98-3.14 (4H, m, SCH₂CH both sides).

δ_c (150 MHz CDCl₃) 173.8 (COOAlloc), 170.4 (COOFmoc), 157.6 (COOH), 156.2 (COOallyl), 143.8 (C-6 Fmoc), 141.4 (C-1 Fmoc), 132.4 (CH₂CH=CH₂ allyl), 131.3 (CH₂CH=CH₂ Alloc), 127.9 (C-3 Fmoc), 127.2 (C-4 Fmoc), 125.3 (C-5 Fmoc), 120.1 (C-2 Fmoc), 119.5 (CH₂CH=CH₂ allyl), 118.3 (CH₂CH=CH₂ Alloc), 67.7 (CH₂ Fmoc), 66.7 (CH₂CH=CH₂ allyl), 66.2 (CH₂CH=CH₂ Alloc), 54.5 (CHNHFmoc), 53.8 (CHNHAlloc), 47.2 (CH Fmoc), 35.2 & 35.0 (SCH₂ both sides).

MS: *m/z* (ES⁺) 577.2 ([M+Na]⁺, 100%); HRMS C₂₈H₃₀N₂O₈Na ([M+Na]⁺) requires 577.1621, found 577.1613.

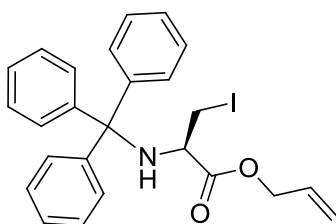
ν_{max} (CHCl₃) 3320 (NH stretch, broad), 2950 (OH stretch, broad), 1710 (C=O stretch, broad), 1515 (C-N amide bend).

$[\alpha]_D^{25}$ -19.0 (c 1.0, CH₃OH).

7.2.3 Experimental for Large Scale Synthesis

Large scale synthesis was carried out at the European Knowledge Centre of Eisai Ltd. in Hatfield, UK. Preparation of trityl allyl serine (**138**) and doubly protected cystine (**135**) was outsourced to Oxygen Healthcare, Cambridge, UK, which is part of Piramal Enterprises Ltd, Mumbai, India, who produced 100 g of each compound following the procedures developed during the small scale investigations.

***(R)*-Allyl 3-iodo-2-(trimethylphenylamino)propanoate 139**



Medium Scale:

(S)-allyl 3-hydroxy-2-(trimethylphenylamino)propanoate (**138**) (10.0 g, 25.8 mmol, 1 eq.) was dissolved in dry CH₂Cl₂ (16 mL) at room temperature in the presence of triphenylphosphine (10.2 g, 38.7 mmol, 1.5 eq.). The solution was cooled to -10 °C using an acetone/ice/water bath. The temperature was monitored throughout the reaction by the presence of a thermometer within the reaction vessel. Diethylazodicarboxylate (6.10 mL, 38.7 mmol, 1.5 eq.) in CH₂Cl₂ (5 mL) was then added dropwise over 30 min, ensuring the internal temperature did not exceed 12 °C. The reaction was left for 5 min before the addition of methyl iodide over 5 min (2.41 mL, 38.7 mmol, 1.5 eq.). The reaction was left to stir for a

further 3 h at -10 °C and then purified directly by column chromatography (Biotage KP-SIL 340 g snap column, 0 – 50% ethyl acetate in hexane over 15 column volumes) to yield the product as a pale yellow viscous oil (8.36 g, 16.8 mmol, 65%).

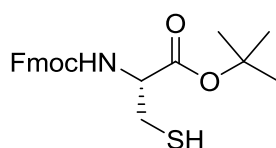
Large Scale:

(S)-allyl 3-hydroxy-2-(trimethylphenylamino)propanoate (**138**) (30.0 g, 77.4 mmol, 1 eq.) was dissolved in dry CH₂Cl₂ (66 mL) at room temperature in the presence of triphenylphosphine (30.5 g, 116.1 mmol, 1.5 eq.). The solution was cooled to -10 °C using an acetone/ice/water bath. The temperature was monitored throughout the reaction by the presence of a thermometer within the reaction vessel. Diethylazodicarboxylate (18.3 mL, 116 mmol, 1.5 eq.) in CH₂Cl₂ (20 mL) was then added dropwise over 45 min, ensuring the temperature did not exceed 12 °C. The reaction was left for 5 min before the addition of methyl iodide over 5 min (7.20 mL, 116 mmol, 1.5 eq.) in CH₂Cl₂ (10 mL). The reaction was left to stir for a further 3 h and then purified directly by column chromatography (Biotage KP-SIL 340 g snap column, 0 – 50% ethyl acetate in hexane over 15 column volumes) to yield the product as a pale yellow viscous oil (18.1 g, 36.4 mmol, 47%).

NMR: δ_H (400 MHz CDCl₃) 7.50 (6H, m, trityl) 7.27 (9H, m, trityl), 5.77 (1H, ddt, J 17.2, 10.5, 6.0 Hz, CH₂CH=CH₂), 5.22 (2H, m, CH₂CH=CH₂), 4.27 (1H, dddd, J 13.0, 6.0, 1.5, 1.2 Hz, CHH'CH=CH₂), 4.13 (1H, dddd, J 13.0, 6.0, 1.5, 1.2 Hz, CHH'CH=CH₂), 3.54 (1H, m, CHCH₂I), 3.35 (1H, dd, J 9.8, 3.5 Hz, CHCHH'I), 3.23 (1H, dd, J 9.8, 6.0 Hz, CHCHH'I), 2.92 (1H, d, J 9.8 Hz, NH).

Spectroscopic data obtained is identical to that obtained from the small scale reaction.

(R)-tert-butyl 2-((9(fluorenylmethoxycarbonyl))amino)-3-mercaptopropanoate (62)



Medium Scale:

Dithiothreitol (2.90 g, 18.8 mmol, 1.5 eq.) was added to a stirred solution of (2R,2'R)-tert-butyl 3,3'-disulfanediyldis(2-(9(fluorenylmethoxycarbonyl))aminopropanoate) (**135**) (10.0 g, 12.5 mmol, 1 eq.) in dry CH₂Cl₂ (150 mL). To this, triethylamine (2.62 mL, 18.8 mmol, 1.5 eq.) was added and the solution was left to stir for 1 h. The solution was then washed with sodium bicarbonate (2 x 100 mL) and water (2 x 100 mL), dried (MgSO₄) and concentrated *in vacuo* to yield the product as a colourless oil (9.51 g, 23.8 mmol, 95%).

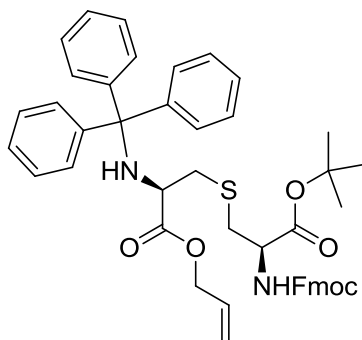
Large Scale:

Dithiothreitol (8.71 g, 56.5 mmol, 1.5 eq.) was added to a stirred solution of (2*R*,2'*R*)-*tert*-butyl 3,3'-disulfanediylbis(2-(9(fluorenylmethoxycarbonyl))aminopropanoate) (**135**) (30.0 g, 37.6 mmol, 1 eq.) in dry CH₂Cl₂ (450 mL). To this, triethylamine (7.90 mL, 56.5 mmol, 1.5 eq.) was added and the solution was left to stir for 1 h. The solution was then washed with sodium bicarbonate (2 x 400 mL) and water (2 x 400 mL), dried (MgSO₄) and concentrated *in vacuo* to yield the product as a colourless oil (28.7 g, 71.9 mmol, 95%).

NMR: δ_{H} (600 MHz CDCl₃) 7.77 (2H, d, *J* 7.4 Hz, Fmoc H_a) 7.62 (2H, d, *J* 7.4 Hz, Fmoc H_d), 7.41 (2H, t, *J* 7.4 Hz, Fmoc H_b), 7.33 (2H, t, *J* 7.4 Hz, Fmoc H_c) 5.76 (1H, d, *J* 7.2 Hz, NH), 4.56 (1H, m, SCH₂CH), 4.41 (2H, d, *J* 6.9 Hz, CH₂Fmoc), 4.24 (1H, t, *J* 6.9 Hz, CHFmoc), 3.00 (2H, m, SCH₂CH), 1.51 (9H, s, *t*Bu).

Spectroscopic data obtained is identical to that obtained from the small scale reaction.

(R)-Allyl 3-((R)-2-((9-fluorenylmethoxycarbonyl))amino-3-tert-butoxy-3-oxopropylthio)-2-(tritylamino)propanoate 140



Medium Scale:

(R)-allyl 3-iodo-2-(trimethylphenylamino)propanoate (7.36 g, 14.8 mmol, 1 eq.) **139** and (R)-tert-butyl 2-((9-fluorenylmethoxycarbonyl))amino-3-mercaptopropanoate (**62**) (5.91 g, 14.8 mmol, 1 eq.) were dissolved in DMF (140 mL) at 4 °C. Dry cesium carbonate (2.41 g, 7.39 mmol, 0.5 eq.) was added and the reaction stirred for 2 h before the addition of a second portion of cesium carbonate (2.41 g, 7.39 mmol, 0.5 eq.). The reaction was left to stir for a further 2 h before ethyl acetate (140 mL) was added and the mixture washed with cold citric acid (4 °C, 5% aq. w/v, 3 x 140 mL). The organic layer was dried over MgSO₄ and concentrated *in vacuo*. Purification by column chromatography (Biotage KP-SIL 340 g snap column, 0 – 50% ethyl acetate in hexane over 15 column volumes) yielded the title compound as a white solid (6.84 g, 8.90 mmol, 61%).

Large Scale:

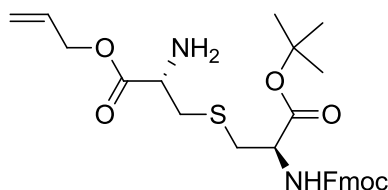
(R)-allyl 3-iodo-2-(trimethylphenylamino)propanoate (18.1 g, 36.4 mmol, 1 eq.) **139** and (R)-tert-butyl 2-((9-fluorenylmethoxycarbonyl))amino-3-mercaptopropanoate (**62**) (14.5 g, 36.4 mmol, 1 eq.) were dissolved in DMF (300 mL) at 4 °C. Dry cesium carbonate (5.95 g, 18.2 mmol, 0.5 eq.) was added and the reaction stirred for 2 h before the addition of a second portion of cesium carbonate (5.95 g, 18.2 mmol, 0.5 eq.). The reaction was left to stir for a further 2 h and then excess ethyl acetate (250 mL) was added and the mixture washed with cold citric acid (4 °C, 5% aq. w/v, 3 x 250 mL). The organic layer was dried over MgSO₄ and concentrated *in vacuo*. Purification by column chromatography (Biotage KP-SIL 340 g snap column, 0 – 50% ethyl acetate in hexane over 15 column volumes) yielded the title compound as a white solid (13.5 g, 17.6 mmol, 48%).

NMR: δ_H (600 MHz CDCl₃) 7.75 (2H, m, Fmoc H_a), 7.60 (2H, m, Fmoc H_d), 7.49 (6H, d, *J* 7.6 Hz, trityl), 7.39 (2H, m, Fmoc H_c), 7.29 (2H, m, Fmoc H_b), 7.24 (6H, t, *J* 7.5 Hz, trityl), 7.17 (3H, t, *J* 7.5 Hz, trityl), 5.70 (1H, ddt, *J* 17.0, 10.7, 7.1 Hz, CH₂CH=CH₂), 5.63 (1H, d, *J* 7.9 Hz, NH),

5.20 (2H, m, CH₂CH=CH₂), 4.49 (1H, m, SCH₂CH α side), 4.35 (2H, m, CH₂Fmoc), 4.21 (1H, t, *J* 7.1 Hz, CHFmoc), 4.14 (1H, dd, *J* 13.1, 7.1 Hz, CHH'CH=CH₂), 3.99 (1H, dd, *J* 13.1, 7.1 Hz, CHH'CH=CH₂), 3.55 (1H, m, SCH₂CH β side), 2.97 (1H, d, *J* 7.4 Hz, SCH₂CH α side), 2.81 (1H, m, SCH₂CH β side), 1.59 (1H, br s, NH), 1.48 (9H, s, *t*Bu).

Spectroscopic data obtained is identical to that obtained from the small scale reaction.

(R)*-Allyl 3-((*R*)-2-((9(*fluorenylmethoxycarbonyl*))amino-3-*tert*-butoxy-3-oxopropylthio)-2-(amino)propanoate **159*



Medium Scale:

A solution of trifluoroacetic acid (9.82 mL, 127 mmol, 10 eq.) in CH₂Cl₂ (20 mL) was added to a stirred solution of triethylsilane (20.4 mL, 127.4 mmol, 10 eq.) and (*R*)-allyl 3-((*R*)-2-((9(*fluorenylmethoxycarbonyl*))amino-3-*tert*-butoxy-3-oxopropylthio)-2-(tritylamino)propanoate **140** (9.80 g, 12.7 mmol, 1 eq.) in CH₂Cl₂ (80 mL) at 4 °C. The internal temperature was maintained at 20 °C throughout the addition. Once addition was complete, the ice bath was removed and the reaction was left to stir at room temperature for 4 h. After this time, excess CH₂Cl₂ (100 mL) was added and the organic layer was washed with sodium bicarbonate (2 x 100 mL) and brine (100 mL) before being dried over MgSO₄ and concentrated *in vacuo*. The product was then purified by column chromatography (Biotage KP-NH 375 g snap column, 20 – 80% ethyl acetate in hexane over 10 column volumes) to yield the product as a colourless oil (2.92 g, 5.54 mmol, 44%).

Large Scale:

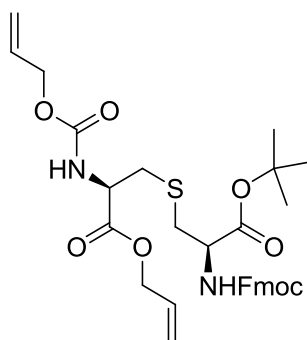
A solution of trifluoroacetic acid (20.4 mL, 265 mmol, 10 eq.) in CH₂Cl₂ (50 mL) was added to a stirred solution of triethylsilane (42.2 mL, 265 mmol, 10 eq.) and (*R*)-allyl 3-((*R*)-2-((9(*fluorenylmethoxycarbonyl*))amino-3-*tert*-butoxy-3-oxopropylthio)-2-(tritylamino)propanoate **140** (20.3 g, 26.5 mmol, 1 eq.) in CH₂Cl₂ (150 mL) on ice. The temperature inside the reaction vessel was maintained at 20 °C throughout the addition. The temperature was monitored throughout the reaction by the presence of a thermometer within the reaction vessel. Once addition was complete, the ice bath was removed and the reaction was left to stir at room temperature for 4 h. After this time, excess CH₂Cl₂ (200 mL) was added and the organic layer was washed with sodium bicarbonate (2 x 200 mL) and brine

(200 mL) before being dried over MgSO_4 and concentrated *in vacuo*. The product was then purified by column chromatography (Biotage KP-NH 375 g snap column, 20 – 80% ethyl acetate in hexane over 10 column volumes) to yield the product as a colourless oil (7.61 g, 14.5 mmol, 55%).

NMR: δ_{H} (600 MHz CDCl_3) 7.76 (2H, m, Fmoc H_a) 7.61 (2H, m, Fmoc H_d), 7.40 (2H, t, J 7.4 Hz, Fmoc H_b), 7.31 (2H, t, J 7.4 Hz, Fmoc H_c), 6.09 (1H, m, NH), 5.88 (1H, ddt, J 17.2, 10.9, 5.7 Hz, $\text{CH}_2\text{CH}=\text{CH}_2$), 5.28 (2H, m, $\text{CH}_2\text{CH}=\text{CH}_2$), 4.61 (2H, m, $\text{CH}_2\text{CH}=\text{CH}_2$), 4.51 (1H, m, CHNH_2), 4.38 (2H, d, J 7.1 Hz, CH_2Fmoc), 4.23 (1H, t, J 7.1, CHFmoc), 3.71 (1H, m, SCH_2CH β side), 3.02 (3H, m, $\text{SCHH}'\text{CH}$ α side and SCH_2CH β side), 2.85 (1H, m, $\text{SCHH}'\text{CH}$ α side), 1.49 (9H, s, tBu).

Spectroscopic data obtained is identical to that obtained from the small scale reaction.

(*R*)-Allyl 3-((*R*)-2-((9-fluorenylmethoxycarbonyl))amino-3-*tert*-butoxy-3-oxopropylthio)-2-(allyloxycarbonylamino)propanoate 141



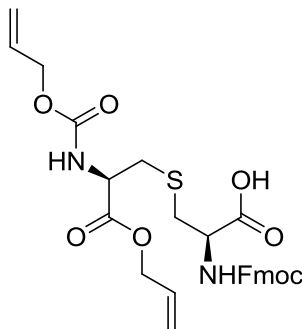
Sodium bicarbonate (6.68 g, 39.8 mmol, 4 eq.) was added to a solution of (*R*)-allyl 3-((*R*)-2-((9-fluorenylmethoxycarbonyl))amino-3-*tert*-butoxy-3-oxopropylthio)-2-(amino)propanoate **159** (10.5 g, 19.9 mmol, 1 eq.) in 1,4-dioxane (120 mL). The reaction was cooled to 0 °C and allyl chloroformate (4.24 mL, 39.8 mmol, 2 eq.) was added. The reaction was left to stir for 18 h before the addition of excess CH_2Cl_2 (250 mL). The organic layer was washed with saturated aqueous sodium bicarbonate (2 x 150 mL) and brine (150 mL), dried over MgSO_4 and concentrated *in vacuo* to yield the title product as a colourless oil (10.3 g, 16.9 mmol, 85%).

NMR: δ_{H} (500 MHz CDCl_3) 7.77 (2H, d, J 7.5 Hz, Fmoc H_a) 7.61 (2H, d, J 7.5 Hz, Fmoc H_d), 7.40 (2H, t, J 7.5 Hz, Fmoc H_b), 7.31 (2H, t, J 7.5 Hz, Fmoc H_c), 5.89 (2H, m, $\text{CH}_2\text{CH}=\text{CH}_2$ allyl and Alloc), 5.64 (1H, m, NH), 5.32 (1H, m, $\text{CH}_2\text{CH}=\text{CHH}'$ allyl), 5.29 (1H, m, $\text{CH}_2\text{CH}=\text{CHH}'$ Alloc), 5.24 (1H, m, $\text{CH}_2\text{CH}=\text{CHH}'$ allyl), 5.19 (1H, m, $\text{CH}_2\text{CH}=\text{CHH}'$ Alloc), 4.64 (2H, d, J 5.7 Hz, $\text{CH}_2\text{CH}=\text{CH}_2$ allyl), 4.57-4.59 (3H, m, CHNH Alloc and $\text{CH}_2\text{CH}=\text{CH}_2$ Alloc), 4.48 (1H, m, CHNH

Fmoc), 4.40 (2H, m, CH_2 Fmoc), 4.24 (1H, t, J 7.5 Hz, CH Fmoc), 2.93-3.04 (4H, m, SCH_2CH both sides), 1.48 (9H, s, $t\text{Bu}$).

Spectroscopic data obtained is identical to that obtained from the small scale reaction.

(*R*)-Allyl 3-((*R*)-2-((9-fluorenylmethoxycarbonyl))amino-3-*tert*-butoxy-3-oxopropylthio)-2-(allyloxycarbonylamino)propanoic acid **142**



(*R*)-allyl 3-((*R*)-2-((9-fluorenylmethoxycarbonyl))amino-3-*tert*-butoxy-3-oxopropylthio)-2-(allyloxycarbonylamino)propanoate **141** (5.00 g, 8.19 mmol, 1 eq.) was dissolved in a solution of trifluoroacetic acid (50 mL, 650 mmol, 79 eq.), triethylsilane (1.31 mL, 8.19 mmol, 1 eq.) and CH_2Cl_2 (50 mL) and stirred for 2 h before concentrating *in vacuo*. Removal of trifluoroacetic acid was aided by the addition of toluene (20 mL). The product was then re-dissolved in toluene (50 mL) with heating and then left in the freezer for 72 h. After this time, the toluene was decanted off to give the product as a white solid. The filtrate was concentrated and recrystallised for a second time. The solid was filtered and combined with the previous crystallisation to afford the desired product as a white solid (3.00 g, 5.42 mmol, 66%).

NMR: δ_{H} (600 MHz CDCl_3) 9.40 (1H, br s, COOH), 7.75 (2H, m, H_a), 7.56 (2H, m, H_d), 7.38 (2H, m, H_b), 7.30 (2H, t, J 7.4, H_c), 6.86 (1H, d, J 6.9, NH), 5.97 (1H, d, J 7.3, NH Fmoc), 5.79-5.89 (2H, m, $\text{CH}_2\text{CH}=\text{CH}_2$ allyl and Alloc), 5.16-5.35 (4H, m, $\text{CH}_2\text{CH}=\text{CH}_2$ allyl and Alloc), 4.60-4.63 (2H, m, SCH_2CH both sides), 4.53-4.58 (4H, m, $\text{CH}_2\text{CH}=\text{CH}_2$ allyl and Alloc), 4.39 (2H, m, CH_2Fmoc), 4.22 (1H, t, J 6.8 CHFmoc), 2.98-3.14 (4H, m, SCH_2CH both sides).

Spectroscopic data obtained is identical to that obtained from the small scale reaction.

7.3 Experimental for Peptide Synthesis (Chapter 3)

7.3.1 General Experimental for Peptide Synthesis

The peptides were either synthesised using a peptide synthesiser or by hand using the same timings and solution volumes. Microwave couplings were carried out using a Personal Chemistry Smith Creator microwave loaded with 5 mL reaction vials. In all cases, the vial was

irradiated for 5 min at 60 °C before transfer of the resin back to the reaction syringe. DMF was used as the primary solvent throughout the peptide synthesis.

Peptides were centrifuged using an Eppendorf Centrifuge, model 5810R and were lyophilised using a Thermo Scientific Heto PowerDry LL1500 freeze-dryer. Peptides were agitated using an IKA KS130 basic platform shaker.

Method 1: Automated Peptide Synthesis

Peptides were synthesised on a MultiSynTech Syro Peptide Synthesiser (Model MP-60). The peptide synthesiser contains an agitation block capable of holding 2 mL and 5 mL syringes with frits, connected to a vacuum pump to remove solutions. Amino acid and reagent concentrations were calculated based on the quantity and loading of the resin. The total volume of all reagents in each step was 1.5 mL. All reagents were dissolved in HPLC grade DMF.

Fmoc Deprotection: All Fmoc deprotections were carried out using a solution of 40% piperidine in DMF, which was added to the syringe containing the resin. The mixture was agitated for 20 sec every minute for a total of 3 min before removal of reagent by filtration under vacuum. The resin was washed with DMF (4 x 1.5 mL) before addition of a second portion of piperidine in DMF solution (40% v/v, 0.75 mL), followed by DMF (0.75 mL) to make an overall 20% v/v solution of piperidine in DMF. This mixture was agitated for 20 sec every minute for a total of 10 min. The reagents were removed by filtration under vacuum and the resin washed with DMF (6 x 1.5 mL).

Amino Acid Coupling: Fmoc-protected amino acid (4 eq.) was added to the reaction syringe with HBTU (4 eq.) and DIPEA (8 eq.). The mixture was agitated for 20 sec every 3 min for a total of 40 min. The reagents were removed by filtration under vacuum and the resin washed with DMF (4 x 1.5 mL).

Lanthionine Coupling: (S)-allyl 3-((S)-2-((9(flourenylmethoxycarbonyl))amino-3-*tert*-butoxy-3-oxopropylthio)-2-(allyloxycarbonylamino)propanoic acid **142** (3 eq.), PyAOP (5 eq.) and HOAt (5 eq.) were dissolved in DMF (4 mL). To this, *N,N*-diisopropylethylamine (10 eq.) was added and left to react for 1 min before addition to a microwave vial containing the resin. The vial was irradiated for 5 min at 60 °C before transfer of the resin back to the reaction syringe. The resin was then washed with DMF (4 x 1.5 mL).

Allyl/Alloc Deprotection: Simultaneous deprotection of both the allyl and Alloc ester groups was performed using tetrakis(triphenyl)phosphine palladium (0) (1 eq.) and 1,3-

dimethylbarbituric acid (10 eq.) in a 1 : 1 solution of chloroform : DMF (2 mL). This was left to react for 2 h in the dark under argon before removal of the solution by filtration. The resin was then washed with CH₂Cl₂ (10 x 1.5 mL), sodium diethyldithiocarbamate (5 % w/v, 15 x 1.5 mL) and DMF (10 x 1.5 mL).

Lanthionine Cyclisation: *N,N*-diisopropylethylamine (10 eq.) was added to a solution of PyAOP (5 eq.) and HOAt (5 eq.) in DMF (4 mL). The solution was left to react for 1 min before addition to a microwave vial containing the resin. The vial was irradiated for 5 min at 60 °C before transfer of the resin back to the reaction syringe. The resin was then washed with DMF (4 x 1.5 mL).

Method 2: Manual Peptide Synthesis

Manual peptide synthesis was carried out using an IKA KS130 basic platform shaker to agitate the solutions. Reactions were carried out in 5 mL syringes with frits, which were evacuated by hand at the end of each reaction. Amino acid and reagent concentrations were calculated based on the quantity and loading of the resin. The total volume of all reagents in each step was 1.5 mL. All reagents were dissolved in HPLC grade DMF.

Fmoc Deprotection: All Fmoc deprotections were carried out using a solution of 40% piperidine in DMF, which was added to the syringe containing the resin. The mixture was agitated for 3 min before removal of reagent by filtration. A second portion of piperidine in DMF solution (40% v/v, 0.75 mL) was added, followed by DMF (0.75 mL) to make an overall 20% v/v solution of piperidine in DMF. This mixture was agitated for a total of 10 min. The reagents were removed by filtration and the resin washed with DMF (6 x 1.5 mL).

Amino Acid Coupling: Fmoc-protected amino acid (0.6 mL, 4 eq.) was added to the reaction syringe with HBTU (0.6 mL, 4 eq.) and DIPEA (0.3 mL, 8 eq.). The mixture was agitated for a total of 40 min. The reagents were removed by filtration and the resin washed with DMF (4 x 1.5 mL).

Lanthionine Coupling: (*S*)-allyl 3-((*S*)-2-((9-fluorenylmethoxycarbonyl))amino-3-*tert*-butoxy-3-oxopropylthio)-2-(allyloxycarbonylamino)propanoic acid **142** (3 eq.), PyAOP (5 eq.) and HOAt (5 eq.) were dissolved in DMF (4 mL). To this, *N,N*-diisopropylethylamine (10 eq.) was added and left to react for 1 min before addition to a microwave vial containing the resin. The vial was irradiated for 5 min at 60 °C before transfer of the resin back to the reaction syringe. The resin was then washed with DMF (4 x 1.5 mL).

Allyl/Alloc Deprotection: Simultaneous deprotection of both the allyl and Alloc ester groups was performed using tetrakis(triphenylphosphine) palladium (0) (1 eq.) and 1,3-dimethylbarbituric acid (10 eq.) in a 1 : 1 solution of chloroform : DMF (2 mL). This was left to react for 2 h in the dark under argon before removal of the solution by filtration. The resin was then washed with CH₂Cl₂ (10 x 1.5 mL), sodium diethyldithiocarbamate (5% w/v, 15 x 1.5 mL) and DMF (10 x 1.5 mL).

Lanthionine Cyclisation: *N,N*-diisopropylethylamine (10 eq.) was added to a solution of PyAOP (5 eq.) and HOAt (5 eq.) in DMF (4 mL). The solution was left to react for 1 min before addition to a microwave vial containing the resin. The vial was irradiated for 5 min at 60 °C before transfer of the resin back to the reaction syringe. The resin was then washed with DMF (4 x 1.5 mL).

Cleavage and Purification

Cleavage and purification procedures were the same for both peptides made manually and those made using the peptide synthesiser.

Cleavage from the Resin: Peptides were first washed with DMF (4 x 1.5 mL), CH₂Cl₂ (4 x 1.5 mL), methanol (4 x 1.5 mL) and diethyl ether (4 x 1.5 mL) before drying in a desiccator for 45 min. A solution of 94% TFA, 2.5% water, 2.5% EDT and 1% TIPS (2.5 mL) was then added to the resin and left to agitate for 30 min on the platform shaker. After this time, the entire solution was transferred to a Falcon tube and 12 mL of diethyl ether was added to precipitate the peptide. The cleavage procedure was then repeated with fresh cleavage solution (2.5 mL containing 94% TFA, 2.5% water, 2.5% EDT and 1% TIPS) and left to agitate for a further 40 min. The entire solution was again transferred to a Falcon tube before addition of 12 mL of diethyl ether to precipitate the peptide.

The Falcon tubes were then centrifuged for 10 min at 4000 rpm and 4 °C before decanting off the diethyl ether solution. This process was performed 3 times in total before re-dissolving the peptide in water and lyophilising.

HPLC Purification: The peptides were analysed and purified *via* reverse phase HPLC using either a Varian ProStar system with a Model 210 solvent delivery module and a Model 320 UV detector or a Dionex system with a PDA-100 photodiode array detector and a model ASI-100 automated sample injector. The preparative purification was performed using an ACE C8-300 semi-preparative column (150 x 10 mm, flow rate of 8.0 mL/min), with UV detection at 215 and 254 nm, loaded with 200 – 1850 µL aliquots of a 10-20 mg/mL solution of peptide dissolved in water.

The mobile phase was a decreasing gradient of water in acetonitrile. Exact gradients have been reported for each peptide. The fractions containing the correct peak were pooled, the solvent removed under reduced pressure to approximately 2 mL and the solution freeze-dried.

Analysis

HPLC Analysis: The purified peptide was analysed by analytical HPLC using an ACE C8-300 analytical column (150 x 10 mm, flow rate of 1.0 mL/min), with UV detection at 215 and 254 nm. Linear gradient: 2 – 98% B over 20 min (A = water, B = acetonitrile). The analysis of the chromatograms was conducted using Chromeleon Software version 2.0.

ESI-MS analysis: This was performed on a Waters Acquity Ultra Performance LC/MS machine using a linear gradient of 5 – 95% B over 5 min (A = water, B = acetonitrile, 0.1% TFA). The analysis of the chromatograms was conducted using MassLynx software version 4.0.

Disulfide Bond Cyclisation: Peptides were dissolved in pure water (concentration = 0.1 mg/mL) and left to stir at 4 °C for 7 – 10 days before concentrating down to approximately 2 mL. The solution was then flash frozen and lyophilised to yield the cyclised peptide as a white solid.

7.3.2 Synthesis of ProTX-II and Disulfide Analogues

ProTX-II (22)



The reaction was carried out on a 100 mg scale using pre-loaded Fmoc-Trp(Boc)-NovaSyn® TGT resin resin (loading = 0.20 mmol/g) and using the amounts listed below:

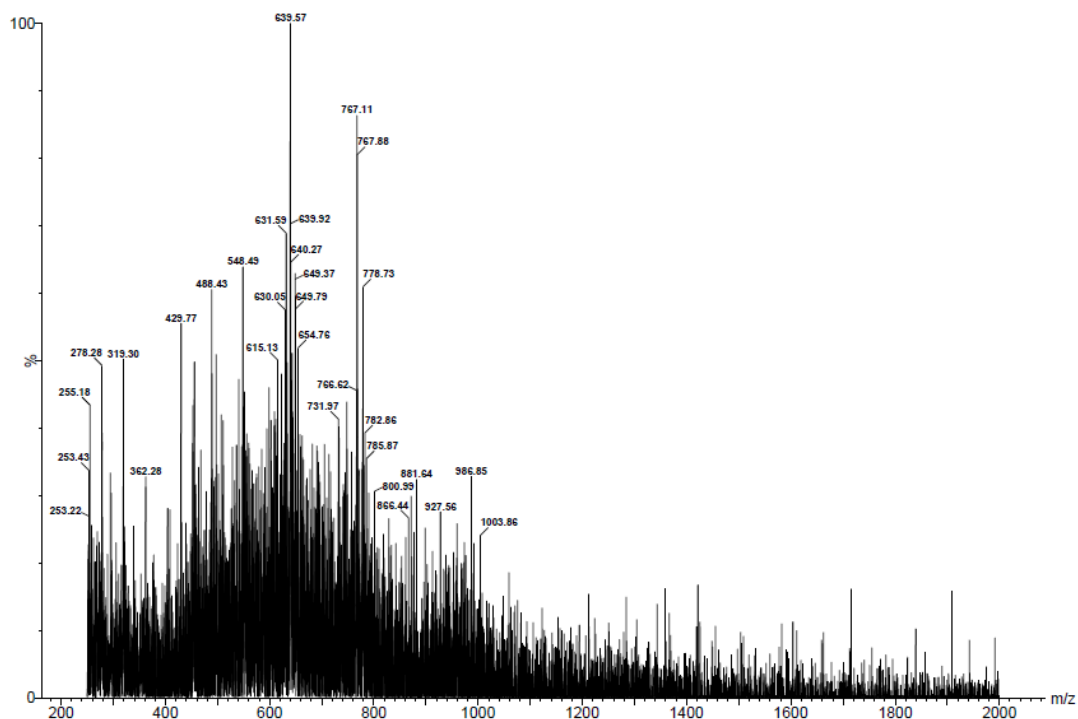
Amino Acid	Mass (g)	Vol. DMF (mL)
Fmoc-Cys(Trt)-OH	0.2811	3.6
Fmoc-Asp(O ^t Bu)-OH	0.0329	0.6
Fmoc-Glu(O ^t Bu)-OH	0.0681	1.2
Fmoc-Gly-OH	0.0238	0.6
Fmoc-Lys(Boc)-OH	0.1874	3.0
Fmoc-Leu-OH	0.0565	1.2
Fmoc-Met-OH	0.0594	1.2
Fmoc-Gln(Trt)-OH	0.0489	0.6
Fmoc-Arg(Pbf)-OH	0.1038	1.2
Fmoc-Ser(^t Bu)-OH	0.0307	0.6
Fmoc-Thr(^t Bu)-OH	0.0318	0.6
Fmoc-Val-OH	0.0272	0.6
Fmoc-Trp(Boc)-OH	0.1685	2.4
Fmoc-Tyr(^t Bu)-OH	0.0368	0.6

The resin was added to a reaction syringe, washed with DMF (4 x 1.5 mL) and left to swell for 30 min in 1.5 mL DMF. After this time, protected leucine (0.6 mL, 4 eq.) was added to the reaction syringe and coupled using HBTU (30.3 mg in 0.6 mL DMF, 4 eq.) and DIPEA (27.7 μ L in 0.2723 mL DMF, 8 eq.). Successive Fmoc deprotections and amino acid couplings were carried out using general method 1 with 0.6 mL of protected amino acid solution per coupling step.

The peptide was cleaved under standard conditions, washed with ether and lyophilised. The peptide was purified using a gradient of 35 – 60 % B over 15 min (A = water, B = acetonitrile) and left to cyclise for 10 days in pure water at 4 °C to yield 10 mg of product (13%).

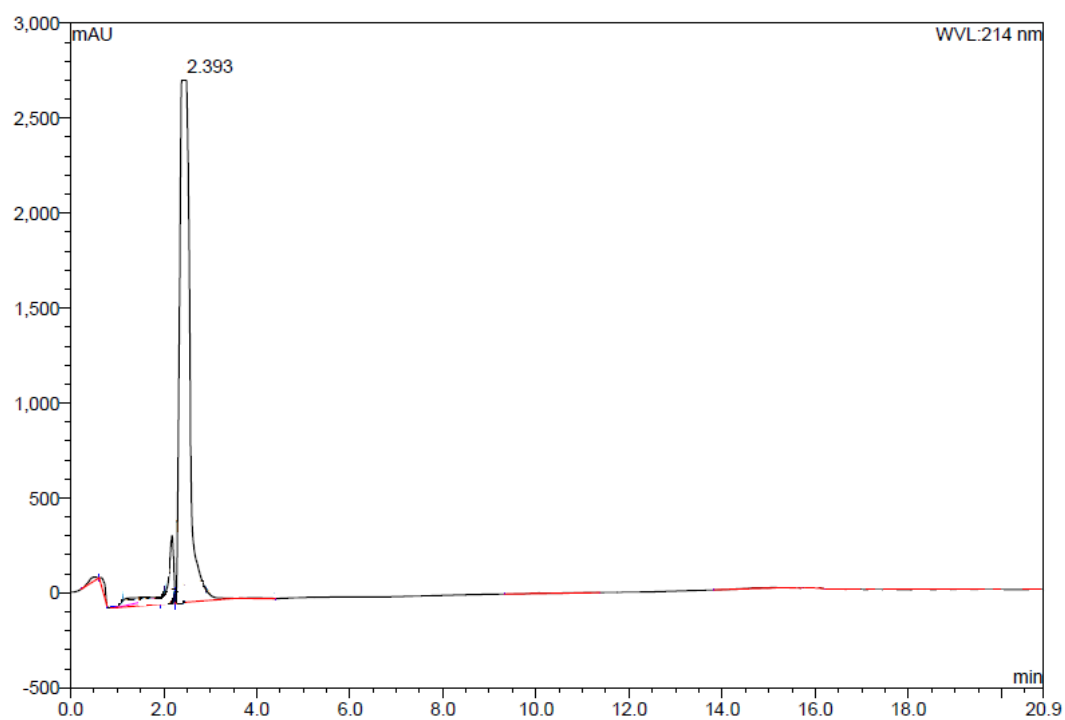
Uncyclised peptide:

LCMS:



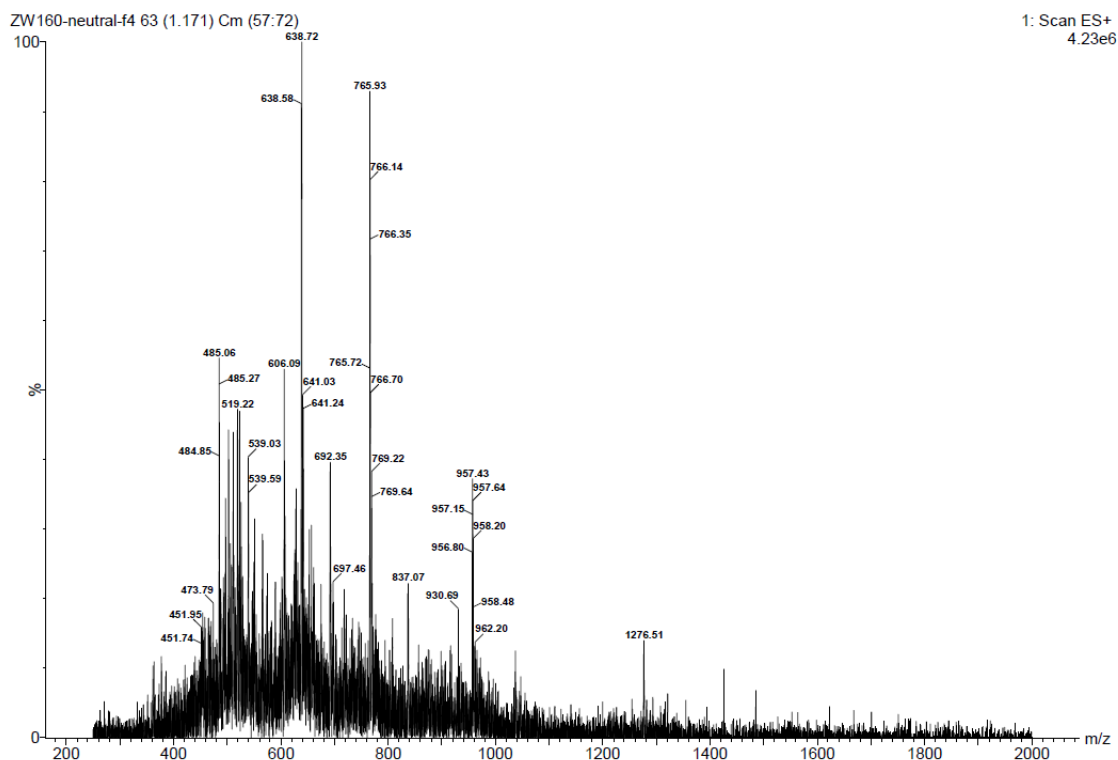
Analysis: m/z (ES^+) 765.93 ($[M + 5H]^{5+}$), 639.57 ($[M + 6H]^{6+}$).

Analytical HPLC: The purified peptide was analysed by analytical HPLC using an ACE C8-300 analytical column (150 x 10 mm, flow rate of 1.0 mL/min), with a linear gradient of 2 – 98% B over 20 min (A = water, B = acetonitrile).



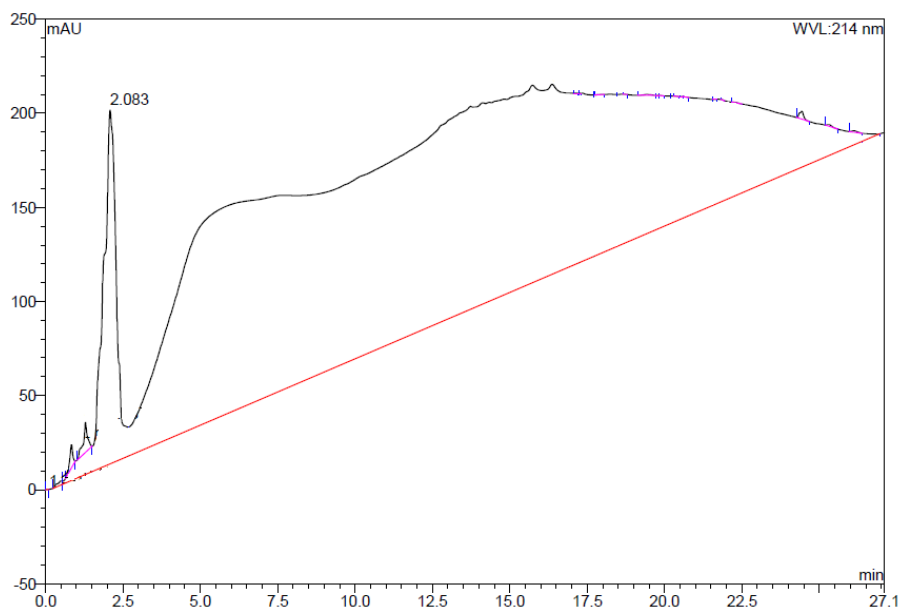
Cyclised peptide:

LCMS:

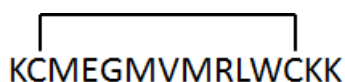


Analysis: m/z (ES⁺) 1276.51 ([M + 3H]³⁺), 957.43 ([M + 4H]⁴⁺), 765.93 ([M + 5H]⁵⁺), 638.72 ([M + 6H]⁶⁺).

Analytical HPLC: The purified peptide was analysed by analytical HPLC using an ACE C8-300 analytical column (150 x 10 mm, flow rate of 1.0 mL/min), with a linear gradient of 2 – 98% B over 20 min (A = water, B = acetonitrile).



C-Terminal Disulfide Single Ring 191



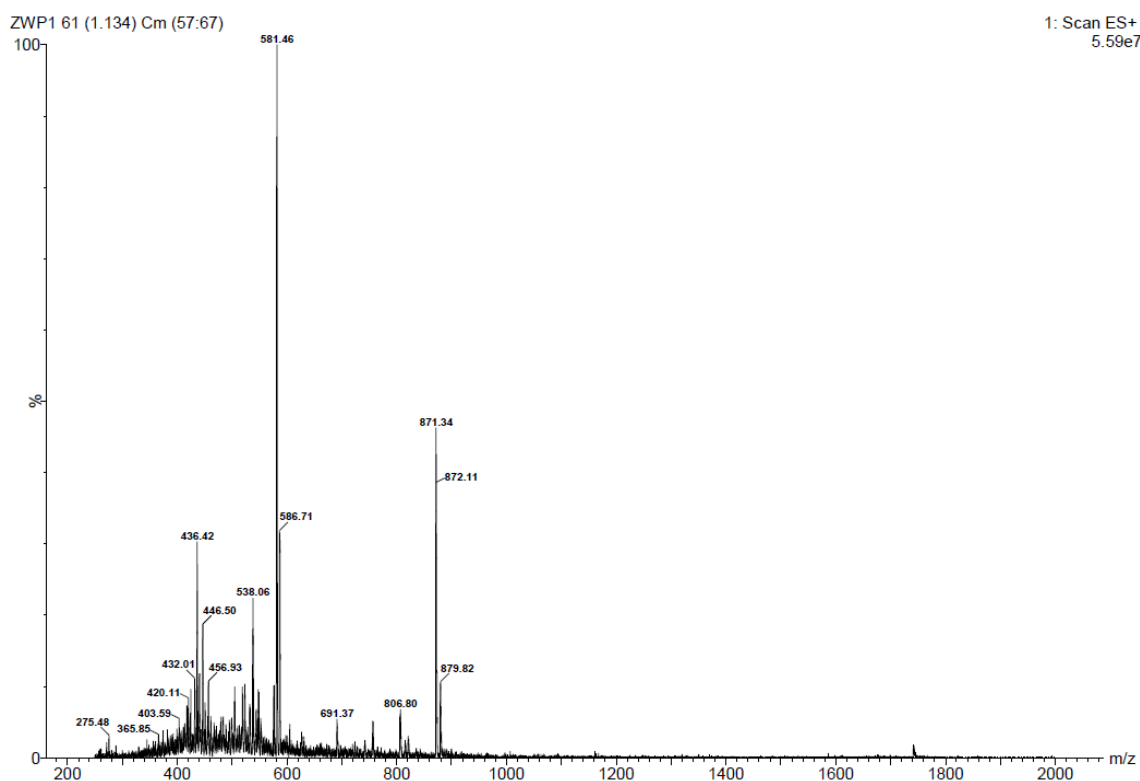
The reaction was carried out on a 100 mg scale using pre-loaded H-Lys(Boc)-2-Cl-Trt resin (loading = 0.75 mmol/g) and using the amounts listed below:

Amino Acid	Mass (g)	Vol. DMF (mL)
Fmoc-Cys(Trt)-OH	0.3514	1.2
Fmoc-Glu(O ^t Bu)-OH	0.1276	0.6
Fmoc-Gly-OH	0.0892	0.6
Fmoc-Lys(Boc)-OH	0.4217	1.8
Fmoc-Leu-OH	0.1060	0.6
Fmoc-Met-OH	0.3343	1.8
Fmoc-Arg(Pbf)-OH	0.1946	0.6
Fmoc-Val-OH	0.1018	0.6
Fmoc-Trp(Boc)-OH	0.1580	0.6

The resin was added to a reaction syringe, washed with DMF (4 x 1.5 mL) and left to swell for 30 min in 1.5 mL DMF. After this time, protected leucine (0.6 mL, 4 eq.) was added to the reaction syringe and coupled using HBTU (113.7 mg in 0.6 mL DMF, 4 eq.) and DIPEA (103.8 μ L in 0.1962 mL DMF, 8 eq.). Successive Fmoc deprotections and amino acid couplings were carried out using general method 1 with 0.6 mL of protected amino acid solution per coupling step.

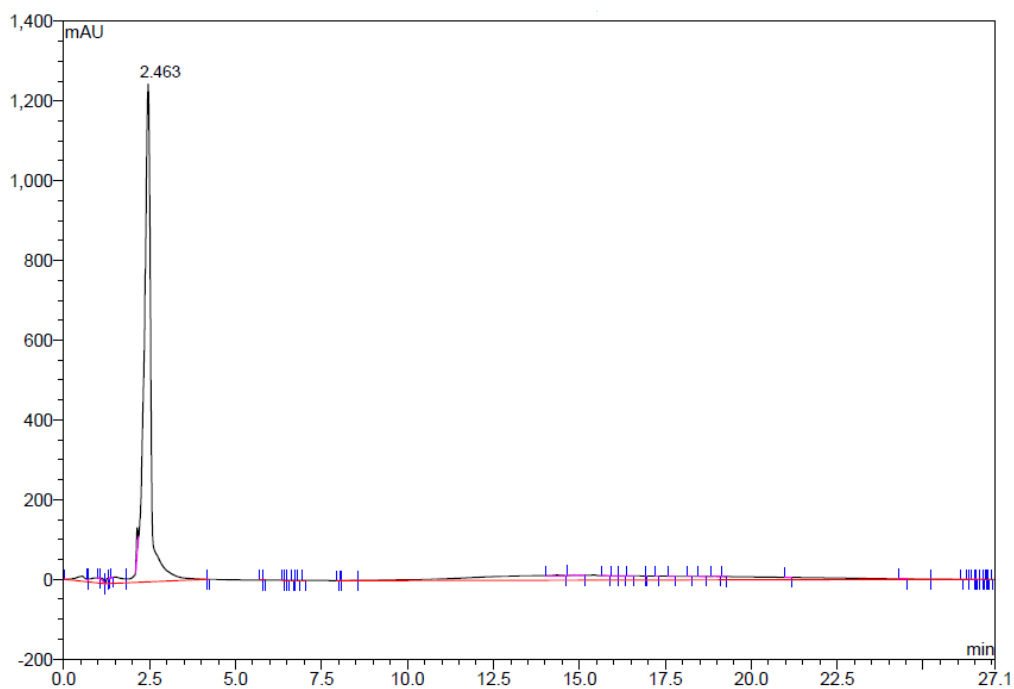
The peptide was cleaved under standard conditions, washed with ether and lyophilised. The peptide was purified using a gradient of 40 – 80 % B over 15 min (A = water, B = acetonitrile) and left to cyclise for 10 days in pure water at 4 °C to yield 13 mg of product (10%).

LCMS:

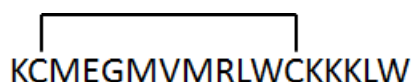


Analysis: m/z (ES⁺) 871.34 ($[M + 2H]^{2+}$), 581.41 ($[M + 3H]^{3+}$).

Analytical HPLC: The purified peptide was analysed by analytical HPLC using an ACE C8-300 analytical column (150 x 10 mm, flow rate of 1.0 mL/min), with a linear gradient of 2 – 98% B over 20 min (A = water, B = acetonitrile).



C-Terminal Disulfide Single Ring with KKLW tail 192



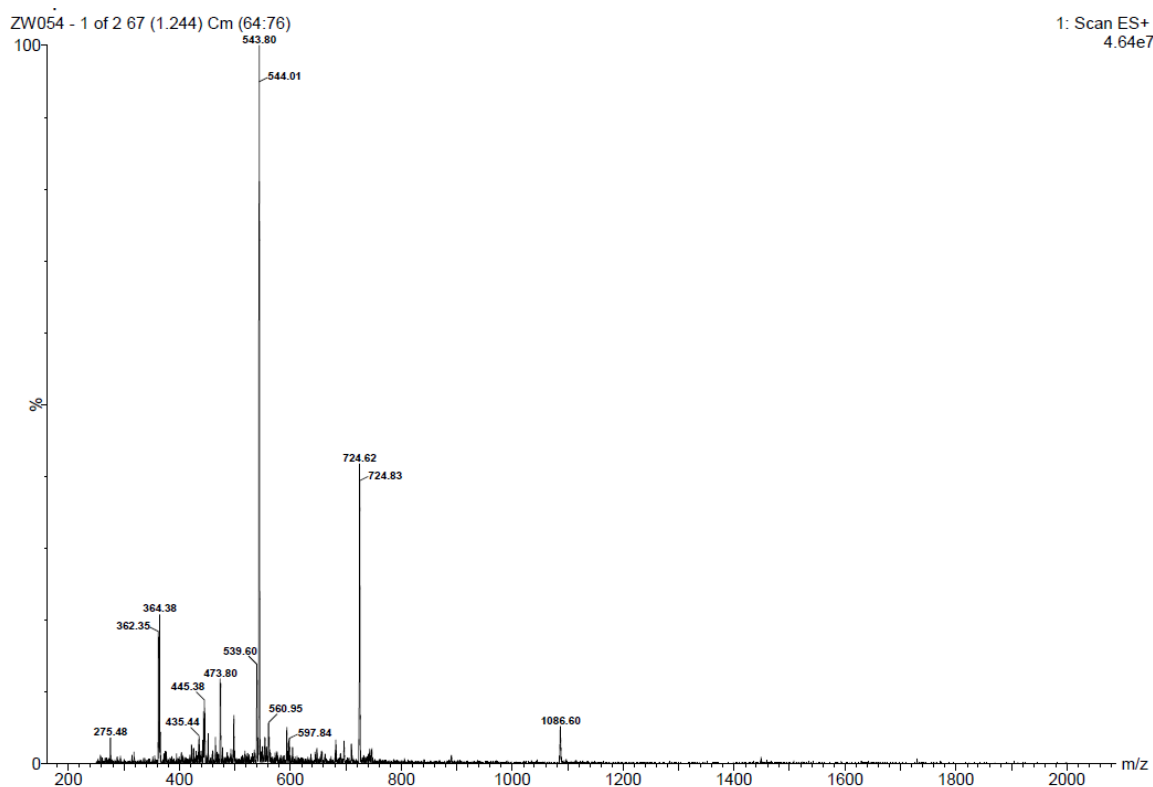
The reaction was carried out on a 100 mg scale using pre-loaded Fmoc-Trp(Boc)-NovaSyn® TGT resin (loading 0.20 mmol/g) using the amounts listed below:

Amino Acid	Mass (g)	Vol. DMF (mL)
Fmoc-Cys(Trt)-OH	0.0937	1.2
Fmoc-Glu(O ^t Bu)-OH	0.0340	0.6
Fmoc-Gly-OH	0.0238	0.6
Fmoc-Lys(Boc)-OH	0.1499	2.4
Fmoc-Leu-OH	0.0565	1.2
Fmoc-Met-OH	0.0891	1.8
Fmoc-Arg(Pbf)-OH	0.0519	0.6
Fmoc-Val-OH	0.0272	0.6
Fmoc-Trp(Boc)-OH	0.0843	1.2

The resin was added to a reaction syringe, washed with DMF (4 x 1.5 mL) and left to swell for 30 min in 1.5 mL DMF. After this time, the Fmoc group was removed using the standard Fmoc deprotection step described in method 1 above. Protected leucine (0.6 mL, 4 eq.) was added to the reaction syringe and coupled using HBTU (30.3 mg in 0.6 mL DMF, 4 eq.) and DIPEA (27.7 µL in 0.2723 mL DMF, 8 eq.). Successive Fmoc deprotections and amino acid couplings were carried out using general method 1 with 0.6 mL of protected amino acid solution per coupling step.

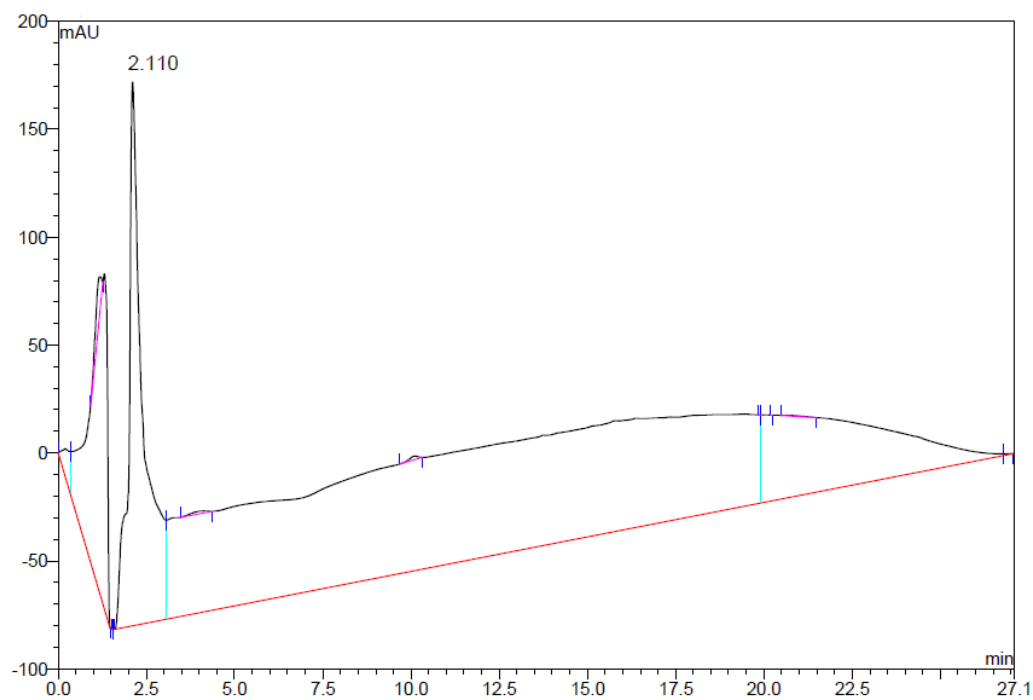
The peptide was cleaved under standard conditions, washed with ether and lyophilised. The peptide was purified using a gradient of 40 – 80 % B over 15 min (A = water, B = acetonitrile) and left to cyclise for 10 days in pure water at 4 °C to yield 7 mg of product (16%).

LCMS:

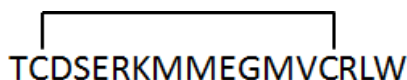


Analysis: m/z (ES⁺) 1086.60 ([M + 2H]²⁺), 724.62 ([M + 3H]³⁺), 543.80 ([M + 4H]⁴⁺).

Analytical HPLC: The purified peptide was analysed by analytical HPLC using an ACE C8-300 analytical column (150 x 10 mm, flow rate of 1.0 mL/min), with a linear gradient of 2 – 98% B over 20 min (A = water, B = acetonitrile).



Middle Disulfide Single Ring 193



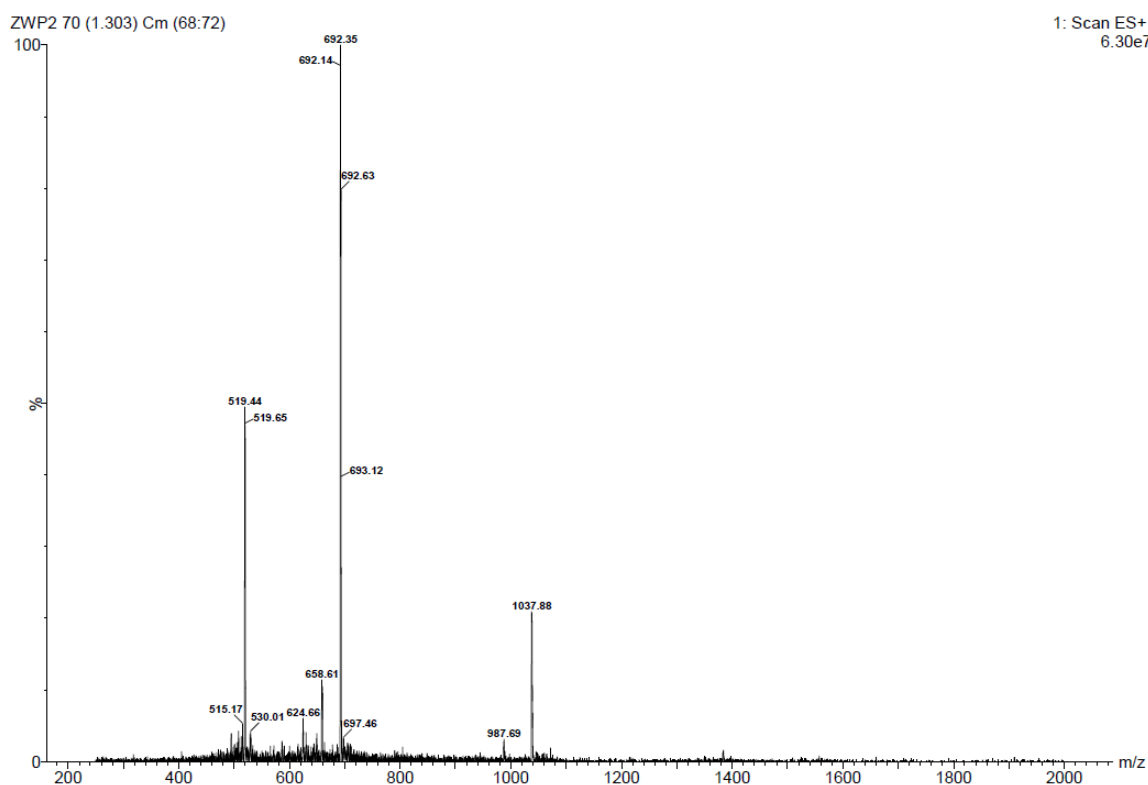
The reaction was carried out on a 100 mg scale using pre-loaded Fmoc-Trp(Boc)-NovaSyn® TGT resin (loading 0.20 mmol/g) using the amounts listed below:

Amino Acid	Mass (g)	Vol. DMF (mL)
Fmoc-Cys(Trt)-OH	0.0937	1.2
Fmoc-Asp(O ^t Bu)-OH	0.0329	0.6
Fmoc-Glu(O ^t Bu)-OH	0.0681	1.2
Fmoc-Gly-OH	0.0238	0.6
Fmoc-Lys(Boc)-OH	0.0750	0.6
Fmoc-Leu-OH	0.0891	0.6
Fmoc-Met-OH	0.0489	1.8
Fmoc-Arg(Pbf)-OH	0.0519	1.2
Fmoc-Ser(^t Bu)-OH	0.0307	0.6
Fmoc-Thr(^t Bu)-OH	0.0318	0.6
Fmoc-Val-OH	0.0843	0.6
Fmoc-Trp(Boc)-OH	0.0368	0.6

The resin was added to a reaction syringe, washed with DMF (4 x 1.5 mL) and left to swell for 30 min in 1.5 mL DMF. After this time, the Fmoc group was removed using the standard Fmoc deprotection step described in method 1 above. Protected leucine (0.6 mL, 4 eq.) was added to the reaction syringe and coupled using HBTU (30.3 mg in 0.6 mL DMF, 4 eq.) and DIPEA (27.7 μ L in 0.2723 mL DMF, 8 eq.). Successive Fmoc deprotections and amino acid couplings were carried out using general method 1 with 0.6 mL of protected amino acid solution per coupling step.

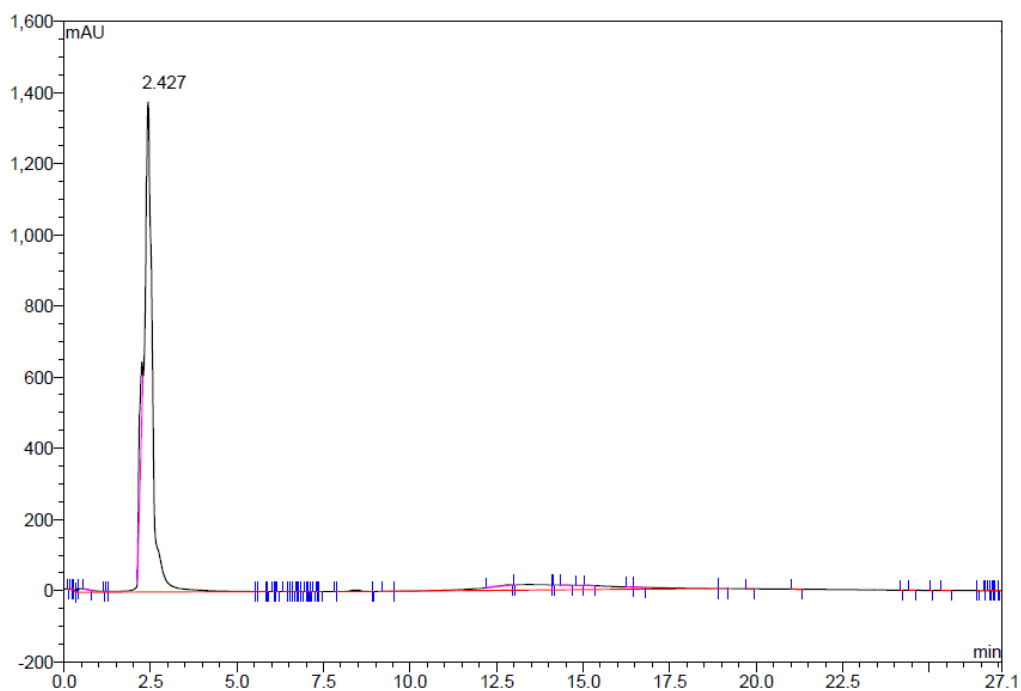
The peptide was cleaved under standard conditions, washed with ether and lyophilised. The peptide was purified using a gradient of 40 – 80 % B over 15 min (A = water, B = acetonitrile) and left to cyclise for 10 days in pure water at 4 °C to yield 1.5 mg of product (4%).

LCMS:

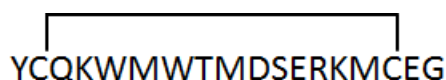


Analysis: m/z (ES⁺) 1037.88 ([M + 2H]²⁺), 692.35 ([M + 3H]³⁺), 519.44 ([M + 4H]⁴⁺).

Analytical HPLC: The purified peptide was analysed by analytical HPLC using an ACE C8-300 analytical column (150 x 10 mm, flow rate of 1.0 mL/min), with a linear gradient of 2 – 98% B over 20 min (A = water, B = acetonitrile).



N-Terminal Disulfide Single Ring 194



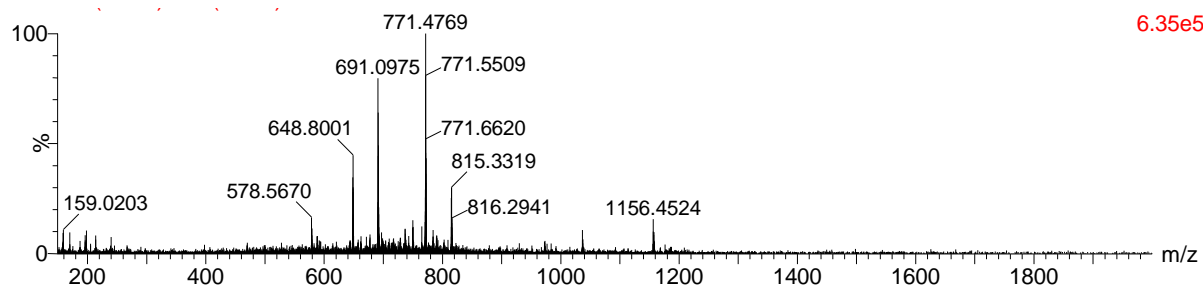
The reaction was carried out on a 100 mg scale using pre-loaded Fmoc-Gly-NovaSyn® TGT resin (loading = 0.20 mmol/g) using the amounts listed below:

Amino Acid	Mass (g)	Vol. DMF (mL)
Fmoc-Cys(Trt)-OH	0.0937	1.2
Fmoc-Asp(O ^t Bu)-OH	0.0329	0.6
Fmoc-Glu(O ^t Bu)-OH	0.0681	1.2
Fmoc-Gly-OH	0.0238	0.6
Fmoc-Lys(Boc)-OH	0.0750	1.2
Fmoc-Met-OH	0.0891	1.8
Fmoc-Gln(Trt)-OH	0.0489	0.6
Fmoc-Arg(Pbf)-OH	0.0519	0.6
Fmoc-Ser(^t Bu)-OH	0.0307	0.6
Fmoc-Thr(^t Bu)-OH	0.0318	0.6
Fmoc-Trp(Boc)-OH	0.0843	1.2
Fmoc-Tyr(^t Bu)-OH	0.0368	0.6

The resin was added to a reaction syringe, washed with DMF (4 x 1.5 mL) and left to swell for 30 min in 1.5 mL DMF. After this time, the Fmoc group was removed using the standard Fmoc deprotection step described in method 1 above. Protected glycine (0.6 mL, 4 eq.) was added to the reaction syringe and coupled using HBTU (27.7 mg in 0.6 mL DMF, 4 eq.) and DIPEA (27.7 μ L in 0.2723 mL DMF, 8 eq.). Successive Fmoc deprotections and amino acid couplings were carried out using general method 1 with 0.6 mL of protected amino acid solution per coupling step.

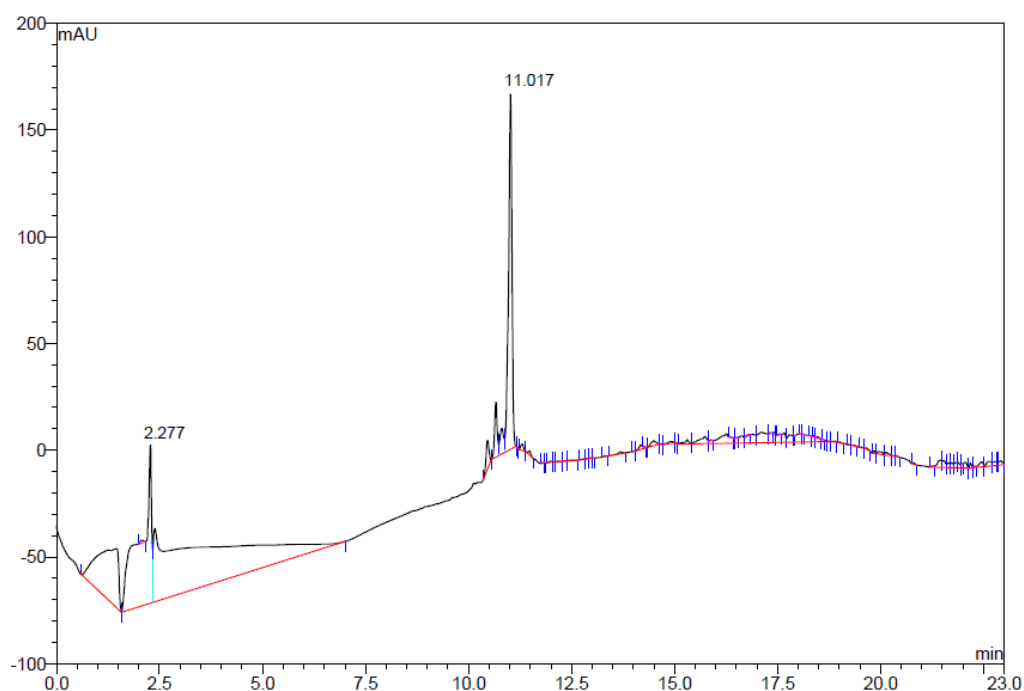
The peptide was cleaved under standard conditions, washed with ether and lyophilised. The peptide was purified using a gradient of 10 – 60 % B over 30 min (A = water, B = acetonitrile) and left to cyclise for 10 days in pure water at 4 °C to yield 12 mg of product (26%).

LCMS:



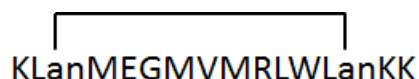
Analysis: m/z (ES⁺) 1156.45 ([M + 2H]²⁺), 771.48 ([M + 3H]³⁺) 578.57 ([M + 4H]⁴⁺).

Analytical HPLC: The purified peptide was analysed by analytical HPLC using an ACE C8-300 analytical column (150 x 10 mm, flow rate of 1.0 mL/min), with a linear gradient of 2 – 98% B over 20 min (A = water, B = acetonitrile).



7.3.3 Optimisation of the Synthesis of Lanthionine-Containing Analogues

All optimisation was carried out using the C-terminal single ring structure **205**.



Preparation of Low-Loading Chlorotrityl Resin: The low-loading chlorotrityl resin was prepared from the pre-loaded chlorotrityl resin (220 mg, loading = 0.75 mmol/g). The resin was first swelled in DMF (2 mL) for 45 min before evacuating the syringe. Acetic anhydride (13.5 μL , 0.143 mmol, 0.85 eq.) was then added and the resin was left to agitate for 30 min on a platform shaker before evacuating the syringe. The resin was washed with DMF (6 x 1.5 mL). To calculate the new loading of the resin, 20 mg of the resin was removed. To this, Fmoc-Gly-OH (5.0 mg in 0.82 mL DMF), DIPEA (30.0 μL in 2.29 mL DMF) and HBTU (20.0 mg in 2.60 mL DMF) were added and left to react for 1 h. The syringe was then evacuated and the peptide was washed with DMF (6 x 1.5 mL). A solution of DBU in DMF (2% v/v, 2 mL) was added and left to react for 30 min before the addition of acetonitrile (8 mL). 2 mL of this solution was removed and diluted with a further portion of acetonitrile (23 mL). The UV spectrum of this solution was measured and the optical density at 304 nm recorded against a

reference sample of DBU in DMF (2% v/v, 2 mL) made to the same concentration in acetonitrile. To calculate the resin loading, the following equation was used:^{8,9}

$$\text{Loading} = (\text{absorbance} \times \text{volume}) / (\text{extinction coefficient} \times \text{path length} \times \text{mass of resin})$$

For the knock-down lysine resin, the loading was calculated to be 0.109 mmol/g.

The initial trial reactions were carried out on a 50 mg scale using pre-loaded resins according to Table 7.2. The second set of trial reactions were carried out on a 100 mg scale to allow determination of yields using pre-loaded resins according to Table 7.3.

The resin was added to a reaction syringe, washed with DMF (4 x 1.5 mL) and left to swell for 30 min in 1.5 mL DMF. After this time, the Fmoc group was removed using the standard Fmoc deprotection step described in method 1 above. Protected lysine (4 eq.) was added to the reaction syringe and coupled using HBTU (4 eq. in 0.6 mL DMF) and DIPEA (8 eq. in 0.2636 mL DMF). Successive Fmoc deprotections and amino acid couplings were carried out using general method 2 with 0.6 mL of protected amino acid solution per coupling step.

Lanthionine was added to the peptide sequence and left to react according to the conditions in Table 7.2 and Table 7.3 using PyAOP (5 eq.), HOAt (5 eq.) and DIPEA (10 eq.) for both the coupling and cyclisation steps. The simultaneous allyl and Alloc deprotection was carried out according to the general protocol described above using tetrakis(triphenylphosphine) palladium (0) (1 eq.) and 1,3-dimethylbarbituric acid (10 eq.).

The peptide was cleaved under standard conditions, washed with ether and lyophilised. To obtain yields, the peptides synthesised according to Table 7.3 were purified using a gradient of 5 – 50 % B over 15 min (A = water, B = acetonitrile) to yield 3 mg of product (8%).

Entry	Resin	Loading (mmol/g)	Temp (°C)	Time (mins)	Peptide Formed
1	NovaSyn TGT	0.2	60	5	✓
2	NovaSyn TGT	0.2	60	7	✓
3	NovaSyn TGT	0.2	70	5	✓
4	LL Cl-Trt	0.11	60	5	✓
5	LL Cl-Trt	0.11	60	7	✓
6	LL Cl-Trt	0.11	70	5	✓
7	Cl-Trt	0.73	60	5	Polymerisation
8	Cl-Trt	0.73	60	7	Polymerisation
9	Cl-Trt	0.73	70	5	Polymerisation

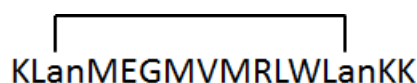
Table 7.2: Summary of Preliminary Investigations into the Use of the Microwave for Incorporation of Lanthionine (142) into the Peptide Sequence

Entry	Resin	Temp (°C)	Time (mins)	Yield (%)
1	NovaSyn TGT	60	5	8
2	NovaSyn TGT	60	10	2
3	NovaSyn TGT	70	5	4
4	LL Cl-Trt	60	5	0
5	LL Cl-Trt	60	10	0
6	LL Cl-Trt	70	5	0
7	NovaSyn TGT	RT, no μ W	120	8 (+ 3 peptide – lanthionine)

Table 7.3: Summary of Further Investigations into the Use of the Microwave for Incorporation of Lanthionine (**142**) into the Peptide Sequence

7.3.4 Synthesis of Lanthionine-Containing Analogues

C-Terminal Lanthionine Single Ring 205



The reaction was carried out on a 100 mg scale using pre-loaded Fmoc-Lys(Boc)-NovaSyn® resin (loading 0.24 mmol/g) using the amounts listed below:

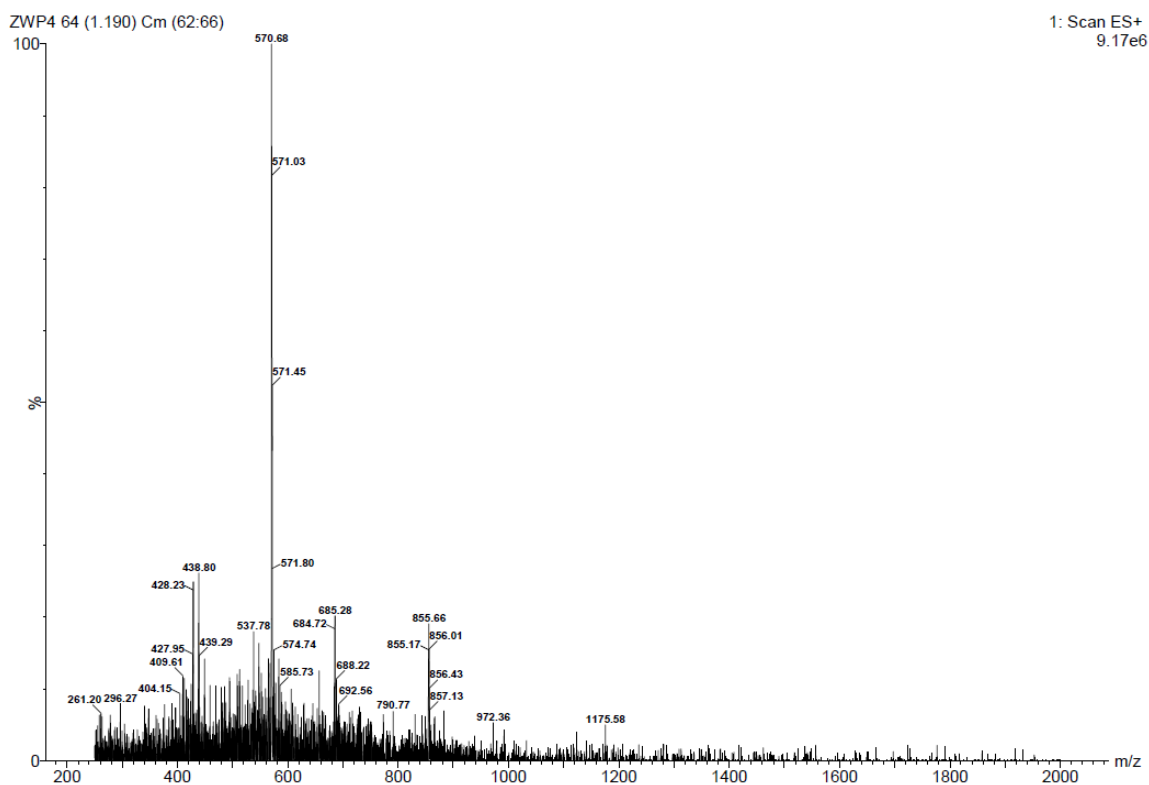
Amino Acid	Mass (g)	Vol. DMF (mL)
Lanthionine 142	0.0399	4.0
Fmoc-Glu(O ^t Bu)-OH	0.0408	0.6
Fmoc-Gly-OH	0.0285	0.6
Fmoc-Lys(Boc)-OH	0.1349	1.8
Fmoc-Leu-OH	0.0339	0.6
Fmoc-Met-OH	0.1070	1.8
Fmoc-Arg(Pbf)-OH	0.0623	0.6
Fmoc-Val-OH	0.0326	0.6
Fmoc-Trp(Boc)-OH	0.0506	0.6

The resin was added to a reaction syringe, washed with DMF (4 x 1.5 mL) and left to swell for 30 min in 1.5 mL DMF. After this time, the Fmoc group was removed using the standard Fmoc deprotection step described in method 1 above. Protected lysine (0.6 mL, 4 eq.) was added to the reaction syringe and coupled using HBTU (33.2 mg in 0.6 mL DMF, 4 eq.) and DIPEA (36.4 μ L in 0.2636 mL DMF, 8 eq.). Successive Fmoc deprotections and amino acid couplings were carried out using general method 1 with 0.6 mL of protected amino acid solution per coupling step.

Lanthionine was added to the peptide sequence using the microwave protocol described in the general experimental section, using PyAOP (62.5 mg, 5 eq.), HOAt (16.3 mg, 5 eq.) and DIPEA (41.5 μ L, 10 eq.) for both the coupling and cyclisation steps. The simultaneous allyl and Alloc deprotection was carried out according to the general protocol described above using tetrakis(triphenyl)phosphine palladium (0) (27.7 mg, 1 eq.) and 1,3-dimethylbarbituric acid (37.5 mg, 10 eq.).

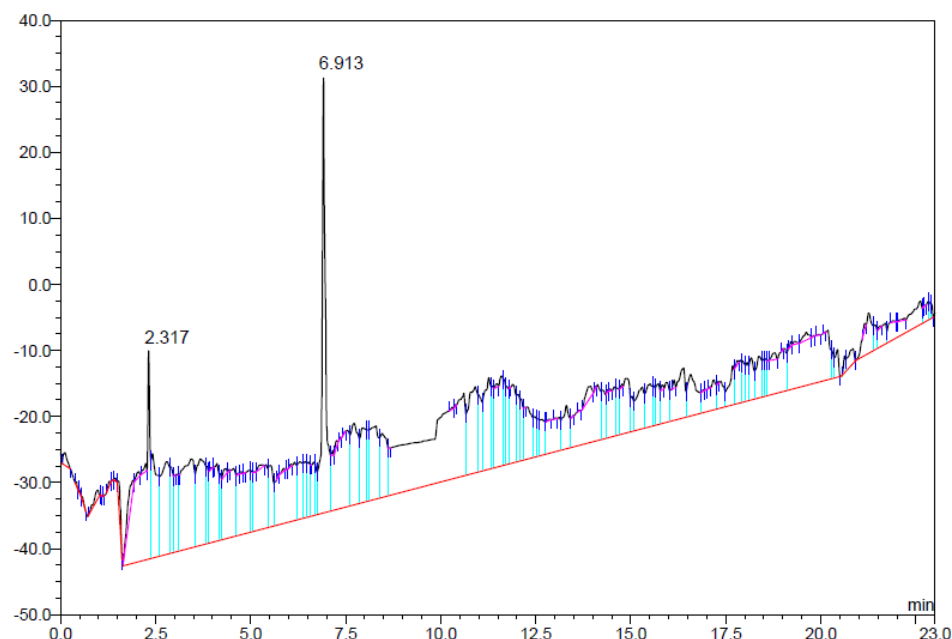
The peptide was cleaved under standard conditions, washed with ether and lyophilised. The peptide was purified using a gradient of 5 – 50 % B over 15 min (A = water, B = acetonitrile) to yield 3 mg of product (8%).

LCMS:

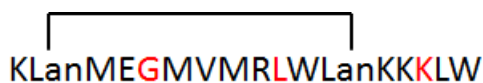


Analysis: m/z (ES^+) 855.66 ($[M + 2H]^{2+}$), 570.68 ($[M + 3H]^{3+}$) 428.23 ($[M + 4H]^{4+}$).

Analytical HPLC: The purified peptide was analysed by analytical HPLC using an ACE C8-300 analytical column (150 x 10 mm, flow rate of 1.0 mL/min), with a linear gradient of 2 – 98% B over 20 min (A = water, B = acetonitrile).



C-Terminal Lanthionine Single Ring with KKLW tail 206



The reaction was carried out on a 100 mg scale using pre-loaded Fmoc-Trp(Boc)-NovaSyn® resin (loading 0.20 mmol/g) using the amounts listed below:

Amino Acid	Mass (g)	Vol. DMF (mL)
Lanthionine 142	0.0332	4.0
Fmoc-Glu(O ^t Bu)-OH	0.0340	0.6
Fmoc-(FmocHmb)-Gly-OH	0.0347	0.6
Fmoc-Lys(Boc)-OH	0.1124	1.8
Fmoc-(FmocHmb)-Lys(Boc)-OH	0.0662	0.6
Fmoc-Leu-OH	0.0283	0.6
Fmoc-(FmocHmb)-Leu-OH	0.0569	0.6
Fmoc-Met-OH	0.0891	1.8
Fmoc-Arg(Pbf)-OH	0.0519	0.6
Fmoc-Val-OH	0.0272	0.6
Fmoc-Trp(Boc)-OH	0.0843	1.2

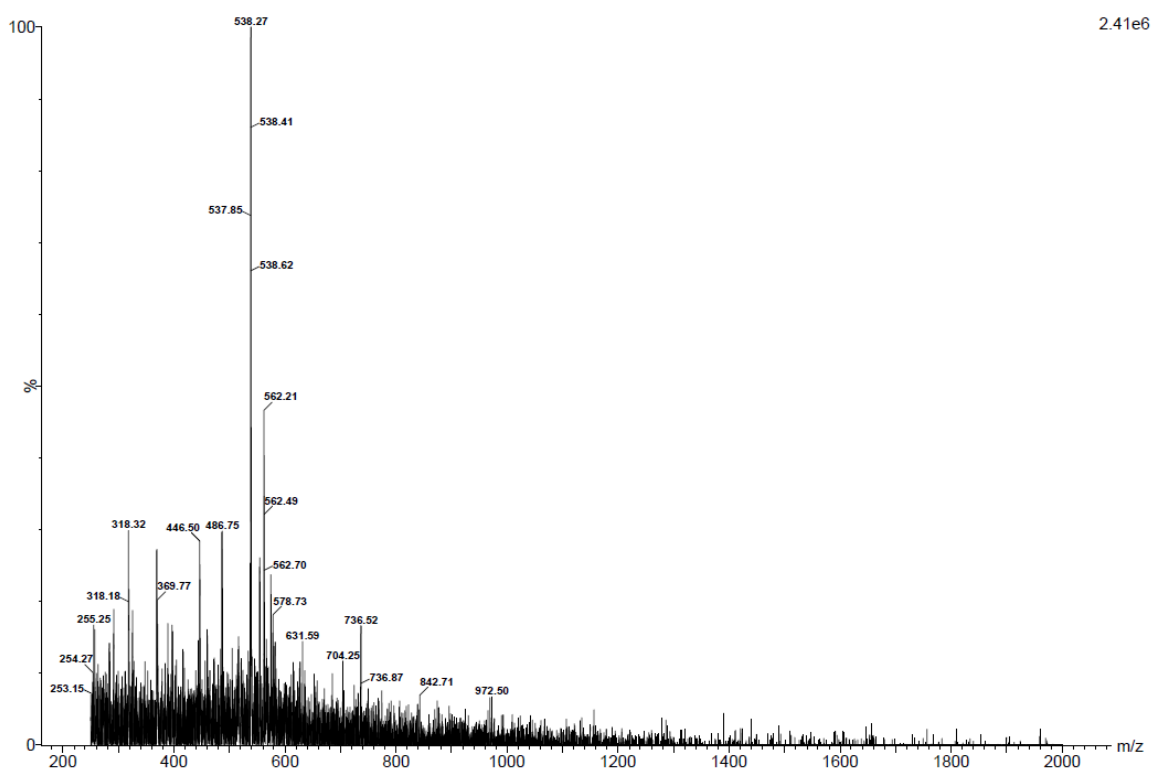
The resin was added to a reaction syringe, washed with DMF (4 x 1.5 mL) and left to swell for 30 min in 1.5 mL DMF. After this time, the Fmoc group was removed using the standard Fmoc deprotection step described in method 2 above. Protected glycine (0.6 mL, 4 eq.) was added to the reaction syringe and coupled using HBTU (33.2 mg in 0.6 mL DMF, 4 eq.) and

DIPEA (36.4 μ L in 0.2636 mL DMF, 8 eq.). Successive Fmoc deprotections and amino acid couplings were carried out using general method 2 with 0.6 mL of protected amino acid solution per coupling step. Each coupling step was repeated a second time prior to each deprotection with fresh amino acid solution, giving a total agitation time of 80 min.

Lanthionine was added to the peptide sequence using the microwave protocol described in the general experimental section, using PyAOP (52.1 mg, 5 eq.), HOAt (13.6 mg, 5 eq.) and DIPEA (34.6 μ L, 10 eq.) for both the coupling and cyclisation steps. The simultaneous allyl and Alloc deprotection was carried out according to the general protocol described above using tetrakis(triphenylphosphine) palladium (0) (23.1 mg, 1 eq.) and 1,3-dimethylbarbituric acid (31.2 mg, 10 eq.).

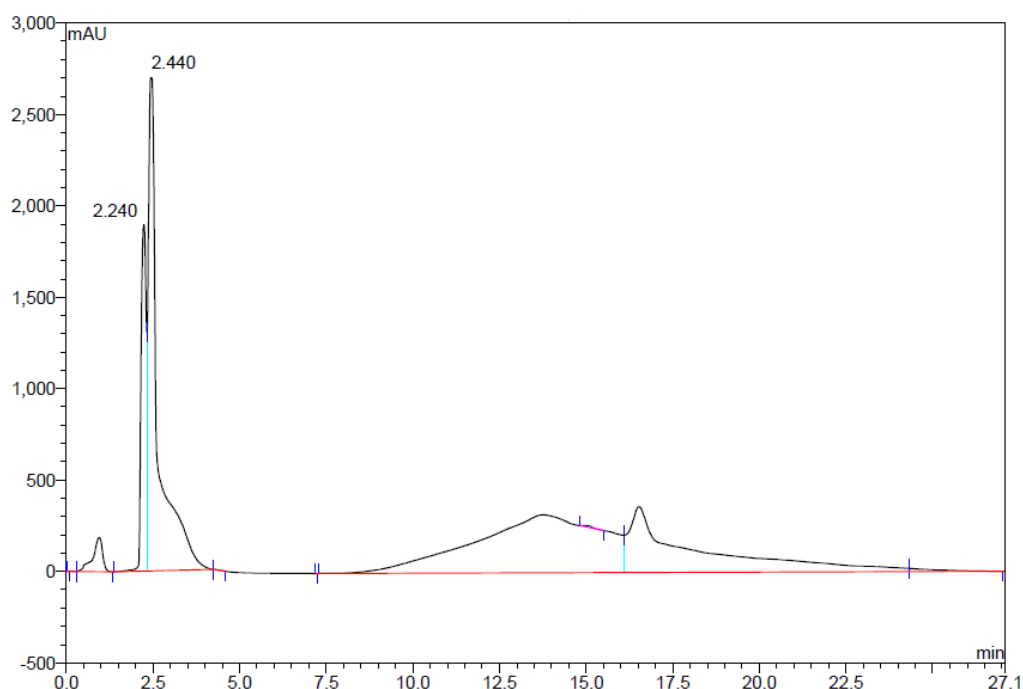
The peptide was cleaved under standard conditions, washed with ether and lyophilised. The peptide was purified using a gradient of 10 – 55 % B over 8 min (A = water, B = acetonitrile) to yield 4 mg of product (9%).

LCMS:

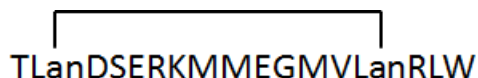


Analysis: m/z (ES^+) 538.27 ($[M + 4H]^{4+}$).

Analytical HPLC: The purified peptide was analysed by analytical HPLC using an ACE C8-300 analytical column (150 x 10 mm, flow rate of 1.0 mL/min), with a linear gradient of 2 – 98% B over 20 min (A = water, B = acetonitrile).



Middle Single Ring with Lanthionine 207



The reaction was carried out on a 100 mg scale using pre-loaded Fmoc-Trp(Boc)-NovaSyn® resin (loading 0.20 mmol/g) using the amounts listed below:

Amino Acid	Mass (g)	Vol. DMF (mL)
Lanthionine 142	0.0332	4.0
Fmoc-Asp(O ^t Bu)-OH	0.0329	0.6
Fmoc-Glu(O ^t Bu)-OH	0.0681	1.2
Fmoc-Gly-OH	0.0238	0.6
Fmoc-Lys(Boc)-OH	0.0375	0.6
Fmoc-Leu-OH	0.0283	0.6
Fmoc-Met-OH	0.0891	1.8
Fmoc-Arg(Pbf)-OH	0.1038	1.2
Fmoc-Ser(^t Bu)-OH	0.0307	0.6
Fmoc-Thr(^t Bu)-OH	0.0318	0.6
Fmoc-Val-OH	0.0272	0.6
Fmoc-Trp(Boc)-OH	0.0421	0.6

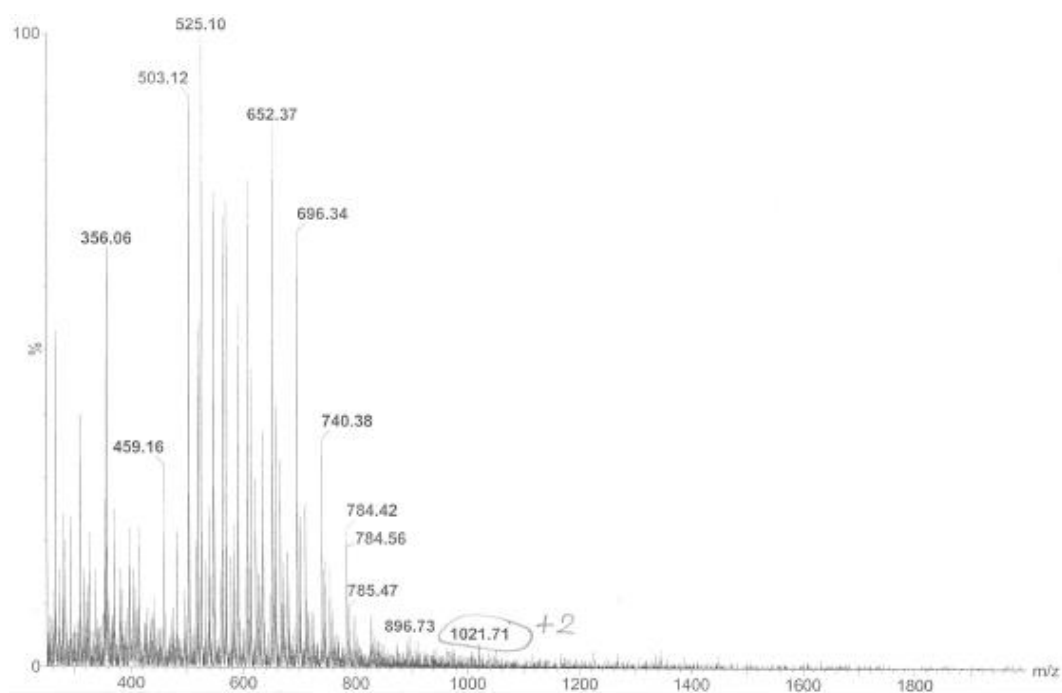
The resin was added to a reaction syringe, washed with DMF (4 x 1.5 mL) and left to swell for 30 min in 1.5 mL DMF. After this time, the Fmoc group was removed using the standard Fmoc deprotection step described in method 1 above. Protected glycine (0.6 mL, 4 eq.) was

added to the reaction syringe and coupled using HBTU (33.2 mg in 0.6 mL DMF, 4 eq.) and DIPEA (36.4 μ L in 0.2636 mL DMF, 8 eq.). Successive Fmoc deprotections and amino acid couplings were carried out using general method 1 with 0.6 mL of protected amino acid solution per coupling step.

Lanthionine was added to the peptide sequence using the microwave protocol described in the general experimental section, using PyAOP (52.1 mg, 5 eq.), HOAt (13.6 mg, 5 eq.) and DIPEA (34.6 μ L, 10 eq.) for both the coupling and cyclisation steps. The simultaneous allyl and Alloc deprotection was carried out according to the general protocol described above using tetrakis(triphenylphosphine) palladium (0) (23.1 mg, 1 eq.) and 1,3-dimethylbarbituric acid (31.2 mg, 10 eq.).

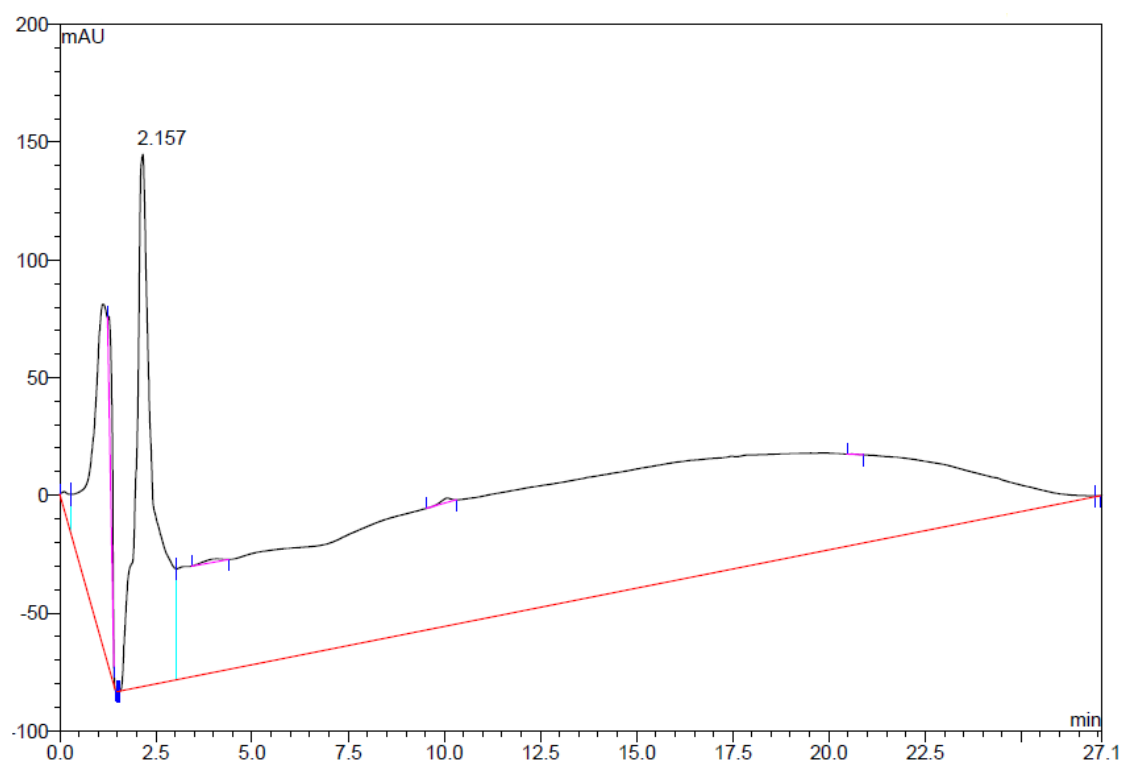
The peptide was cleaved under standard conditions, washed with ether and lyophilised. The peptide was purified using a gradient of 5 – 50 % B over 15 min (A = water, B = acetonitrile) to yield 0.5 mg of product (1%).

LCMS:

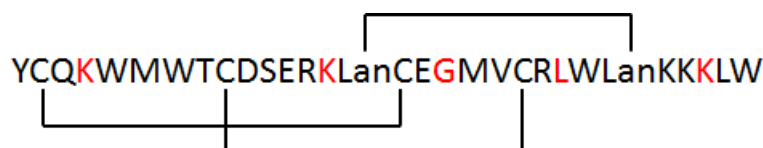


Analysis: m/z (ES^+) 1021.71 ($[M + 2H]^{2+}$).

Analytical HPLC: The purified peptide was analysed by analytical HPLC using an ACE C8-300 analytical column (150 x 10 mm, flow rate of 1.0 mL/min), with a linear gradient of 2 – 98% B over 20 min (A = water, B = acetonitrile).



Triple Ring with C-Terminal Lanthionine (214)



(red indicates the use of an Hmb protected amino acid)

The reaction was carried out on a 100 mg scale using pre-loaded Fmoc-Trp(Boc)-NovaSyn® resin (loading 0.20 mmol/g) using the amounts listed below:

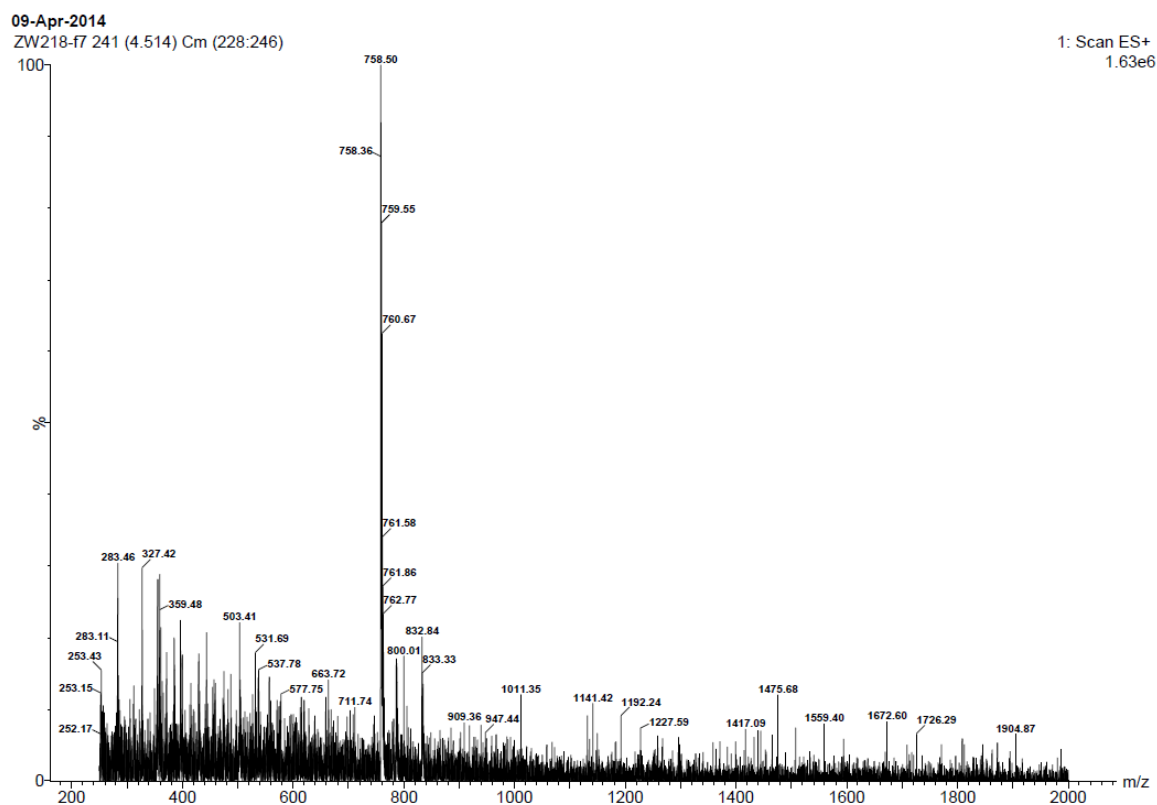
Amino Acid	Mass (g)	Vol. DMF (mL)
Lanthionine 142	0.0332	4.0
Fmoc-Cys(Trt)-OH	0.1874	2.4
Fmoc-Asp(O ^t Bu)-OH	0.0329	0.6
Fmoc-Glu(O ^t Bu)-OH	0.0681	1.2
Fmoc-(FmocHmb)-Gly-OH	0.0347	0.6
Fmoc-Lys(Boc)-OH	0.0750	1.2
Fmoc-(FmocHmb)-Lys(Boc)-OH	0.1985	1.8
Fmoc-Leu-OH	0.0283	0.6
Fmoc-(FmocHmb)-Leu-OH	0.0569	0.6
Fmoc-Met-OH	0.0594	1.2
Fmoc-Gln(Trt)-OH	0.0489	0.6
Fmoc-Arg(Pbf)-OH	0.1038	1.2
Fmoc-Ser(^t Bu)-OH	0.0307	0.6
Fmoc-Thr(^t Bu)-OH	0.0318	0.6
Fmoc-Val-OH	0.0272	0.6
Fmoc-Trp(Boc)-OH	0.1685	2.4
Fmoc-Tyr(^t Bu)-OH	0.368	0.6

The resin was added to a reaction syringe, washed with DMF (4 x 1.5 mL) and left to swell for 30 min in 1.5 mL DMF. After this time, the Fmoc group was removed using the standard Fmoc deprotection step described in method 2 above. Protected glycine (0.6 mL, 4 eq.) was added to the reaction syringe and coupled using HBTU (33.2 mg in 0.6 mL DMF, 4 eq.) and DIPEA (36.4 µL in 0.2636 mL DMF, 8 eq.). Successive Fmoc deprotections and amino acid couplings were carried out using general method 2 with 0.6 mL of protected amino acid solution per coupling step. Each coupling step was repeated a second time prior to each deprotection with fresh amino acid solution, giving a total agitation time of 80 min.

Lanthionine was added to the peptide sequence using the microwave protocol described in the general experimental section, using PyAOP (52.1 mg, 5 eq.), HOAt (13.6 mg, 5 eq.) and DIPEA (34.6 µL, 10 eq.) for both the coupling and cyclisation steps. The simultaneous allyl and Alloc deprotection was carried out according to the general protocol described above using tetrakis(triphenyl)phosphine palladium (0) (23.1 mg, 1 eq.) and 1,3-dimethylbarbituric acid (31.2 mg, 10 eq.).

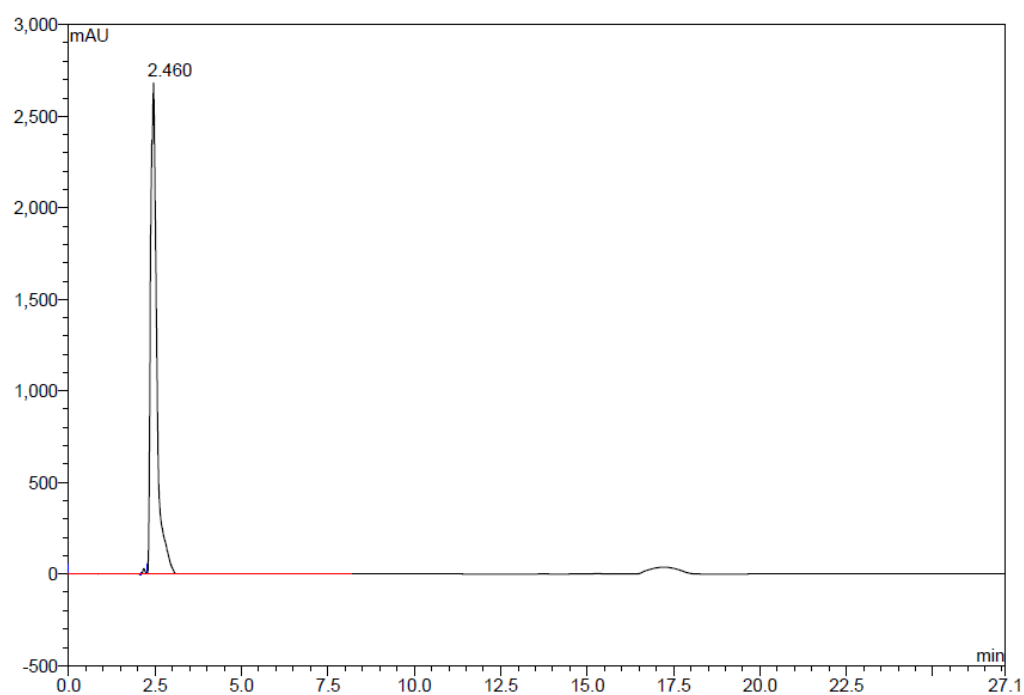
The peptide was cleaved from the resin using a solution of 96.5% TFA, 2.5% water and 1% TIPS (2.5 mL) and left to stir for 1 h. After this time, the entire solution was transferred to a Falcon tube and 12 mL of diethyl ether was added to precipitate the peptide. The Falcon tube was then centrifuged for 10 min at 4000 rpm and 4 °C before decanting off the diethyl ether solution. This process was performed 3 times in total before re-dissolving the peptide in water and lyophilising. The peptide was purified using a gradient of 10 – 55 % B over 15 min (A = water, B = acetonitrile) to yield 0.3 mg of product (0.4%).

LCMS:



Analysis: m/z (ES^+) 758.50 ($[M + 5H]^5+$).

Analytical HPLC: The purified peptide was analysed by analytical HPLC using an ACE C8-300 analytical column (150 x 10 mm, flow rate of 1.0 mL/min), with a linear gradient of 2 – 98% B over 20 min (A = water, B = acetonitrile).



Triple Ring 2nd Ring Lanthionine (215)



(red indicates the use of an Hmb protected amino acid)

The reaction was carried out on a 100 mg scale using pre-loaded Fmoc-Trp(Boc)-NovaSyn® resin (loading 0.20 mmol/g) using the amounts listed below:

Amino Acid	Mass (g)	Vol. DMF (mL)
Lanthionine 142	0.0332	4.0
Fmoc-Cys(Trt)-OH	0.1874	2.4
Fmoc-Asp(O ^t Bu)-OH	0.0329	0.6
Fmoc-Glu(O ^t Bu)-OH	0.0681	1.2
Fmoc-(FmocHmb)-Gly-OH	0.0347	0.6
Fmoc-Lys(Boc)-OH	0.0750	1.2
Fmoc-(FmocHmb)-Lys(Boc)-OH	0.1985	1.8
Fmoc-Leu-OH	0.0283	0.6
Fmoc-(FmocHmb)-Leu-OH	0.0569	0.6
Fmoc-Met-OH	0.0594	1.2
Fmoc-Gln(Trt)-OH	0.0489	0.6
Fmoc-Arg(Pbf)-OH	0.1038	1.2
Fmoc-Ser(^t Bu)-OH	0.0307	0.6
Fmoc-Thr(^t Bu)-OH	0.0318	0.6
Fmoc-Val-OH	0.0272	0.6
Fmoc-Trp(Boc)-OH	0.1685	2.4
Fmoc-Tyr(^t Bu)-OH	0.368	0.6

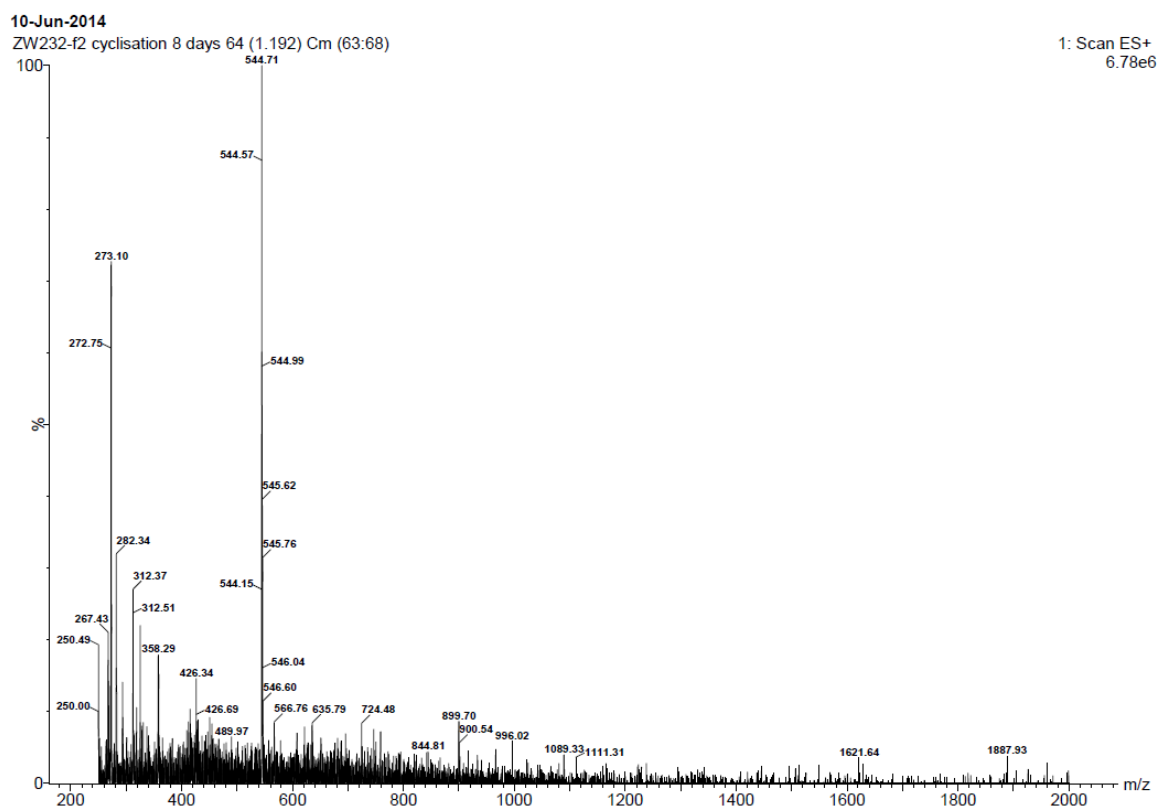
The resin was added to a reaction syringe, washed with DMF (4 x 1.5 mL) and left to swell for 30 min in 1.5 mL DMF. After this time, the Fmoc group was removed using the standard Fmoc deprotection step described in method 2 above. Protected glycine (0.6 mL, 4 eq.) was added to the reaction syringe and coupled using HBTU (33.2 mg in 0.6 mL DMF, 4 eq.) and DIPEA (36.4 µL in 0.2636 mL DMF, 8 eq.). Successive Fmoc deprotections and amino acid couplings were carried out using general method 2 with 0.6 mL of protected amino acid solution per coupling step. Each coupling step was repeated a second time prior to each deprotection with fresh amino acid solution, giving a total agitation time of 80 min.

Lanthionine was added to the peptide sequence using the microwave protocol described in the general experimental section, using PyAOP (52.1 mg, 5 eq.), HOAt (13.6 mg, 5 eq.) and DIPEA (34.6 µL, 10 eq.) for both the coupling and cyclisation steps. The simultaneous allyl and Alloc deprotection was carried out according to the general protocol described above using tetrakis(triphenylphosphine) palladium (0) (23.1 mg, 1 eq.) and 1,3-dimethylbarbituric acid (31.2 mg, 10 eq.).

Selective deprotection of the S(Tmp) groups from the orthogonally protected cysteine residues was carried out using 5% DTT in 0.1M NMM in DMF (1.5 mL) (3 x 30 min) before washing with DMF (4 x 1.5 mL). The deprotected cysteines were then cyclised using *N*-chlorosuccinimide (53.4 mg, 2 eq.) in DMF (2 mL) for 1.5 h before again washing with DMF (4 x 1.5 mL).

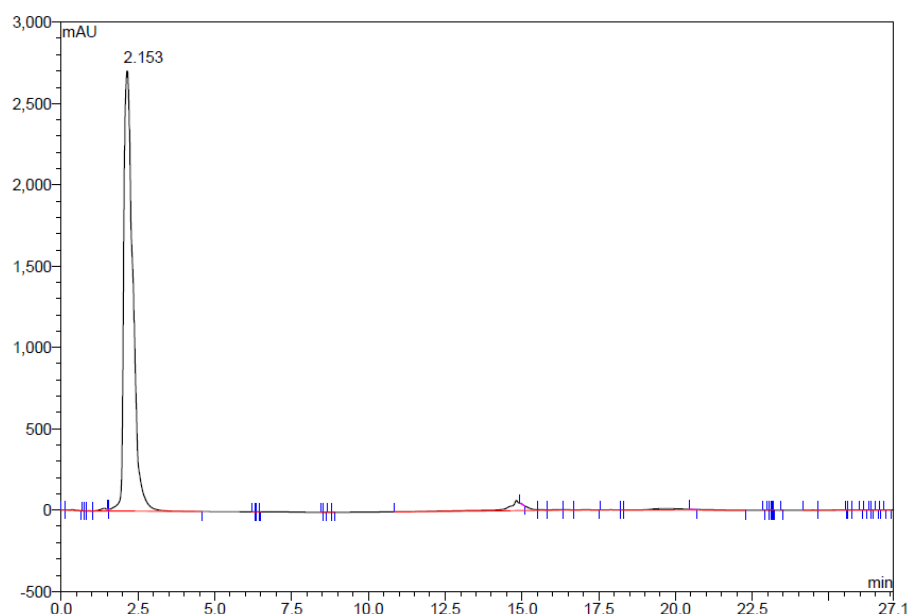
The peptide was cleaved from the resin using a solution of 96.5% TFA, 2.5% water and 1% TIPS (2.5 mL) and left to stir for 1 h. After this time, the entire solution was transferred to a Falcon tube and 12 mL of diethyl ether was added to precipitate the peptide. The Falcon tube was then centrifuged for 10 min at 4000 rpm and 4 °C before decanting off the diethyl ether solution. This process was performed 3 times in total before re-dissolving the peptide in water and lyophilising. The peptide was purified using a gradient of 10 – 55 % B over 15 min (A = water, B = acetonitrile) to yield 5 mg of product (7%).

LCMS:

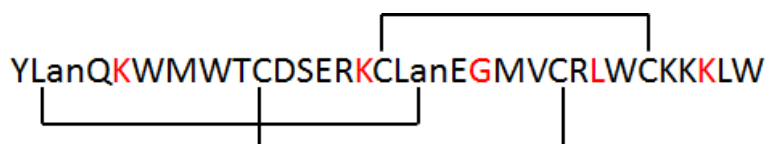


Analysis: m/z (ES^+) 544.64 ($[M + 7H]^7+$).

Analytical HPLC: The purified peptide was analysed by analytical HPLC using an ACE C8-300 analytical column (150 x 10 mm, flow rate of 1.0 mL/min), with a linear gradient of 2 – 98% B over 20 min (A = water, B = acetonitrile).



Triple Ring 3rd Ring Lanthionine (216)



(red indicates the use of an Hmb protected amino acid)

The reaction was carried out on a 100 mg scale using pre-loaded Fmoc-Trp(Boc)-NovaSyn® resin (loading 0.20 mmol/g) using the amounts listed below:

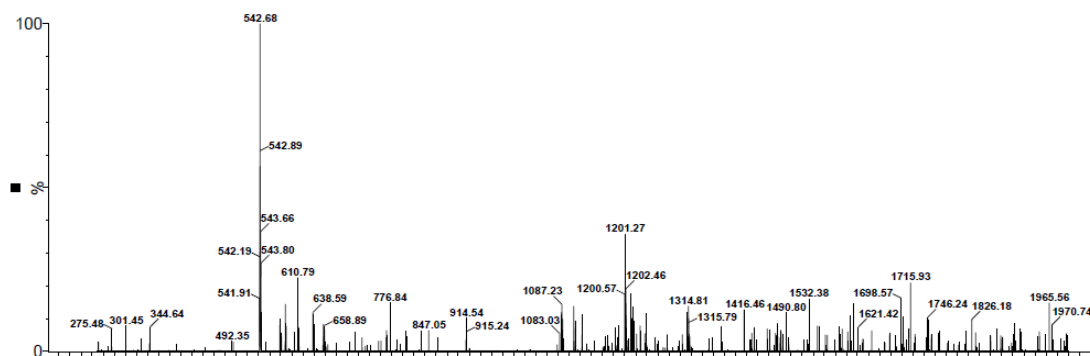
Amino Acid	Mass (g)	Vol. DMF (mL)
Lanthionine 142	0.0332	4.0
Fmoc-Cys(Trt)-OH	0.1874	2.4
Fmoc-Asp(O ^t Bu)-OH	0.0329	0.6
Fmoc-Glu(O ^t Bu)-OH	0.0681	1.2
Fmoc-(FmocHmb)-Gly-OH	0.0347	0.6
Fmoc-Lys(Boc)-OH	0.0750	1.2
Fmoc-(FmocHmb)-Lys(Boc)-OH	0.1985	1.8
Fmoc-Leu-OH	0.0283	0.6
Fmoc-(FmocHmb)-Leu-OH	0.0569	0.6
Fmoc-Met-OH	0.0594	1.2
Fmoc-Gln(Trt)-OH	0.0489	0.6
Fmoc-Arg(Pbf)-OH	0.1038	1.2
Fmoc-Ser(^t Bu)-OH	0.0307	0.6
Fmoc-Thr(^t Bu)-OH	0.0318	0.6
Fmoc-Val-OH	0.0272	0.6
Fmoc-Trp(Boc)-OH	0.1685	2.4
Fmoc-Tyr(^t Bu)-OH	0.368	0.6

The resin was added to a reaction syringe, washed with DMF (4 x 1.5 mL) and left to swell for 30 min in 1.5 mL DMF. After this time, the Fmoc group was removed using the standard Fmoc deprotection step described in method 2 above. Protected glycine (0.6 mL, 4 eq.) was added to the reaction syringe and coupled using HBTU (33.2 mg in 0.6 mL DMF, 4 eq.) and DIPEA (36.4 μ L in 0.2636 mL DMF, 8 eq.). Successive Fmoc deprotections and amino acid couplings were carried out using general method 2 with 0.6 mL of protected amino acid solution per coupling step. Each coupling step was repeated a second time prior to each deprotection with fresh amino acid solution, giving a total agitation time of 80 min.

Lanthionine was added to the peptide sequence using the microwave protocol described in the general experimental section, using PyAOP (52.1 mg, 5 eq.), HOAt (13.6 mg, 5 eq.) and DIPEA (34.6 μ L, 10 eq.) for both the coupling and cyclisation steps. The simultaneous allyl and Alloc deprotection was carried out according to the general protocol described above using tetrakis(triphenylphosphine) palladium (0) (23.1 mg, 1 eq.) and 1,3-dimethylbarbituric acid (31.2 mg, 10 eq.).

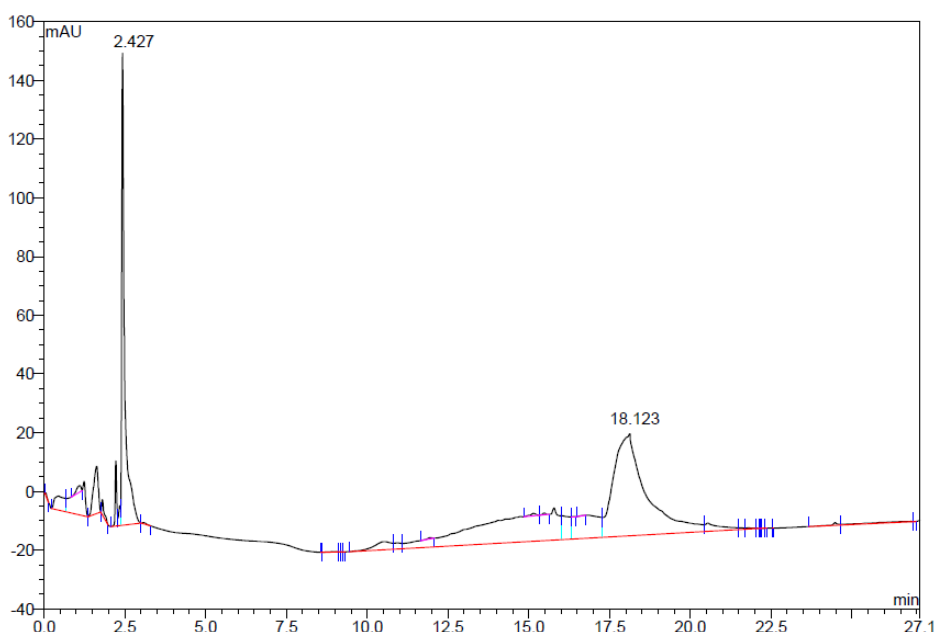
The peptide was cleaved from the resin using a solution of 96.5% TFA, 2.5% water and 1% TIPS (2.5 mL) and left to stir for 1 h. After this time, the entire solution was transferred to a Falcon tube and 12 mL of diethyl ether was added to precipitate the peptide. The Falcon tube was then centrifuged for 10 min at 4000 rpm and 4 °C before decanting off the diethyl ether solution. This process was performed 3 times in total before re-dissolving the peptide in water and lyophilising. The peptide was purified using a gradient of 10 – 55 % B over 15 min (A = water, B = acetonitrile) to yield 0.8 mg of product (1%).

LCMS:



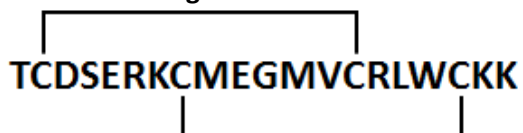
Analysis: m/z (ES⁻) 544.64 ([M - 7H]⁷⁺).

Analytical HPLC: The purified peptide was analysed by analytical HPLC using an ACE C8-300 analytical column (150 x 10 mm, flow rate of 1.0 mL/min), with a linear gradient of 2 – 98% B over 20 min (A = water, B = acetonitrile).



7.3.5 Attempted Syntheses of Double Ring Analogues of ProTx-II

C-Terminal Double Ring Disulfide Analogue 195



The reaction was carried out on a 100 mg scale using pre-loaded Fmoc-Lys(Boc)-NovaSyn® TGT resin (loading = 0.20 mmol/g). The cysteine side chains were protected either with trityl, mmt or AcM groups and using the amounts listed below:

Amino Acid	Mass (mg)	Vol. DMF (mL)
Fmoc-Cys(Trt)-OH	93.7	1.2
Fmoc-Cys(MMT)-OH	98.5	1.2
Fmoc-Cys(Acm)-OH	66.3	1.2
Fmoc-Asp(O ^t Bu)-OH	32.9	0.6
Fmoc-Glu(O ^t Bu)-OH	68.1	1.2
Fmoc-Gly-OH	23.8	0.6
Fmoc-Lys(Boc)-OH	112.4	1.8
Fmoc-Leu-OH	28.3	1.2
Fmoc-Met-OH	59.4	1.2
Fmoc-Arg(Pbf)-OH	103.8	0.6
Fmoc-Ser(^t Bu)-OH	30.7	0.6
Fmo-Thr(^t Bu)-OH	31.8	0.6
Fmoc-Val-OH	27.2	0.6
Fmoc-Trp(Boc)-OH	42.1	0.6

The resin was added to a reaction syringe, washed with DMF (4 x 1.5 mL) and left to swell for 30 min in 1.5 mL DMF. After this time, protected lysine (0.6 mL, 4 eq.) was added to the reaction syringe and coupled using HBTU (30.3 mg in 0.6 mL DMF, 4 eq.) and DIPEA (27.7 μ L in 0.2723 mL DMF, 8 eq.). Successive Fmoc deprotections and amino acid couplings were carried out using general method 1 with 0.6 mL of protected amino acid solution per coupling step.

The peptide was then washed with DMF (4 x 1.5 mL), CH₂Cl₂ (4 x 1.5 mL), methanol (4 x 1.5 mL) and diethyl ether (4 x 1.5 mL) before drying in a desiccator for 45 min. Cleavage and cyclisation conditions varied depending on the combination of protecting groups as summarised below.

Double Trityl Protection: The peptide was cleaved using a solution of 94% TFA, 2.5% water, 2.5% EDT and 1% TIPS (2.5 mL) was then added to the resin and left to agitate for 30 min on the platform shaker. After this time, the entire solution was transferred to a Falcon tube and 12 mL of diethyl ether was added to precipitate the peptide. The cleavage procedure was then repeated with fresh cleavage solution (2.5 mL containing 94% TFA, 2.5% water, 2.5% EDT and 1% TIPS) and left to agitate for a further 40 min. The entire solution was again transferred to a Falcon tube before addition of 12 mL of diethyl ether to precipitate the peptide. The Falcon tube was then centrifuged for 10 min at 4000 rpm and 4 °C before decanting off the diethyl ether solution. This process was performed 3 times in total before re-dissolving the peptide in water and lyophilising. The peptide was dissolved in water (0.1 mg/mL) and left for 7 days before concentrating *in vacuo*.

Trityl/MMT protection: The peptide was cleaved using a solution of 10% v/v trifluoroethanol and 10% v/v acetic acid in CH₂Cl₂ which was left to stir for 1h before filtering off the liquid and concentrating *in vacuo*. The peptide was dissolved in 1% v/v trifluoroacetic acid in DCM and left to stir overnight before concentrating *in vacuo*. The peptide was then re-dissolved in a solution of 96.5% TFA, 2.5% water and 1% TIPS (2.5 mL) and left to stir for 1 h. After this time, the entire solution was transferred to a Falcon tube and 12 mL of diethyl ether was added to precipitate the peptide. The Falcon tube was then centrifuged for 10 min at 4000 rpm and 4 °C before decanting off the diethyl ether solution. This process was performed 3 times in total before re-dissolving the peptide in water and lyophilising.

Trityl/Acm protection:

Method 1: The peptide was cleaved from the resin using a solution of 96.5% TFA, 2.5% water and 1% TIPS (2.5 mL) and left to stir for 1 h. After this time, the entire solution was

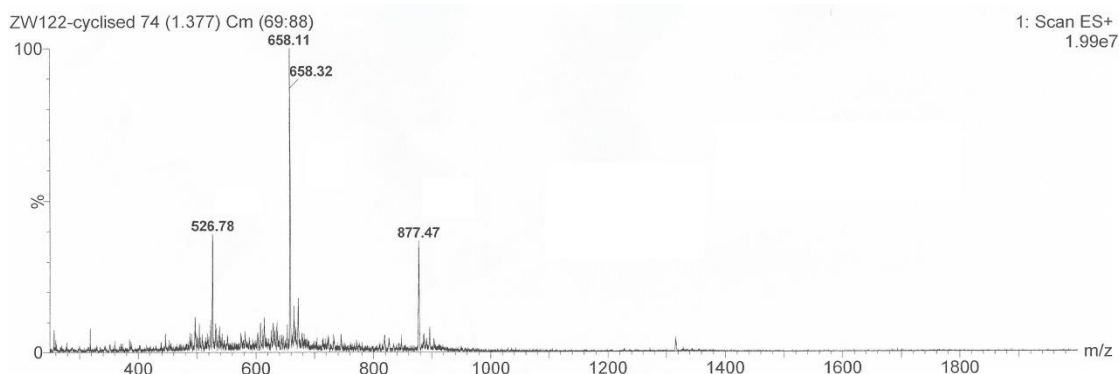
transferred to a Falcon tube and 12 mL of diethyl ether was added to precipitate the peptide. The Falcon tube was then centrifuged for 10 min at 4000 rpm and 4 °C before decanting off the diethyl ether solution. This process was performed 3 times in total before re-dissolving the peptide in water and lyophilising. The peptide was then left to stir in water for 2 days to cyclise. The peptide was re-dissolved in DMF (1.2 mL) and added drop-wise to a stirred solution of iodine (20.6 mg, 0.081 mmol, 8 eq.) in DMF (12 mL) over 30 min. The reaction was left to stir for a further 20 min before dilution with CH₂Cl₂ (15 mL). Ascorbic acid (10 mL, 0.2 M) and sodium acetate (10 mL, 0.5 M) were added and the product was extracted twice with 10% v/v methanol in chloroform (10 mL) and once with CH₂Cl₂ (10 mL). The combined organic layers were washed with water (20 mL), dried (Na₂SO₄) and most of the solvent was removed *in vacuo* before precipitation in diethyl ether. The solution was transferred to a Falcon tube and centrifuged for 10 min at 4000 rpm and 4 °C before decanting off the diethyl ether solution. The peptide was then re-dissolved in water and lyophilised.

Method 2: Iodine (15.2 mg, 0.12 mmol, 6 eq.) in a 3:1 solution of hexafluoroisopropanol to chloroform (2 mL) was added to the peptide syringe and left to stir for 30 min. After this time, the peptide was washed with chloroform (10 x 1.5 mL) and DMF (5 x 1.5 mL). A second portion of iodine (15.2 mg, 0.12 mmol, 6 eq.) in DMF (2 mL) was then added and left to stir for a further 30 min. After this time, the peptide was washed again with chloroform (10 x 1.5 mL) and DMF (5 x 1.5 mL). The peptide was then cleaved from the resin using a solution of 96.5% TFA, 2.5% water and 1% TIPS (2.5 mL), which was left to agitate on the platform shaker for 1 h. After this time, the entire solution was transferred to a Falcon tube and 12 mL of diethyl ether was added to precipitate the peptide. The Falcon tube was then centrifuged for 10 min at 4000 rpm and 4 °C before decanting off the diethyl ether solution. This process was performed 3 times in total before re-dissolving the peptide in water and lyophilising.

None of these methods produced the desired product.

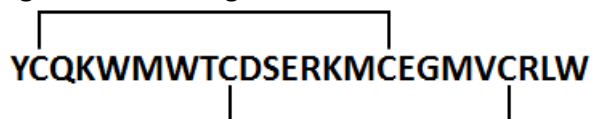
HPLC purification from the use of Trt/MMT protecting groups, isolated a small amount of the peptide minus the terminal tryptophan (MW = 2629).

LC-MS trace:



Analysis: m/z (ES^+) 877.46 ($[M + 3H]^{3+}$), 658.11 ($[M + 4H]^{4+}$), 526.78 ($[M + 5H]^{5+}$).

N-Terminal Double Ring Disulfide Analogue 196



The reaction was carried out on a 100 mg scale using pre-loaded Fmoc-Trp(Boc)-NovaSyn® TGT resin resin (loading = 0.20 mmol/g). The cysteine side chains were protected either with trityl, mmt, Acn or S^tBu groups and using the amounts listed below:

Amino Acid	Mass (mg)	Vol. DMF (mL)
Fmoc-Cys(Trt)-OH	93.7	1.2
Fmoc-Cys(MMT)-OH	98.5	1.2
Fmoc-Cys(Acm)-OH	66.3	1.2
Fmoc-Cys(S ^t Bu)-OH	69.1	1.2
Fmoc-Asp(O ^t Bu)-OH	32.9	0.6
Fmoc-Glu(O ^t Bu)-OH	68.1	1.2
Fmoc-Gly-OH	23.8	0.6
Fmoc-Lys(Boc)-OH	75.0	1.2
Fmoc-Leu-OH	28.3	0.6
Fmoc-Met-OH	89.1	1.8
Fmoc-Gln(Trt)-OH	48.9	0.6
Fmoc-Arg(Pbf)-OH	103.8	1.2
Fmoc-Ser(^t Bu)-OH	30.7	0.6
Fmoc-Thr(^t Bu)-OH	31.8	0.6
Fmoc-Val-OH	27.2	0.6
Fmoc-Trp(Boc)-OH	42.1	0.6
Fmoc-Tyr(^t Bu)-OH	36.8	0.6

The resin was added to a reaction syringe, washed with DMF (4 x 1.5 mL) and left to swell for 30 min in 1.5 mL DMF. After this time, protected lysine (0.6 mL, 4 eq.) was added to the reaction syringe and coupled using HBTU (30.3 mg in 0.6 mL DMF, 4 eq.) and DIPEA (27.7 μ L in 0.2723 mL DMF, 8 eq.). Successive Fmoc deprotections and amino acid couplings were

carried out using general method 1 with 0.6 mL of protected amino acid solution per coupling step.

The peptide was then washed with DMF (4 x 1.5 mL), CH₂Cl₂ (4 x 1.5 mL), methanol (4 x 1.5 mL) and diethyl ether (4 x 1.5 mL) before drying in a desiccator for 45 min. Cleavage and cyclisation conditions varied depending on the combination of protecting groups as summarised below.

Double Trityl Protection: The peptide was cleaved using a solution of 94% TFA, 2.5% water, 2.5% EDT and 1% TIPS (2.5 mL) was then added to the resin and left to agitate for 30 min on the platform shaker. After this time, the entire solution was transferred to a Falcon tube and 12 mL of diethyl ether was added to precipitate the peptide. The cleavage procedure was then repeated with fresh cleavage solution (2.5 mL containing 94% TFA, 2.5% water, 2.5% EDT and 1% TIPS) and left to agitate for a further 40 min. The entire solution was again transferred to a Falcon tube before addition of 12 mL of diethyl ether to precipitate the peptide. The Falcon tube was then centrifuged for 10 min at 4000 rpm and 4 °C before decanting off the diethyl ether solution. This process was performed 3 times in total before re-dissolving the peptide in water and lyophilising. The peptide was dissolved in water (0.1 mg/mL) and left for 7 days before concentrating *in vacuo*.

Trityl/MMT protection: The peptide was cleaved using a solution of 10% v/v trifluoroethanol and 10% v/v acetic acid in CH₂Cl₂ which was left to stir for 1h before filtering off the liquid and concentrating *in vacuo*. The peptide was dissolved in 1% v/v trifluoroacetic acid in DCM and left to stir overnight before concentrating *in vacuo*. The peptide was then re-dissolved in a solution of 96.5% TFA, 2.5% water and 1% TIPS (2.5 mL) and left to stir for 1 h. After this time, the entire solution was transferred to a Falcon tube and 12 mL of diethyl ether was added to precipitate the peptide. The Falcon tube was then centrifuged for 10 min at 4000 rpm and 4 °C before decanting off the diethyl ether solution. This process was performed 3 times in total before re-dissolving the peptide in water and lyophilising.

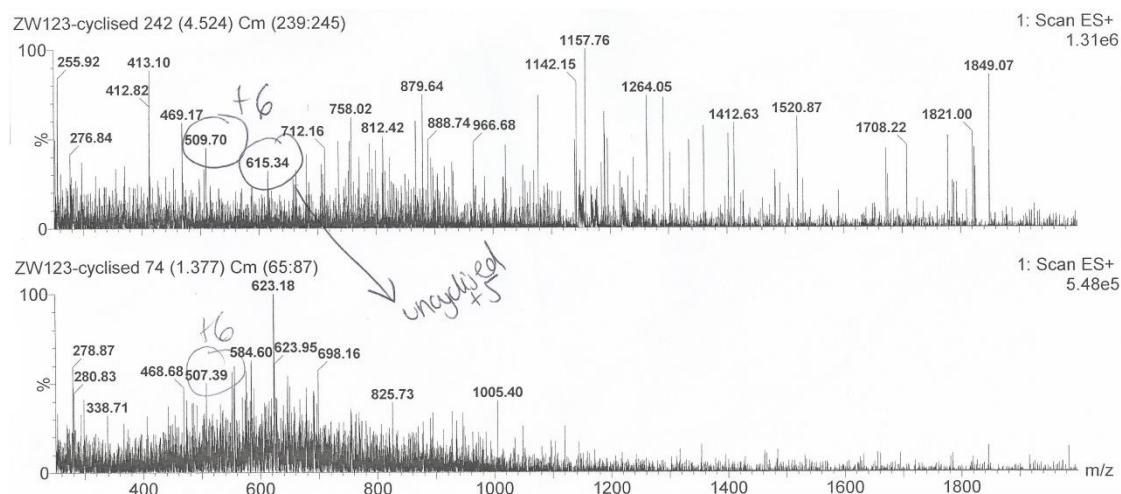
Trityl/Acm protection: The peptide was cleaved from the resin using a solution of 96.5% TFA, 2.5% water and 1% TIPS (2.5 mL) and left to stir for 1 h. After this time, the entire solution was transferred to a Falcon tube and 12 mL of diethyl ether was added to precipitate the peptide. The Falcon tube was then centrifuged for 10 min at 4000 rpm and 4 °C before decanting off the diethyl ether solution. This process was performed 3 times in total before re-dissolving the peptide in water and lyophilising. The peptide was then left to stir in water for 2 days to cyclise. The peptide was re-dissolved in DMF (1.2 mL) and added drop-wise to a

stirred solution of iodine (20.6 mg, 0.081 mmol, 8 eq.) in DMF (12 mL) over 30 min. The reaction was left to stir for a further 20 min before dilution with CH₂Cl₂ (15 mL). Ascorbic acid (10 mL, 0.2 M) and sodium acetate (10 mL, 0.5 M) were added and the product was extracted twice with 10% v/v methanol in chloroform (10 mL) and once with CH₂Cl₂ (10 mL). The combined organic layers were washed with water (20 mL), dried (Na₂SO₄) and most of the solvent was removed *in vacuo* before precipitation in diethyl ether. The solution was transferred to a Falcon tube and centrifuged for 10 min at 4000 rpm and 4 °C before decanting off the diethyl ether solution. The peptide was then re-dissolved in water and lyophilised.

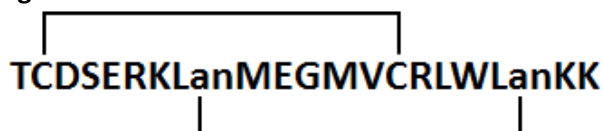
Trityl/S^tBu protection: The peptide was cleaved from the resin using a solution of 96.5% TFA, 2.5% water and 1% TIPS (2.5 mL) and left to stir for 30 min. After this time, the entire solution was transferred to a Falcon tube and 12 mL of diethyl ether was added to precipitate the peptide. The process was repeated with fresh cleavage solution and left to stir for a further 40 min before again precipitating in to diethyl ether. The Falcon tube was then centrifuged for 10 min at 4000 rpm and 4 °C before decanting off the diethyl ether solution. This process was performed 3 times in total before re-dissolving the peptide in water and lyophilising. The peptide was then left to stir in water for 4 days to cyclise before concentrating *in vacuo*. To remove the S^tBu group, the peptide was re-dissolved in TFA (5 mL) and trichloromethylsilane (2.0 mL, 17.0 mmol, 250 eq.) and diphenyl sulfoxide (0.275 g, 1.36 mmol, 20 eq.) were added. The solution was left to stir for 2 h before addition of ether to precipitate the peptide. The solution was transferred to a Falcon tube and centrifuged for 10 min at 4000 rpm and 4 °C before decanting off the diethyl ether solution. The peptide was washed twice more with ether before re-dissolving in water and lyophilising.

None of these methods produced the desired product.

LCMS trace shows a mixture an inseparable mixture of the +6 and uncyclised +5 ions:



C-Terminal Double Ring with Terminal Lanthionine 210



The reaction was carried out on a 100 mg scale using pre-loaded Fmoc-Lys(Boc)-NovaSyn® TGT resin resin (loading = 0.20 mmol/g) and using the amounts listed below:

Amino Acid	Mass (mg)	Vol. DMF (mL)
Lanthionine 142	33.2	4.0
Fmoc-Cys(Trt)-OH	93.7	1.2
Fmoc-Asp(O ^t Bu)-OH	32.9	0.6
Fmoc-Glu(O ^t Bu)-OH	68.1	1.2
Fmoc-Gly-OH	23.8	0.6
Fmoc-Lys(Boc)-OH	112.4	1.8
Fmoc-Leu-OH	28.3	1.2
Fmoc-Met-OH	59.4	1.2
Fmoc-Arg(Pbf)-OH	103.8	0.6
Fmoc-Ser(^t Bu)-OH	30.7	0.6
Fmo-Thr(^t Bu)-OH	31.8	0.6
Fmoc-Val-OH	27.2	0.6
Fmoc-Trp(Boc)-OH	42.1	0.6

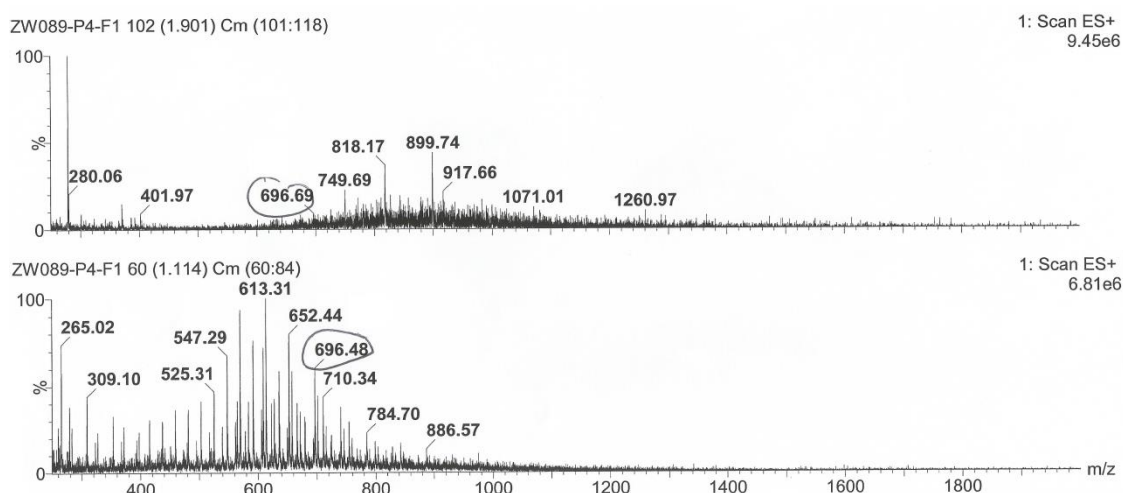
The resin was added to a reaction syringe, washed with DMF (4 x 1.5 mL) and left to swell for 30 min in 1.5 mL DMF. After this time, the Fmoc group was removed using the standard Fmoc deprotection step described in method 2 above. Protected glycine (0.6 mL, 4 eq.) was added to the reaction syringe and coupled using HBTU (33.2 mg in 0.6 mL DMF, 4 eq.) and DIPEA (36.4 µL in 0.2636 mL DMF, 8 eq.). Successive Fmoc deprotections and amino acid couplings were carried out using general method 2 with 0.6 mL of protected amino acid

solution per coupling step. Each coupling step was repeated a second time prior to each deprotection with fresh amino acid solution, giving a total agitation time of 80 min.

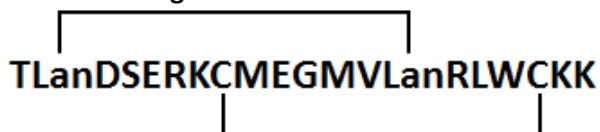
Lanthionine was added to the peptide sequence using the microwave protocol described in the general experimental section, using PyAOP (52.1 mg, 5 eq.), HOAt (13.6 mg, 5 eq.) and DIPEA (34.6 μ L, 10 eq.) for both the coupling and cyclisation steps. The simultaneous allyl and Alloc deprotection was carried out according to the general protocol described above using tetrakis(triphenylphosphine) palladium (0) (23.1 mg, 1 eq.) and 1,3-dimethylbarbituric acid (31.2 mg, 10 eq.). The peptide was cleaved under standard conditions, washed with ether and lyophilised.

None of the desired product was produced.

LCMS traces shows a peak close to the mass of the +4 ion (circled) but is not the desired mass:



C-Terminal Double with Middle Ring Lanthionine 211



The reaction was carried out on a 100 mg scale using pre-loaded Fmoc-Lys(Boc)-NovaSyn® TGT resin resin (loading = 0.20 mmol/g) and using the amounts listed below:

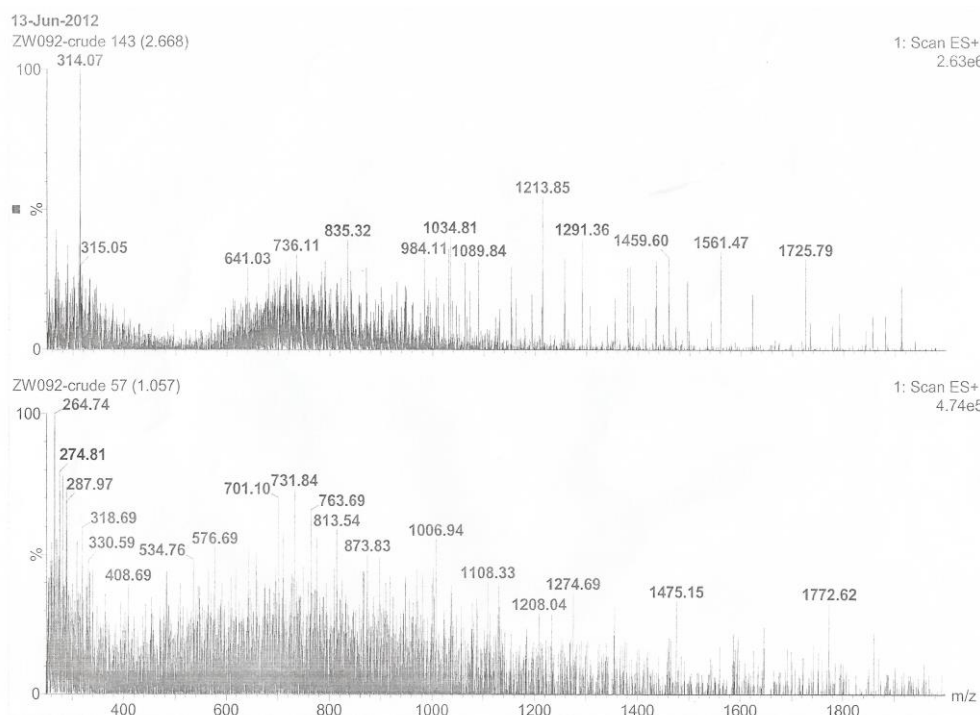
Amino Acid	Mass (mg)	Vol. DMF (mL)
Lanthionine 142	33.2	4.0
Fmoc-Cys(Trt)-OH	93.7	1.2
Fmoc-Asp(O ^t Bu)-OH	32.9	0.6
Fmoc-Glu(O ^t Bu)-OH	68.1	1.2
Fmoc-Gly-OH	23.8	0.6
Fmoc-Lys(Boc)-OH	112.4	1.8
Fmoc-Leu-OH	28.3	1.2
Fmoc-Met-OH	59.4	1.2
Fmoc-Arg(Pbf)-OH	103.8	0.6
Fmoc-Ser(^t Bu)-OH	30.7	0.6
Fmo-Thr(^t Bu)-OH	31.8	0.6
Fmoc-Val-OH	27.2	0.6
Fmoc-Trp(Boc)-OH	42.1	0.6

The resin was added to a reaction syringe, washed with DMF (4 x 1.5 mL) and left to swell for 30 min in 1.5 mL DMF. After this time, the Fmoc group was removed using the standard Fmoc deprotection step described in method 2 above. Protected glycine (0.6 mL, 4 eq.) was added to the reaction syringe and coupled using HBTU (33.2 mg in 0.6 mL DMF, 4 eq.) and DIPEA (36.4 μ L in 0.2636 mL DMF, 8 eq.). Successive Fmoc deprotections and amino acid couplings were carried out using general method 2 with 0.6 mL of protected amino acid solution per coupling step. Each coupling step was repeated a second time prior to each deprotection with fresh amino acid solution, giving a total agitation time of 80 min.

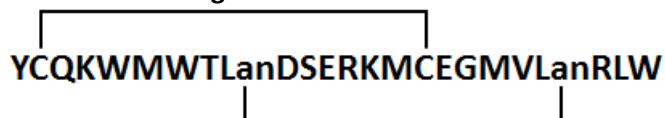
Lanthionine was added to the peptide sequence using the microwave protocol described in the general experimental section, using PyAOP (52.1 mg, 5 eq.), HOAt (13.6 mg, 5 eq.) and DIPEA (34.6 μ L, 10 eq.) for both the coupling and cyclisation steps. The simultaneous allyl and Alloc deprotection was carried out according to the general protocol described above using tetrakis(triphenylphosphine) palladium (0) (23.1 mg, 1 eq.) and 1,3-dimethylbarbituric acid (31.2 mg, 10 eq.). The peptide was cleaved under standard conditions, washed with ether and lyophilised.

None of the desired product was produced.

LCMS trace shows none of the desired product:



N-Terminal Double with Middle Ring Lanthionine 212



The reaction was carried out on a 100 mg scale using pre-loaded Fmoc-Trp(Boc)-NovaSyn® TGT resin resin (loading = 0.20 mmol/g) and using the amounts listed below:

Amino Acid	Mass (mg)	Vol. DMF (mL)
Lanthionine 142	33.2	4.0
Fmoc-Cys(Trt)-OH	93.7	1.2
Fmoc-Asp(O ^t Bu)-OH	32.9	0.6
Fmoc-Glu(O ^t Bu)-OH	68.1	1.2
Fmoc-Gly-OH	23.8	0.6
Fmoc-Lys(Boc)-OH	75.0	1.2
Fmoc-Leu-OH	28.3	0.6
Fmoc-Met-OH	89.1	1.8
Fmoc-Gln(Trt)-OH	48.9	0.6
Fmoc-Arg(Pbf)-OH	103.8	1.2
Fmoc-Ser(^t Bu)-OH	30.7	0.6
Fmoc-Thr(^t Bu)-OH	31.8	0.6
Fmoc-Val-OH	27.2	0.6
Fmoc-Trp(Boc)-OH	42.1	0.6
Fmoc-Tyr(^t Bu)-OH	36.8	0.6

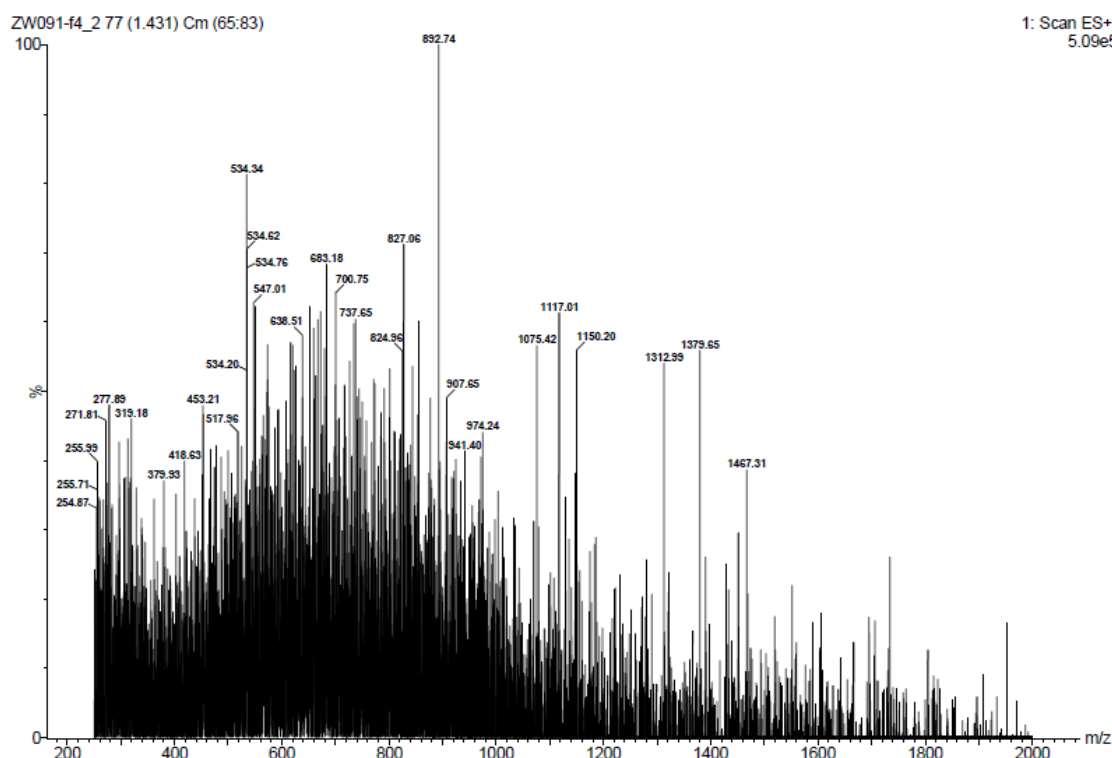
The resin was added to a reaction syringe, washed with DMF (4 x 1.5 mL) and left to swell for 30 min in 1.5 mL DMF. After this time, the Fmoc group was removed using the standard

Fmoc deprotection step described in method 2 above. Protected glycine (0.6 mL, 4 eq.) was added to the reaction syringe and coupled using HBTU (33.2 mg in 0.6 mL DMF, 4 eq.) and DIPEA (36.4 μ L in 0.2636 mL DMF, 8 eq.). Successive Fmoc deprotections and amino acid couplings were carried out using general method 2 with 0.6 mL of protected amino acid solution per coupling step. Each coupling step was repeated a second time prior to each deprotection with fresh amino acid solution, giving a total agitation time of 80 min.

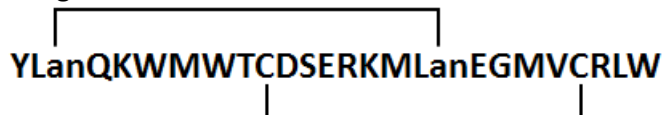
Lanthionine was added to the peptide sequence using the microwave protocol described in the general experimental section, using PyAOP (52.1 mg, 5 eq.), HOAt (13.6 mg, 5 eq.) and DIPEA (34.6 μ L, 10 eq.) for both the coupling and cyclisation steps. The simultaneous allyl and Alloc deprotection was carried out according to the general protocol described above using tetrakis(triphenylphosphine) palladium (0) (23.1 mg, 1 eq.) and 1,3-dimethylbarbituric acid (31.2 mg, 10 eq.). The peptide was cleaved under standard conditions, washed with ether and lyophilised.

None of the desired product was produced.

LCMS trace shows none of the desired product:



N-Terminal Double Ring with Terminal Lanthionine 213



The reaction was carried out on a 100 mg scale using pre-loaded Fmoc-Trp(Boc)-NovaSyn® TGT resin resin (loading = 0.20 mmol/g) and using the amounts listed below:

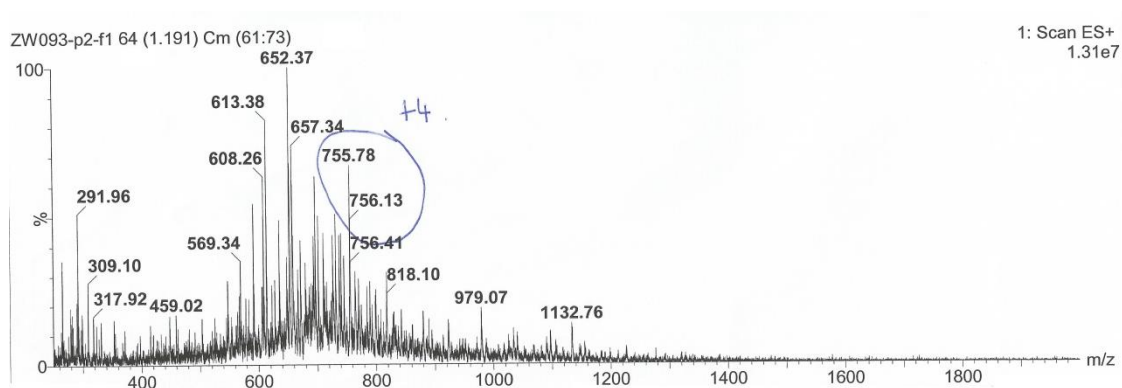
Amino Acid	Mass (mg)	Vol. DMF (mL)
Lanthionine 142	33.2	4.0
Fmoc-Cys(Trt)-OH	93.7	1.2
Fmoc-Asp(O ^t Bu)-OH	32.9	0.6
Fmoc-Glu(O ^t Bu)-OH	68.1	1.2
Fmoc-Gly-OH	23.8	0.6
Fmoc-Lys(Boc)-OH	75.0	1.2
Fmoc-Leu-OH	28.3	0.6
Fmoc-Met-OH	89.1	1.8
Fmoc-Gln(Trt)-OH	48.9	0.6
Fmoc-Arg(Pbf)-OH	103.8	1.2
Fmoc-Ser(^t Bu)-OH	30.7	0.6
Fmoc-Thr(^t Bu)-OH	31.8	0.6
Fmoc-Val-OH	27.2	0.6
Fmoc-Trp(Boc)-OH	42.1	0.6
Fmoc-Tyr(^t Bu)-OH	36.8	0.6

The resin was added to a reaction syringe, washed with DMF (4 x 1.5 mL) and left to swell for 30 min in 1.5 mL DMF. After this time, the Fmoc group was removed using the standard Fmoc deprotection step described in method 2 above. Protected glycine (0.6 mL, 4 eq.) was added to the reaction syringe and coupled using HBTU (33.2 mg in 0.6 mL DMF, 4 eq.) and DIPEA (36.4 µL in 0.2636 mL DMF, 8 eq.). Successive Fmoc deprotections and amino acid couplings were carried out using general method 2 with 0.6 mL of protected amino acid solution per coupling step. Each coupling step was repeated a second time prior to each deprotection with fresh amino acid solution, giving a total agitation time of 80 min.

Lanthionine was added to the peptide sequence using the microwave protocol described in the general experimental section, using PyAOP (52.1 mg, 5 eq.), HOAt (13.6 mg, 5 eq.) and DIPEA (34.6 µL, 10 eq.) for both the coupling and cyclisation steps. The simultaneous allyl and Alloc deprotection was carried out according to the general protocol described above using tetrakis(triphenyl)phosphine palladium (0) (23.1 mg, 1 eq.) and 1,3-dimethylbarbituric acid (31.2 mg, 10 eq.). The peptide was cleaved under standard conditions, washed with ether and lyophilised.

None of the desired product was produced.

LCMS shows the +4 ion as part of an inseparable mixture:

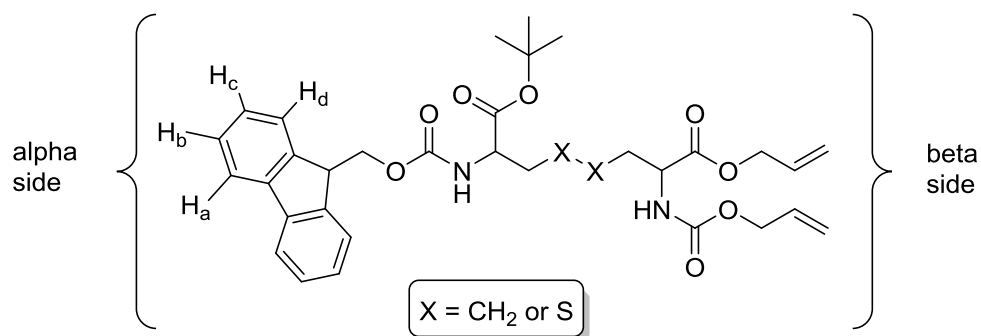


7.4 Experimental for the Synthesis of Cystathionine (Chapter 4)

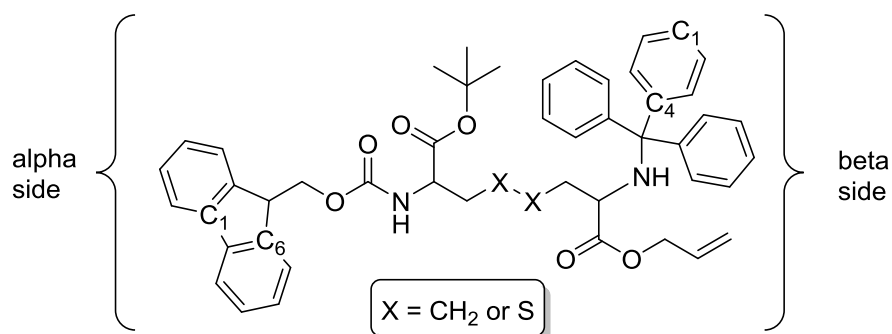
7.4.1 Key to NMR Assignments:

The following nomenclature is used throughout this chapter when assigning NMRs:

¹H NMR:

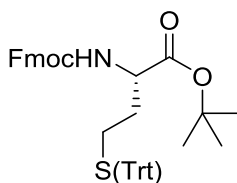


¹³C NMR:



7.4.2 Experimental for Cystathionine Synthesis Work

(S)-tert-Butyl N-(9(Fluorenylmethoxycarbonyl))tritylhomocysteinate (263)



Fmoc-L-HomoCys(Trt)-OH (**262**) (500 mg, 0.833 mmol, 1.0 eq.) was dissolved in CH₂Cl₂ (7 mL). To this, *tert*-butyl-2,2,2-trichloroacetimidate (373 μ L, 2.08 mmol, 2.5 eq.) was added and the resulting solution was left to stir at rt for 16 h. The reaction was then concentrated *in vacuo* before redissolving in ethyl acetate (10 mL). The organic layer was washed with saturated sodium bicarbonate (2 x 10 mL) and brine (10 mL) and dried (Na₂SO₄) before concentrating *in vacuo* to yield the desired product as a white solid (540 mg, 99%) which was used without further purification.

NMR: δ_{H} (600 MHz, CDCl₃) 7.76 (2H, m, H_a), 7.57 (2H, dd, *J* 12.4, 7.5 Hz, H_d), 7.40 (6H, d, *J* 7.5 Hz, trityl), 7.30 (2H, m, H_b), 7.25 (9H, m, trityl), 7.18 (2H, t, *J* 7.5 Hz, H_c), 5.08 (1H, d, *J* 8.3 Hz, NH), 4.35 (2H, d, *J* 7.1 Hz, CH₂Fmoc), 4.18 (1H, t, *J* 7.1 Hz, CHFmoc), 4.12 (1H, m, CHCH₂CH₂S(Trt)), 2.23 – 2.30 (1H, m, CHCH₂CHH'S(Trt)), 2.13 – 2.19 (1H, m, CHCH₂CHH'S(Trt)), 1.76 – 1.86 (1H, m, CHCHH'CH₂S(Trt)), 1.58 – 1.65 (1H, m, CHCHH'CH₂S(Trt)), 1.48 (9H, s, CO₂^tBu).

δ_{C} (150 MHz, CDCl₃) 171.3 (COO^tBu), 156.1 (COOFmoc), 144.7 (C-4 trityl), 143.9 (C-6 Fmoc), 141.4 (C-1 Fmoc), 129.7 (aromatic C), 128.0 (aromatic C), 127.8 (aromatic C), 127.7 (aromatic C), 127.2 (aromatic C), 126.8 (aromatic C), 125.2 (aromatic C), 120.1 (aromatic C), 91.9 (CPh₃), 82.5 (C(CH₃)₃), 67.9 (CH₂ Fmoc), 53.9 (CHCH₂CH₂S), 47.2 (CH Fmoc), 37.2 (CHCH₂CH₂S), 28.0 (C(CH₃)₃), 27.9 (CHCH₂CH₂S).

MS: *m/z* (ES⁺) 678.3 ([M+Na]⁺, 100%); HRMS C₄₂H₄₁NO₄SNa ([M+Na]⁺) requires 678.2654, found 678.2676

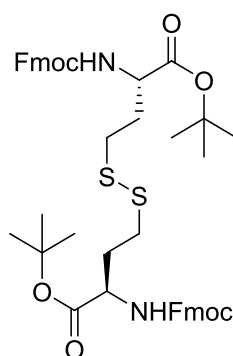
ν_{max} : (CH₃OH) 3324 (NH stretch, broad), 1711 & 1642 (C=O stretch, broad), 1448 (aromatic stretch).

$[\alpha]_{\text{D}}^{20}$: + 42.5 (c 1.0, CH₃OH).

Melting point: 64-68 °C.

Results are in agreement with literature values.¹⁰

Di-*tert*-butyl 4,4'-disulfanediylbis(2-(9(fluorenylmethoxycarbonyl))amino)butanoate) 264



(*S*)-*tert*-Butyl *N*-(9(Fluorenylmethoxycarbonyl))tritylhomocysteinate (**263**) (550 mg, 0.883 mmol, 1.0 eq.) was dissolved in 5 mL of CH₂Cl₂. To this solution, trifluoroacetic acid (646 μ L, 8.83 mmol, 10.0 eq.) and triethylsilane (1.34 mL, 8.83 mmol, 10.0 eq.) were added and the resulting mixture left to stir for 4h at rt. After this time, excess CH₂Cl₂ was added (10 mL) and water (10 mL). The organic layer was washed with saturated sodium bicarbonate (2 x 10 mL) and brine (10 mL) and dried (Na₂SO₄) before concentrating *in vacuo*. The resulting oil was purified by column chromatography (CH₂Cl₂, R_f = 0.4) to yield the product as a colourless oil (360 mg, 98%).

NMR: δ_H (600 MHz, CDCl₃) 7.78 (2H, d, *J* 7.4 Hz, H_a), 7.61 (2H, d, *J* 7.4 Hz, H_d), 7.41 (2H, t, *J* 7.4 Hz, H_b), 7.33 (2H, t, *J* 7.4 Hz, H_c), 5.44 (1H, d, *J* 8.2 Hz, NH), 4.39 – 4.47 (3H, m, CH₂Fmoc and CHCH₂CH₂S), 4.23 (1H, t, *J* 6.9 CHFmoc), 2.50 – 2.64 (2H, m, CHCH₂CH₂S), 2.10 – 2.17 (1H, m, CHCHH'CH₂S), 1.91 – 1.98 (1H, m, CHCHH'CH₂S), 1.49 (9H, s, CO₂^tBu).

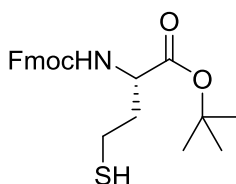
δ_C (150 MHz, CDCl₃) 171.3 (COO^tBu), 156.1 (COOFmoc), 143.8 (C-6 Fmoc), 141.4 (C-1 Fmoc), 127.9 (C-3 Fmoc), 127.7 (C-4 Fmoc), 125.2 (C-5 Fmoc), 120.1 (C-2 Fmoc), 82.7 (C(CH₃)₃), 67.1 (CH₂ Fmoc), 53.4 (CHCH₂CH₂S), 47.3 (CH Fmoc), 37.5 (CHCH₂CH₂S), 28.1 (C(CH₃)₃), 20.8 (CHCH₂CH₂S).

MS: *m/z* (ES⁺) 843.5 ([M+NH₄]⁺, 100%), 826.5 ([M+H]⁺, 30%), 769.5 ([M+H-^tBu]⁺, 38%); HRMS C₄₆H₅₂N₂O₈S₂Na ([M+Na]⁺) requires 849.3219, found 849.3220.

ν_{max} : (CH₃OH) 3326 (NH stretch, broad), 1703 & 1641 (C=O stretch, broad).

$[\alpha]_D^{20}$: + 34.4 (c 1.0, CH₃OH).

(S)-tert-Butyl N-(9(fluorenylmethoxycarbonyl))-homocysteinate (257)



Di-*tert*-butyl 4,4'-disulfanediylbis(2-(9(fluorenylmethoxycarbonyl))amino)butanoate) **264** (344 mg, 0.417 mmol, 1.0 eq.) was dissolved in CH₂Cl₂ (10 mL). To this, dithiothreitol (385 mg, 2.50 mmol, 1.5 eq.) and triethylamine (348 μ L, 2.50 mmol, 1.5 eq.) were added and the resulting solution was left to stir at rt for 0.5 h. The organic layer was washed with saturated sodium bicarbonate (10 mL) and water (2 x 10 mL) and dried (Na₂SO₄) before concentrating *in vacuo* to yield the desired product as a yellow oil (280 mg, 81%) which was used without further purification.

NMR: δ_H (600 MHz, CDCl₃) 7.77 (2H, d, *J* 7.5 Hz, H_a), 7.60 (2H, d, *J* 7.5 Hz, H_d), 7.41 (2H, t, *J* 7.5 Hz, H_b), 7.33 (2H, t, *J* 7.5 Hz, H_c), 5.38 (1H, d, *J* 8.2 Hz, NH), 4.37 – 4.46 (3H, m, CH₂Fmoc and CHCH₂CH₂S), 4.22 (1H, t, *J* 6.9 Hz, CHFmoc), 2.48 – 2.62 (2H, m, CHCH₂CH₂S), 2.09 – 2.16 (1H, m, CHCHH'CH₂S), 1.90 – 1.98 (1H, m, CHCHH'CH₂S), 1.48 (9H, s, CO₂^tBu).

δ_C (150 MHz, CDCl₃) 171.3 (COO^tBu), 156.1 (COOFmoc), 143.8 (C-6 Fmoc), 141.4 (C-1 Fmoc), 127.9 (C-3 Fmoc), 127.2 (C-4 Fmoc), 125.2 (C-5 Fmoc), 120.1 (C-2 Fmoc), 82.3 (C(CH₃)₃), 67.1 (CH₂ Fmoc), 53.4 (CHCH₂CH₂S), 47.3 (CH Fmoc), 37.5 (CHCH₂CH₂S), 28.1 (C(CH₃)₃), 20.3 (CHCH₂CH₂S).

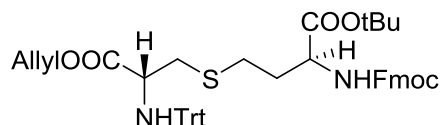
MS: *m/z* (ES⁺) 436.2 ([M+Na]⁺, 100%); HRMS C₂₃H₂₇NO₄Na ([M+Na]⁺) requires 436.1559, found 436.1578

ν_{max} : (CH₃OH) 3329 (NH stretch, broad), 1704 & 1638 (C=O stretch, broad), 1525 (amide bend).

$[\alpha]_D^{20}$: - 16.3 (c 1.0, CH₃OH).

Results are in agreement with literature values.¹⁰

***tert*-Butyl-*N*-(9(flourenylmethoxycarbonyl))-*S*-(3-(allyloxy)-3-oxo-2-(tritylamino)propyl)homocysteinate (250)**



(*R*)-Allyl 3-iodo-2-(trimethylphenylamino)propanoate **139** (337 mg, 0.677 mmol, 1.0 eq.) and (*S*)-*tert*-butyl *N*-(9(flourenylmethoxycarbonyl))-homocysteinate (**257**) (280 mg, 0.18 mmol, 1.0 eq.) were added together in 3 mL of DMF and cooled on ice. To this, cesium carbonate (110 mg, 0.339 mmol, 0.5 eq.) was added and the solution left to stir for 2 h. After this time, a second portion of cesium carbonate (110 mg, 0.339 mmol, 0.5 eq.) was added and the solution left to stir for a further 2 h. Excess ethyl acetate (10 mL) was then added and the organic layer was washed with pre-cooled citric acid (5% w/v, 4 °C, 3 x 10 mL). The organic layer was dried (Na₂SO₄) and concentrated *in vacuo*. The resulting oil was purified by column chromatography (petrol: ethyl acetate 1 : 4, R_f = 0.6) to yield the product as a colourless oil (25 mg, 0.0320 mmol, 5%).

NMR: δ_{H} (600 MHz, CDCl₃) 7.77 (2H, d, *J* 8.4 Hz, H_a Fmoc) 7.59 (2H, d, *J* 8.5 Hz, H_d Fmoc), 7.51 (6H, d, *J* 8.5 Hz, H_o trityl), 7.40 (2H, t, *J* 7.4 Hz, H_b Fmoc), 7.24 – 7.34 (9H, m, trityl), 7.17 (2H, t, *J* 7.4 Hz, H_c Fmoc), 5.70 (1H, ddt, *J* 17.0, 11.3, 5.6 Hz, CH₂CH=CH₂), 5.38 (1H, m, NH Fmoc), 5.14 – 5.20 (2H, m, CH₂CH=CH₂), 4.31 – 4.43 (3H, m, CH₂Fmoc and CHNHFmoc), 4.21 (1H, t, *J* 7.4 Hz CHFmoc), 4.16 (1H, dd, *J* 13.3, 6.4 Hz, CHH'CH=CH₂), 3.98 (1H, dd, *J* 13.9, 6.4 Hz, CHH'CH=CH₂), 3.54 (1H, m, CHNHtrityl), 2.87 (1H, dd, *J* 13.5, 5.5 Hz, CHH'CHNHtrityl), 2.69 (1H, dd, *J* 13.5, 8.4 Hz, CHH'CHNHtrityl), 2.50 (2H, m, CH₂CH₂CHNHFmoc), 2.04 – 2.11 (1H, m, CH₂CHH'NHFmoc), 1.84 – 1.93 (1H, m, CH₂CHH'NHFmoc), 1.47 (9H, s, CO₂^tBu).

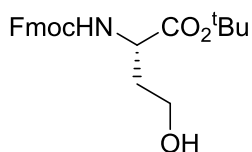
δ_{C} (150 MHz, CDCl₃) 173.5 (CO₂^tBu), 171.1 (COOFmoc), 156.0 (COOallyl), 145.8 (C-4 trityl), 143.9 (C-6 Fmoc), 141.4 (C-1 Fmoc), 131.9 (CH₂CH=CH₂ allyl), 128.9 (trityl), 128.1 (trityl), 127.8 (C-3 Fmoc), 127.2 (trityl), 126.7 (C-4 Fmoc), 125.2 (C-5 Fmoc), 120.1 (C-2 Fmoc), 118.6 (CH₂CH=CH₂ allyl), 82.7 (C(CH₃)₃), 71.2 (CPh₃), 67.1 (CH₂ Fmoc), 65.8 (CH₂CH=CH₂ allyl), 56.3 (CHNHtrityl), 53.8 (CHNHFmoc), 47.3 (CH Fmoc), 37.3 (CH₂CHNHtrityl), 32.9 (CH₂CH₂CHNHtrityl), 28.5 (CH₂CH₂CHNHtrityl), 28.1 (C(CH₃)₃).

MS: *m/z* (ESI⁺) 783.7 ([M+H]⁺, 100%); HRMS C₄₈H₅₁N₂O₆S ([M+H]⁺) requires 783.3462, found 783.3468.

ν_{max} : (CH₃OH) 3331 (NH stretch, broad), 1720 & 1641 (C=O stretch, broad), 1448 (alkene stretch).

$[\alpha]_D^{20}$: + 30.8 (c 1.0, CH₃OH).

(S)-tert-Butyl 2-(9(fluorenylmethoxycarbonylamino))-4-hydroxybutanoate (254)¹⁰



L-Homoserine (**247**, 2.00 g, 16.8 mmol, 1.0 eq.) and sodium carbonate (1.78 g, 16.8 mmol, 1.0 eq.) were dissolved in water (35 mL) and chilled on ice. To this, a solution of Fmoc succinimide (5.67 g, 16.8 mmol, 1 eq.) in 1,4-dioxane (15 mL) was added slowly. The reaction was allowed to warm to rt and left to stir for 7 h. After this time, the 1,4-dioxane was removed *in vacuo* and the remaining mixture was washed with ethyl acetate (35 mL) before acidifying the aqueous layer to pH 2 with 2M HCl. The resulting precipitate was extracted with ethyl acetate (3 x 30 mL). The organic layer was dried (Na₂SO₄) and concentrated *in vacuo* to yield the title product as a white solid. The solid was re-dissolved in CH₂Cl₂ (60 mL) and THF (15 mL). To this, *tert*-butyl-2,2,2-trichloroacetimidate (7.52 mL, 42.0 mmol, 2.5 eq.) was added and the reaction was left to stir for 14 h. After this time, the reaction was concentrated *in vacuo*, before re-dissolving in ethyl acetate (40 mL). The organic layer was washed with saturated sodium bicarbonate (40 mL) and brine (40 mL) before drying (Na₂SO₄) and concentrating *in vacuo*. Purification by column chromatography (CH₂Cl₂, R_f = 0.35) yielded the title product as a white waxy solid (4.0 g, 10.1 mmol, 60%).

NMR: δ_H (600 MHz, CDCl₃) 7.77 (2H, d, *J* 7.4 Hz, H_a), 7.60 (2H, d, *J* 7.4 Hz, H_d), 7.41 (2H, td, *J* 7.4, 2.1 Hz, H_b), 7.33 (2H, t, *J* 7.4 Hz, H_c), 5.64 (1H, d, *J* 7.5 Hz, NH), 4.48 (1H, dd, *J* 10.6, 7.5 Hz, CHCH₂CH₂OH), 4.37 – 4.46 (2H, m, CH₂Fmoc), 4.22 (1H, t, *J* 6.8 Hz, CHFmoc), 3.68 – 3.73 (1H, m, CHCH₂CHH'OH), 3.57 – 3.63 (1H, m, CHCH₂CHH'OH), 2.13 – 2.20 (1H, m, CHCHH'CH₂OH), 1.59 – 1.65 (1H, m, CHCHH'CH₂OH), 1.48 (9H, s, CO₂^tBu).

δ_C (150 MHz, CDCl₃) 171.9 (COO^tBu), 157.1 (COOFmoc), 143.8 (C-6 Fmoc), 141.4 (C-1 Fmoc), 127.9 (C-3 Fmoc), 127.2 (C-4 Fmoc), 125.2 (C-5 Fmoc), 120.1 (C-2 Fmoc), 82.9 (C(CH₃)₃), 67.3 (CHCH₂CH₂OH), 58.4 (CHCH₂CH₂OH), 51.5 (CH₂ Fmoc), 47.3 (CH Fmoc), 36.3 (CHCH₂CH₂OH), 28.1 (C(CH₃)₃).

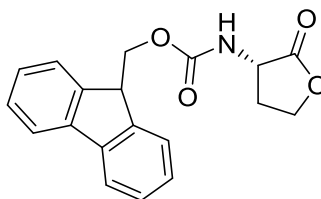
MS: *m/z* (ES⁺) 420.2 ([M+Na]⁺, 100%); HRMS C₂₃H₂₇NO₅Na ([M+Na]⁺) requires 420.1787, found 420.1784.

ν_{max} : (CH₃OH) 3359 (NH stretch, broad), 2973 (CH stretch), 1694 (C=O stretch, broad).

$[\alpha]_D^{20}$: - 6.3 (c 1.0, CH₃OH).

Results are in agreement with literature values.¹¹

(S)-9-(Fluorenylmethoxycarbonylamino)-(2-oxotetrahydrofuran-3-yl)carbamate (268)¹²



NMR: δ_H (600 MHz, $CDCl_3$) 7.76 (2H, d, J 7.5 Hz, H_a), 7.63 (2H, dd, J 13.1, 7.5 Hz, H_d), 7.40 (2H, t, J 7.5 Hz, H_b), 7.30 (2H, t, J 7.5 Hz, H_c), 6.19 (1H, d, J 7.7 Hz, NH), 4.39 (2H, m, CH_2 Fmoc), 4.32 (1H, m, $CHCH_2CH_2OH$), 4.24 (1H, t, J 7.4 Hz, $CHFmoc$), 3.46 – 3.51 (1H, m, $CHCH_2CH_2$), 2.05 – 2.11 (1H, m, $CHCHH'CH_2OH$), 1.97 – 2.04 (1H, m, $CHCHH'CH_2OH$).

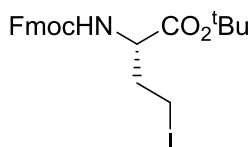
δ_C (150 MHz, $CDCl_3$) 171.4 (COO^tBu), 156.2 ($COOFmoc$), 144.0 (C-6 Fmoc), 141.4 (C-1 Fmoc), 127.8 (C-3 Fmoc), 127.1 (C-4 Fmoc), 125.3 (C-5 Fmoc), 120.1 (C-2 Fmoc), 66.9 (CH_2 Fmoc), 58.7 ($CHCH_2CH_2$), 53.7 ($CHCH_2CH_2$), 47.3 (CH Fmoc), 31.8 ($CHCH_2CH_2$).

MS: m/z (ES^+) 324.1 ($[M+H]^+$, 100%); HRMS $C_{19}H_{18}NO_4$ ($[M+H]^+$) requires 324.1236, found 324.1243.

ν_{max} : (CH_3OH) 3367 (NH stretch, broad), 2973 (CH stretch), 1692 & 1615 (C=O stretch, broad).

$[\alpha]_D^{20}$: -16.7 (c 1.0, CH_3OH).

(S)-tert-Butyl 2-((9-(fluorenylmethoxycarbonylamino)-4-iodobutanoate 258



To a stirred solution of triphenylphosphine (790 mg, 3.01 mmol, 1.2 eq.) and imidazole (205 mg, 3.01 mmol, 1.2 eq.) in CH_2Cl_2 (20 mL). Iodine (765 mg, 3.01 mmol, 1.2 eq.) was added portionwise over 5 min. The mixture was left to stir until no pieces of iodine were visible. To this mixture, a solution of (S)-tert-Butyl 2-(9-(Fluorenylmethoxycarbonylamino))-4-hydroxybutanoate (**254**) (1.00 g, 2.51 mmol, 1 eq.) in CH_2Cl_2 (10 mL) was added and left to stir for 1 h. After this time, the reaction was filtered and concentrated *in vacuo*. Purification by column chromatography (petrol: ethyl acetate 9 : 1, R_f = 0.85) yielded the title product as a colourless oil (667 mg, 1.31 mmol, 53%).

NMR: δ_H (600 MHz, $CDCl_3$) 7.77 (2H, d, J 7.5 Hz, H_a), 7.60 (2H, d, J 7.5 Hz, H_d), 7.41 (2H, t, J 7.5 Hz, H_b), 7.33 (2H, m, H_c), 5.41 (1H, d, J 8.0 Hz, NH), 4.43 (2H, dt, J 19.0, 7.0 Hz, CH_2 Fmoc),

4.26 – 4.31 (1H, m, CHCH₂CH₂I), 4.20 – 4.25 (1H, m, CHFmoc), 3.09 – 3.16 (1H, m, CHCH₂CH₂I), 2.38 – 2.44 (1H, m, CHCHH'CH₂I), 2.15 – 2.21 (1H, m, CHCHH'CH₂I), 1.48 (9H, s, CO₂^tBu).

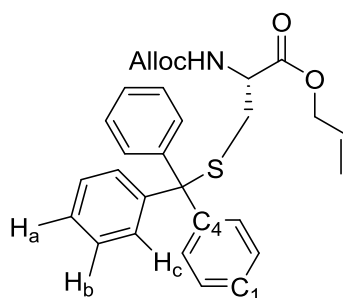
δ_c (150 MHz, CDCl₃) 170.5 (COO^tBu), 156.1 (COOFmoc), 143.7 (C-6 Fmoc), 141.4 (C-1 Fmoc), 127.8 (C-3 Fmoc), 127.2 (C-4 Fmoc), 125.2 (C-5 Fmoc), 120.1 (C-2 Fmoc), 83.1 (C(CH₃)₃), 67.1 (CH₂ Fmoc), 55.4 (CHCH₂CH₂I), 47.3 (CH Fmoc), 37.5 (CHCH₂CH₂I), 28.1 (C(CH₃)₃), -0.57 (CHCH₂CH₂I).

MS: m/z (ES⁺) 530.1 ([M+Na]⁺, 100%); HRMS C₂₃H₂₆NO₄INa ([M+Na]⁺) requires 530.0804, found 530.0827.

ν_{max} : (CH₃OH) 3335 (NH stretch, broad), 2974 (CH stretch), 1717 (C=O stretch, broad).

$[\alpha]_D^{20}$: - 21.3 (c 1.0, CH₃OH).

(S)-Allyl N-((allyloxy)carbonyl)tritylcysteinate (252)¹⁰



(S)-trityl-L-Cysteine (**251**, 1.00 g, 2.75 mmol, 1.0 eq.) and sodium carbonate (292 mg, 2.75 mmol, 1.0 eq.) were suspended in water/acetonitrile (10 mL : 5 mL) and chilled on ice before the dropwise addition of allyl chloroformate (292 μ L, 2.75 mmol, 1.0 eq.). The reaction was allowed to warm to rt and left to stir under argon for 18 h. After this time, the acetonitrile was removed *in vacuo* and additional water (10 mL) added. The pH was adjusted to 2 using 2M HCl forming a precipitate which was extracted with ethyl acetate (3 x 20 mL). The combined organic fractions were dried (Na₂SO₄) and concentrated *in vacuo* before redissolving in DMF (10 mL). Sodium hydrogen carbonate (231 mg, 2.75 mmol, 1.0 eq.) and allyl bromide (262 μ L, 3.03 mmol, 1.1 eq.) were added and the reaction left to stir under argon for a further 24 h. After this time, the reaction was concentrated *in vacuo* and redissolved in ethyl acetate (10 mL). The organic layer was washed with water (10 mL) and 1 M KHSO₄ (2 x 10 mL) before being dried (Na₂SO₄) and concentrated *in vacuo* to yield the product as a yellow oil (1.06 g, 2.17 mmol, 79%) which was used without further purification.

NMR: δ_H (600 MHz, CDCl₃) 7.37 – 7.41 (6H, m, H_c) 7.25 – 7.30 (6H, m, H_b), 7.22 (3H, t, *J* 7.3 Hz, H_a), 5.90 (1H, ddt, *J* 17.3, 10.6, 5.7 Hz, CH₂CH=CH₂ allyl), 5.87 (1H, ddt, *J* 17.3, 10.6, 5.5 Hz,

CH₂CH=CH₂ Alloc), 5.20 – 5.35 (4H, m, CH₂CH=CH₂ allyl and Alloc), 4.57 – 4.74 (2H, m, CH₂CH=CH₂ allyl), 4.54 (2H, d, *J* 5.5 Hz, CH₂CH=CH₂ Alloc), 4.32 – 4.37 (1H, m, CHCH₂S), 2.67 (1H, dd, *J* 12.5, 6.2 Hz, CHCHH'S), 2.58 (1H, dd, *J* 12.5, 4.6 Hz, CHCHH'S).

δ_c (150 MHz, CDCl₃) 170.3 (COOAlloc), 155.5 (COOallyl), 144.3 (C-4 trityl), 132.6 (CH₂CH=CH₂ allyl), 131.5 (CH₂CH=CH₂ Alloc), 129.6 (C-3 trityl), 128.1 (C-2 trityl), 127.1 (C-1 trityl), 118.9 (CH₂CH=CH₂ allyl), 117.9 (CH₂CH=CH₂ Alloc), 67.1 (CPh₃), 66.4 (CH₂CH=CH₂ allyl), 66.2 (CH₂CH=CH₂ Alloc), 53.0 (CHCH₂S), 34.2 (CHCH₂S).

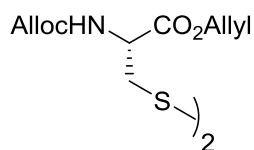
MS: *m/z* (ESI⁺) 510.2 ([M+Na]⁺, 100%); HRMS C₂₉H₂₉NO₄SN_a ([M+Na]⁺) requires 510.1715, found 510.1719.

*ν*_{max} (CH₃OH) 3326 (NH stretch, broad), 1718 (C=O stretch, broad), 1490 & 1443 (alkene stretch), 1050 (C-N stretch), 701 (C-S stretch).

[α]_D²⁰ + 28.9 (c 1.0, CH₃OH).

Results are in agreement with literature values.¹⁰

Diallyl 3,3'-disulfanediyl(2*R*,2'*R*)-bis(2-(allyloxycarbonylamino)propanoate) **266**



To a solution of (*R*)-allyl 2-(allyloxycarbonylamino)-3-(tritylthio)propanoate (**252**) (2.24 g, 4.58 mmol, 1.0 eq.) in CH₂Cl₂, trifluoroacetic acid (3.53 mL, 45.8 mmol, 10.0 eq.) and triethylsilane (7.32 mL, 45.8 mmol, 10.0 eq.) were added. The reaction was left to stir for 4 h before addition of excess CH₂Cl₂ (20 mL) and water (30 mL). The organic layer was separated and washed with saturated sodium bicarbonate (2 x 30 mL) and brine (30 mL) before drying (Na₂SO₄) and concentrating *in vacuo*. Purification by column chromatography (petrol: ethyl acetate 4 : 1, R_f = 0.35) yielded the final product as a yellow oil (0.900 g, 1.84 mmol, 80%).

NMR: δ_H (600 MHz, CDCl₃) 5.87 – 5.97 (2H, m, CH₂CH=CH₂ allyl and Alloc), 5.21 – 5.39 (4H, m, CH₂CH=CH₂ allyl and Alloc), 4.77 (2H, d, *J* 5.5 Hz, CH₂CH=CH₂ Alloc), 4.55 – 4.64 (3H, m, CH₂CH=CH₂ allyl and CHCH₂S), 2.88 – 3.13 (2H, m, CHCH₂S).

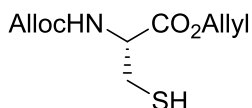
δ_c (150 MHz, CDCl₃) 171.5 (COOAlloc), 156.4 (COOallyl), 129.6 (CH₂CH=CH₂ Alloc), 128.4 (CH₂CH=CH₂ allyl), 119.1 (CH₂CH=CH₂ allyl), 118.4 (CH₂CH=CH₂ Alloc), 66.4 (CH₂CH=CH₂ allyl), 65.3 (CH₂CH=CH₂ Alloc), 53.6 (CHCH₂S), 31.1 (CHCH₂S).

MS: m/z (ESI⁺) 489.1 ([M+H]⁺, 100%); HRMS C₂₀H₂₉N₂O₈S₂ ([M+H]⁺) requires 489.1365, found 489.1360.

ν_{max} : (CH₃OH) 3335 (NH stretch, broad), 2925 (CH stretch), 1696 (C=O stretch, broad), 1513 & 1335 (alkene stretch).

$[\alpha]_D^{20}$: - 10.2 (c 1.0, CH₃OH).

(R)-Allyl 2-(allyloxycarbonylamino)-3-mercaptopropanoate (253)



Dithiothreitol (426 mg, 2.76 mmol, 1.5 eq.) and triethylamine (385 μ L, 2.76 mmol, 1.5 eq.) were added to a stirred solution of diallyl 3,3'-disulfanediyl(2*R*,2'*R*)-bis(2-(allyloxycarbonylamino)propanoate) **266** (0.900 g, 1.84 mmol, 1.0 eq.) in CH₂Cl₂ (10 mL). The reaction was left to stir for 1 h before washing with saturated sodium bicarbonate (10 mL) and brine (2 x 10 mL). The organic layer was dried (Na₂SO₄) and concentrated *in vacuo* to yield the title product as a pale yellow oil (753 mg, 3.10 mmol, 84%).

NMR: δ_H (600 MHz, CDCl₃) 5.88 – 5.96 (2H, m, CH₂CH=CH₂ allyl and Alloc), 5.66 (1H, d, *J* 7.4 Hz, NH), 5.38 (1H, d, *J* 1.3 Hz, CH₂CH=CHH' allyl), 5.35 (1H, d, *J* 1.2 Hz, CH₂CH=CHH' Alloc), 5.29 (1H, dd, *J* 10.4, 1.3 Hz, CH₂CH=CHH' allyl), 5.24 (1H, dd, *J* 10.4, 1.2 Hz, CH₂CH=CHH' Alloc), 4.65 – 4.73 (3H, m, CH₂CH=CH₂ allyl and CHCH₂S), 4.60 (2H, d, *J* 5.0 Hz, CH₂CH=CH₂ Alloc), 2.96 – 3.09 (2H, m, CHCH₂S).

δ_C (150 MHz, CDCl₃) 169.8 (COOAlloc), 155.6 (COOallyl), 132.5 (CH₂CH=CH₂ Alloc), 131.7 (CH₂CH=CH₂ allyl), 119.5 (CH₂CH=CH₂ allyl), 118.2 (CH₂CH=CH₂ Alloc), 66.6 (CH₂CH=CH₂ allyl), 66.2 (CH₂CH=CH₂ Alloc), 55.3 (CHCH₂S), 27.1 (CHCH₂S).

MS: m/z (ESI⁺) 246.3 ([M+H]⁺, 20%), 142.3 ([M+H-CH₂SH-C₃H₅]⁺, 100%);

HRMS C₁₀H₁₄NO₄S ([M-H]⁺) requires 244.0644, found 244.0652.

ν_{max} : (CH₃OH) 3360 (NH stretch, broad), 2927 (CH stretch), 1706 (C=O stretch, broad), 1507 & 1335 (alkene stretch).

$[\alpha]_D^{20}$: - 1.2 (c 1.0, CH₃OH).

Results are in agreement with literature values.¹⁰

Optimisation of the Synthesis of (S)-Allyl 2-(allyloxycarbonylamino)-4-hydroxybutanoate (248)

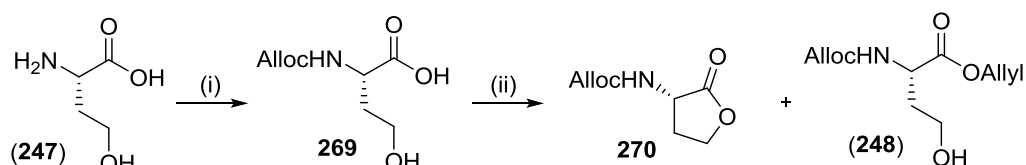


Figure 7.2: Attempts to Synthesise allyl/Alloc Homoserine (248)

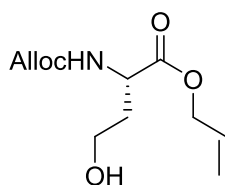
Reagents and Conditions: (i) allyl chloroformate, Na_2CO_3 , CH_2Cl_2 (ii) see table

L-Homoserine (500 g, 4.20 mmol, 1.0 eq.) and sodium carbonate (445 mg, 4.20 mmol, 1.0 eq.) were dissolved in water/acetonitrile (5 mL : 2.5 mL) and cooled to 0 °C. Allyl chloroformate (446.4 μL , 4.20 mmol, 1.0 eq.) was added dropwise and the reaction allowed to warm back to rt and left to stir for 24 h. After this time, the reaction was concentrated *in vacuo* and re-dissolved in ethyl acetate (10 mL). The organic layer was washed with water (10 mL) before being dried (Na_2SO_4) and concentrated *in vacuo*. The reaction was then re-dissolved in DMF (10 mL) and sodium hydrogen carbonate and allyl bromide were added and left to stir according to the conditions in Table 7.4. The reaction was again concentrated *in vacuo* and re-dissolved in ethyl acetate (10 mL). The organic layer was washed with water (3 x 10 mL), dried (Na_2SO_4) and concentrated *in vacuo* to yield the product as a white waxy solid (200 mg, 0.823 mmol, 20%) which was used without further purification.

Entry	Reaction Conditions (ii)	Results
1	1.1 eq. allyl bromide, NaHCO_3 , 24 h	100% lactone 270
2	1.1 eq. allyl bromide, NaHCO_3 , 65 h	100% lactone 270
3	1.1 eq. allyl bromide, NaHCO_3 , then additional 0.6 eq. allyl bromide after 24 h. total stirring time =36 h	100% lactone 270
4	1.1 eq. allyl bromide, NaHCO_3 , 8 h, on ice	1:1 lactone 270 and homoserine (248) mix, 20% yield
5	1.1 eq. allyl bromide, NaHCO_3 , 24 h, no work up	2:3 lactone 270 and homoserine (248) mix, 25% yield

Table 7.4: Attempts to Synthesise allyl/Alloc Homoserine (248)

(S)-Allyl 2-(allyloxycarbonylamino)-4-hydroxybutanoate (248)



NMR: δ_{H} (600 MHz, CDCl_3) 5.87 – 5.96 (2H, m, $\text{CH}_2\text{CH}=\text{CH}_2$ allyl and Alloc), 5.63 (1H, d, J 7.9 Hz, NH), 5.22 – 5.37 (4H, m, $\text{CH}_2\text{CH}=\text{CH}_2$ allyl and Alloc), 4.66 (2H, d, J 5.8 Hz, $\text{CH}_2\text{CH}=\text{CH}_2$

Alloc), 4.54 – 4.62 (3H, m, $\text{CH}_2\text{CH}=\text{CH}_2$ allyl and $\text{CHCH}_2\text{CH}_2\text{OH}$), 3.65 – 3.78 (2H, m, $\text{CHCH}_2\text{CH}_2\text{OH}$), 2.16 – 2.25 (1H, m, $\text{CHCHH}'\text{CH}_2\text{OH}$), 1.68 – 1.75 (1H, m, $\text{CHCHH}'\text{CH}_2\text{OH}$), 1.62 (1H, br s, OH).

δ_{C} (150 MHz, CDCl_3) 172.4 (COOallyl), 156.8 (COOAlloc), 132.5 ($\text{CH}_2\text{CH}=\text{CH}_2$ Alloc), 131.4 ($\text{CH}_2\text{CH}=\text{CH}_2$ allyl), 119.2 ($\text{CH}_2\text{CH}=\text{CH}_2$ Alloc), 118.3 ($\text{CH}_2\text{CH}=\text{CH}_2$ allyl), 66.3 & 65.9 ($\text{CH}_2\text{CH}=\text{CH}_2$ allyl and Alloc), 58.5 ($\text{CHCH}_2\text{CH}_2\text{OH}$), 51.2 ($\text{CHCH}_2\text{CH}_2\text{OH}$), 36.0 ($\text{CHCH}_2\text{CH}_2\text{OH}$).

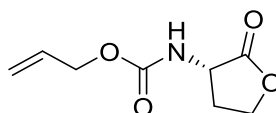
MS: m/z (ESI^+) 244.6 ($[\text{M}+\text{H}]^+$, 100%); HRMS $\text{C}_{11}\text{H}_{18}\text{NO}_5$ ($[\text{M}+\text{H}]^+$) requires 243.1185, found 244.1191.

ν_{max} : (CH_3OH) 3325 (OH stretch, broad), 1703 & 1649 ($\text{C}=\text{O}$ stretch, broad).

$[\alpha]_{\text{D}}^{20}$: - 39.5 (c 1.0, CH_3OH).

Results are in agreement with literature values.¹³

(S)-Allyl(2-oxotetrahydrofuran-3-yl)carbamate 270



NMR: δ_{H} (600 MHz, CDCl_3) 5.91 (1H, ddt, J 16.3, 10.9, 6.0 Hz, $\text{CH}_2\text{CH}=\text{CH}_2$), 5.32 (1H, d, J 17.2 Hz, NH), 5.23 (2H, m, $\text{CH}_2\text{CH}=\text{CH}_2$), 4.59 (2H, d, J 5.2 Hz, $\text{CH}_2\text{CH}=\text{CH}_2$), 4.46 (2H, t, J 9.1 Hz, $\text{CHCH}_2\text{CH}_2\text{O}$ lactone), 4.41 (1H, m, $\text{CHCH}_2\text{CH}_2\text{O}$ lactone), 2.78 (1H, m, $\text{CHCH}_2\text{CHH}'\text{O}$ lactone), 2.22 (1H, ddq, J 11.9, 9.1, 8.9 Hz, $\text{CHCH}_2\text{CHH}'\text{O}$ lactone).

δ_{C} (150 MHz, CDCl_3) 175.1 (COOlactone), 156.1 (COOAlloc), 132.4 ($\text{CH}_2\text{CH}=\text{CH}_2$), 118.3 ($\text{CH}_2\text{CH}=\text{CH}_2$), 66.3 ($\text{CH}_2\text{CH}=\text{CH}_2$), 65.9 ($\text{CHCH}_2\text{CH}_2\text{OH}$), 50.6 ($\text{CHCH}_2\text{CH}_2\text{OH}$), 30.5 ($\text{CHCH}_2\text{CH}_2\text{OH}$).

MS: m/z (ESI^+) 186.5 ($[\text{M}+\text{H}]^+$, 100%); HRMS $\text{C}_8\text{H}_{12}\text{NO}_4$ ($[\text{M}+\text{H}]^+$) requires 186.0766, found 186.0773.

ν_{max} : (CH_3OH) 3339 (NH stretch, broad), 1701 & 1647 ($\text{C}=\text{O}$ stretch, broad), 1260 & 1198 (lactone stretch).

$[\alpha]_{\text{D}}^{20}$: - 43.2 (c 1.0, CH_3OH).

Attempts to Ring Open Lactone (270) to form (S)-Allyl 2-(allyloxycarbonylamino)-4-hydroxybutanoate (248)



General Method 1:

(S)-Allyl(2-oxotetrahydrofuran-3-yl)carbamate **270** (80.0 mg, 0.432 mmol, 1.0 eq.) was dissolved in allyl alcohol (5 mL). To this, a few drops of concentrated hydrochloric acid was added and the reaction was left to stir overnight. The reaction was then dissolved in ethyl acetate (5 mL), washed once with water (5 mL) before drying (Na_2SO_4) and concentrating *in vacuo*. NMR showed no reaction occurred.

General Method 2:

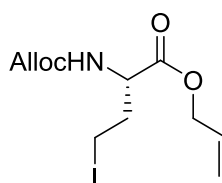
(S)-Allyl(2-oxotetrahydrofuran-3-yl)carbamate **270** (100.0 mg, 0.541 mmol, 1.0 eq.) was dissolved in ethanol (2 mL). To this, sodium hydroxide (21.6 mg, 0.541 mmol, 1.0 eq.) was added and the reaction was left to stir at room temperature for 30 min. After this time, the reaction was concentrated *in vacuo*, re-dissolved in ethanol (2 mL) and concentrated *in vacuo* a second time.

After this, the crude product was dissolved in DMF (2 mL) and allyl bromide was added (46.7 μL , 0.649 mmol, 1.2 eq.). The reaction was left to stir for the amount of time detailed in Table 7.5 before concentrating *in vacuo*. The reaction was then dissolved in ethyl acetate (5 mL), washed once with water (5 mL) before drying (Na_2SO_4) and concentrating *in vacuo*. NMR showed no reaction occurred.

Entry	Method	Results
1	General Method 1	100% lactone 270
2	General Method 2, 8 h	100% lactone 270
3	General Method 2, 21 h	100% lactone 270

Table 7.5: Attempts to Open Alloc Lactone **270**

(S)-Allyl 2-(allyloxycarbonylamino)-4-iodobutanoate 259



(S)-Allyl 2-(allyloxycarbonylamino)-4-hydroxybutanoate (**248**) (500 mg, 2.06 mmol, 1.0 eq.) was dissolved in CH_2Cl_2 (30 mL) and treated with mesyl chloride (190 μL , 2.47 mmol, 1.2 eq.)

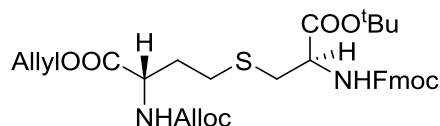
and triethylamine (344 μ L, 2.47 mmol, 1.2 eq.). The reaction was left to stir for 45 min before addition of sodium iodide (925 mg, 2.06 mmol, 1.0 eq.) in acetone (20 mL). The reaction was left to stir for 16 h before concentrating *in vacuo*. The resulting mixture was re-dissolved in ethyl acetate (10 mL), washed once with water (10 mL), dried (Na_2SO_4) and concentrated *in vacuo* to yield the crude product. Purification by column chromatography (petrol: ethyl acetate, 2:1, R_f = 0.5) yielded the desired product as a yellow oil (60 mg, 8%).

NMR: δ_H (600 MHz, CDCl_3) 5.85 – 5.94 (2H, m, $\text{CH}_2\text{CH}=\text{CH}_2$ allyl and Alloc), 5.38 (1H, d, J 7.1 Hz, NH), 5.19 – 5.36 (4H, m, $\text{CH}_2\text{CH}=\text{CH}_2$ allyl and Alloc), 4.64 (2H, d, J 5.8 Hz, $\text{CH}_2\text{CH}=\text{CH}_2$ allyl), 4.56 (2H, d, J 5.4 Hz, $\text{CH}_2\text{CH}=\text{CH}_2$ Alloc), 4.42 (1H, m, $\text{CHCH}_2\text{CH}_2\text{I}$), 3.35 – 3.44 (1H, m, $\text{CHCH}_2\text{CHH}'\text{I}$), 3.05 – 3.10 (1H, m, $\text{CHCH}_2\text{CHH}'\text{I}$), 2.39 – 2.48 (1H, m, $\text{CHCHH}'\text{CH}_2\text{I}$), 2.18 – 2.26 (1H, m, $\text{CHCHH}'\text{CH}_2\text{I}$).

δ_C (150 MHz, CDCl_3) 171.1 (COOallyl), 155.9 (COOAlloc), 132.5 ($\text{CH}_2\text{CH}=\text{CH}_2$ Alloc), 131.3 ($\text{CH}_2\text{CH}=\text{CH}_2$ allyl), 119.2 ($\text{CH}_2\text{CH}=\text{CH}_2$ allyl), 118.2 ($\text{CH}_2\text{CH}=\text{CH}_2$ Alloc), 66.5 ($\text{CH}_2\text{CH}=\text{CH}_2$ allyl), 66.1 ($\text{CH}_2\text{CH}=\text{CH}_2$ Alloc), 54.8 ($\text{CHCH}_2\text{CH}_2\text{I}$), 17.5 ($\text{CHCH}_2\text{CH}_2\text{I}$), -0.65 ($\text{CHCH}_2\text{CH}_2\text{I}$).

MS: m/z (ESI⁺) 354.2 ($[\text{M}+\text{H}]^+$, 60%), 268.2 ($[\text{M}+\text{H}-\text{Alloc}]^+$, 100%).

(*R*)-tert-Butyl 2-((9*H*-fluoren-9-yl)methoxycarbonylamino)-3 (((*S*)-3-(allyloxy)-2-(allyloxycarbonylamino)-3-oxobutyl)thio)propanoate (250)



(*S*)-Allyl 2-(allyloxycarbonylamino)-4-iodobutanoate **259** (66.0 mg, 0.180 mmol, 1.0 eq.) was added to a stirred solution of (*R*)-tert-butyl 2-((9-fluorenylmethoxycarbonyl))amino)-3-mercaptopropanoate (**62**) (74.0 mg, 0.180 mmol, 1.0 eq.) and cesium carbonate (60.0 mg, 0.180 mmol, 1.0 eq.) in dry DMF (1 mL). The reaction was left to stir overnight before addition of excess ethyl acetate (5 mL). The solution was washed with cold citric acid (5% w/v, 4 °C, 3 x 5 mL) before drying (Na_2SO_4) and concentrating *in vacuo*. Purification by column chromatography (4:1 petrol: ethyl acetate, R_f = 0.35) yielded the title product as a yellow oil (57 mg, 0.0913 mmol, 51%).

NMR: δ_H (600 MHz, CDCl_3) 7.72 – 7.80 (2H, m, H_a), 7.57 – 7.65 (2H, m, H_d), 7.36 – 7.43 (2H, m, H_b), 7.27 – 7.35 (2H, m, H_c), 5.84 – 5.96 (2H, m, $\text{CH}_2\text{CH}=\text{CH}_2$ allyl and Alloc), 5.75 (1H, d, J 7.6 Hz, NH), 5.70 (1H, d, J 7.1 Hz, NH), 5.17 – 5.43 (2H, m, $\text{CH}_2\text{CH}=\text{CH}_2$ allyl and Alloc), 4.46 – 4.69 (6H, m, NHCH both sides and $\text{CH}_2\text{CH}=\text{CH}_2$ allyl and Alloc), 4.34 – 4.43 (2H, m, CH_2Fmoc), 4.18 – 4.27 (1H, m, CHFmoc), 3.16 – 3.26 (1H, m, $\text{CHCHH}'\text{S}$), 2.93 – 3.03 (1H, m,

CHCHH'S), 2.59 – 2.67 (2H, m, CHCH₂CH₂S), 2.11 – 2.18 (1H, m, CHCHH'CH₂S), 1.91 – 2.03 (1H, m, CHCHH'CH₂S), 1.50 (9H, s, CO₂^tBu).

δ_c (150 MHz, CDCl₃) 171.5 (COOAllyl), 156.5 (COOAlloc), 155.6 (COOFmoc), 143.8 (C-6 Fmoc), 141.4 (C-1 Fmoc), 132.6 & 131.5 (CH₂CH=CH₂ allyl and Alloc), 127.9 (C-3 Fmoc), 127.2 (C-4 Fmoc), 125.3 (C-5 Fmoc), 120.1 (C-2 Fmoc), 119.2 & 118.0 (CH₂CH=CH₂ allyl and Alloc), 83.0 (C(CH₃)₃), 67.3 (CH₂ Fmoc), 66.4 & 66.1 (CH₂CH=CH₂ allyl and Alloc), 54.7 & 53.1 (NHCH both sides), 47.2 (CH Fmoc), 34.9 (CHCH₂S), 32.5 (CHCH₂CH₂S), 29.8 (CHCH₂CH₂S), 28.1 (C(CH₃)₃).

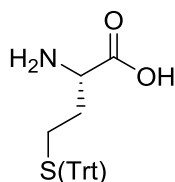
MS: m/z (ES⁺) 647.2 ([M+Na]⁺, 100%); HRMS C₃₃H₄₀N₂O₈Na ([M+Na]⁺) requires 647.2403, found 647.2417.

ν_{max} : (CH₃OH) 3334 (NH stretch, broad), 2944 (CH stretch), 1653 (C=O stretch, broad), 1448 & 1409 (alkene stretch).

$[\alpha]_D^{20}$: - 6.1 (c 1.0, CH₃OH).

Results are in agreement with literature values.¹⁰

(S)-Trityl-L-homocysteine (271)



Fmoc-L-HomoCys(Trt)-OH (**262**) (300 mg, 0.500 mmol, 1.0 eq.) was dissolved in DMF (1.2 mL). To this, piperidine (0.8 mL) was added and the resulting solution was left to stir at rt for 2 h before concentrating *in vacuo*. The product was precipitated from toluene to yield a white solid (159 mg, 0.421 mmol, 84%) which was used without further purification.

NMR: δ_H (600 MHz, CDCl₃) 7.30 (6H, t, J 7.3 Hz, trityl), 7.27 (6H, d, J 7.3 Hz, trityl), 7.23 (3H, t, J 7.3 Hz, trityl), 3.04 (1H, m, CHCH₂CH₂S(Trt)), 2.18 – 2.26 (1H, m, CHCH₂CH₂S(Trt)), 1.74 – 1.82 (1H, m, CHCHH'CH₂S(Trt)), 1.57 – 1.65 (1H, m, CHCHH'CH₂S(Trt)).

δ_c (150 MHz, CDCl₃) 170.9 (COOH), 144.5 (C-4 trityl), 129.1 (C-3 trityl), 128.1 (C-2 trityl), 126.8 (C-1 trityl), 65.9 (CPh₃), 53.6 (CHCH₂CH₂S), 28.0 (CHCH₂CH₂S), 23.4 (CHCH₂CH₂S).

MS: m/z (ES⁺) 400.1 ([M+Na]⁺, 20%), 356.1 ([M+Na - CO₂H]⁺, 35%), 340.2 ([M+Na - CO₂H - NH₂]⁺, 100%); HRMS C₂₃H₂₃NO₂Na ([M+Na]⁺) requires 400.1347, found 400.1339

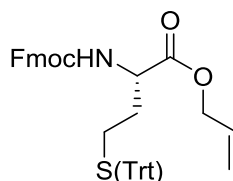
ν_{max} : (CH₃OH) 3345 (NH stretch, broad), 1701 & 1638 (C=O stretch, broad), 1509 (amide bend).

$[\alpha]_D^{20}$: - 6.2 (c 1.0, CH₃OH).

Mp = 162 – 166 °C.

Results are in agreement with literature values.¹⁴

(S)-Allyl N-(9(flourenylmethoxycarbonyl))tritylhomocysteinate 273



Cesium carbonate (54.3 mg, 0.167 mmol, 0.5 eq.) was added to a stirred solution of Fmoc-L-HomoCys(Trt)-OH (**262**) (200 mg, 0.333 mmol, 1.0 eq.) in methanol (3 mL) and left to stir for 15 min. After this time, the reaction was concentrated *in vacuo*. The resulting cesium salt was then dissolved in DMF (2 mL). Allyl bromide (29.0 μ L, 0.333 mmol, 1.0 eq.) was added dropwise and the reaction was left to stir for 16 h. Excess ethyl acetate (10 mL) was added and the solution washed with pre-cooled citric acid (5% w/v, 4 °C, 5 x 10 mL). The organic layer was dried (Na₂SO₄) and concentrated *in vacuo* to yield the desired product as a white solid (200 mg, 0.313 mmol, 94%) which was used without further purification.

NMR: δ_H (600 MHz, CDCl₃) 7.76 (2H, m, H_a) 7.57 (2H, dd, *J* 12.1, 7.4 Hz, H_d), 7.41 (6H, m, trityl), 7.23 – 7.35 (11H, trityl & Fmoc), 7.19 (2H, t, *J* 7.4 Hz, H_c), 5.79 - 5.88 (1H, m, CH₂CH=CH₂), 5.21 - 5.31 (2H, m, CH₂CH=CH₂), 4.96 (1H, d, *J* 8.3 Hz, NH), 4.55 (2H, m, CH₂CH=CH₂), 4.33 – 4.40 (2H, m, CH₂Fmoc), 4.23 – 4.27 (1H, m, CHCH₂CH₂S), 4.20 (1H, t, *J* 6.9 Hz, CHFmoc), 2.26 – 2.33 (1H, m, CHCH₂CHH'S(Trt)), 2.16 – 2.21 (1H, m, CHCH₂CHH'S(Trt)), 1.78 – 1.84 (1H, m, CHCHH'CH₂S(Trt)), 1.56 – 1.64 (1H, m, CHCHH'CH₂S(Trt)).

δ_C (150 MHz, CDCl₃) 171.6 (COO^tBu), 155.9 (COOFmoc), 144.7 (C-4 trityl), 143.8 (C-6 Fmoc), 141.4 (C-1 Fmoc), 131.5 (CH₂CH=CH₂), 129.7 (aromatic C), 128.0 (aromatic C), 127.9 (aromatic C), 127.3 (aromatic C), 127.2 (aromatic C), 126.8 (aromatic C), 125.2 (C-5 Fmoc), 120.1 (C-2 Fmoc), 119.1 (CH₂CH=CH₂ allyl), 82.2 (CPh₃), 67.1 (CH₂ Fmoc), 66.2 (CH₂CH=CH₂), 53.4 (CHCH₂CH₂S(Trt)), 47.2 (CH Fmoc), 31.6 (CHCH₂CH₂S(Trt)), 27.9 (CHCH₂CH₂S(Trt)).

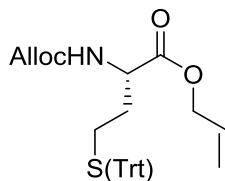
MS: *m/z* (ESI⁺) 662.23 ([M+Na]⁺, 100%); HRMS C₄₁H₃₇NO₄Na ([M+Na]⁺) requires 662.2341, found 662.2365.

ν_{max} (CH₃OH) 3331 (NH stretch, broad), 1649 (C=O stretch, broad), 740 (C-S stretch).

$[\alpha]_D^{20} + 15.7$ (c 1.0, CH₃OH).

Melting point: 71-74 °C.

(S)-Allyl N-((allyloxy)carbonyl)tritylhomocysteinate 274



Piperidine (1 mL) was added to a stirred solution of (S)-Allyl N-(9(fluorenylmethoxycarbonyl))tritylhomocysteinate **273** (200 mg, 0.312 mmol, 1.0 eq.) in DMF (1.5 mL). The reaction was left to stir for 1 h before concentrating *in vacuo*. This was then re-dissolved in acetonitrile (2 mL) and sodium carbonate (40.0 mg, 0.374 mmol, 1.2 eq.) in water (1 mL) was added. The solution was cooled to 0 °C, before the careful dropwise addition of allyl chloroformate (66.3 μ L, 0.624 mmol, 2.0 eq.). The reaction was allowed to warm to rt and left to stir for 16 h before concentrating *in vacuo*. The product was redissolved in ethyl acetate (5 mL) and washed with water (3 x 5 mL). The organic layer was dried (Na₂SO₄) and concentrated *in vacuo* to yield the desired product as a yellow oil (148 mg, 0.295 mmol, 89%) which was used without further purification.

NMR: δ_H (600 MHz, CDCl₃) 7.40 (6H, d, *J* 7.7 Hz, trityl), 7.29 (6H, t, *J* 7.7 Hz, trityl), 7.22 (3H, t, *J* 7.7 Hz, trityl), 5.79 – 5.94 (2H, m, CH₂CH=CH₂ allyl and Alloc), 5.19 – 5.33 (4H, m, CH₂CH=CH₂ allyl and Alloc), 4.96 (1H, d, *J* 8.0 Hz, NH), 4.54 (4H, m, CH₂CH=CH₂ allyl and Alloc), 4.24 – 4.29 (1H, m, CHFmoc), 2.26 – 2.33 (1H, m, CHCH₂CHH'S(Trt)), 2.15 – 2.22 (1H, m, CHCH₂CHH'S(Trt)), 1.77 – 1.85 (1H, m, CHCHH'CH₂S(Trt)), 1.56 – 1.65 (1H, m, CHCHH'CH₂S(Trt)).

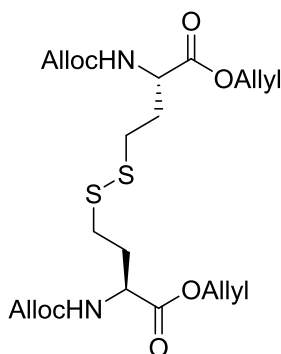
δ_C (150 MHz, CDCl₃) 171.6 (COOallyl), 155.7 (COOAlloc), 144.7 (C-4 trityl), 132.7 (CH₂CH=CH₂ Alloc), 131.5 (CH₂CH=CH₂ allyl), 129.7 (trityl), 128.0 (trityl), 126.9 (trityl), 119.2 (CH₂CH=CH₂ Alloc), 117.9 (CH₂CH=CH₂ allyl), 67.1 (CPh₃), 66.2 & 65.6 (CH₂CH=CH₂ allyl and Alloc), 53.4 (CHCH₂CH₂S(Trt)), 32.0 (CHCH₂CH₂S(Trt)), 27.9 (CHCH₂CH₂S(Trt)).

MS: *m/z* (ES⁺) 524.19 ([M+Na]⁺, 100%); HRMS C₃₀H₃₁NO₄SNa ([M+Na]⁺) requires 524.1872, found 524.1890.

ν_{max} (CH₃OH) 3327 (NH stretch, broad), 1702 (C=O stretch, broad), 1489 (aromatic stretch), 1019 (NH bend), 742 (C-S stretch).

$[\alpha]_D^{20} + 11.7$ (c 1.0, CH₃OH).

Diallyl 4,4'-disulfanediyl(2*S*,2'*S*)-bis(2-(allyloxycarbonylamino)butanoate) 275



(*S*)-Allyl *N*-((allyloxy)carbonyl)tritylhomocysteinate **274** (225 mg, 0.449 mmol, 1.0 eq.) was dissolved in 5 mL of CH₂Cl₂. To this solution, trifluoroacetic acid (345.6 μ L, 4.49 mmol, 10.0 eq.) and triethylsilane (716 mL, 4.49 mmol, 10.0 eq.) were added and the resulting mixture left to stir for 2 h at rt. After this time, excess CH₂Cl₂ was added (10 mL) and water (10 mL). The organic layer was washed with saturated sodium bicarbonate (2 x 10 mL) and brine (10 mL) and dried (Na₂SO₄) before concentrating *in vacuo*. The resulting oil was purified by column chromatography (CH₂Cl₂, R_f = 0.4) to yield the product as a colourless oil (44.0 mg, 8.52 mmol, 19 %).

NMR: δ_H (600 MHz, CDCl₃) 5.88 – 5.97 (2H, m, CH₂CH=CH₂ allyl and Alloc), 5.19 – 5.37 (4H, m, CH₂CH=CH₂ allyl and Alloc), 4.66 (2H, d, *J* 5.8 Hz, CH₂CH=CH₂ Alloc), 4.58 (2H, d, *J* 5.5 Hz, CH₂CH=CH₂ allyl), 4.56 (1H, m, CHCH₂CH₂S), 4.24 – 4.29 (1H, m, CHFmoc), 2.54 – 2.67 (2H, m, CHCH₂CH₂S), 2.13 – 2.20 (1H, m, CHCHH'CH₂S), 1.95 – 2.03 (1H, m, CHCHH'CH₂S).

δ_C (150 MHz, CDCl₃) 171.8 (COOallyl), 156.1 (COOAlloc), 132.6 (CH₂CH=CH₂ Alloc), 131.4 (CH₂CH=CH₂ allyl), 119.4 (CH₂CH=CH₂ Alloc), 118.2 (CH₂CH=CH₂ allyl), 66.4 (CH₂CH=CH₂ Alloc), 66.1 (CH₂CH=CH₂ allyl), 65.9 (CHCH₂CH₂S), 37.2 (CHCH₂CH₂S), 20.8 (CHCH₂CH₂S).

MS: *m/z* (ES⁺) 535.8 ([M+NH₄]⁺, 100%); HRMS C₂₂H₃₂N₂O₈S₂Na ([M+Na]⁺) requires 539.1498, found 539.1478.

ν_{max} (CH₃OH) 3324 (NH stretch, broad), 1711 & 1642 (C=O stretch, broad), 740 (C-S stretch).

$[\alpha]_D^{20}$ - 2.2 (c 1.0, CH₃OH).

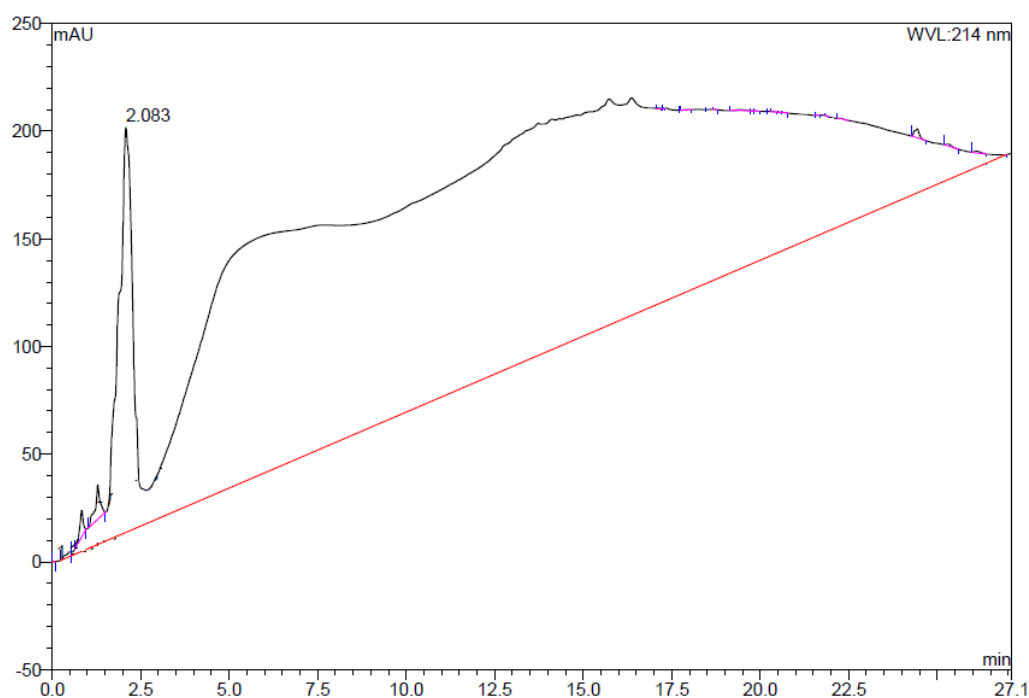
7.5 Experimental for the Analysis of the Connectivity of ProTx-II (Chapter 5)

HPLC Analysis: The purified peptide was analysed by analytical HPLC using an ACE C8-300 analytical column (150 x 10 mm, flow rate of 1.0 mL/min), with UV detection at 215 and 254 nm. Linear gradient: 2 – 98% B over 20 min (A = water, B = acetonitrile). The analysis of the chromatograms was conducted using Chromeleon Software version 2.0.

7.5.1 Preparation of ProTx-II (**22**)

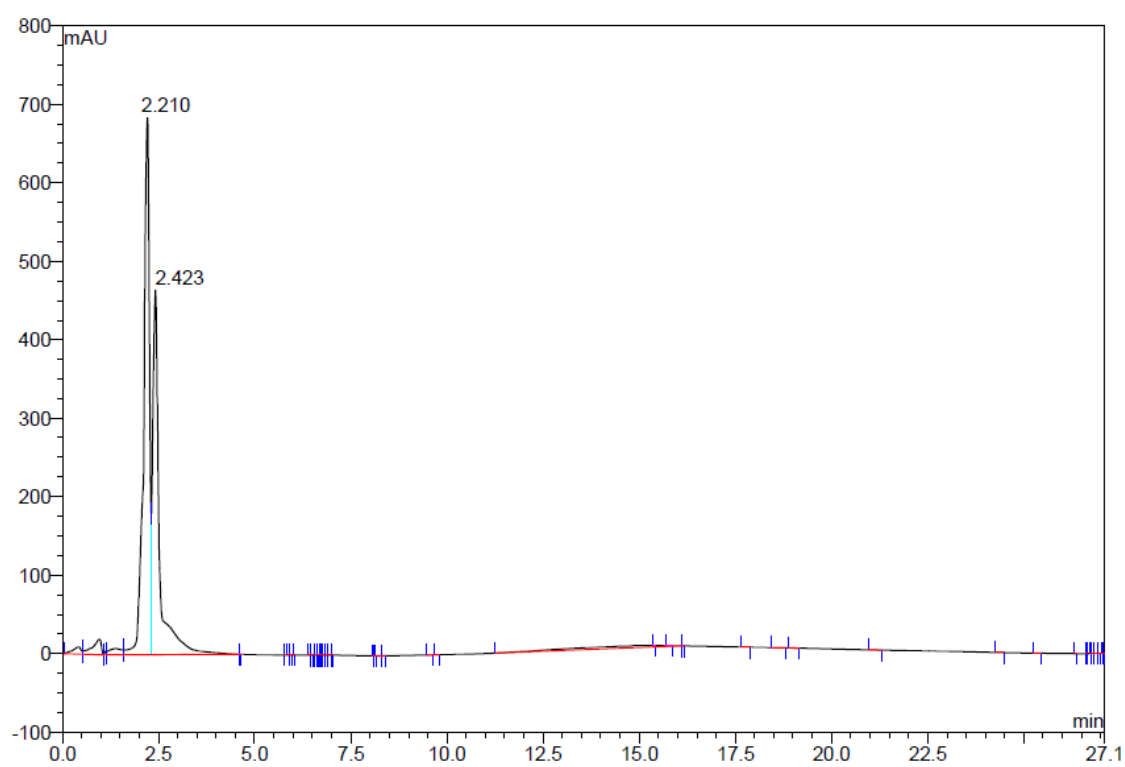
Disulfide Bond Cyclisation – Original Method: Purified linear ProTx-II (**22**) was dissolved in pure water (concentration = 0.1 mg/mL) and left to stir at 4 °C for 7 – 10 days before concentrating down to approximately 2 mL. The solution was then flash frozen and lyophilised to yield the cyclised peptide as a white solid.

Analytical HPLC:

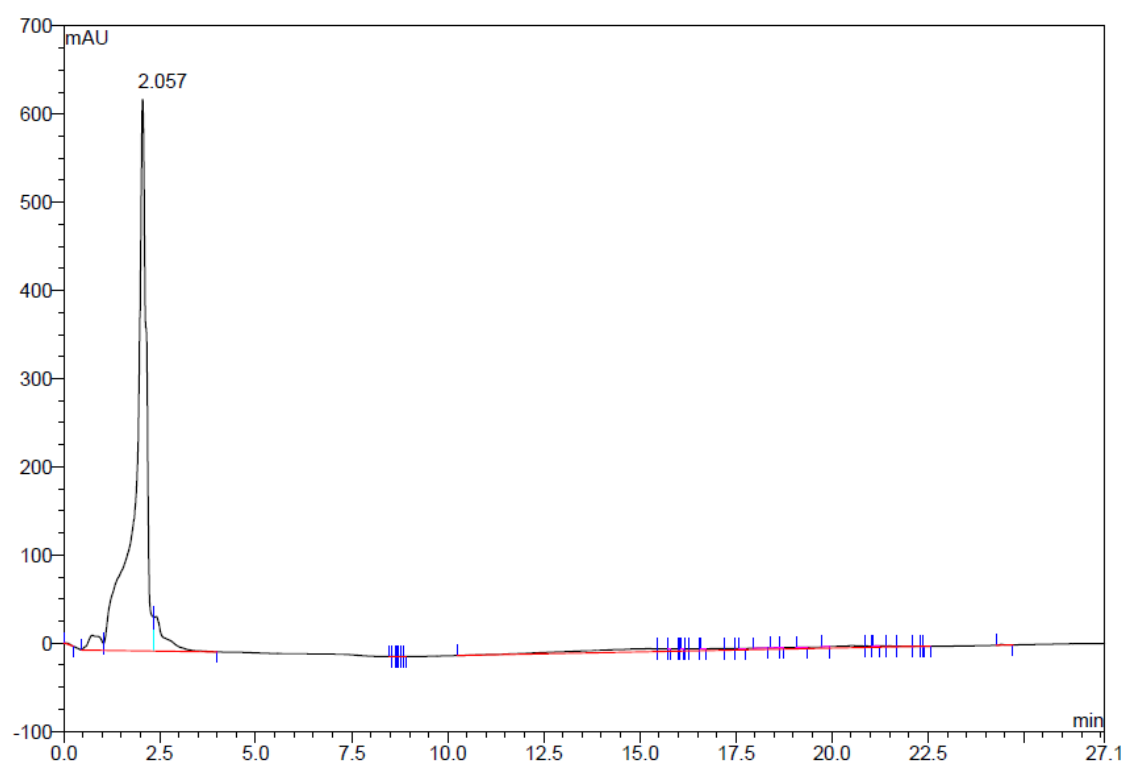


Disulfide Bond Cyclisation – Park Method¹⁵: Glutathione(0.15 mM) and glutathione disulfide (0.3 mM) were added to a mixture of urea (2 M) and Tris-HCl (0.1 M) in water. The pH was adjusted to 8.0 using saturated aqueous sodium bicarbonate. A solution of crude linear ProTx-II (**22**) was added at a concentration of 0.1 mg/mL and left to stir for 24 h at room temperature. After this time, the pH of the solution was adjusted to 3 using HCl (2 M). The peptide was purified by analytical HPLC using an ACE C8-300 analytical column (150 x 10 mm, flow rate of 1.0 mL/min), with UV detection at 215 and 254 nm. Linear gradient: 2 – 98% B over 20 min (A = water, B = acetonitrile).

Analytical HPLC trace before purification:



Analytical HPLC of purified product:



Analytical HPLC Traces for Commercial Sources of ProTx-II and Combined Injections:

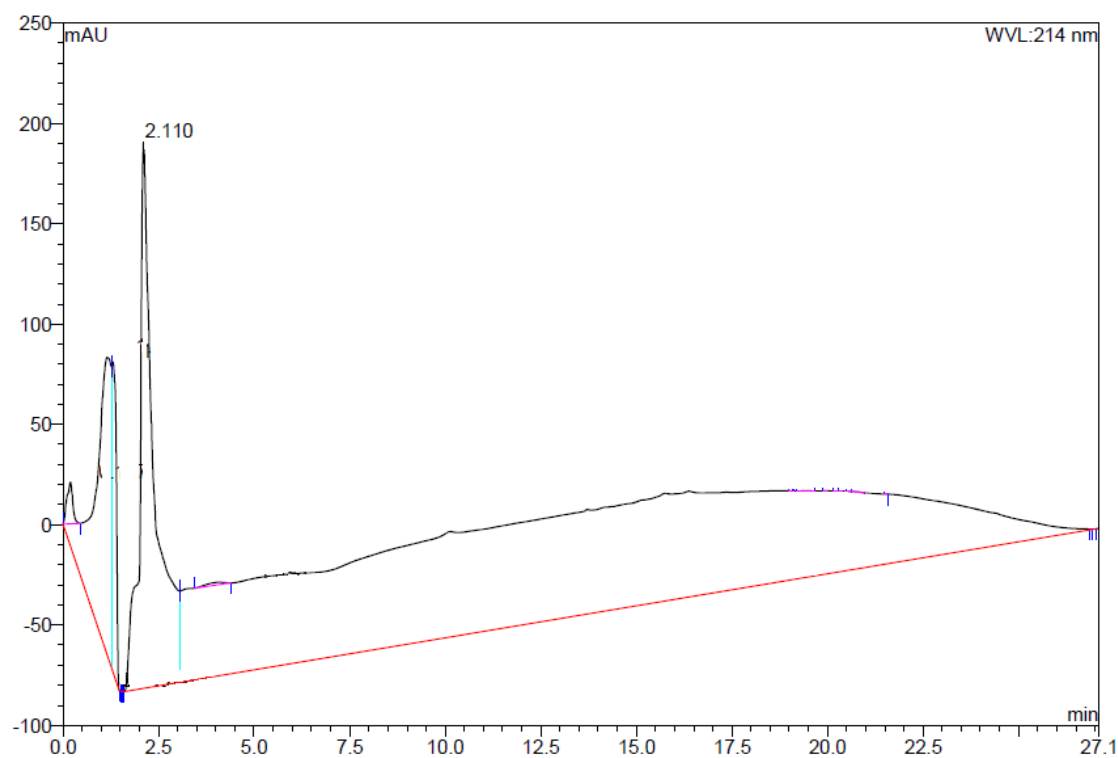


Figure 7.3: HPLC Trace Showing Injection of Tocris ProTx-II

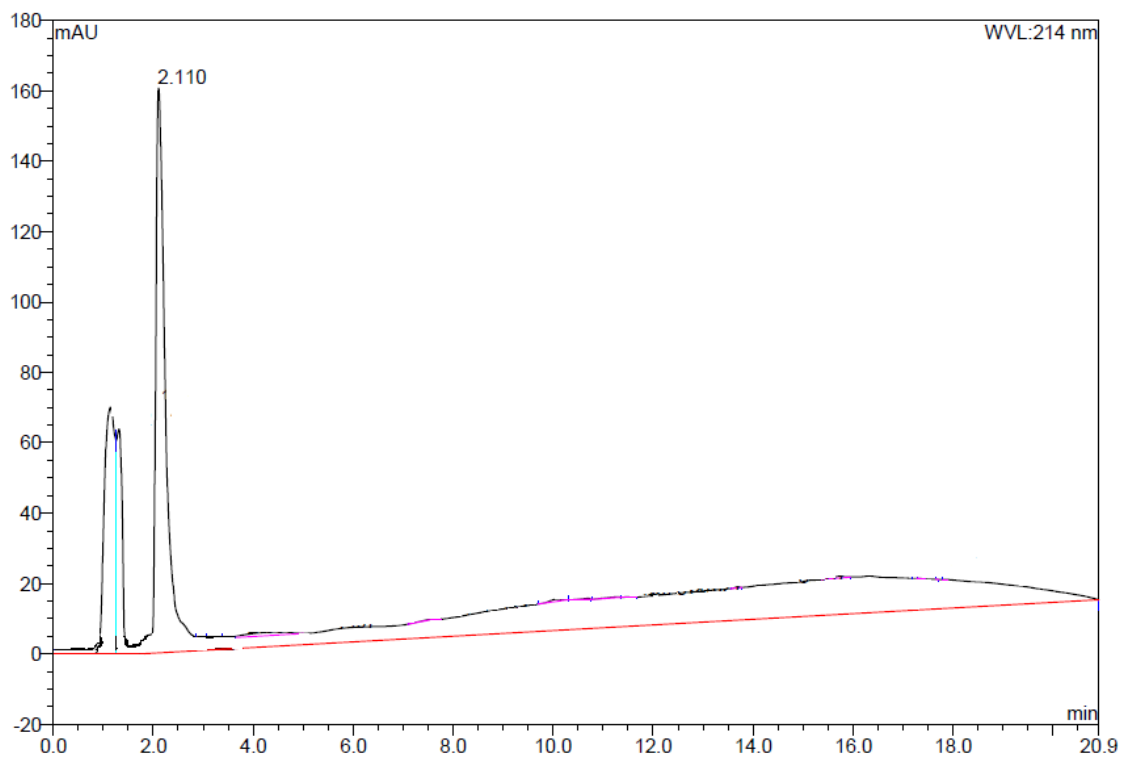


Figure 7.4: HPLC Trace Showing Combined Injection of Tocris ProTx-II and Original Cyclisation Method for Synthesis of ProTx-II in-house

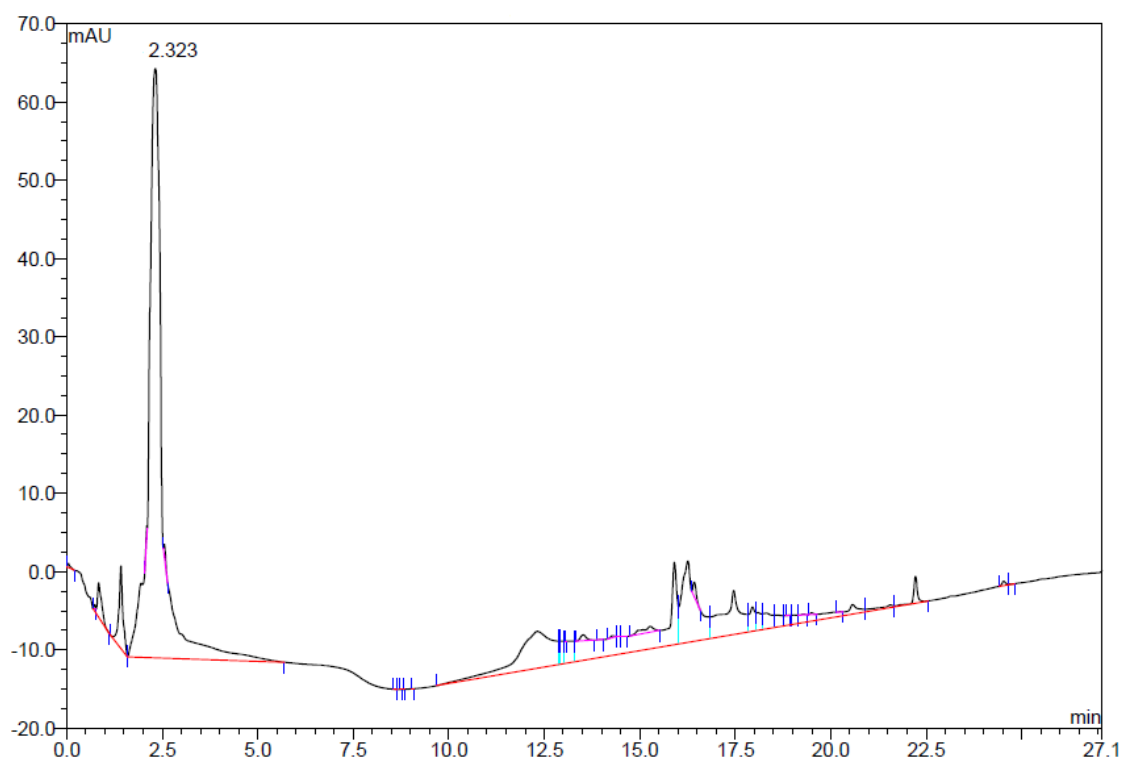


Figure 7.5: HPLC Trace Showing Smartox ProTx-II

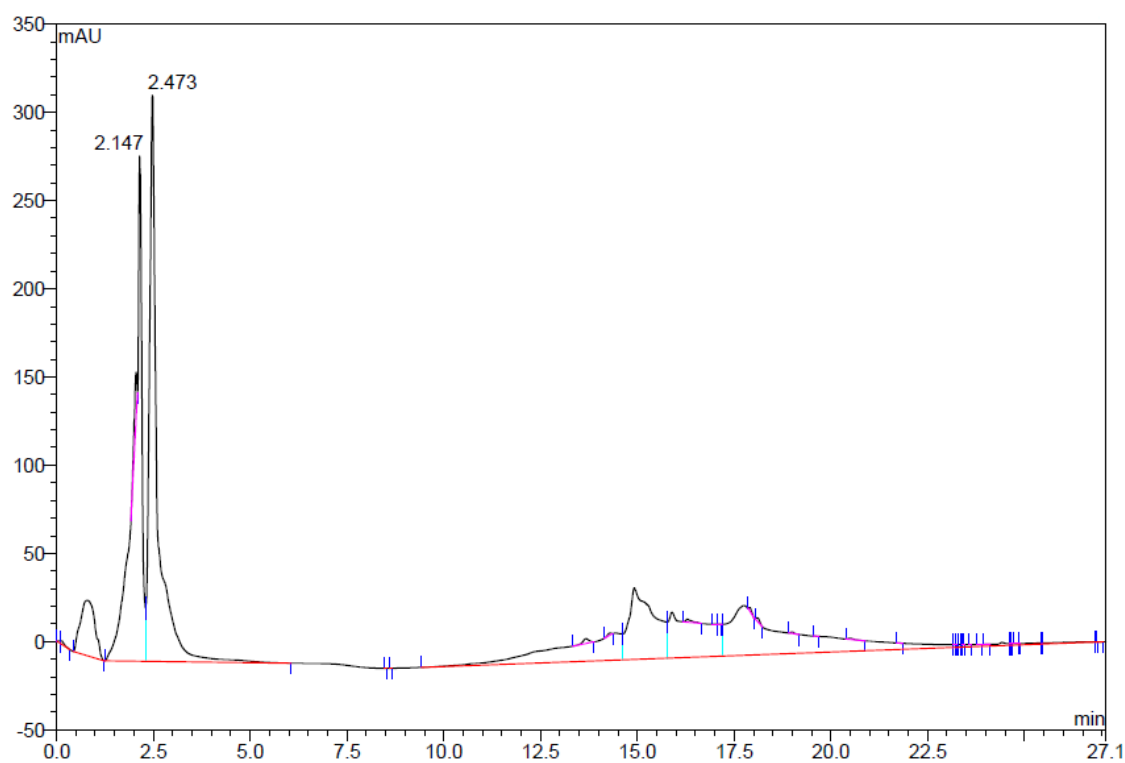


Figure 7.6: HPLC Trace Showing Combined Injection of Smartox ProTx-II and Original Cyclisation Method for Synthesis of ProTx-II in-house

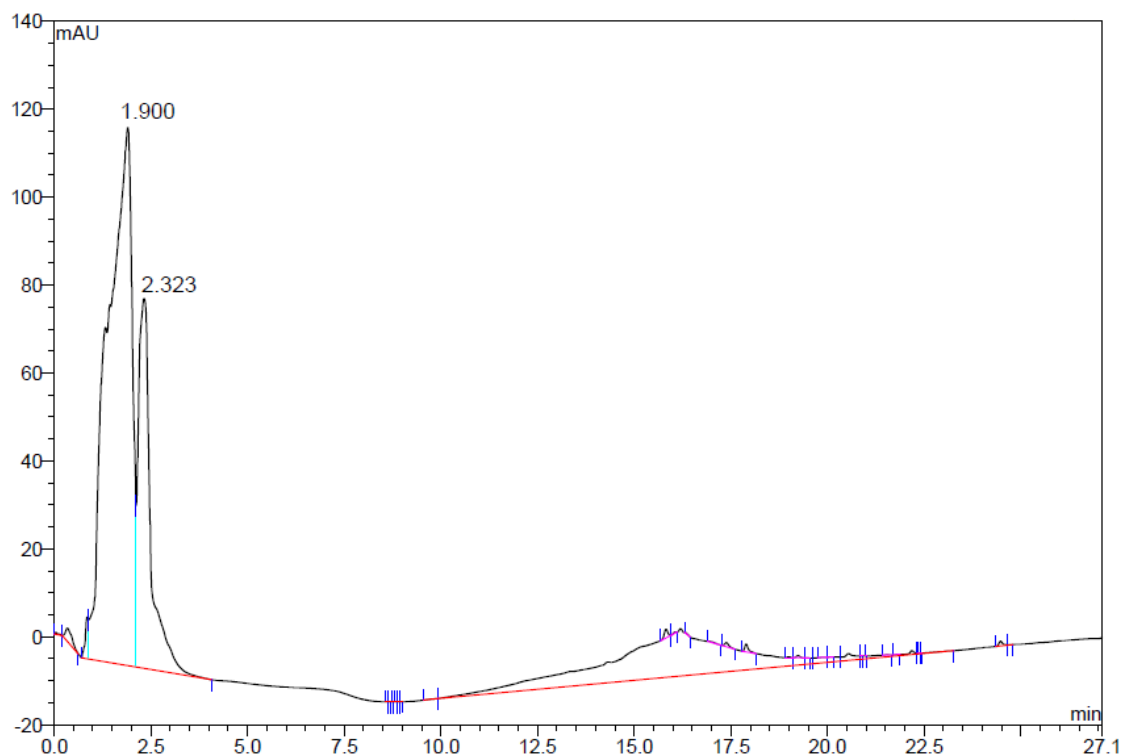


Figure 7.7: HPLC Trace Showing Combined Injection of Smartox ProTx-II and Park Cyclisation Method for Synthesis of ProTx-II in-house

7.5.2 Maleimide Experiments

All reactions were carried out in a solution containing 57.5% water, 40% acetonitrile and 2.5% DMF. ProTx-II was diluted to a concentration of 100 μ M and TCEP and 2,3-dibromomaleimide were diluted to a concentration of 10 mM in this solution.

Addition of 2,3-dibromomaleimide: Maleimide (19.8 μ L, 11.0 eq) was added to a solution of ProTx-II (180 μ L, 1.0 eq.). The solution was mixed and data recorded over the course of 1 h. In all cases, no addition of maleimide was observed (see Table 7.6).

Reduction of ProTx-II: TCEP (18.0 μ L, 10.0 eq) was added to ProTx-II (180 μ L, 1.0 eq.). The solution was mixed and left for 1 h. After this time, 2,3-dibromomaleimide was added to the solution as indicated in the above protocol.

Entry	Experiment	Mass Recorded	Result
1	In-house ProTx-II	3826	Control
2	In-house ProTx-II, Park Cyclisation conditions	3826	Control
3	Smartox Peptide	3826	Control
4	In-house ProTx-II + Maleimide (284)	3826	No Maleimide addition
5	In-house ProTx-II, Park Cyclisation conditions + Maleimide (284)	3826	No Maleimide addition
6	Smartox Peptide + Maleimide (284)	3826	No Maleimide addition
7	In-house ProTx-II + TCEP + Maleimide (284)	4111	Peptide + 3 maleimides
8	In-house ProTx-II, Park Cyclisation conditions + TCEP + Maleimide (284)	3826	No Maleimide addition
9	Smartox Peptide + TCEP + Maleimide (284)	3826	No Maleimide addition

Table 7.6: Results from the Maleimide End-Capping Experiments

7.5.3 Digestion Experiments

First Digestion Method (Chapter 3): ProTx-II, Trypsin and Glu-C were diluted to a concentration of 1.0 mg/mL in 100 mM ammonium bicarbonate solution. Trypsin (5.0 μ L) was added to a solution of ProTx-II (100 μ L) and left to stir at 37 °C for 18 h before addition of Glu-C (10 μ L). The mixture was left to stir for a further 18 h before submitting the solution directly for analysis.

Second Digestion Method (Chapter 3): ProTx-II (50 μ g) was first dissolved in 50 μ L of 75 mM ammonium bicarbonate solution and then added to a spin column containing immobilised trypsin (TT0010, Sigma-Aldrich). Digestion was carried out according to the manufactures protocol and the product collected, flash frozen and lyophilised. The digested ProTx-II was redissolved in 50 μ L of 100 mM ammonium bicarbonate solution. Glu-C was diluted to a concentration of 1.0 mg/mL in 100 mM ammonium bicarbonate solution. Glu-C (2.5 μ L) was added to the ProTx-II solution and left at 37 °C for 18 h before submitting the solution directly for analysis.

Third Digestion Method (Chapter 5): ProTx-II was solubilised in 50 mM ammonium bicarbonate solution containing 0.1% RapiGest™ to give a concentration of 1.0 mg/mL. The solution was heated to 40 °C for 10 min before the condensate was spun down using a techno mini low revolution centrifuge. Trypsin (2.0 μ L, 0.5 mg/mL in 50 mM ammonium bicarbonate solution) was added to the solution and left at 37 °C for 2 h. After this time, a second portion of trypsin (2 μ L) was added and the solution was left at 37 °C for a further 18 h. Glu-C (2.5 μ L, 1.0 mg/mL in 50 mM ammonium bicarbonate solution) was then added

and the solution left overnight at 37 °C. After this time, the solution was flash frozen and lyophilised before submission for analysis.

7.5.4 Computer Modelling

Computer modelling was carried out using Molecular Operating Environment software (MOE) version 2009.10 with the Amber94 forcefield and Born solvation.¹⁶ This uses the DSSP hydrogen bond estimation algorithm to assign secondary structure to amino acids.

ProTx-II was modelled using the homology modelling function within the software and the structure was built from the solution phase NMR structure of PaTx-I.¹⁷ Lanthionine bonds were modelled by creating the disulfide bond-containing compound, removing one sulfur atom *in silico* and using the program to re-calculate the energies and position of the atoms to give a rough estimate of the lanthionine bond in the system.

¹ Pangborn, A. B.; Giardello, M. A.; Grubbs, R. H.; Rosen, R. K.; Timmers, F. J., *Organometallics*, **15**, 1518-1520 (1996)

² Liu, L.; Tanke, R. S.; Miller, M. J., *J. Org. Chem.*, **51**, 26, 5332-5337 (1986)

³ Hida, T.; Hayashi, K.; Yukishige, K.; Tanida, S.; Kawamura, N.; Harada, S., *J. Antibiotics*, **48**, 7, 589-603 (1995)

⁴ Barlos, K.; Papaioannou, D.; Theodoropoulos, D., *J. Org. Chem.*, **47**, 1324-1326 (1982)

⁵ Turner, J. J.; Sikkema, F. D.; Filippov, D. V.; van der Marel, G. A.; van Boom, J. H., *Synlett*, **11**, 1727-1730 (2001)

⁶ Mustapa, M. F.; Harris, R.; Esposito, D.; Chubb, N. A. L.; Mould, J.; Schultz, D.; Driscoll, P. C.; Tabor, A. B., *J. Org. Chem.*, **68**, 8193-8198 (2003)

⁷ Pattabiraman, V. R.; McKinnie, S. M. K.; Vederas, J. C., *Angew. Chem. Int. Ed.*, **47**, 9472-9475 (2008)

⁸ Gude, M.; Ryf, J.; White, P. D., *Lett. Pept. Sci.*, **9**, 203-206 (2003)

⁹ Simon, M. L.; *Methods in Enzymology: Constitutive Activity in Receptors and Other Proteins, Part B*, **485**, 110 (2010)

¹⁰ Knerr, P. J.; Tzekou, A.; Ricklin, D.; Qu, H.; Chen, H.; van der Donk, W. A.; Lambris, J. D., *ACS Chem. Biol.*, **6**, 753-760 (2011)

¹¹ Saucedo, J. C.; Duke, R. M.; Nitz, M., *ChemBioChem*, **8**, 391-394 (2007)

¹² Son, J.-K.; Ramalingam, K.; Woodard, R. W., *Synthesis*, **1**, 3, 240-242 (1988)

¹³ Carrasco, M. R.; Brown, R. T.; Serafimova, I. M.; Silva, O., *J. Org. Chem.*, **68**, 1, 195-197 (2003)

¹⁴ Adamczyk, M.; Fishpaugh, J. R.; Thiruazhi, M., *Tetrahedron: Asymmetry*, **10**, 21, 4151-4156 (1999)

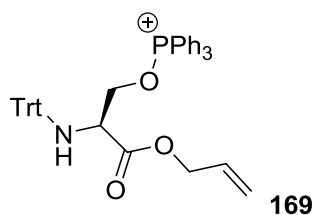
¹⁵ Park, J. H.; Carlin, K. P.; Wu, G.; Ilyin, V. I.; Musza, L. L.; Blake, P. R.; Kyle, D. J., *J. Med. Chem.*, **57**, 6623-6631 (2014)

¹⁶ *Molecular Operating Environment (MOE)*, 2010.10; Chemical Computing Group Inc., 1010 Sherbooke St. West, Suite #910, Montreal, QC, Canada, H3A 2R7, **2015**

¹⁷ Chagot, B.; Escoubas, P.; Villegas, E.; Bernard, C.; Ferrat, G.; Corzo, G.; Lazdunski, M.; Darbon, H., *Prot. Sci.*, **13**, 1197-1208 (2004)

Appendix: LC-MS Data from Mitsunobu Experiments

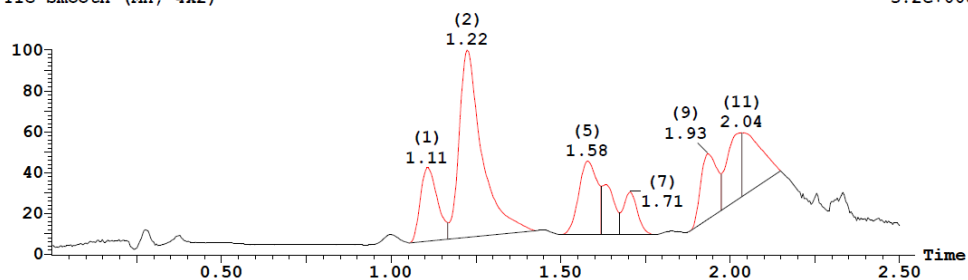
Evidence for Formation of Phosphine Adduct **169**



Chemical Formula: $C_{43}H_{39}NO_3P^+$
 Exact Mass: 648.27
 Molecular Weight: 648.76

MS ES+ :TIC Smooth (Mn, 4x2)

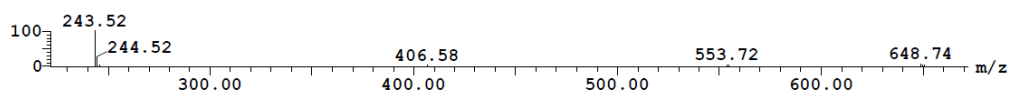
3.2e+008



Peak ID	Compound	Time	Mass Found
5		1.58	

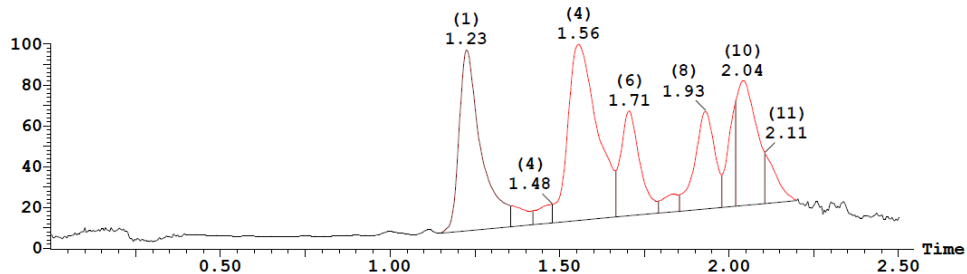
SAMPLE: 1:3 Combine (376:400- (339:350+426:437))

5.4e+007



MS ES+ :TIC Smooth (Mn, 4x2)

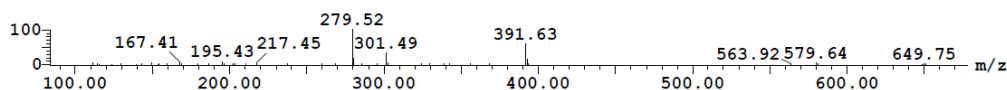
2.1e+008



Peak ID	Compound	Time	Mass Found
3		1.48	

SAMPLE: 2:33 Combine (351:375- (314:325+401:412))

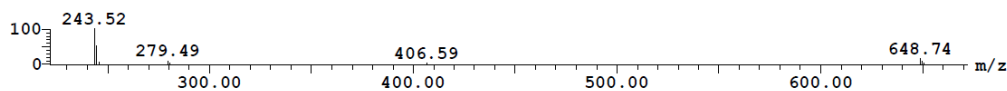
2.4e+006



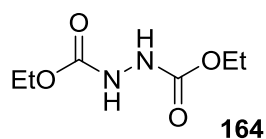
Peak ID	Compound	Time	Mass Found
5		1.57	

SAMPLE: 2:33 Combine (374:398- (337:348+424:435))

6.5e+007



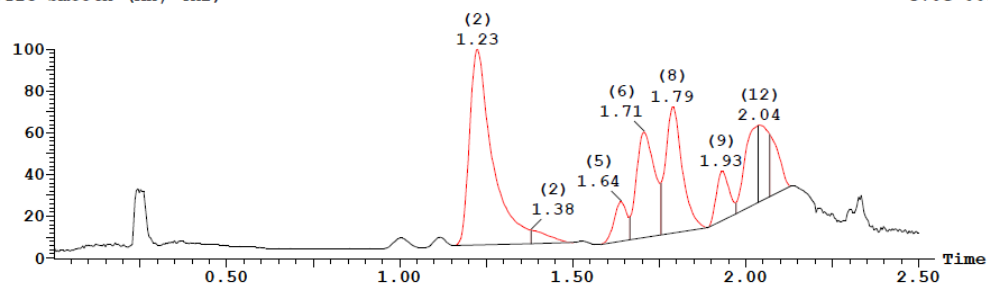
Evidence for Formation of DEAD Adduct **164**



Chemical Formula: C₆H₁₂N₂O₄
 Exact Mass: 176.08
 Molecular Weight: 176.17

MS ES+ :TIC Smooth (Mn, 4x2)

3.0e+008

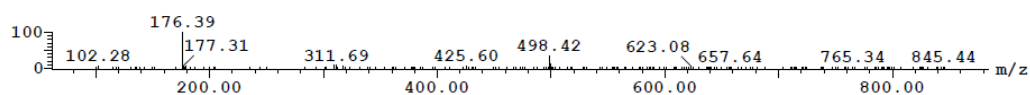


Peak ID Compound Time Mass Found

7 1.77

SAMPLE: 1:2 Combine (422:446-(385:396+472:483))

1.6e+005

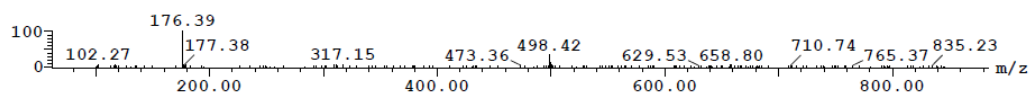


Peak ID Compound Time Mass Found

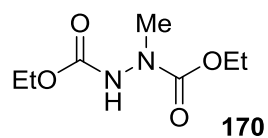
8 1.79

SAMPLE: 1:2 Combine (428:452-(391:402+478:489))

1.7e+005



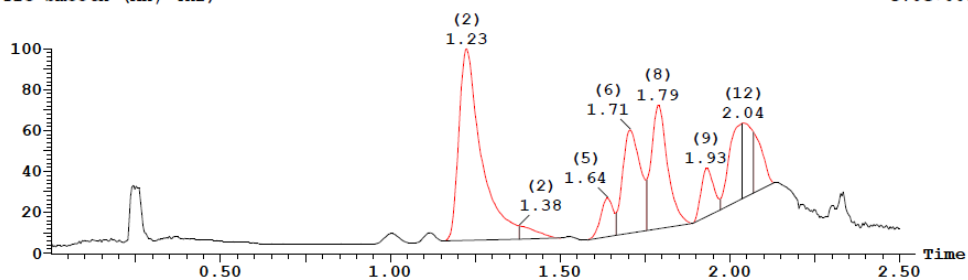
Evidence for Formation of DEAD Adduct **170**



Chemical Formula: $C_7H_{14}N_2O_4$
 Exact Mass: 190.10
 Molecular Weight: 190.20

MS ES+ :TIC Smooth (Mn, 4x2)

3.0e+008

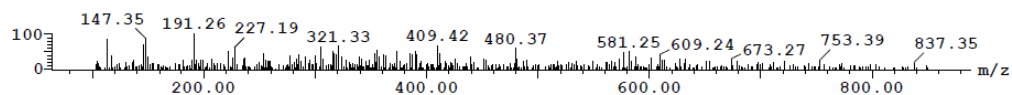


Peak ID Compound Time Mass Found

2 1.23

SAMPLE: 1:2 Combine (292:316-(255:266+342:353))

1.3e+004



Peak ID Compound Time Mass Found

4 1.48

SAMPLE: 1:2 Combine (351:375-(314:325+401:412))

2.3e+004

